Investigation into the role of the SUMO-like domains of the *Schizosaccharomyces pombe* DNA repair protein Rad60

A thesis submitted to the University of Sussex
for the degree of Doctor of Philosophy

by

Lara Katrina Boyd

November 2009

Declaration

I hereby declare that this thesis has not been, and will not be, submitted in whole or in part to another university for the award of any other degree. The work described herein is my own work except where otherwise stated.

Lara Katrina Boyd
November 2009

Acknowledgements

I would like to thank my supervisor, Dr. Felicity Watts, and co-supervisor, Dr. Simon Morley, for their supervision, guidance and support throughout the course of my PhD. I would like to express my deepest thanks to Prof. Tony Carr for providing both practical and emotional support when it was most needed. I am forever grateful.

I would like to acknowledge and thank Dr. Darren Thompson and Dr. Nigel Brisset for their help in modelling the SUMO-like domains, and Dr. Helfrid Hochegger, Dr. Ewan Smith and Clare Vesely for their generosity and their help with Southern blotting. I am grateful to all members of the GDSC and would like to express particular thanks to the support staff who make life just that little bit easier.

For all those in the Watts and Hoffman (Team Hoff) labs, I would like to say thank you for the useful discussions, good advice and for bringing a little bit of fun into the lab. Particular thanks have to go to Sharada, who has been a constant rock, and Andi, with whom I started and finished this journey with and, undoubtedly, would never have made it this far without.

From the heart: I am eternally grateful to my Mum and Dad for their love, support and encouragement throughout my entire life. Last, but certainly not least, a huge thank you to Chris, who has been there for me always, no matter what, providing love, laughter and encouragement.

University of Sussex
Lara Katrina Boyd
D Phil

Investigation into the role of the SUMO-like domains of the *Schizosaccharomyces pombe* DNA repair protein Rad60

Summary

Ubiquitin and ubiquitin-like (UBLs) proteins are post-translational modifiers that share a characteristic ββαββαβ fold. SUMO (small ubiquitin-like modifier) is one of a number of ubiquitin-like proteins. Unlike ubiquitin, SUMO does not appear to have a role in protein degradation. Instead it has been shown to have roles in facilitating protein-protein interactions, altering protein localisation and modulating protein activity. Analysis of protein databases indicates the existence of ubiquitin-fusion proteins, which act to functionally mimic ubiquitination by interacting with the proteosome. During the course of this project a family of SUMO-like domain (SLD) proteins has been identified and termed the RENi family after its best-studied members *S. pombe* Rad60, *S. cerevisiae* Esc2 and *M. musculus* Nip45.

I have initiated an investigation into the importance of the two SUMO-like domains for *S. pombe* Rad60 function. A *rad60* mutant deleted for SLD1 (*rad60-SLD1Δ*) is not viable suggesting that SLD1 is required for the essential role of Rad60. A *rad60* mutant deleted for SLD2 (*rad60-ct*) is viable but cells are sensitive to DNA damaging agents. This implies that SLD2 is not required for the essential function of Rad60 but is required for the response to DNA damage. The C-terminally truncated Rad60 protein (Rad60-ct) is mis-localised in *rad60-ct* cells. Provision of an NLS to the C-terminus of the Rad60-ct protein restores nuclear localisation but does not rescue the HU and MMS sensitivity of *rad60-ct* cells. Instead, expression of the Rad60-ctNLS protein has a dominant-negative effect in both wild-type and *rad60-ct* cells. The same phenomenon was observed when SLD2 was replaced with SUMO. This suggests that SLD2 is required not only to localise Rad60 to the nucleus, but also for the DNA damage response itself.

Molecular modelling suggests that SLD1 and SLD2 can adopt the characteristic ββαββαβ fold. A novel 'recombinase-mediated cassette-exchange' system was used to initiate a structure/function study of Rad60 SLD2 by mutating residues predicted to help maintain the hydrophobic core. The DNA damage sensitive phenotype of L348G, L338G, L346G and I334G substitutions support the hypothesis that the SLD2 adopts a SUMO-like fold.

Sumoylation of Rad60, *in vitro*, can be enhanced by the SUMO E3 ligase, Pli1 but not Nse2. Rad60 is sumoylated in a manner dependent on the C-terminus, which has is required to interact with the Hus5 conjugator, *in vitro*. This suggests that SLD2 may act to recruit Hus5 for sumoylation of itself and/or other proteins.

Table of Contents

List of Figures

List of Tables

Abbreviations

4-NQO	4-Nitroquinoline oxide
5-FOA	5-fluoroorotic acid
6-4PDs	(6-4) pyrimidone photodimers
9-1-1	Rad9-Rad1-Hus1
AP	apurinic or apyrimidinic
APS	ammonium persulfate
AT	ataxia-telangiectesia
ATM	ataxia telangeictesia mutated
ATP	adenosine triphosphate
ATR	ATM and Rad3 related
ATRIP	ATR-interacting protein
BER	base excision repair
BSA	bovine serum albumin
C. elegans	*Caenorhabditis elegans*
Cdk	cyclin-dependent kinase
cDNA	complementary DNA
ChIP	chromatin immununoprecipitation
CPD	cyclobutane pyrimidine dimmer
D. melangostar	*Drosophilla melanogastar*
DMSO	dimethyl sulfoxide
dNTP	deoxyribonucleotide triphosphate
DSB	double strand break
DSBR	double strand break repair
DTT	dithiothreitol
DUB	de-ubiquitinating enzyme
E. coli	*Escherichia coli*
ECL	Enhanced chemi-luminescence
EDTA	ethylenediaminetetraacetic acid
ELN	extra low nitrogen
EMM2	Edinburgh minimal media 2
EtOH	ethanol
GFP	green fluorescent protein
GG-NER	global genome NER
GST	glutathione-S-transferase
H. sapiens	*Homo sapiens*
HDAC	histone deacetylase
HJ	Holliday junction
HR	homologous recombination
HU	hydroxyurea
IMS	industrial methylated spirits
IOA	iodoacetamide
IPTG	isopropyl-β-D-thiogalactopyranoside
IR	ionising radiation
LB	L-broth
M. musculus	*Mus musculus*
MCM	mini-chromosome maintenance
MMR	mismatch repair
MMS	methyl methanesulfonate
MRN	Mre11-Rad40-Nbs1
MRX	Mre11-Rad40-Xrs2
NEM	N-ethylmaleimide
NER	nucleotide excision repair
NHEJ	non-homologous end joining
NLS	nuclear localisation signal
NP	nonidet P40
NPC	nuclear pore complex
Nse	non-Smc element

PBS	phosphate buffered saline
PCNA	proliferating cell nuclear antigen
PCR	polymerase chain reaction
PEG	polyethylene glycol
PIK	phosphoinositid-3-kinase
PML	promyelocytic leukaemia
PMSF	phenylmethylsulphonyl flouride
Pol	polymerase
Pre-RC	pre-replication complex
PRR	post replication repair
PVDF	polyvinylidene difluoride
rDNA	ribosomal DNA
RFC	replication factor complex
RMCE	recombinase mediated cassette exchange
RNA	ribonucleic acid
RNAP	RNA polymerase
ROS	reactive oxygen species
S. cerevisiae	*Saccharomyces cerevisiae*
S. pombe	*Schizosaccaromyces pombe*
SAE	SUMO activating enzyme
SBM	SUMO binding motif
SDS	sodium dodecyl sulphate
SDSA	Synthesis-dependent strand-annealing
SDS-PAGE	sodium dodecyl sulphate polyacrylamide gel electrophoresis
SIM	SUMO interacting motif
SLD	SUMO-like domain
SMC	structural maintenance of chromosomes
SSA	single strand annealing
SSB	single strand break
ssDNA	single strand DNA
STUbL	SUMO-targeted ubiquitin ligase
SUMO	small ubiquitin-like modifier
TBE	tris borate
TBZ	thiabendozole
TCA	trichloroacetic acid
TC-NER	transcription-coupled NER
TDG	thymine-DNA glycosylase
TEMED	tetramethylethylenediamine
TLS	translesion synthesis
TTD	Trichothiodystrophy
Ub	ubiquitin
UBA	ubiquitin associated domain
UBD	ubiquitin-binding domain
UBL	ubiquitin-like protein
UBM	ubiquitin-binding motif
UV	ultraviolet
UVDE	UV dependent endonuclease
UVER	UV excision repair
X-Gal	f-bromo-4-chloro-3indolyl-β-D galactopyranoside
YE	yeast extract
YEA	yeast extract agar
YNB	yeast nitrogen base
YNBA	yeast nitrogen base agar

CHAPTER 1
INTRODUCTION

1.1 Introduction

The integrity of the genome is under constant threat from both endogenous and exogenous sources, which can result in damage to the DNA. DNA lesions must be repaired to prevent the loss, or incorrect transmission, of genetic information, which could result in developmental abnormalities, tumourigenesis and even cell death. To prevent aberrations of the DNA from occurring, organisms have developed a number of complex cellular processes allowing DNA damage to be detected and, if necessary, repaired. In recent years, the mechanisms controlling the cell cycle and DNA repair have been the focus of much research, which is providing valuable insight into the cause and potential therapeutic treatments of many diseases including cancer.

The work in this thesis focuses on an investigation of the role of the SUMO-like domains of the *S. pombe* DNA repair protein Rad60. In this chapter, I shall provide an introduction into the cell cycle, DNA damage and the mechanisms that exist to ensure that genomic integrity is not compromised, as well as an introduction into some of the functional roles of the small ubiquitin-like modifier (SUMO).

1.2 *S. pombe* as a model organism

The mechanisms controlling the cell cycle and DNA repair have been the focus of scientists for many years, but, as with many other fields of research, the study of the human cell cycle is technically and ethically difficult. To overcome the problems associated with human research, 'model organisms' have proved invaluable as experimental systems to allow basic research to be carried out. This has enabled the study of a number of cellular processes that would otherwise be impossible. Since many features of eukaryotic life are conserved to some extent, 'basic research' using simpler 'model organisms' has often provided a basis for the study of more complex organisms Frequently used model organisms include prokaryotes such as *E. coli*, unicellular eukaryotes including the budding yeast *S. cerevisiae* and fission yeast *S. pombe*, multicellular eukaryotes, such as the nematode *C. elegans* and

vertebrates such as the mouse *M. musculus*. The fission yeast *S. pombe* has a number of characteristics that make it the ideal tool to study eukaryotic life and in particular the cell cycle and DNA damage repair processes.

S. pombe was first isolated from an East African millet beer, called *Pombe.* One advantage of using the fission yeast is its simplicity. *S. pombe* is a single rod-shaped cell that grows in length and divides by medial fission at a constant length. Cell size and length can therefore give a good visual indication of cell-cycle stage. The *S. pombe* cell cycle does, however, differ from other eukaryotic cell cycles by having a shorter G1 phase and a longer G2 phase. *S. pombe* spends approximately 70% of its cell cycle in the G2 phase, where bulk DNA replication has been completed. Due to the short generation time of *S. pombe,* it is easy to culture a large number of cells for study. The *S. pombe* cell cycle is discussed in further detail in section 1.4.2.

Another advantage of using *S. pombe* as a model for studies is the ability to perform genetic analysis. Unlike mammalian cells, *S. pombe* exists predominantly in a haploid state, allowing the phenotypic analysis of recessive mutants. Under conditions of nitrogen starvation, the haploid yeast is able to undergo mating and forms diploid zygotes, which form four spores when they undergo meiosis. The individual spores can be analysed by tetrad dissection, which is useful for genetic analysis and for the study of genetic recombination. The publication of the whole genome sequence in 2002 (Wood, Gwilliam et al. 2002) makes *S. pombe* an ideal tool to study eukaryotic cellular processes. Knowledge of the *S. pombe* genome sequence has simplified many existing techniques and allowed the development of new scientific approaches making *S pombe* a useful model.

1.3 Introduction to DNA damage

DNA lesions can occur as a result of damage from both endogenous and exogenous sources. Exogenous sources of DNA damage include UV and γ-irradiation (IR). UV-C light causes covalent joining of adjacent bases, forming mainly cyclobutane pyrimidine dimers (CPDs) and pyrimidine(6-4)pyrimidine photodimers ((6-4)PDs). Such lesions can distort the DNA helix and, therefore, can lead to mis-pairing and mis-incorporation during DNA

synthesis. Exposure to IR can also cause a variety of base alterations including both single-stranded breaks (SSBs) and double-stranded breaks (DSBs) in the phosphodiester backbone. DSBs are highly toxic lesions, which if left unrepaired can result in chromosome breakage and subsequent loss during cell division.

Endogenous processes can also induce DNA damage, for example, hydrolysis can lead to spontaneous DNA depurination. Base damage can occur from the action of reactive oxygen species, which can be generated as a result of some intracellular reactions, as well as IR and UV. In addition, the intricate processes of replication and mitotic chromosome segregation frequently introduce mutations into the genome. Alternatively, abnormal DNA intermediates, such as stalled or collapsed replication forks or unresolved Holliday junctions, may form resulting in DNA, which cannot be replicated. Collapsed replication forks can also result in DNA breaks.

When damage to the DNA is detected during the cell cycle a DNA damage checkpoint is activated and also, if necessary, a DNA repair pathway. DNA repair pathways act mainly on duplex DNA and rely on the excision and subsequent re-synthesis of the damaged sequence based on the information encoded by the complementary strand. However, during DNA replication, unrepaired lesions can impede the progress of replicative DNA polymerases. Stalled replication forks present dangerous structures that can result in either permanent cell cycle arrest or major chromosomal abnormalities. A method to overcome replication blocks is therefore required to ensure genome integrity and cell survival. The cell cycle, checkpoints and DNA repair pathways are discussed in more detail in sections 1.4 and 1.5.

1.4 Sensing DNA damage during the cell cycle

1.4.1 Introduction to the cell cycle

The process of DNA replication and segregation of replicated chromosomes into two identical daughter cells is known as the cell cycle and occurs at distinct and regulated intervals. The eukaryotic cell cycle consists of four phases (Norbury and Nurse 1992). S phase is the phase during which the DNA is replicated and a complete copy of each

chromosome is made. S-phase is preceded by a gap phase called G1, during which the cell prepares for DNA synthesis, and is followed by a gap phase called G2, during which the cell prepares for mitosis (M-phase). During mitosis the newly replicated chromosomes are segregated equally between the two daughter cells as the cells divide. Before commitment to DNA replication, cells in G1 can enter a resting state called G0.

Progression through the cell cycle is a complex process and occurs in a highly ordered series of events that require tight regulation. The alternation of S and M phases and the coordination of growth and division is accomplished by cyclin-dependent kinases (Cdks) and their association with different cyclins during different stages of the cell cycle (Pines 1995). In the Cdk-cyclin pairing, Cdks act as the catalytic subunit for the phosphorylation of serine/threonine residues on target proteins. Cyclins act as the regulatory subunit and are required for targeting Cdks to their target proteins. The cyclic assembly and disassembly of Cdk-cyclin complexes at defined cell stages occur as a consequence of their synthesis, inhibition and ubiquitin-mediated degradation. Furthermore, superimposed onto the cell cycle are a number of 'checkpoints' that act to assess the readiness of the cell to proceed to the next stage in the cycle. I will discuss checkpoints in further detail in section 1.4.3.

1.4.2 The *S pombe* cell cycle

In *S. pombe* the only Cdk directly involved in cell regulation is Cdc2. Cdc2 associates with four different cyclins Cig1, Cig 2, Puc1 and Cdc13**.** Although there are four cyclins in *S. pombe*, only Cdc13 is essential for progression through the cell cycle. This suggests that a single Cdk-cyclin complex (Cdc2-Cdc13) can trigger both S- and M-phase. Progression of the cell cycle is mediated by Cdc2-Cdc13 (Figure 1.1). During G1, Cdc2-Cdc13 activity is low due to the low level of Cdc2. Cdc2 activity is inhibited in two ways. Firstly, any residual Cdc2-Cdc13 activity from the previous M-phase is inhibited by ubiquitin-mediated proteolysis of Cdc13 (Yamaguchi, Murakami et al. 1997; Kitamura, Maekawa et al. 1998). Secondly, the Cdc2 inhibitor Rum1 inhibits the kinase activities of Cdc2-Cdc13 and Cdc2-Cig2 and targets Cdc13 for degradation (Correa-Bordes, Gulli et al. 1997; Benito, Martin-Castellanos et al. 1998). At the G1/S transition, Rum 1 is degraded, thus, increasing Cdc2-Cdc13 activity and sending the cells into S-phase (Benito, Martin-Castellanos et al. 1998).

Figure 1.1: Cell cycle regulation in *S. pombe*

Progression of the *S. pombe* cell cycle is mediated by Cdc2-Cdc13 activity. During G1, Cdc2-Cdc13 activity is inhibited by Rum1. At the G1/S transition, Rum 1 is degraded, thus, increasing Cdc2-Cdc13 activity and promoting entry into S-phase. During G2, phosphorylation on Cdc2 Tyr15 by Wee1 inactivates Cdc2-Cdc13. At the G2/M transition the inactivating phosphate group is removed by Cdc25 phosphatase, promoting Mitosis At the end of mitosis, the ubiquitin ligase (APC) targets mitotic cyclins for degradation, thus, lowering the levels of Cdc2-Cdc13.

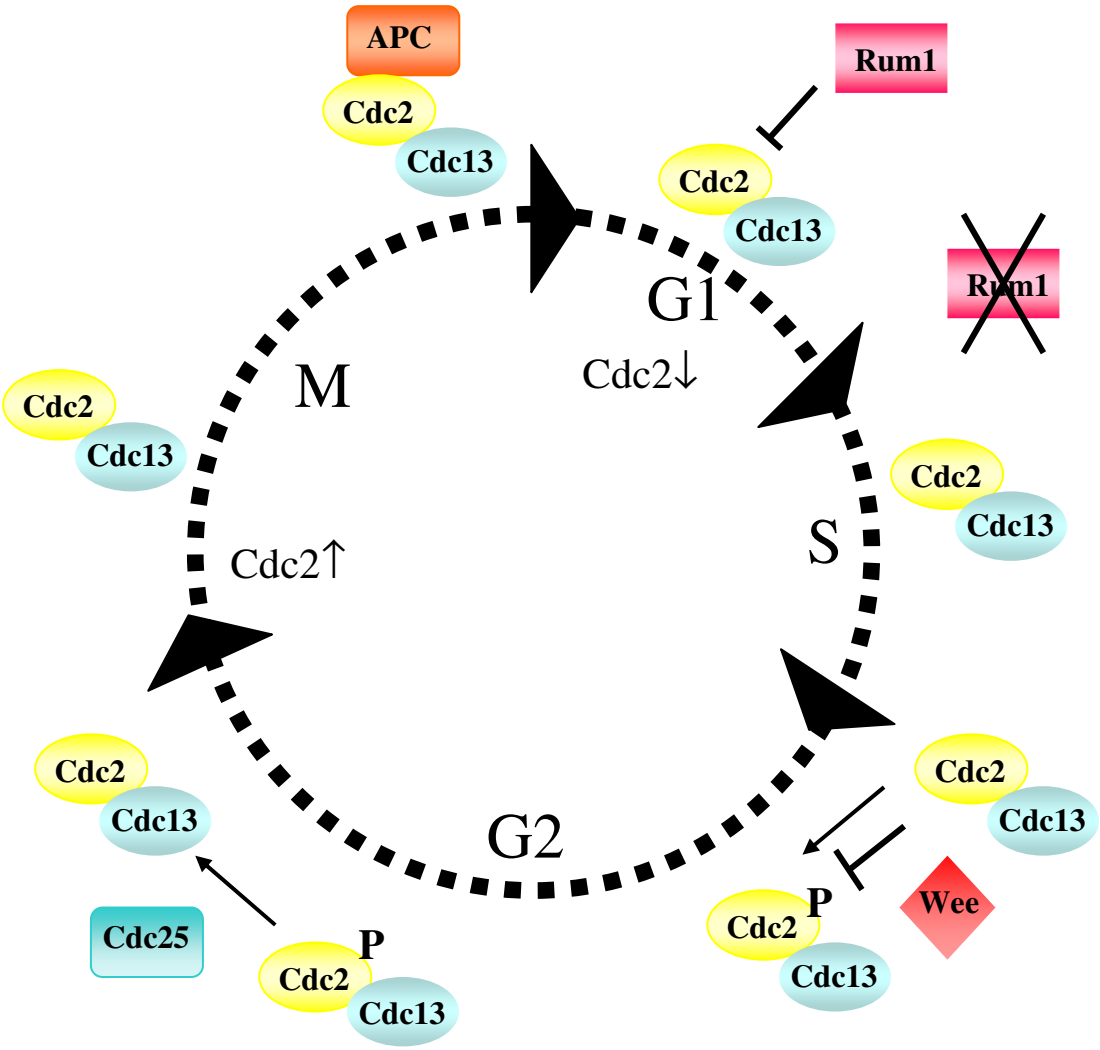

Figure 1.1: **Cell cycle regulation in *S. pombe***

Active S-phase Cdc2-Cdc13 complexes phosphorylate proteins that make up the pre-replication complex, which is assembled during G1. During G2, phosphorylation on Tyr15 of Cdc2 by the Wee1 kinase renders Cdc2-Cdc13 inactive. At the G2/M transition the inactivating phosphate group is removed by Cdc25 phosphatase, further increasing the activity of Cdc2-Cdc13 (Moreno, Nurse et al. 1990). The increased activity of Cdc2-Cdc13, which is synthesised but inactivated during G1 and S phase, promotes the initiation of Mitosis by stimulating downstream proteins required for chromosome condensation and mitotic spindle assembly. At the end of M-phase, the ubiquitin ligase known as the anaphase promoting complex (APC) targets mitotic cyclins for degradation, thus, lowering the levels of Cdc2-Cdc13 and ensuring that telophase and cytokinesis can continue.

1.4.3 DNA damage checkpoints

The periodic activation of cyclins acts to control cell cycle progression. However, the faithful transmission of genetic information from one cell to its daughters requires not only accuracy in DNA replication and chromosome distribution, but also the ability to survive both spontaneous and induced DNA damage. Cells have evolved a number of mechanisms that 'sense' DNA damage during the cell cycle and consequently slow or arrest the cell cycle, thereby, allowing cells to repair the damage (Weinert and Hartwell 1988). The precise 'checkpoint' response is dependent on both the stage of the cell cycle and the exact type of DNA damage encountered. Different types of DNA damage are discussed in further detail in section 1.5.

The best-defined checkpoints are the G1/S, intra-S and G2/M checkpoints. When DNA damage is sensed in G1, the G1/S checkpoint is activated to prevent cells from entering S-phase, therefore inhibiting the initiation of DNA replication. The G2/M checkpoint (also known as the DNA damage checkpoint) is activated in G2 and acts to prevent cells from undergoing mitosis when damage is present. The intra-S-phase checkpoint is activated when DNA damage is detected in S-phase. Unlike the G1/S and G2/M checkpoints, which respond to DNA damage, the intra-S-phase checkpoint also has to recognise and respond to replication intermediates and stalled replication forks that can prevent the progression of replicative polymerases that can cause DNA breaks. Although these checkpoints are

distinct, many of the proteins required for the response to DNA damage are shared. There are three main classes of checkpoint proteins: sensors that detect replication blocks or DNA damage; transducers that relay this signal; and effectors that act on targets of the checkpoint. At any point in the cell cycle, the response to DNA damage follows the same sequence of events; 1) DNA damage is first detected by 'sensor' proteins, 2) a group of 'signal transducer' proteins convey the signal to specific 'effector' proteins, 3) The 'effector' proteins activate a cascade of events that result in cell cycle arrest and DNA repair. In addition to the signal transduction proteins mentioned above, a number of other 'mediator' proteins are involved in the DNA damage response. These proteins are mainly cell cycle specific and associate with the sensors, signal transducers and effector proteins at particular phases of the cell cycle to provide signal transduction specificity. Conserved proteins of the signal transduction pathway (and *S. pombe* homologues) can be seen figure 1.2.

1.4.3.1 The checkpoint response

The checkpoint mechanism is best understood for its role in the response to DSBs. Checkpoint initiation is dependent on the transient recruitment of the Mre11/Rad50/Nbs1 (MRN) complex to sites of DSBs followed by the recruitment and activation of the ataxia-telangiectasia mutated (ATM) protein (Lee and Paull 2005). ATM is a member of the phosphoinositide 3-kinase (PI3K) protein family and is considered to function as a DNA damage 'sensor' protein in the checkpoint response. Two other PI3K 'sensor' proteins, ATM and Rad3-related' (ATR) and DNA-dependent protein kinase (DNA-PK), are activated in response to DSBs. However, unlike ATM and DNA-PK, which function in response to DSBs, the primary function of ATR is in the initiation of the DNA damage response to stalled replication forks. The *S. pombe* homologues of ATM and ATR are Tel1 and Rad3 respectively. In contrast to the *H. sapiens* sensor proteins ATM and ATR, which activate checkpoints in response to DSBs and UV/replicative stress respectively, *S. pombe* Rad3 activates both checkpoint pathways (al-Khodairy and Carr 1992).

ATM exists as inactive dimers, which, when recruited to sites of DNA damage, dissociate and autophosphorylate on multiple residues. This autophosphorylation is believed to be

Figure 1.2: The checkpoint response

(A) The signal transduction pathway **(B)** Checkpoint proteins identified in *H. sapiens* and their *S. pombe* homologues.

A

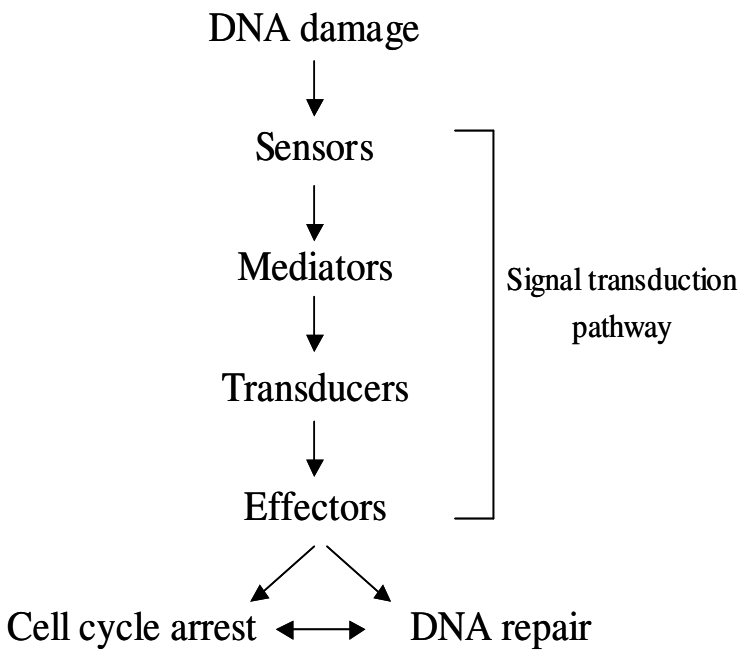

B

Function	Class	*H. Sapiens*	*S. pombe*
Sensors	RFC1-like protein complexes	Rad17	Rad17
		Rfc2-5	Rfc2-5
	PCNA-like complexes	Rad9	Rad9
		Rad1	Rad1
		Hus1	Hus1
	PI3K like complexes	ATM	Tel1
		ATR	Rad3
		ATRIP	Rad26
	MRN complexes	Mre11	Mre11
		Rad50	Rad50
		Nbs1	Nbs1
Mediators	BRCT-containing	BRCA1	Crb2
		TopBP1	Rad4
		53BP1	
		Mdc1	
		Claspin	Mrc1
Transducers	Protein kinase	Chk1	Chk1
		Chk2	Cds1

Figure 1.2: The checkpoint response

important for maintaining ATM activation (Bakkenist and Kastan 2003). Active ATM phosphorylates target proteins, which are essential for the response to DNA damage and its subsequent repair. For example, histone H2AX is phosphorylated at sites of damage by ATM, ATR or DNA-PK (Rogakou, Pilch et al. 1998). Phosphorylated H2AX (γ-H2AX) signals for the recruitment of other proteins that are essential for the chromatin remodelling process that is necessary for the process of DNA repair. Other proteins recruited to sites of DSBs include the so-called 'mediator' proteins, which act downstream of ATM and ATR (Stewart, Wang et al. 2003). Checkpoint mediators may assist in promoting interactions between ATM/ATR and their substrates by recruiting additional substrates and acting as scaffolds upon which to assemble complexes. Mediator proteins include Claspin and the BRCA1 C terminus (BRCT) repeat domain proteins 53BP1, Mdc1, BRCA1 and TopBP1. Different mediator proteins associate with proteins of the signal transduction pathway in response to DNA damage at specific stages of the cell cycle. The DNA damage checkpoint mediators Mdc1, 53BP1, and BRCA1 are largely linked to the ATM pathway, whereas TopBP1 and Claspin have been proposed to co-regulate the ATR pathway (Kumagai, Kim et al. 2004; Stucki and Jackson 2004; Garcia, Furuya et al. 2005). *S. pombe* homologues of Claspin, BRCA1, and TopBP1 are Mrc1, Crb2 and Rad4 respectively.

As well as functioning upstream, the MRN complex is also a substrate of ATM. Phosphorylation of the MRN complex by activated ATM is important for downstream signalling (Uziel, Lerenthal et al. 2003). MRN complex mediated resection of DSBs is followed by the coating of single-stranded DNA with replication protein A (RPA) (Byun, Pacek et al. 2005). RPA binding protects the DNA ends from further processing and acts to recruit ATR and its binding partner ATRIP (ATR-interacting protein) (Zou and Elledge 2003), subsequently leading to ATR-dependent phosphorylation of proteins such as the mediator proteins Claspin and BRCA1. Additionally, the ssDNA-RPA complex recruits the Rad17 clamp loader and the PCNA-like (proliferating cell nuclear antigen) 9-1-1 (Rad9-Rad1-Hus1) complex onto DNA (Melo, Cohen et al. 2001; Zou and Elledge 2003). ATR phosphorylates Rad17 and the 9-1-1 complex, which is important for down-stream signalling (Caspari, Dahlen et al. 2000). The ATR, ATRIP, Rad17, Rad9, Rad1 and Hus1

are conserved in *S. pombe* and are encoded by the *rad3*, *rad26*, *rad17*, *rad1* and *hus1* genes respectively.

Activated ATM and ATR mediate the phosphorylation and activation of the so-called 'tranducer' proteins, Chk1 and Chk2. Chk1 and Chk2 are serine threonine kinases that act to phosphorylate target proteins, such as p53 and the Cdc25 family of proteins that control cell cycle arrest (Bartek and Lukas 2001). Although there is some redundancy, Chk1 and Chk2 function in different pathways. In mammalian cells, Chk1 is phosphorylated and activated in an ATR dependent manner in response to UV or replication stress, whereas Chk2 is and activated in an ATM-dependent manner in response to IR induced DSBs (Liu, Guntuku et al. 2000; Melchionna, Chen et al. 2000). In *S. pombe* the ATR homologue, Rad3 activates both Chk1 and Cds1 (Chk2 homologue). However, Chk1 and Cds1 respond to different checkpoint signals (Brondello, Boddy et al. 1999). Chk1 activation occurs most commonly when DNA damage is detected after the DNA damage has been replicated (Walworth and Bernards 1996). In contrast, Cds1 is activated in response to replication stress, (Lindsay, Griffiths et al. 1998). Under conditions where Cds1 activity is lost, replication damage results in the collapse of stalled replication forks and Chk1 can be activated (Lindsay, Griffiths et al. 1998).

Below the level of signal transduction is a group of proteins termed the 'effector' proteins. Activated transducer kinases Chk1 and Chk2 (Cds1 in *S. pombe*), act upon effector proteins to produce a number of different cellular responses, including signalling for DNA repair, regulation of transcription, inducing apoptosis and controlling cell cycle transitions. The best-studied examples of effector proteins in mammalian cells are the p53 tumour suppressor protein and the Cdc25 family of phosphatases. In mammalian cells, the p53 tumour suppressor plays an important role in the decision to undergo either cell cycle arrest or apoptosis in response to stresses including DNA damage (Giaccia and Kastan 1998). Under normal conditions the level of p53 is kept low by Mdm2-mediated ubiquitination and degradation. When DNA damage is detected, ATM and ATR phosphorylate Ser15 of p53 (Banin, Moyal et al. 1998; Canman, Lim et al. 1998). Phosphorylation of p53 inhibits its interaction with Mdm2, thus, resulting in p53 stabilisation (Shieh, Taya et al. 1999).

Activated p53 transactivates p21, which inhibits two G1/S-promoting cyclin-dependent kinases, Cdk2 and Cdk4, thus inhibiting G1/S transition (el-Deiry, Tokino et al. 1993; Harper, Adami et al. 1993) The Cdc25 family of protein phosphatases act to remove the phosphate group from Cdks that act to regulate the cell cycle transitions (Boutros, Dozier et al. 2006). For example, when DNA damage is detected in G2, Chk1 and/or Chk2 phosphorylate Cdc25-A, resulting in its ubiquitination and subsequent degradation. Inactivation of Cdc25-A leads to an accumulation of Tyr15 phosphorylated Cdc2, resulting in mitotic arrest. (Zhao, Watkins et al. 2002; Xiao, Chen et al. 2003). In an analogous manner, *S. pombe* Cdc25 is phosphorylated in a Rad3-Crb2-Chk1- (sensor-mediator-transducer) dependent manner, thereby mediating cell cycle arrest by promoting Tyr15 phosphorylation of Cdc2.

1.4.3.2 Targets of the *S. pombe* Cds1 checkpoint kinase

The *S. pombe* checkpoint kinase Cds1 plays an important role in stabilising stalled replication forks and promoting recovery (Kai and Wang 2003). Three proteins have been identified as targets of Cds1 and they are likely to play an important role in preventing mutations during replication and promoting recovery after replication stalling. These proteins are the Mus81-Eme complex, Rqh1 and Rad60 (Murray, Lindsay et al. 1997; Boddy, Shanahan et al. 2003).

When replication is perturbed, Cds1 interacts with the nuclease Mus81 via its FHA (forkhead associated) domain. Cds1 regulated phosphorylation of Mus81 reduces the chromatin binding ability of the Mus81-Eme1 complex (Boddy, Shanahan et al. 2003; Kai and Wang 2003). This suggests that one of the ways that Cds1 may prevent the occurrence of deletion mutations caused by the Mus81-Eme1 nuclease in replication stressed cells is by reducing the chromatin binding ability of Mus81. Like Mus81, in response to replication stress, Cds1 interacts with the Rad60 via its FHA domain (Boddy, Shanahan et al. 2003). Rad60 is associated with the Smc5/6 complex (Section 1.6 and section 1.9) and is required for the repair of DSBs by recombination repair (Morishita, Tsutsui et al. 2002). In response to replication stress by HU treatment, Cds1-dependent phosphorylation of Rad60 by Cds1 results in Rad60 delocalisation from the nucleus (Boddy, Shanahan et al. 2003). This

suggests that removal of Rad60 from the nucleus, may be another method by which Cds1 acts to prevent non-productive and inappropriate recombination repair events during replication stalling (Boddy, Shanahan et al. 2003; Kai and Wang 2003). The *S. pombe* RecQ helicase, Rqh1, is required for the recovery from HU-induced S-phase arrest (Stewart, Chapman et al. 1997). In *S. cerevisiae*, following HU treatment, the Rqh1 homologue, Sgs1, is required to maintain polymerases α and ε at stalled replication forks (Cobb, Bjergbaek et al. 2003). This suggests that after replication fork stalling, Sgs1 plays a role in resolving aberrant strand exchange events and a third way in which Cds1 may act to allow recovery from replication induced arrest.

1.5 DNA damage repair pathways

Due to the diverse nature of DNA damage a number of different DNA repair pathways have evolved to ensure faithful transmission of the genome. In this section, I will discuss the different DNA repair mechanisms known to exist in the cell.

1.5.1 Nucleotide excision repair

Nucleotide excision repair (NER) occurs in both prokaryotes and eukaryotes and exists to remove bulky DNA lesions that distort the DNA helix. This includes lesions induced by UV damage such as 6-4 photoproducts and CPDs, and also other types of damage such as inter- and intra-strand cross-links. In brief, the NER repair mechanism acts by making incisions on both sides of the damaged nucleotide, removing the fragment containing the damage and then re-synthesising the excised fragment. In humans, defects in the NER pathway are associated with several disorders including Xeroderma pigmentosum, which is characterised by an extreme sensitivity to sunlight and an elevated risk of skin cancer (Cleaver 1968). Other NER associated disorders include Trichothiodystrophy and Cockayne Syndrome (Lehmann 1995; Lehmann 2003)

Two sub-pathways of NER pathways have been identified; global genome NER (GG-NER) and transcription-coupled NER (TC-NER). As their names suggest, GG-NER repairs DNA lesions throughout the genome whereas TC-NER is confined to the repair of DNA lesions in transcribed strands and is coupled to active transcription. The main difference between

the TC-NER and GG-NER pathways is the requirement of different factors for the recognition of the DNA lesion. Following recognition, both pathways require the same core NER factors for the assembly of a functional NER complex. TC-NER specific factors are recruited when the RNAPII complex is stalled at a DNA lesion. The stalled polymerase must be displaced to make the lesion accessible for repair. Recognition requires the CSA and CSB proteins along with XAB2 and HMGN1 (Nakatsu, Asahina et al. 2000; Bustin 2001; Fousteri, Vermeulen et al. 2006). In GG-NER, XPC-Rad23B along with UV-DDB recognises the site of DNA damage. Once the lesion has been recognised XPA, TFIIH and RPA are recruited (Park, Mu et al. 1995; Sugasawa, Okamoto et al. 2001; Volker, Mone et al. 2001). The basal transcription factor TFIIH has an essential role in NER as two of its components XPB and XPD exert their DNA-dependent ATPase and helicase activity respectively to unwind about 20-25 bp of DNA around the DNA lesion (Drapkin, Reardon et al. 1994; Wang, Buratowski et al. 1995). In an ATP-dependent reaction, XPG recruits the heterodimer ERCC1-XPF to form Pre-initiation complex I. The XPG and XPF-ERCC1 endonucleases make incisions 3' and 5' to the lesion respectively (O'Donovan, Davies et al. 1994; Sijbers, van der Spek et al. 1996). This results in the release of the DNA fragment containing the lesion. Following excision of the lesion, replication factor C (RFC), proliferating cell nuclear antigen (PCNA), DNA polymerase δ or ε, DNA ligase and RPA are required for gap filling and ligation (Aboussekhra, Biggerstaff et al. 1995; Shivji, Podust et al. 1995; Araujo, Tirode et al. 2000).

The NER pathway has been well characterised in *S. pombe.* The *S. pombe* homologues of XPA, XPB, XPD, XPF, XPG and ERCC1 are Rhp14, Ptr8, Rad15, Rad16, Rad13, and Swi10 respectively (Marti, Kunz et al. 2002).

1.5.2 UV damage excision repair

In contrast to *S. cerevisiae, S. pombe* NER mutants are still able to excise UV-induced damaged DNA, suggesting the existence of an alternative pathway for the excision of UV lesions in *S. pombe* (Murray, Doe et al. 1992; McCready, Carr et al. 1993; Carr, Schmidt et al. 1994; Murray, Tavassoli et al. 1994). The UV damage excision repair (UVER) pathway is dependent on an *S. pombe* specific protein known as the UV damage endonuclease

(UVDE) (Freyer, Davey et al. 1995; Yonemasu, McCready et al. 1997). UVDE shares structural similarity to the AP endonucleases, recognising both 6-4 photoproducts and CPDs, and functions by nicking the phosphodiester backbone 5'to the DNA lesion. Following cleavage, Rad2 is required to process the UVDE nick (Alleva and Doetsch 1998). The DNA is then re-synthesised through the action of DNA polymerases and ligases.

A *rad2 rad13* double mutant is repair proficient suggesting the existence of an alternative Rad2-independent pathway exists to process UVDE nicks. This pathway requires functional Rhp51, Rqh1 and TopIII proteins for activity, although the precise mechanism of action is unknown (McCready, Osman et al. 2000).

1.5.3 Base excision repair

The majority of cellular DNA damage occurs as a consequence of cellular metabolism. Small lesions, including apurinic and apyrimidinic (AP) sites, form as a result of spontaneous hydrolysis and oxidative damage to bases by reactive oxygen species (ROS), as well as from IR and UV damage. The most common way to remove such damage is through the action of the BER pathway. In BER, the damaged base is removed through the action of a group of DNA glycosylases. DNA glycosylases can be subdivided by their ability to recognise a particular type of base modification. For example, thymine DNA glycosylase specifically recognise and remove thymine residues found in G:T mispairs, which arise through deamination of 5-methylcytosine (Krokan, Nilsen et al. 2000; Norbury and Hickson 2001). The DNA glycosylase cleaves the N-glycosidic bond between the modified base and the deoxyribose sugar, leaving an AP site in the DNA. An AP-endonuclease (APE) cleaves the AP site to generate 3' OH and 5' deoxyribose phosphate termini (Doetsch and Cunningham 1990). Following cleavage, the AP site is removed by a phosphodiesterase and the gap in the DNA is re-synthesised through DNA polymerase and DNA ligase activity.

Two different BER mechanisms exist: short-patch and long-patch BER. In the short-patch BER model, only the damaged base is excised leaving a 1-nucleotide gap (Kubota, Nash et al. 1996). In this situation, the DNA strand is re-synthesised by DNA polymerase β and

ligated by the ligase III/XRCC1 complex (Kubota, Nash et al. 1996). In the long-patch BER model, excision of the damaged base leaves a repair patch of 2-8 nucleotides. DNA polymerase β, DNA polymerase δ/ε, PCNA and the FEN1 endonuclease are required for long-patch repair synthesis, and DNA ligase I is required to close the gap (Krokan, Nilsen et al. 2000; Sokhansanj, Rodrigue et al. 2002). The choice between long-patch and short-patch BER may depend on whether cleavage by the APE occurs 5' or 3' to the AP site respectively.

The BER pathway is conserved from bacteria to mammals. In mammals the balance between the use of long-patch and short-patch BER repair may be tissue specific, but it is generally believed that short-patch BER is the more commonly used (Karahalil, Hogue et al. 2002)**.**

1.5.4 Mismatch repair

Errors can occur during normal DNA metabolism and DNA processing reactions, including DNA replication, recombination and repair. Cells have evolved a DNA repair mechanism known as mismatch repair (MMR) to remove such mismatches and thus prevent mutations becoming permanent. Because MMR reduces the number of replication-associated errors, mutations associated with the inactivation of human MMR proteins have been associated with hereditary and sporadic cancers such as HNPCC (Fishel, Lescoe et al. 1993; Leach, Tokino et al. 1993; Papadopoulos, Nicolaides et al. 1994).

The MMR pathway has been extensively studied in *E. coli* and is initiated by the MutS, MutL and MutH proteins. A homodimer of the 'mismatch recognition' protein, MutS, recognises base-base mismatches and small nucleotide insertion/deletion loops (Modrich and Lahue 1996). After MutS binding, MutL interacts with MutS to enhance mismatch recognition and recruit MutH. MutL functions as a homodimer and possesses ATPase activity. MutL binding facilitates the assembly of a functional MMR complex, by stimulating the loading and processivity of helicase II at the MMR initiation site (Dao and Modrich 1998). MutL is able to interact with the clamp loader subunits of pol III, suggesting that MMR is coupled with DNA replication. Upon its recruitment and activation

by MutS and MutL in the presence of ATP, MutH specifically cleaves the daughter strand at a hemimethylated dGATC 5' or 3' to the located mismatch (Modrich and Lahue 1996; Junop, Obmolova et al. 2001). This strand-specific nick provides the initiation site for mismatch excision. The precise method in which the mismatched base is cleaved remains unclear. However, it is believed that in the presence of MutL, helicaseII loads at the nick and unwinds the duplex DNA from the nick towards the site of mismatch, generating single stranded DNA, which is rapidly bound by the single-stranded binding (SSB) protein and, thus, protected from nuclease attack (Ramilo, Gu et al. 2002). Depending on the position of the nick, relative to the mismatch, ExoI or ExoX (3'-5' exonuclease), or ExoVII or RecJ (5' -3' exonuclease) excise the nicked strand, from the initial dGATC, up to and slightly beyond the mismatch. The resulting single-stranded gap is repaired by the action of DNA pol III, SSB and DNA ligase (Modrich and Lahue 1996).

The mismatch repair pathway is conserved in eukaryotes. However, differences are present. For example, whilst *E.coli* MutS and MutL are homodimers, they function as hetrerodimers in eukaryotes. To date, no homologues of MutH have been identified in eukaryotes. In *H. sapiens*, the MutS related heterodimers; MSH2-MSH6 (MutSα) and MSH2-MSH3 (MutSβ) recognise the mismatch site. *S. pombe* does not require the MSH2-MSH3 heterodimer for MMR. Although most eukaryotes utilise the MutL-related heterodimer, MLH1-PMS1, multiple MutL-related proteins have been identified (Marti, Kunz et al. 2002).

1.5.5 Post replicative repair

Most types of DNA damage cannot be accommodated by the active site of the replicative DNA polymerases. Under normal circumstances the DNA lesion is removed by DNA repair pathways, such as BER and NER, before the replicative machinery encounters it. However, if the damage fails to be removed before the polymerase encounters it, the replication fork will stall. The post replicative repair (PRR pathway) allows the replication fork to bypass the site of damage, preventing prolonged stalling of DNA replication.

PCNA is an essential replication factor and an important factor for S-phase DNA repair. PCNA is regulated by both ubiquitin and SUMO modification (Section 1.7 and section 1.8). In *S. cerevisiae*, stalled DNA replication forks induce monoubiquitination of PCNA Lys164, catalysed by the Rad6 ubiquitin conjugating enzyme and the Rad18 RING finger E3 ligase (Bailly, Lamb et al. 1994; Ulrich and Jentsch 2000; Hoege, Pfander et al. 2002). PCNA monoubiquitination of Lys164 signals for the replacement of the replicative polymerase by translesion synthesis (TLS) family polymerases that are capable of bypassing DNA lesions in an 'error-prone' manner (TLS). Alternatively, in the presence of the Rad18/Rad6 complex, MMS2-Ubc13 ubiquitin conjugating enzyme and the Rad5 RING finger E3 ligase can catalyse the formation of K63-linked polyubiquitin chains onto the monoubiquitin on PCNA K164 (Bailly, Lamb et al. 1994; Ulrich and Jentsch 2000; Hoege, Pfander et al. 2002). Polyubiquitination of PCNA directs a second 'error-free' PRR pathway (also referred to as the error-free damage avoidance pathway), which uses the newly synthesised sister chromatid as a template to bypass the DNA lesion through a template switching mechanism. PCNA, therefore, acts to initiate and choose between an error-prone pathway, translesion synthesis, and an error-free DNA damage tolerance pathway (Hoege, Pfander et al. 2002; Stelter and Ulrich 2003).

Mammalian homologues of the PRR proteins have been identified suggesting that PRR is well conserved through evolution.

1.5.6 Double-strand break repair

Double-stranded breaks (DSBs) are amongst the most deleterious damage that cellular DNA repair systems must contend with. In fact, a single unrepaired DSB can result in cell death. Double stranded breaks can be induced by both exogenous sources, such as IR, and endogenous processes of DNA metabolism. If in a dividing cell the damage is left unrepaired, the chromosomal region unconnected to the centromere is unable to segregate to the daughter cell. This can lead to chromosomal deletions and potentially to cell death. If incorrectly repaired, DSBs can lead to other aberrations such as translocations (Pierce, Stark et al. 2001). In *H. sapiens* defects in the DSB repair pathway can result in disorders

such as Nijmegen Breakage Syndrome and Ataxia telangiectasia (Shiloh 1997; Carney, Maser et al. 1998).

In eukaryotes, DSBs can be repaired either by non-homologous end-joining (NHEJ) or by homology-dependent repair mechanisms such as homologous recombination (HR), and the HR-associated, single-strand annealing (SSA) and synthesis-dependent strand-annealing (SDSA) pathways. NHEJ joins two DNA ends irrespective of their sequence, consequentially generating errors if the two ends are unrelated. HR on the other hand is an error free DSB repair mechanism that uses homologous DNA sequences, often from sister chromatids, as templates for repairing broken ends. Although it is not clear which factors determine the choice between HR and NHEJ for DSB repair, it is believed that the stage of the cell cycle must play an important role. This is because the homologous template, which is necessary for HR, is only present during the S and G2 phases of the cell cycle. This suggests that NHEJ is the predominant repair pathway in G1 and M phases.

1.5.6.1 Homologous recombination

Whilst the primary role of HR in mitotic cells is the repair of double stranded breaks, HR is also essential for a number of other processes required for the maintenance of genomic stability such as telomere maintenance. In meiotic cells, HR is required to ensure the correct disjunction at the first meiotic division by establishing a physical connection between homologous chromosomes. In addition, HR is necessary for meiotic crossover events required to generate genetic diversity. The current model for HR-dependent double-strand break repair can be described in 6 stages; 1) DSB detection, 2) 5'-3'-resection, 3) strand-invasion/ D-loop formation, 4) branch migration, 5) gap filling and ligation/ double Holiday Junction formation 6) Holliday junction resolution (Figure 1.3).

When a DSB is detected, the DNA damage checkpoint is activated resulting in the phosphorylation of histone H2AX and the recruitment of proteins required for the repair of the DSB. The MRN complex is required for the initiation of DSB repair events, including both HR and NHEJ. Mre11 displays both 3'-5' exonuclease and endonuclease activity and is important for the processing of DSB ends. Rad50 shows structural similarity to the SMC

Figure 1.3 Homology-mediated double strand break repair in *S. pombe*

Overview of the homology-mediated double strand break repair mechanisms in *S. pombe*. HR: homologous recombination, SDSA: synthesis dependent strand annealing, SSA: single strand annealing. Figure adapted from (Raji and Hartsuiker 2006).

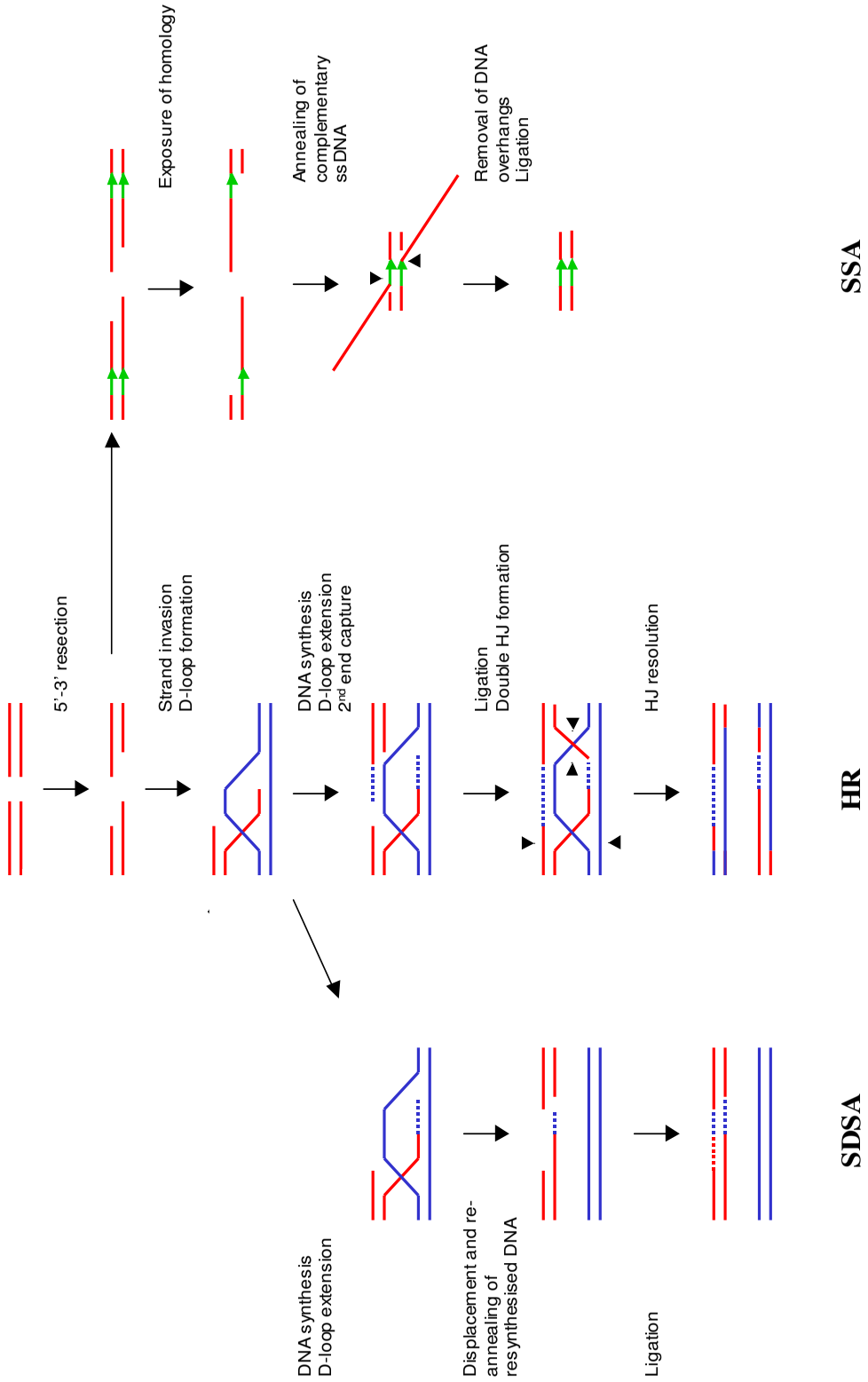

Figure 1.3: Homology mediated double strand break repair in *S. pombe*

(structural maintenance of chromosomes) proteins (Section 1.6), and is thought to form a globular ATPase domain. Nbs1 is a substrate of ATM (Tel1 in *S. pombe*) and is able to recruit the MRN complex to the site of a DSB through interaction of its FHA and BRCT domains with γ-H2AX. Despite having 3'-5' nuclease activity, the MRN complex has been implicated in the processing of the DSB ends by 5' to 3' resection. The resulting 3' single-stranded overhangs are able to invade a homologous DNA strand (Furuse, Nagase et al. 1998; Moreau, Ferguson et al. 1999). Following resection, the 3' single-stranded DNA overhangs are subsequently coated with the single-stranded binding protein RPA, which is thought to help remove secondary structures before Rad51 (Rhp51 in *S. pombe*) is loaded onto the DNA. Since RPA has a higher affinity for ssDNA than Rad51 does, recombination mediator proteins are required to overcome RPA inhibition and assist Rad51 binding. One such mediator protein is Rad52 (Rad22 in *S. pombe*), which interacts with Rad51. Loading of the Rad52-Rad51 complex onto single-stranded DNA facilitates the formation of Rad51 nucleoprotein filaments (Essers, Houtsmuller et al. 2002; Jackson, Dhar et al. 2002). Once assembled, the Rad51 nuceloprotein filament is capable of interacting with the homologous template DNA, thus initiating strand exchange. When the damaged DNA strand invades the undamaged DNA duplex a structure known as the D-loop forms. Using the undamaged homologous strand as a template, DNA Polymerase I extends the damaged strand and the ends are ligated by DNA ligase I. A double Holliday junction (HJ) is formed when a single crossover covalently joins two recombining duplexes. Following HR, structure specific endonucleases, such as Mus81, resolve the HJs into two duplexes (Haber 1999).

According to this HR model, equal crossover and non-crossover events are generated due to the alternate Holliday junction resolution. However, recent studies suggest that crossover and non-crossover events are generated from different recombination intermediates (Allers and Lichten 2001). To explain the low level of associated crossover events in mitotic cells, the synthesis-dependent strand-annealing **(**SDSA) model has been proposed (Section 1.5.6.3).

1.5.6.2 Synthesis-dependent strand-annealing

According to the HR model above, resolution of the HJ results in gene conversion, thus, yielding both crossover and non-crossover products. The synthesis-dependent strand-annealing (SDSA) model was proposed to explain the low number of associated crossovers seen in non-meiotic cells (Ferguson and Holloman 1996). Like HR, SDSA is initiated by strand invasion, but after branch migration, the newly synthesised DNA strand is displaced from the template and returned to the broken DNA molecule. This event results in homologous repair without associated crossovers (Figure 1.3).

1.5.6.3 Single-strand annealing

The Rad51-dependent recombination pathway discussed in section 1.5.6.1 is the most efficient pathway to repair DSBs. However, an alternative Rad51-independent recombination pathway does exist. The single-strand annealing (SSA) pathway can repair DSBs found between two nearly homologous repeats. Like HR, SSA is initiated by DSB detection, followed by 5'-3'-resection. However, 5'-3'-resection is followed by further resection of the DSB ends by an endonuclease until two small regions of homology are revealed on either side of the break. The homologous sequences anneal in a Rad52-dependent manner, leaving long single-stranded non-homologous DNA ends. The endonuclease activity of Rad1-Rad10 is required to trim off the 3' non-homologous ssDNA tails that can form after annealing (Baumann and West 1998; Norbury and Hickson 2001). Like HR, duplex DNA is restored through the action of DNA Pol I and DNA ligase I. Unlike HR, SSA is error prone and results in the deletion of the sequence between the homologous sequences flanking the DSB (Figure 1.3).

1.5.6.4 Non-homologous end-joining

Unlike HR, NHEJ requires little or no sequence homology and joins two DNA ends irrespective of their sequence. NHEJ is, therefore, potentially a less accurate form of DSB repair. NHEJ consists of three stages; 1) the capture of capture of both ends of the broken DNA molecule, 2) the formation of a molecular bridge to bring the two DNA ends back together and 3) the re-ligation of the broken DNA molecule. The NHEJ pathway has been well characterised in *H. sapiens* and is Rad52-independent. Instead, NHEJ requires the

action of XRCC1, Ku70, Ku80, DNA ligase IV and DNA-PKcs (DNA protein kinase catalytic subunit). The NHEJ process is initiated by the binding of the Ku70/Ku80 heterodimer to both ends of the broken DNA molecule. Binding of the Ku70/80 heterodimer protects the ends of the DSB from further processing and creates a scaffold for the recruitment of other NHEJ proteins. In an early stage of NHEJ, the DNA-dependent protein kinase catalytic subunit (DNA-PK_{cs}) is recruited to the site of the DSB (Gottlieb and Jackson 1993; Singleton, Torres-Arzayus et al. 1999). This kinase facilitates the formation of a synaptic complex, which brings the DNA ends together. Finally, the ligase IV/XRCC4 complex catalyses the ligation of the two DNA ends, regardless of homology (Ramsden and Gellert 1998; Nick McElhinny, Snowden et al. 2000).

1.6 The Smc5/6 complex and its role in DNA repair

1.6.1 Introduction to SMC proteins

The structural maintenance of chromosomes (SMC) protein family is well conserved across eubacteria, archaea, and eukaryotes. SMC proteins form a superfamily of proteins sharing a common structure. Globular N- and C-terminal domains, containing Walker A and B motifs respectively, are separated by two long coiled-coils joined by a flexible 'hinge' (Haering, Lowe et al. 2002; Hirano and Hirano 2002; Sergeant, Taylor et al. 2005). The hinge allows the molecule to fold back on itself, allowing the two coiled-coils to interact in an anti-parallel manner bringing the N- and C-terminal domains into close proximity of one another thus generating an ATPase active site (Melby, Ciampaglio et al. 1998).

In eukaryotes six SMC proteins comprise three SMC complexes; Smc1/Smc3 (cohesin), Smc2/Smc4 (condensin) and the Smc5/Smc6 complex (Michaelis, Ciosk et al. 1997; Hirano 1999; Fousteri and Lehmann 2000). The SMC heterodimers are formed by intermolecular interactions of the hinge domains of the two SMC proteins. Unlike eukaryotes, only one *smc* gene exists in prokaryotes where the SMC protein forms a homodimer rather than a heterodimer (Hirano and Hirano 1998). SMC proteins are conserved in all eukaryotes and are essential for viability. The Smc1 and Smc3 proteins form the core of cohesin, a complex required to hold the sister chromatids together, and Smc2 and Smc4 form the core of condensin, which as the name suggests has an important

role in condensing the chromosomes during mitosis (For reviews see (Nasmyth and Haering 2005; Hirano 2006)). The Smc5 and Smc6 proteins form the core of the Smc5/Smc6 complex, whose role has been implicated in the repair of DNA damage (Michaelis, Ciosk et al. 1997; Fousteri and Lehmann 2000; Sergeant, Taylor et al. 2005). Although, each of the three complexes is required for a different aspect of chromosome segregation and repair, interplay between DSB repair and segregation seems to be well conserved since many prokaryotes also contain SMC-like proteins involved in both processes (Cobbe and Heck 2004).

1.6.2 The Smc5/6 complex

1.6.2.1 Architecture of the Smc5/6 complex

The Smc5/6 complex was initially defined in *S. pombe* by a hypomorphic allele of *smc6*, formally known as *rad18* (Lehmann, Walicka et al. 1995). The Smc5/6 complex is composed of eight subunits including the structural maintenance of chromosomes proteins Smc5 and Smc6 and six non-SMC proteins Nse1-6 (McDonald, Pavlova et al. 2003; Sergeant, Taylor et al. 2005; Pebernard, Wohlschlegel et al. 2006). Like Smc5 and Smc6, Nse1-4 are essential for viability in *S. pombe*, whereas Nse5 and Nse6 are not essential but are required for the DNA repair function of the Smc5/6 complex. An additional, loosely associated subunit, Rad60, is required for both DNA repair and the essential function of the complex (Morishita, Tsutsui et al. 2002; Boddy, Shanahan et al. 2003). Rad60 is discussed in further detail in section 1.9.

Prior to the identification of the Nse5 and Nse6 subunits, *in vitro* studies indicated that the Smc5/6 complex consists of two sub-complexes (Sergeant, Taylor et al. 2005). In the first sub-complex, Smc5 and Smc6 interact via their hinge domains to form the core of the complex. Nse2 was also found bound to the coiled-coil region of the Smc5 protein. The second sub-complex consists of Nse1, Nse3 and Nse4, which bind to one another. The two complexes were thought to be bridged by a weak interaction between Nse2 and Nse3 (Sergeant, Taylor et al. 2005).

More recently, the Nse1-Nse3-Nse4 sub-complex has been shown to bind directly to Smc5, independently of Nse2 (Pebernard, Wohlschlegel et al. 2006). Two additional Nse proteins, designated Nse5 and Nse6, were identified by their ability to interact with the Smc5 and Nse4 proteins (Pebernard, Wohlschlegel et al. 2006). This is consistent with there being six Nse proteins in the *S. cerevisiae* Smc5/6 complex (Hazbun, Malmstrom et al. 2003). The *S. pombe* Nse5 and Nse6 proteins form a heterodimer that binds directly to Smc5/6, independently of Nse1-4, although the site of interaction is not known (Pebernard, Wohlschlegel et al. 2006). The binding of Nse5 and Nse6 to both Smc5 and Smc6 was confirmed in a separate study (Palecek, Vidot et al. 2006). In this study, Nse4 was shown to bind both SMC proteins. Structural predictions suggest Nse4 is related to the cohesin kleisin, Scc1, with a helix turn helix motif at its N-terminus and a winged helix domain at its C-terminus (Palecek, Vidot et al. 2006). Kleisins are found in both cohesin and condensin, and act to bridge the head domains of the SMC proteins, allowing them to form closed ring-like structures. Scc1 has a separase cleavage site that allows opening of the cohesin complex so that sister chromatids can separate (Uhlmann, Wernic et al. 2000). No such cleavage sites have been identified in Nse4 (Palecek, Vidot et al. 2006). This suggests that, if the Smc5/6 complex does open and close, a different mechanism is likely to be in place. The current model (Palecek, Vidot et al. 2006) for the architecture of the Smc5/6 complex can be seen in Figure 1.4.

1.6.2.2 Nse components of the Smc5/6 complex

Studies of the Smc5/6 complex have revealed six non-SMC proteins associated with the complex. Characterisation of these Nse proteins has revealed motifs that may provide a functional role for their association with the Smc5/6 complex.

The Nse1 protein contains a RING finger domain suggesting that it functions as an E3 ubiquitin ligase (Fujioka, Kimata et al. 2002). Although no functional evidence for this activity exists, an *S. cerevisiae nse1* allele (*nse1-C274A*) carrying a mutation in the conserved RING-finger motif shows a higher degree of UV sensitivity than is observed in other non-ubiquitin ligase domain mutants of *nse1* (Santa Maria, Gangavarapu et al. 2007). The UV sensitivity of the PRR mutants *rad18-d* and *rad5-d* is enhanced when they are

Figure 1.4: Architecture of the Smc5/6 complex

The Smc5/6 complex is composed of eight subunits, including the Smc5 and Smc6 proteins and six non-SMC proteins, Nse1-6. The N- and C-terminal globular domains of each SMC subunit self-associate to generate an ATPase. Smc5 and Smc6 interact via their hinge domains to form the core of the complex. Nse2 functions as an SUMO ligase and associates with the coiled-coil region of Smc5. Nse1, Nse3 and Nse4 form a sub-complex that binds to Smc5 independently of Nse2. Nse4 resembles a kleisin and may form a bridge by interacting with both SMC proteins. Nse5 and Nse6 form a heterodimer, independent of the other Nse proteins. Nse5 and Nse6 associate with the head domains of both Smc5 and Smc6, potentially forming a second bridge. An additional loosely associated subunit, Rad60, is required for both the DNA repair and essential function of the Smc5/6 complex

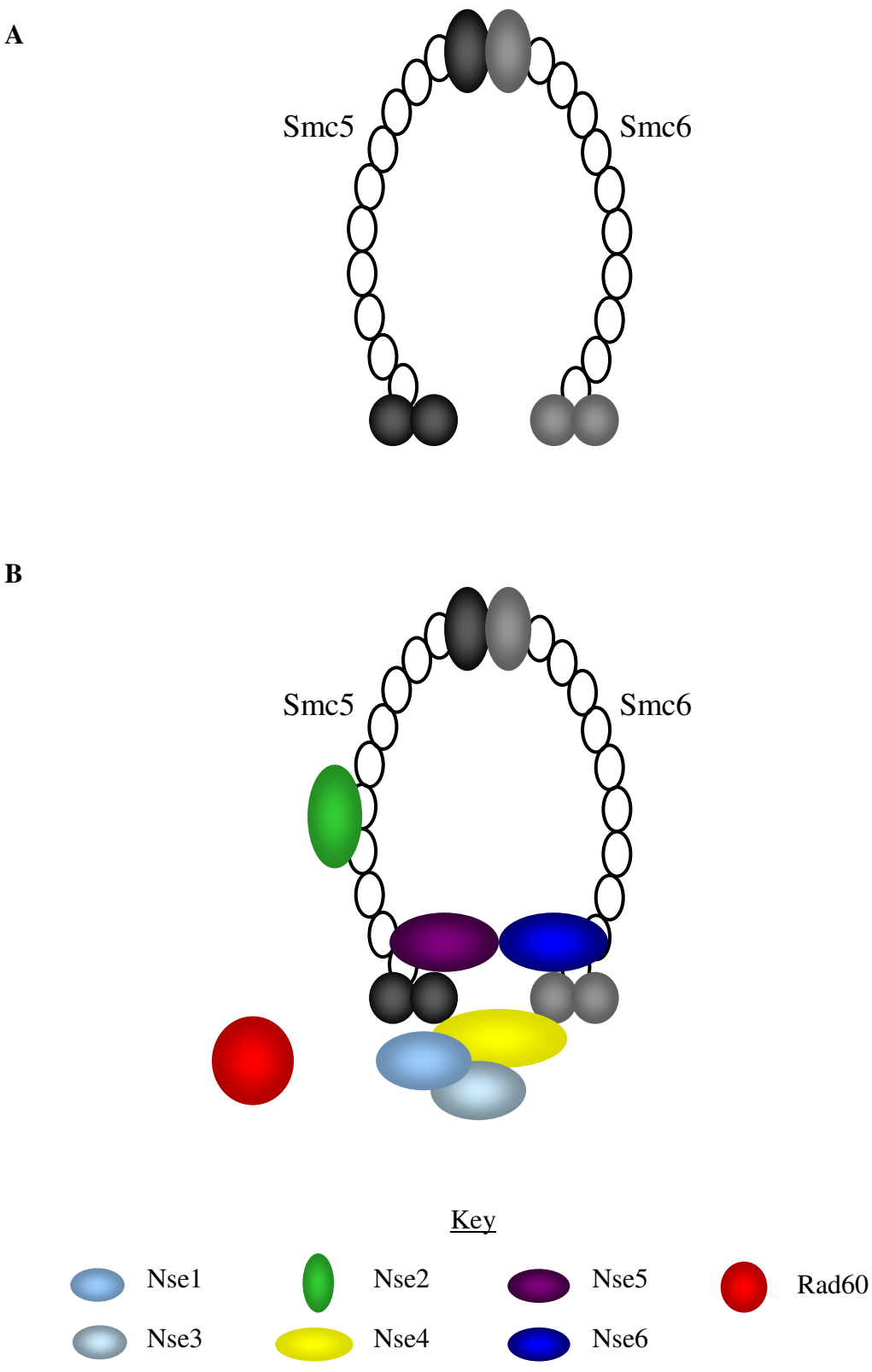

Figure 1.4: Architecture of the Smc5/6 complex

combined with the *nse1-C274A* mutation. In contrast, the UV sensitivity of the *rad52-d* mutant is not altered in combination with *nse1-C274A* (Santa Maria, Gangavarapu et al. 2007). This suggests that, in *S. cerevisiae* at least, the putative ubiquitin ligase, Nse1, contributes to the Rad52 dependent-PRR pathway.

S. pombe Nse2 and its homologues in *S. cerevisiae* and *H. sapiens* (Mms21 and Nse2) contain a PIAS RING-finger like domain attributing to the E3 SUMO ligase function (Andrews, Palecek et al. 2005; Potts and Yu 2005; Zhao and Blobel 2005). Several proteins have been identified as targets of Nse2-dependent sumoylation, including Smc6, Nse3 and Nse2 itself (Andrews, Palecek et al. 2005). It is possible that the weak interaction identified between Nse2 and Nse3 may be a consequence of the Nse2-dependent sumoylation of Nse3 (Andrews, Palecek et al. 2005; Sergeant, Taylor et al. 2005). *nse2-SA* cells which express a ligase-dead variant of Nse2 are partially defective in DSB-repair after IR (Andrews, Palecek et al. 2005). In human cells, Nse2 is not required for the stability of the Smc5-6 complex (Taylor, 2008). Furthermore, in *S. pombe* the Nse2-SA protein is still associated with the Smc5/6 complex, suggesting that Nse2-dependent sumoylation is not required to maintain an intact complex (Andrews, Thesis).

Nse3 contains a MAGE (Melanoma Antigen-Encoding Gene) homology domain (Pebernard, McDonald et al. 2004; Sergeant, Taylor et al. 2005) MAGE domains are found in a large number of mammalian proteins that are highly expressed in tumours. Nse3 is the first example of a MAGE family protein in yeast, although the function of the MAGE domain is currently unknown. Like Smc6, Nse3 has been implicated in the UVER pathway (Lehmann, Walicka et al. 1995; Morikawa, Morishita et al. 2004).

Nse4, previously referred to as Rad62, has no domains predictive of a particular function. Recently, structural predictions suggest that Nse4 may be related to Scc1, with a helix-turn-helix motif at its N-terminus and a winged helix domain at its C-terminus (Palecek, Vidot et al. 2006). This may suggest that like Scc1 of cohesin, Nse4 acts as a kleisin molecule for the Smc5/6 complex. No experimental evidence for this exists at present.

Nse5 and Nse6 are the most recently identified subunits of the Smc5/6 complex. Like the Nse1-4 subunits Nse5 and Nse6 are essential for viability in *S cerevisiae*. In *S. pombe*, however, Nse5 and Nse6 are not essential. Mutants of these proteins display many of the phenotypes observed for hypomorphic mutants of Smc5/6, suggesting that the Nse5/6 heterodimer specifically facilitates some of the DNA repair functions of the Smc5/6 complex (Pebernard, McDonald et al. 2004). Nse6 is a member of the ARM/HEAT repeat family. ARM/HEAT repeats provide protein-protein interfaces and are found in factors associated with both cohesin and condensin. Like Rad60, Nse5/6 mutants are dependent on Mus81 and Rqh1 for viability (Pebernard, McDonald et al. 2004). This would suggest that, since Mus81 and Rqh1 have been implicated in the processing of Holliday junctions that can form as a result of HR, Holliday junctions accumulate in Nse5/6 mutant cells (Pebernard, McDonald et al. 2004).

1.6.2.3 Functional roles of the Smc5/6 complex

Unlike the other SMC complexes, the Smc5/6 complex has a poorly defined role in DNA repair. The Smc5/6 complex was first identified in *S. pombe* when *smc6* was shown to complement a DNA-damage sensitive mutant (Lehmann, Walicka et al. 1995). Epistasis analysis of *smc6* mutants with an *rhp51-d* strain implicated the Smc5/6 complex in the HR pathway (Lehmann, Walicka et al. 1995). *nse1*, *nse2, nse4* and *nse6* are also epistatic with *rhp51-d* in response to IR (McDonald, Pavlova et al. 2003; Morikawa, Morishita et al. 2004; Pebernard, Wohlschlegel et al. 2006). Following IR-induced DNA damage in G2, hypomorphic *smc5*, *smc6* and *nse* mutants are unable to repair damaged chromosomes (Verkade, Bugg et al. 1999; Morikawa, Morishita et al. 2004; Lindroos, Vinnere et al. 2006). Smc6-X mutant cells are proficient in Cds1-dependent mitotic arrest in response to HU. However, after release from HU they undergo aberrant mitosis (Miyabe, Morishita et al. 2006). These aberrant mitoses can be suppressed by deletion of *rhp51* or *rhp55* (Ampatzidou, Irmisch et al. 2006; Miyabe, Morishita et al. 2006). This is consistent with the requirement of Smc6 during a late stage in recombination at a subset of stalled replication forks that collapse. A similar phenomenon has been observed for *rad60* mutants, suggesting Rad60 functions with the Smc5/6 complex at a late stage of repair (Miyabe, Morishita et al. 2006). Rad60 is discussed in further detail in section 1.8.1.

Ambiguously, both *S. cerevisiae* and *S. pombe* can accommodate the complete loss of HR but loss of Smc5/6 function is lethal. Furthermore, the lethality caused by Smc6 loss cannot be reversed by the additional loss of HR function (Torres-Rosell, Machin et al. 2005; Cost and Cozzarelli 2006). This suggests an additional, HR-independent, role of the Smc5/6 complex.

Two mutant alleles of *smc6* have been extensively characterised in *S. pombe,* namely *smc6-X* and *smc6-74* (Lehmann, Walicka et al. 1995; Verkade, Bugg et al. 1999). *smc6-X* cells have a R706C mutation in the second coiled-coil region close to the hinge and are sensitive to DNA damaging agents including UV, IR and MMS. UV-induced damage is removed less efficiently in *smc6-X* than in wild type cells (Lehmann *et al,* 1995). However, *smc6* mutants are not epistatic to mutants in the conserved NER pathway (Section 1.4.3). Instead, Smc6 is thought to be involved in UVER (Section 1.4.4), a secondary UV damage removal pathway that involves the *rad2* and *rhp51* genes (Lehmann, Walicka et al. 1995; Murray, Lindsay et al. 1997). Deletion of *rhp51* rescues the sensitivity of *nse6-d*, *nse2-1*and *nse4-1* cells to UV at low doses, suggesting that in the mutant cells, UV damage is converted into a toxic structure by the HR protein Rad51 (Morikawa, Morishita et al. 2004; Pebernard, Wohlschlegel et al. 2006).

smc6-74 cells have an A151T mutation that maps to the highly conserved arginine finger in the N-terminal globular domain, and have a phenotype similar to that observed for *smc6-X* (Verkade, Bugg et al. 1999). Unlike *smc6-X,* which remains cell cycle arrested after induction of DNA damage, *smc6-74* cells show a DNA damage checkpoint of wild-type duration. However, *smc6-74* cells re-enter the cell cycle following aberrant mitoses, suggesting that *smc6-74* cells are proficient in initiating the checkpoint but deficient in maintaining checkpoint arrest (Verkade, Bugg et al. 1999). In *S. pombe* Brc1 has been identified as an allele-specific multi-copy suppresser of the *smc6-74* allele (Verkade, Bugg et al. 1999). Brc1 is a protein consisting of six BRCT repeats and is required for mitotic fidelity. Brc1-dependent *smc6-74* suppression is dependent on the activity of structure-specific nucleases (Slx1/4 and Mus81/Eme1) and HR function. *brc1-d* is synthetic lethal with both *smc6-X* and *smc6-74* (Verkade, Bugg et al. 1999). Taken together, these

observations suggest that Brc1 acts downstream of Smc6 in a function that is defective in *smc6-74* but not *smc6-X*.

It would appear that the HR defect of Smc5/6 mutants is a genome-wide phenomenon. Several studies have focused on the consequence of Smc5/6 defects for ribosomal DNA (rDNA) replication and stability. Chromatin IP (ChIP) studies show that Smc5/6 is enriched on the *S. cerevisiae* rDNA, although this is not evident at the rDNA in *S. pombe* (Torres-Rosell, Machin et al. 2005; Ampatzidou, Irmisch et al. 2006). However, in both *S. pombe* and *S. cerevisiae* a significant proportion of Smc6 localises to the nucleolus, which is home to ~200 rDNA repeat units (Torres-Rosell, Machin et al. 2005; Ampatzidou, Irmisch et al. 2006). Smc5/6 complex has implied functions not only in response to DNA damage and collapsed replication forks during mitosis`, but also during meiosis (Taylor, Moghraby et al. ; Pebernard, McDonald et al. 2004).

The Smc5/6 complex is architecturally similar to cohesin. Until recently, studies of cohesin have focused on its function in unchallenged cells, whereas Smc5/6 function has been investigated from a DNA repair perspective. Recently, the defect in recombination of Smc5/6 mutants has been attributed to a defect in the ability of Smc5/6 mutants to recruit cohesin to sites of DSBs (Potts, Porteus et al. 2006). In mammalian cells, decreased levels of Nse2 or Smc5 disrupt the localisation of cohesin subunits to a site-specific DSB in human cells (Potts, Porteus et al. 2006). This indicates that at least one aspect of the Smc5/6 complex's repair function is to indirectly confer sister chromatid cohesion at the site of damage i.e. to promote damage-induced cohesion. Since the absence of functional Smc5/6 complex delays sister chromatid separation, it is unlikely that the Smc5/6 complex confers sister chromatid cohesion in undamaged cells.

1.7 Ubiquitin

Reversible post-translational modifications are widely used to allow cells to enable them to respond to rapid changes in both their internal and external environments. Post-translation modification of proteins is one such way of regulating protein function. The first example of a protein acting as a post-translational modifier was ubiquitin, which is best known for

its catabolic role in protein degradation via the 26S proteasome (Hershko and Ciechanover 1998). The ubiquitin-proteasome pathway is highly conserved from yeast to mammals.

1.7.1 The ubiquitin pathway

Ubiquitin is synthesised as a precursor molecule that must be processed by de-ubiquitinating enzymes (DUBs) to reveal a diglycine motif at the C-terminus. It is this diglycine motif that acts as the site of attachment to target molecules. Protein ubiquitination is catalysed by the sequential action of E1, E2 and E3 enzymes that activate and transfer ubiquitin to the target protein (Figure 1.3). The activating enzyme (E1) adenylates the C-terminus of ubiquitin, which is then transferred to the E1 cysteinyl side chain via a thiolester linkage (Haas and Siepmann 1997). The ubiquitin moiety is then transferred to a cysteinyl group on the conjugating enzyme (E2). Finally, through the action of an E3 ligase ubiquitin is covalently attached to the ε-amino group of a lysine residue in the target protein. Since the isopeptide bond between ubiquitin and a target protein can be cleaved by deubiquitinating enzymes (DUBs) ubiquitination is a reversible process.

1.7.2 Role of ubiquitin modification

The best-defined role for ubiquitin-conjugation is the targeting of proteins for degradation via the 26S proteasome (Wilkinson 1995; Hochstrasser 1996). Since ubiquitin itself contains 7 lysine residues, the formation of ubiquitin chains is possible. Ubiquitin-mediated targeting of proteins to the proteasome generally requires the assembly of K48-linked ubiquitin chains on target proteins such poly-ubiquitination has been best characterised for K48-linked chains such as p53 (Dulic, Kaufmann et al. 1994).

Ubiquitination has also been shown to play an important role in altering protein function by mechanisms independent of the proteasome. Ubiquitination has been implicated in roles in regulating membrane protein trafficking, signal transduction, transcription, nuclear transport and DNA repair. For example, mammalian histones H2A and H2B are modified by a single ubiquitin moiety (Goldknopf and Busch 1977; Busch and Goldknopf 1981). In *S. cerevisiae* histone H2B mono-ubiquitination functions to regulate chromatin structure

Figure 1.5: The ubiquitin and SUMO modification pathways

The ubiquitin (A) and SUMO (B) conjugation pathways are analogous. Ubiquitin and SUMO are synthesized as precursor molecules (U*/S*) that are cleaved by proteases (P) to reveal a diglycine motif. The mature form of ubiquitin (U) and SUMO (S) are activated by an E1 activating enzyme. They are then transferred to an E2 conjugator enzyme and with the aid of an E3 ligase, conjugated onto the target protein. Proteases can remove the ubiquitin or SUMO from the target.

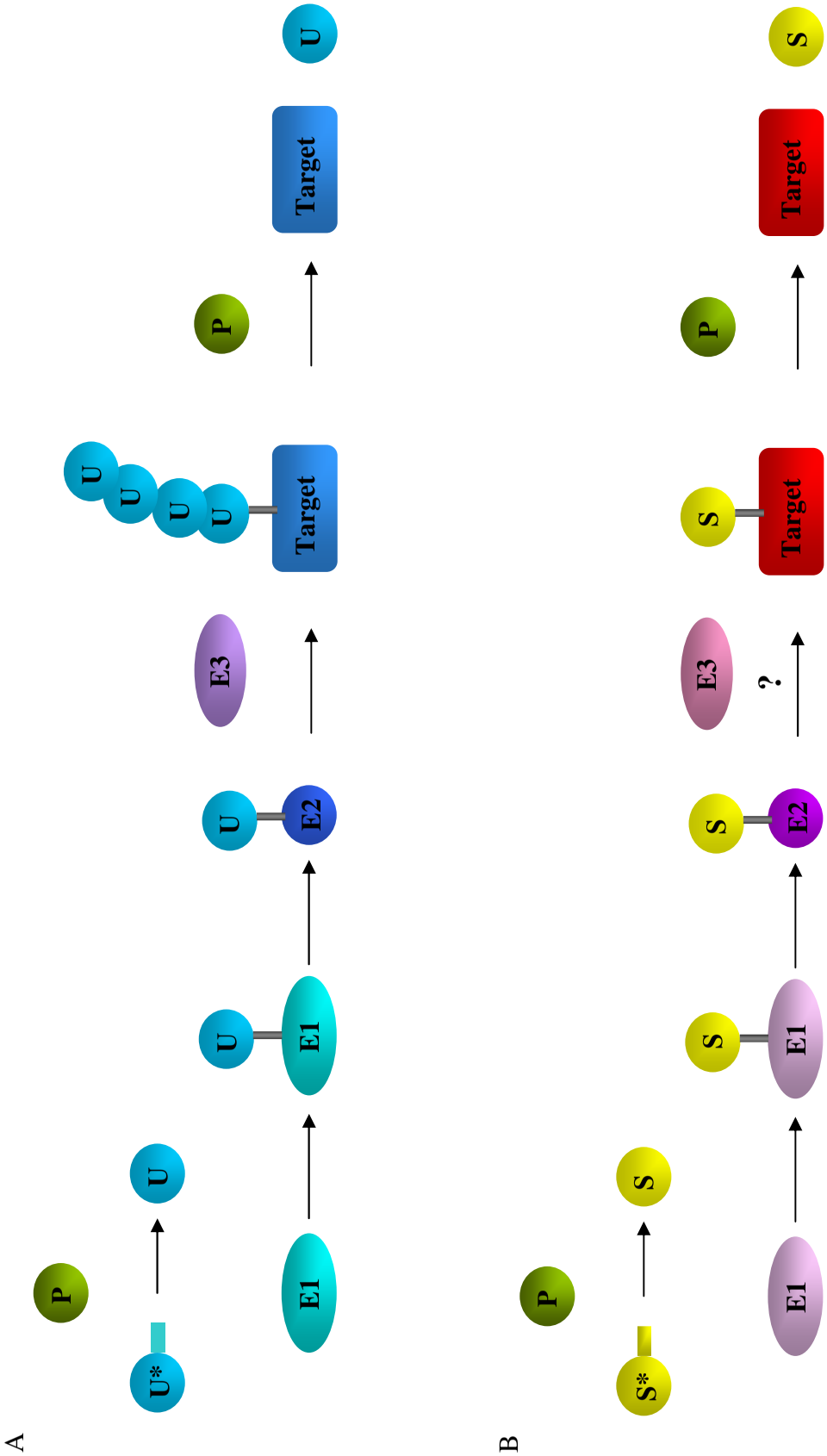

Figure 1.5: The ubiquitin and SUMO modification pathways

and transcription by recruiting a distinct group of methylases, thus, enabling lysine methylation of histone H3 (Briggs, Xiao et al. 2002; Sun and Allis 2002).

The existence of non K48-linked poly-ubiquitin chains, *in vivo*, suggests that simply discriminating between poly- and mono-ubiquitination events is not sufficient to determine the ubiquitin-mediated fate of a protein. Ubiquitin-K63 linkages, mediated by the ubiquitin conjugating heterodimer Mms2-Ubc13, have been observed for a number of cell signalling proteins. For example, in mammalian cells, activation of NFκB requires formation of formation of K63-linked ubiquitin chains on TRAF6 (Wang, Deng et al. 2001). Furthermore, in response to DNA damage, different forms of *S. pombe* PCNA ubiquitin modifications channel DNA lesions into different DNA repair pathways. Mediated by Rad18 and Rad6, mono-ubiquitination of PCNA K164 signals for translesion synthesis (Hoege, Pfander et al. 2002). When Ubc13–Mms2 and Rad5 are present, the K164 ubiquitin monomer is extended into a K63 linked ubiquitin polymer and initiates an error-free DNA damage tolerance pathway (Hoege, Pfander et al. 2002; Stelter and Ulrich 2003). PCNA regulation of PRR is discussed in more detail in section 1.5.5.

1.7.3 Ubiquitin-like domains

Analysis of protein databases suggests that ubiquitin is encoded not only by genes comprising ubiquitin coding sequences, but ubiquitin-like sequences can also be found fused to other open reading frames, e.g. in the case of the *S. cerevisiae* DNA repair proteins Rad23 and Dsk2.

Rad23 is a highly conserved protein involved in NER (Section 1.4.3). It functions in the NER pathway through its interaction with Rad4, the *S. cerevisiae* homologue of *H. sapiens* XPC, through its XPC-binding domain (Masutani, Araki et al. 1997; Sugasawa, Ng et al. 1997). At its N-terminus Rad23 contains an ubiquitin-like (UBL) domain that shares 23% sequence identity with ubiquitin. This domain has been shown to participate in the association of Rad23 with the proteasome (Lambertson, Chen et al. 2003). Like Rad23, Dsk2 has an N-terminal ubiquitin-like domain that is capable of interacting with the proteasome (Funakoshi, Sasaki et al. 2002; Rao and Sastry 2002).

As well as having ubiquitin-like domains (UBLs), Rad23 and Dsk2 also contain ubiquitin-associated (UBA) domains. The UBA domains interact with poly-ubiquitin chains on proteins destined for proteolysis and the UBLs facilitate the interaction between of the Rad23 or Dsk2 with the proteasome (Bertolaet, Clarke et al. 2001; Chen, Shinde et al. 2001; Rao and Sastry 2002). An adaptor model has therefore been proposed for Rad23, Dsk2 and their orthologues. The UBL-UBA proteins deliver polyubiquitinated proteins to the proteasome through binding of their UBA domain to poly-ubiquitinated species and interaction of the ubiquitin-like domain with subunits of the proteasome (Madura 2004).

1.7.4 Ubiquitin-like proteins

Ubiquitin is phylogenetically very well conserved between different organisms, differing only by a small number of conservative substitutions. Besides ubiquitin, 13 more divergent, ubiquitin-like proteins (UBLs) have been identified to date (Kirkin and Dikic 2007). All share the characteristic ββαββαβ fold (also known as the ubiquitin/β-grasp fold) and are conjugated, via their C-terminal diglycine motif, to internal lysine residues of target proteins. The conjugation pathways of the ubiquitin-like proteins are comparable to that of ubiquitin, requiring E1-E2 enzyme activity. (Yeh, Gong et al. 2000). Unlike ubiquitination, E3 ligase activity is not always necessary for conjugation by other UBLs.

The first ubiquitin-like protein to be identified, ISG15, consists of two ubiquitin-like domains. The first of these domains has lost the C-terminal sequence of mature ubiquitin preventing deubiquitinating enzymes from separating the two domains. ISG15 modification has been implicated in a diverse number of biological functions, although the precise role of modification is unknown. Targets include JAK and STAT proteins, suggesting that ISG15 modification has a role in JAK-STAT signal transduction in response to interferon (Malakhov, Kim et al. 2003). An increased level of ISG15 conjugates lead to neurological disorders, whereas decreased levels of ISG15 conjugation has been shown to result in improper monoblast differentiation and possibly to tumorigenic progression of lung tumours (Liu, Ilaria et al. 1999; McLaughlin, Helfrich et al. 2000; Ritchie, Malakhov et al. 2002)

Of the ubiquitin-like proteins, NEDD8 shares the most sequence identity with ubiquitin (~57%). The NEDD8-binding protein, NUB1, contains an N-terminal ubiquitin-like domain, allowing NEDD8 to interact with the proteasome (Kamitani, Kito et al. 2001). Thus, like ubiquitin, NEDD8 can target proteins for degradation. Known targets of NEDD8 include p53 and the cullins. Cullins are subunits of SCF (Skp1-cullin-F-box protein) or SCF-related ubiquitin ligases (Osaka, Kawasaki et al. 1998). NEDD8 modification of the cullin subunit of SCF complexes is necessary for the activity of the ubiquitin ligase (Gagne, Downes et al. 2002). Therefore, modification of ubiquitin E3s by NEDD8 is evidence for cross regulation between the ubiquitin-like proteins.

Two of the most divergent UBLs are APG8 and APG12, which share ~20% sequence identity to each other but no obvious sequence similarity to ubiquitin. Despite the lack of sequence similarity, APG12 folds with a characteristic ubiquitin fold (Paz, Elazar et al. 2000) and like the other UBLs, APG8 and APG12 require E1 and E2 enzymes for their conjugation (Huang and Klionsky 2002). Both APG8 and APG12 function in the starvation response known as autophagy (Mizushima, Noda et al. 1998).

Of all the UBLs, SUMO is the most widely studied. Sumoylation is discussed in more detail in section 1.8.

1.8 SUMO

NMR studies have shown that, like other UBLs, SUMO is structurally similar to ubiquitin (Bayer, Arndt et al. 1998). *H. sapiens* SUMO-1 shares ~18% sequence identity with ubiquitin and contains the characteristic ββαββαβ ubiquitin-fold. SUMO differs from ubiquitin in its surface-charge topology. SUMO has a large negatively charged surface formed by E83, E84, E85 and D86 giving it a much more acidic surface than ubiquitin (Bayer, Arndt et al. 1998). In addition SUMO has a flexible N-terminal extension protruding from the hydrophobic core, which is not found in ubiquitin (Bayer, Arndt et al. 1998). The N-terminal tail is not required for sumoylating activity and can be deleted with only modest effects on SUMO conjugation, indicating the ubiquitin-like domain alone is sufficient for conjugation to most substrates (Bylebyl, Belichenko et al. 2003). These

differences are likely to account for the distinction between SUMO and ubiquitin function and the enzymes that mediate them.

In lower eukaryotes and yeast SUMO is encoded by a single gene, while in higher eukaryotes, such as *H. sapiens*, four isoforms of the protein exist. SUMO-1, SUMO-2 and SUMO–3 may modify both common and different substrates. For example, RanGAP1 is predominantly modified by SUMO-1, whereas Topoisomerase II is predominantly modified by SUMO-2/SUMO-3, which share ~95% sequence identity with each other (Saitoh and Hinchey 2000; Azuma, Arnaoutov et al. 2003; Vertegaal, Ogg et al. 2004; Zhao, Kwon et al. 2004). Cells contain virtually no free SUMO-1, suggesting that the majority of SUMO-1 is conjugated to target proteins. In contrast, cells contain a large pool of SUMO-2 and SUMO-3 (Matunis, Coutavas et al. 1996; Saitoh and Hinchey 2000). Conjugation of SUMO-2 and SUMO–3 is strongly induced in response to stress conditions, suggesting that these isoforms may serve to provide a free pool of SUMO for such stress responses (Saitoh and Hinchey 2000). Unlike SUMO-1, SUMO-2 and SUMO–3 contain a ψKXE SUMO-consensus motif (Section 1.8.5) in their N-terminal extensions, providing a possible site for SUMO-chain formation (Tatham, Jaffray et al. 2001). While poly-SUMO chains are formed predominantly from SUMO-2 and SUMO-3 monomers, the SUMO chains can be terminated by SUMO-1 (Matic, van Hagen et al. 2008). The fourth isoform, SUMO-4, has a restricted level of expression with its highest levels being identified in kidney cells (Bohren, Nadkarni et al. 2004). Unlike the gene encoding the *S.cerevisiae* SUMO-1 homologue, which is essential for viability, the gene encoding the *S. pombe* SUMO-1 homologue (Pmt3) can be deleted. However, cells deleted for this gene are extremely sick exhibiting slow growth and severe defects in genome maintenance (Johnson and Blobel 1997; Tanaka, Nishide et al. 1999).

The SUMO conjugation pathway is analogous to that of ubiquitin (Figure 1.5). However, the enzymes of the SUMO pathway are unique to SUMO and play no role in the conjugation of ubiquitin or any other UBLs. Proteins of the SUMO conjugation pathway are discussed in more detail in sections 1.8.1-1.8.4. Unlike ubiquitination, sumoylation does not target proteins for degradation via the proteasome. However, the precise function

of SUMO conjugation remains unclear and appears much more diverse than that of ubiquitin. SUMO has been implicated with roles in cellular localisation, transcriptional regulation, control of protein stability, and DNA repair to name a few. The role of SUMO modification is discussed in more detail in section 1.8.6.

1.8.1 SUMO proteases

SUMO conjugation is a dynamic process, changing throughout the cell cycle in response to different stimuli (Li and Hochstrasser 1999). Similar to other UBLs, precursor SUMO must first be processed by SUMO-specific C-terminal hydrolases to reveal a diglycine motif. The C-terminal diglycine motif is necessary for SUMO conjugation to occur (Kamitani, Nguyen et al. 1997). Following conjugation, SUMO can be removed from target proteins in a reaction catalysed by SUMO-proteases (Melchior, Schergaut et al. 2003). Some of these proteases function to both process SUMO to its mature form and to cleave the isopeptide bond between SUMO and its target protein (Melchior, Schergaut et al. 2003). All known SUMO-cleaving enzymes contain a ~200 amino acid C-terminal domain, termed the Ulp domain. The Ulp1 domain has SUMO cleaving activity (Mossessova and Lima 2000).

In yeast, two SUMO proteases have been identified, Ulp1 and Ulp2 (Li and Hochstrasser 1999; Li and Hochstrasser 2000; Taylor, Ho et al. 2002). Although Ulp1 exhibits both protease functions mentioned above, the primary role of the *S. pombe* Ulp1 protein is to process SUMO to its mature form (Li and Hochstrasser 1999; Taylor, Ho et al. 2002). Unlike Ulp1, Ulp2, does not cleave the precursor but de-sumoylates a distinct set of conjugates and prevents the accumulation of SUMO chains (Li and Hochstrasser 1999; Bylebyl, Belichenko et al. 2003). Interestingly, Ulp1 and Ulp2 localise to different sub-cellular compartments. Ulp1 is present at the nuclear pore complex, while Ulp2 is present in the nucleoplasm. The two proteases cannot compensate for each other functionally. Whilst deletion of *ulp1* in *S. cerevisiae* is lethal (Li and Hochstrasser), *S. pombe ulp1-d* cells are viable but are deficient in processing precursor SUMO to its mature form and, therefore, show a reduction in the level of SUMO modified species(Taylor, Ho et al. 2002). *ulp2-d* cells are viable in both *S. cerevisiae* and *S. pombe* and show chromosome segregation defects (Bachant, Alcasabas et al. 2002).

1.8.2 The SUMO activating enzyme

The SUMO activating enzyme is a heterodimer containing SAE1 and SAE2 subunits (Dohmen, Stappen et al. 1995; Johnson and Blobel 1997; Desterro, Rodriguez et al. 1999; Gong, Li et al. 1999). The SAE1 and SAE2 subunits are conserved from yeast to human and are related to the N- and C-terminal domains of the yeast ubiquitin E1 activating enzyme Uba1. When assembled together form a functional SUMO activating enzyme. The E1 SUMO-activating enzyme (SAE) initiates the SUMO conjugation process. First, the C-terminal carboxyl group of SUMO attacks ATP, forming a SUMO C-terminal adenylate and releasing pyrophosphate. Next, the thiol group of the active site cysteine in the E1 attacks the SUMO adenylate, releasing AMP and forming a high-energy thiolester bond between the E1 and the C-terminus of SUMO (Johnson and Blobel 1997). The activated SUMO is then ready to be transferred to a cysteine of the E2 enzyme. Most organisms contain a single SUMO-activating enzyme, which is sufficient for the conjugation of all SUMO variants to target proteins. In *S. pombe* the SUMO activating enzyme consists of the Rad31 and Fub2 subunits (Tanaka, Nishide et al. 1999; Ho, Warr et al. 2001).

1.8.3 The SUMO conjugating enzyme

In the second step of the SUMO conjugation pathway SUMO is transferred from the E1 activating enzyme to the active site cysteine of the SUMO-conjugating enzyme (E2), forming a thiolester intermediate (Desterro, Thomson et al. 1997; Johnson and Blobel 1997). Unlike the E2 of other UBL-conjugation pathways, the SUMO-conjugating enzyme can directly recognise substrate proteins and the E2-SUMO thiolester can catalyse the formation of an isopeptide bond between the C-terminal carboxyl group of SUMO and the ε-amino group of the target lysine in the substrate protein, provided that the lysine is part of a SUMO-consensus motif ψKXE (Rodriguez, Dargemont et al. 2001; Bernier-Villamor, Sampson et al. 2002). The SUMO-consensus motif is discussed in further detail in section 1.8.5.

In contrast to ubiquitination, where multiple conjugation enzymes exist, there is only one SUMO-conjugating enzyme (Desterro, Thomson et al. 1997; Johnson and Blobel 1997). In *S. pombe* the SUMO-conjugating enzyme is known as Hus5 (Ho and Watts 2003). Unlike

most organisms, the SUMO-conjugating enzyme is not essential in *S. pombe*, although *hus5* mutants, are very sick and highly sensitive to DNA damaging agents (al-Khodairy, Enoch et al. 1995; Ho and Watts 2003). This implies that sumoylation has a role in the *S. pombe* DNA damage response

1.8.4 The SUMO ligases

In the ubiquitin-conjugation system, substrate recognition is mediated by a family of E3 ubiquitin ligases. The E3 ligase must bind to the E2 conjugator and the target protein, and facilitate the transfer of ubiquitin from the conjugating enzyme to the substrate (Hershko and Ciechanover 1998). Unlike ubiquitination, the requirement of an E3 ligase for the attachment of SUMO to target proteins is not as strict. Although the E2 is sufficient to directly bind and sumoylate the target substrate *in vitro* (Sampson, Wang et al. 2001), E3 SUMO ligases do exist. Ligase activity is likely to play an important role for modulating the efficiency of SUMO attachment to target proteins (Melchior, Schergaut et al. 2003).

Unlike ubiquitin ligases, only a small number of SUMO ligases have been identified to date. The first SUMO ligases to be identified were Siz (*S. cerevisiae*) and PIAS (*H. sapiens*), which define the Siz/PIAS-RING (SP-RING) class of SUMO ligases. The SP-RING family of proteins contain a region homologous to the RING domains of ubiquitin E3 ligases (Hershko and Ciechanover 1998; Hochstrasser 2001). Members of the SP-RING SUMO ligase family include the mammalian PIAS proteins, the *S. cerevisiae* Siz1, Siz2, Mms21 and Zip3 proteins and the *S. pombe* Pli1 and Nse2 proteins. There are a number of other SUMO ligases, which do not conform to the SP-RING class. These include RanBP2, Pc2 and HDAC2 (Pichler, Gast et al. 2002; Kagey, Melhuish et al. 2003; Zhao and Blobel 2005). Interestingly, the different E3 SUMO ligases have distinct sub-cellular localisations; RanBP2 is associated with the nuclear pore complex, the PIAS (SP-RING) proteins are found in the nucleoplasm and nuclear bodies and Pc2 is found in the subnuclear structure called a Polycomb body (Sachdev, Bruhn et al. 2001; Pichler, Gast et al. 2002; Kagey, Melhuish et al. 2003). Localisation of the SUMO ligases may contribute to functional specificity.

S. pombe Pli1 and Nse2 are homologues of *S. cerevisiae* Siz1 and Mms21 respectively, and are the only ligases identified to date in *S. pombe* (Xhemalce, Seeler et al. 2004; Andrews, Palecek et al. 2005). Pli1 sumoylation activity is dependent on its SP-RING domain (Xhemalce, Seeler et al. 2004). Deletion of *pli1* results in only a very subtle phenotype despite the level of sumoylation, being dramatically reduced (Xhemalce, Seeler et al. 2004). Unlike *pli1, nse2* is essential for cell viability. However, it is unlikely that the essential function of Nse2 is its ligase activity since *nse2-SA*, a strain in which the RING domain has been mutated to cause loss of SUMO ligase activity, is viable (Andrews, Palecek et al. 2005). The essential function of Nse2 is more likely to be its role a part of the Smc5/6 complex. Nse2 facilitates the sumoylation of some of the members of the Smc5/6 complex, namely Smc6, Nse3 and Nse2 itself. Nse2 is discussed in further detail in section 1.6.2.2.

1.8.5 Substrate specificity of SUMO.

Typically, the target for SUMO conjugation is a lysine found in a short 'SUMO-consensus motif', ψKxE, where ψ represents a large hydrophobic residue, generally isoleucine, leucine or valine; K is the target lysine; x is any residue; and E is a glutamic acid (Rodriguez, Dargemont et al. 2001). The ψKxE consensus motif is recognised by the E2 conjugating enzyme, which makes key interactions with the motif and transfers SUMO to the target lysine residue (Bernier-Villamor, Sampson et al. 2002; Lin, Tatham et al. 2002). Potential SUMO targets can, therefore, be identified by their interaction with the E2 in the yeast-two hybrid system. However, the ψKXE motif is very short and has been found in many proteins that are not SUMO targets. Several proteins are modified at sites other than the classic ψKxE. PCNA has two sumoylation sites, one of which conforms to the ψKxE motif, whilst the other is a T*K*ET sequence (Hoege, Pfander et al. 2002). In addition a number of proteins have been identified as SUMO targets despite not having a ψKxE motif. This suggests that interactions other than that of the E2 with the target may be necessary for determining substrate specificity.

Many groups have suggested an extended SUMO consensus motif although the functional relevance is not yet known. For example, the synergy consensus motif (SC) is defined by

the presence of proline residues flanking the core SUMO motif (Subramanian, Benson et al. 2003). Similarly an extended motif based on the R-motif repression domain of the transcription factor Elk-1 and the CRD1 domain of p300 has been proposed in which clusters of acidic residues are found downstream of the core SUMO consensus motif (Yang, Jaffray et al. 2003). Recently, a phosphorylation-dependent sumoylation motif (PDSM) has been identified in a subset of substrates that conforms to the extended motif ψKxExxSP (Hietakangas, Anckar et al. 2006). Phosphorylation of the SP motif within the extended consensus has been shown to play an important role in the sumoylation of a number of substrates (Gregoire, Tremblay et al. 2006; Hietakangas, Anckar et al. 2006; Shalizi, Gaudilliere et al. 2006)

1.8.6 Role of SUMO modification

Post-translational modification of target proteins by SUMO has been identified as an important mechanism for regulating a plethora of cellular processes, including cellular localisation, transcription, DNA repair and cell cycle progression. The precise way in which SUMO regulates cellular functions remains poorly understood. A few examples of the role of SUMO modification are described below.

1.8.6.1 Cellular localisation

Post-translational modification by SUMO regulates sub-cellular localisation of many targets including RanGAP1, the first protein identified as a target for sumoylation (Matunis, Coutavas et al. 1996). RanGAP1 is a small GTPase-activating protein for Ran and in its unmodified state is primarily located in the cytoplasm (Matunis, Coutavas et al. 1996; Mahajan, Delphin et al. 1997). During interphase, RanGAP1 is modified on K26 by SUMO-1 (Matunis, Coutavas et al. 1996; Mahajan, Delphin et al. 1997). Modification of RanGAP1 greatly enhances its interaction with the nuclear pore protein RanBP2 (Also known as Nup358) localising RanGAP1 to the nuclear pore (Matunis, Coutavas et al. 1996; Mahajan, Delphin et al. 1997). RanBP2 binding to the modified form of RanGAP1 is dependent on a SUMO-binding motif (section 1.8.7) in RanBP1 (Song, Durrin et al. 2004). This suggests that the SUMO moiety conjugated to RanGAP1 interacts with the SUMO-binding motif on RanBP2 to facilitate the nuclear transport of RanGAP1.

Another example of SUMO-dependent subcellular localisation comes from studies of the tumour suppressor protein PML (promyelocytic leukaemia). PML is a major component of PML nuclear bodies. Sumoylation of PML on K65, K160 and K490 is required for the targeting of PML to nuclear bodies (Muller, Matunis et al. 1998). Mutation of the SUMO-acceptor lysines also causes nuclear body components such as CBP or Sp100 to re-localise in the nucleus (Zhong, Muller et al. 2000; Best, Ganiatsas et al. 2002). This suggests that SUMO-modification of PML supports protein-protein interactions important for either the assembly or stability of the PML bodies.

Whilst sumoylation is most often implicated in promoting localisation of proteins to the nucleus and nuclear bodies, there is evidence to suggest that SUMO modification can function as a signal for nuclear export. *Dictyostelium* MEK1 (Map kinase kinase) is required for the aggregation response and promotes the chemotaxis of cells towards cAMP (Ma, Gamper et al. 1997). MEK1 is transiently sumoylated on K105 in response to cAMP (Sobko, Ma et al. 2002). Unlike many other proteins it is the cytoplasmic and not nuclear fraction of MEK1 that is sumoylated. A MEK1 K105R is retained in the nucleus, suggesting that modification of MEK1 is required for nuclear export into the cytoplasm (Sobko, Ma et al. 2002).

1.8.6.2 Transcriptional regulation

Over half of the SUMO substrates identified to date are transcriptional factors or co-repressors (Shih, Chang et al. 2007). The activity of many transcriptional factors is regulated by their association with PML nuclear bodies. Since the assembly of PML nuclear bodies is dependent on the sumoylation of the PML protein (Section 1.8.6.1), the loss of PML modification has a great effect on transcriptional regulation. For example, sumoylation of the PML protein recruits co-repressor Daxx to PML nuclear bodies, thereby relieving Daxx-mediated transcriptional repression (Seeler and Dejean 2003).

Sumoylation of Elk-1 is required for the repression of genes activated by the MAPK signalling cascade. In the basal state, Elk-1 is modified on K249 and K230, resulting in the

recruitment of histone deacetylase HDAC2 (Yang, Jaffray et al. 2003). SUMO modification of Elk-1 hence influences local histone acetylation levels and repression of target genes (Yang, Jaffray et al. 2003; Yang and Sharrocks 2004). When the pathway is activated by ERK, Elk1 becomes phosphorylated signalling the loss of SUMO-modification and therefore loss of HDAC2 interaction, leading to the activation of target genes (Yang, Jaffray et al. 2003). Alternatively, if the pathway is activated by stress, then SUMO-modification, leading to only partial activation of target genes (Gostissa, Hengstermann et al. 1999).

In general SUMO modification is associated with transcriptional repression. However, in a growing number of cases, SUMO has been shown to play a role in transcription activation. The tumour suppressor p53 is a transcription factor that can inhibit cell cycle progression and in some cases induce apoptosis. p53 is modified at K386, in a region that regulates its DNA binding activity (Muller, Berger et al. 2000). Sumoylation of p53 stimulates its ability to activate reporter genes possibly by competing with Mdm2-mediated ubiquitination, which targets p53 for degradation (Muller, Berger et al. 2000). A p53 K386R mutant that is defective in SUMO conjugation showed a slightly impaired apoptotic activity (Muller, Berger et al. 2000).

1.8.6.3 Cell cycle control

Sumoylation has always had a strong link with mitosis. In fact, the gene encoding SUMO in *S. cerevisiae* was first isolated in a screen for high-copy suppressors of mutations in the gene encoding the centromere binding protein Mif2 (Meluh and Koshland 1995). In addition, mutants in the *S. cerevisiae* E1 (Uba2) and E2 (Ubc9) display cell cycle defects (Seufert, Futcher et al. 1995; Johnson and Blobel 1997). In *S. pombe hus5* and *rad31* mutants exhibit mitotic defects and impaired growth (al-Khodairy, Enoch et al. 1995; Shayeghi, Doe et al. 1997; Ho and Watts 2003).

A number of mitotic targets of SUMO exist. Topoisomerase II (Top 2 in yeast) functions to relax both positive and negative supercoils in DNA. In *S. cerevisiae ulp2-d* strains show loss of centromeric cohesion that can be suppressed by over-expression of a non-

sumoylatable version of Top2 (Topoisomerase 2). SUMO modification of Top2 is, therefore, required to establish the appropriate chromatin environment for centromeric cohesion (Bachant, Alcasabas et al. 2002). This observation suggests that SUMO deconjugation also has a critical role in mitosis.

Septins are required for cytokinesis and bud site selection in *S. cerevisiae* and were the first yeast proteins shown to be sumoylated (Johnson and Blobel 1999; Takahashi, Iwase et al. 1999). SUMO-conjugated forms of the septins Cdc3, Cdc11 and Shs1 are abundant during mitosis (Johnson and Blobel 1999). Conjugation of the septins appears to be tightly regulated and cell cycle dependent with modified forms appearing just before anaphase onset and disappearing abruptly at cytokinesis (Johnson and Blobel 1999). A mutant that eliminates SUMO-conjugation of Cdc3, Cdc11 and Shs1 abolishes almost all mitotic sumoylation at the bud neck and decreases the overall level of SUMO conjugation within G2/M phase (Johnson and Blobel 1999). Despite the drastic loss of sumoylation, the triple sumoylation mutant has near wild-type characteristics and show no sensitivity to conditions of stress. It is possible that a low level of SUMO-conjugation to Septins Cdc10 and Cdc12 is sufficient to compensate for the loss of Cdc3, Cdc11 and Shs1 modification. This is consistent with the synthetic lethality seen between the triple mutant and a *cdc12* temperature sensitive mutant (Johnson and Gupta 2001)

1.8.6.4 Maintaining genomic integrity

Initial genetic experiments indicated that cells lacking components of the SUMO-modification pathway have an impaired ability to repair DNA damage. *S. pombe pmt3* mutants were characterised by aberrant mitosis and defects in chromosomal segregation (Tanaka, Nishide et al. 1999). Furthermore, cells with mutations in the genes encoding Rad31, a component of the SUMO-activating enzyme, and Hus5, the SUMO-conjugating enzyme, exhibit an increased sensitivity to UV, IR and the DNA synthesis inhibitor HU (al-Khodairy, Enoch et al. 1995; Shayeghi, Doe et al. 1997).

Several proteins known to be required for DNA replication and DNA damage repair are modified by SUMO. In *S. cerevisiae*, sumoylation of PCNA occurs during S-phase at K127

and K164 (Hoege, Pfander et al. 2002). K164 is also the site of PCNA ubiquitination, however, ubiquitination is not observed during S-phase. This suggests that sumoylation of PCNA inhibits ubiquitin-dependent post-replicative repair (Section 1.5.5) (Hoege, Pfander et al. 2002). It has been proposed that modification of K164 by SUMO and ubiquitin direct PCNA for different functions (Stelter and Ulrich 2003). Whilst ubiquitination directs PCNA either for translesion synthesis (monoubiquitination) or an error-free DNA damage tolerance pathway (ubiquitin chains), sumoylation of PCNA recruits the Srs2 helicase to disrupt the Rad51-ssDNA filament and prevent inappropriate homologous recombination (Haracska, Torres-Ramos et al. 2004; Papouli, Chen et al. 2005; Pfander, Moldovan et al. 2005). However, there is no evidence to suggest that *S. pombe* PCNA is sumoylated. Instead, *S. pombe* PCNA is ubiquitinated in S-phase. Furthermore, in contrast to *S. cerevisiae*, the DNA-damage sensitivity of mutants in the PRR pathway cannot be suppressed by the deletion of *srs2* (Frampton, Irmisch et al. 2006). This suggests that either polyubiquitination in *S. pombe* has the same function as sumoylation in *S. cerevisiae*, or that the recombination system in *S. pombe* may be less active in S-phase than in *S. cerevisiae*, and it may not be necessary to have a mechanism to suppress it (Frampton, Irmisch et al. 2006).

Another example of how SUMO modification can affect the function of DNA repair proteins is in the case of thymine-DNA glycosylase (TDG), which has an important role in base excision repair. TDG removes thymine and uracil from mismatched G-T and G-U base pairs. Human TDG does not readily dissociate from its product *in vitro* despite the need for dissociation to allow repair of the abasic site generated by TDG. TDG is sumoylated on K330 and the SUMO-modified form of TDG shows a reduced affinity for the DNA substrate suggesting that the TDG reaction cycle is regulated by a SUMO-dependent conformational change (Hardeland, Steinacher et al. 2002).

1.8.7 SUMO-binding motifs

The physiological consequences of SUMO modification are typically mediated by effector proteins that recognise SUMO through SUMO-binding motifs (SBMs), also referred to as SUMO-interacting motifs (SIMs). The first SBM was identified in proteins able to interact

with sumoylated p73 in a yeast-two hybrid screen (Minty, Dumont et al. 2000). Interacting proteins shared a common SXS motif, where S represents a serine residue and X represents any amino acid, flanked by a hydrophobic core on one side and acidic residues on the other. The SXS motif was shown to interact strongly with SUMO in a two-hybrid assay (Minty, Dumont et al. 2000). Subsequently, a second SBM was identified. This SBM is more widely accepted by the scientific community and contains three hydrophobic residues, typically valine, leucine or isoleucine, in a sequence of four amino acids V/I-V/I-X-V/I/L or the reverse orientation V/I-X-V/I-V/I (Song, Durrin et al. 2004; Song, Zhang et al. 2005). This suggested that it was the hydrophobic core flanking the SXS motif that gave it the property of an SBM.

Several proteins including the SUMO-ligases PIASX and RanBP2 and the SUMO-activating enzyme subunit Uba2 contain the V/I-V/I-X-V/I/L motif. In addition, many of the known SBM-containing proteins have nuclear functions, consistent with the general role of sumoylation in the nucleus. Sumoylation of PCNA is important for error-free DNA replication in a process that is dependent on the Srs2 helicase, which is able to disrupt the Rad51 nucleofilaments. Srs2 contains three distinctive domains: a helicase domain, a Rad51 binding domain and a C-terminal PCNA-interaction domain. Sumoylation of PCNA is not a pre-requisite for its interaction with Srs2 (Pfander, Moldovan et al. 2005). However, deletion of the six C-terminal, SBM-containing, residues of Srs2 results in a greatly reduced PCNA binding affinity (Pfander, Moldovan et al. 2005). This suggests that at least one SBM may contribute to the functional interaction between Srs2 and PCNA. More recently, the identification of RING-finger containing proteins, which contain one or more SBM, led to the suggestion that these proteins could target SUMO-modified proteins for ubiquitin mediated proteolysis (Prudden, Pebernard et al. 2007; Sun, Leverson et al. 2007; Uzunova, Gottsche et al. 2007; Xie, Kerscher et al. 2007), SUMO-targeted ubiquitin ligases are discussed in further detail in section 1.8.8.

The structure of SUMO-1 in complex with an SBM-containing PIASX peptide reveals that the residues of the SBM form a β-strand, which are incorporated into a β-sheet together with the second β-strand of SUMO (Song, Zhang et al. 2005). The SBM-binding surface of

SUMO is formed by a groove formed between its α-helix and second β-sheet. A number of hydrophobic residues, including F36 and V38 line the groove to form a conserved hydrophobic patch to accommodate the hydrophobic side chains of the SBM (Song, Durrin et al. 2004; Song, Zhang et al. 2005). Many SBM-containing proteins have a cluster of acidic residues juxtaposed with the hydrophobic core, which may contribute to the specificity of the SBM-SUMO interactions (Song, Zhang et al. 2005; Hecker, Rabiller et al. 2006).

1.8.8 SUMO-targeted ubiquitin ligases.

A novel family of E3 ubiquitin ligases that recognise sumoylated species has recently been identified. The SUMO–targeted ubiquitin ligases (STUbLs) were first identified in *S. cerevisiae*. Two RING-finger domain proteins Slx5 (also known as Hex3) and Slx8 were identified to function as a heterodimer and to be essential for viability in cells lacking the Sgs1 DNA helicase (Rqh1 in *S. pombe*) (Mullen, Kaliraman et al. 2001). The Slx5 protein has also been shown to interact with the homologue of *S. pombe* Nse5 (Hazbun, Malmstrom et al. 2003). In fission yeast, a homologue of Slx8 but not Slx5 can be detected through bioinformatic approaches. In a yeast-two hybrid screen, using Nse5 as bait, an uncharacterised RING-finger protein (Rfp1) was identified and shown, both *in vitro* and *in vivo,* to interact with Slx8 (Prudden, Pebernard et al. 2007). A second *S. pombe* RING-finger protein (Rfp2) has been identified and shown to form a heterodimer with Slx8 (Prudden, Pebernard et al. 2007). Unlike deletion of *slx8,* cells deleted for *rfp1*and *rfp2* are viable. Deletion of both *rfp1* and *rfp2* together results in cells that can survive only a limited number of cell divisions, suggesting a functional redundancy of the Rfp subunits (Sun, Leverson et al. 2007). The Slx8-Rfp1 and Slx8-Rfp2 complexes have been termed collectively Slx8-Rfp. *H. sapiens* RNF4 (RING-finger protein 4) has been identified as a homologue of *S. pombe* Rfp1 and Rfp2 and has been shown to functionally complement *S. pombe* Slx8-Rfp mutants (Kosoy, Calonge et al. 2007; Prudden, Pebernard et al. 2007; Sun, Leverson et al. 2007). This suggests that the STUbL pathway is functionally conserved between yeast and humans.

Several putative STUbLs have been identified in other higher eukaryotes, revealing a common feature of the STUbL family; yeast STUbLs comprise of two proteins, whereas STUbLs in higher eukaryotes consist of a single protein (Perry, Tainer et al. 2008). The yeast Slx8-Slx5 and Slx8-Rfp dimers form via contacts between their RING-finger domains (Yang, Galanis et al. 2006; Prudden, Pebernard et al. 2007). Like Slx5, the Rfp1 and Rfp2 proteins contain a SUMO-binding motif (Section 1.8.7) that has been shown to interact with SUMO in a non-covalent manner (Prudden, Pebernard et al. 2007). In higher eukaryotes, the single bifunctional STUbLs contain a C-terminal RING-finger domain and an N-terminal SUMO-binding motif (Perry, Tainer et al. 2008). It is the presence of the SUMO-binding motif, which distinguishes the STUbL family from other ubiquitin E3 ligases.

By ubiquitinating and promoting the de-sumoylation and/ or degradation of sumoylated target proteins, STUbLs provide cross talk between the ubiquitin and SUMO pathways. STUbL dysfunction causes a specific accumulation of sumoylated protein species and has concomitant defects in DNA repair and genomic integrity (Prudden, Pebernard et al. 2007). In *S. pombe* the lethal phenotype of the *slx8* deletion can be suppressed by deleting the major SUMO ligase, Pli1 (Prudden, Pebernard et al. 2007). In addition over-expressing the isopeptidase Ulp2, which reduces global sumoylation, can suppress the phenotypes associated with deletion of *rfp1* and *rfp2* (Kosoy, Calonge et al. 2007). While this suggests that the maintenance of SUMO pathway homeostasis is critical and that STUbLs are potent regulators of this pathway, the precise mechanism of STUbL function has not been determined.

1.8.8.1 STUbL targets

To date, only a limited number of STUbL targets have been identified. PML is the first protein shown to be degraded by the ubiquitin-mediated pathway. Arsenic triggers SUMO-dependent polyubiquitination of PML through the recruitment of RNF4 (Lallemand-Breitenbach, Jeanne et al. 2008; Tatham, Geoffroy et al. 2008). RNF4 only ubiquitinates the PML protein when it is conjugated to SUMO-2 and preferentially when conjugated to

SUMO-2 polymers (Tatham, Geoffroy et al. 2008). The four N-terminal SUMO-binding motifs of RNF4 are required for this interaction (Tatham, Geoffroy et al. 2008).

Another protein identified as a target of the STUbL protein family is the *S. pombe* DNA repair protein Rad60 (Section 1.9). Rad60 is ubiquitinated *in vitro* by Slx8 in an Rfp1- and SBM-dependent manner (Prudden, Pebernard et al. 2007). Rad60 and Slx8-Rfp mutants display a similar spectrum of DNA damage sensitivities (Prudden, Pebernard et al. 2007). Further more, Rad60 and Slx8-Rfp functions are required for cell viability in the absence of a functional Rqh1 helicase (Prudden, Pebernard et al. 2007). Interestingly, Rad60 belongs to the RENi family of proteins that contain two SUMO-like domains in their C-terminus (Section 1.8.9) (Novatchkova, Bachmair et al. 2005). Like Rad60, *H. sapiens* NIP45 is a member of the RENi family and has been shown to interact with the RNF4 protein. The NIP45-RNF4 interaction is dependent on the C-terminal SUMO-like domains and is enhanced by the co-expression of the mature from of SUMO-1 (Prudden, Pebernard et al. 2007). A mutation in the predicted SBM binding pocket of Rad60 SUMO-like domain 1 abolishes Rfp1 interaction *in vitro*, suggesting that the SUMO-like domains are recognised by the STUbLs. Rad60 is discussed in further detail in section 1.9.

1.8.9 RENI family of proteins

During the course of this project, a family of SUMO-like domain (SLD) proteins have been identified (Novatchkova, Bachmair et al. 2005). The RENi family of proteins has been named after its three best-studied members *S. pombe* Rad60, *S. cerevisiae* Esc2 and *M. musculus* NIP45. All RENi proteins share a similar sequence architecture having an N-terminal low complexity region with many polar and positively charged residues and a C-terminal globular region consisting of one or more SUMO-like domains (Novatchkova, Bachmair et al. 2005). RENi proteins typically contain two SUMO-like domains in their C-terminus. However, only the second SUMO-like domain can be identified in plant members. This second SUMO-like domain has a large negative charged cluster 5-15 residues from the very C-terminus, typical of a SUMO-interaction surface (Bayer *et al*, 1998). The SUMO-like domains of the RENi proteins lack the C-terminal diglycine motif required for conjugation of SUMO to its substrate, suggesting that the SUMO-like domains

are non-cleavable SUMO fusions that can not be conjugated to target proteins (Novatchkova, Bachmair et al. 2005).

Functional information about RENi proteins is restricted to the *S. pombe* Rad60, *S. cerevisiae* Esc2 and *M. musculus* NIP45 proteins. Despite their shared SUMO-like domains, proteins of the RENi family superficially appear to share no functional similarity. However, evidence is emerging to suggest that functional similarities may exist. Esc2 has a role in chromatin silencing via the recruitment or stabilisation of the Sir complex (Dhillon and Kamakaka 2000; Cuperus and Shore 2002). Esc2 is known to interact with the Sir complex protein Sir2, a histone NAD-dependent deacetylase. Sir2 proteins are recruited to chromatin by DNA-bound factors and act by deacetylating histones and transcription factors such as p53 (Imai, Armstrong et al. 2000; Vaziri, Dessain et al. 2001; Rosenberg and Parkhurst 2002). *M. musculus* NIP45 has a role in gene regulation. The binding of tumour necrosis factor TRAF1 to NIP45 blocks the transactivation of the IL-4 promoter (Lieberson, Mowen et al. 2001). TRAF1 may negatively regulate T_h2 differentiation by sequestering NIP45 in the cytosol. This prevents translocation of NIP45 into the nucleus, thereby down-regulating the expression of NIP45-dependent T_h2 cytokines (Bryce, Oyoshi et al. 2006).

S. pombe Rad60 is an essential protein, associated with the Smc5/6 complex and is required for the repair of DSBs (Morishita, Tsutsui et al. 2002; Boddy, Shanahan et al. 2003). Rad60 is discussed in further detail in section 1.8.1. Whilst functionally different, NIP45 and Rad60 have both been shown to interact with STUbLs (section 1.8.8.1), suggesting that the evolutionary conserved SUMO-like domains of the RENi family can functionally mimic SUMO in their interaction with STUbLs.

1.9 Rad60

The gene encoding the Rad60 protein was first identified in a screen to identify *S. pombe* mutants hypersensitive to MMS and synthetically lethal with *rad2*, suggesting a role in recombinational repair (Morishita, Tsutsui et al. 2002). The *rad60* gene is essential for viability in *S. pombe* (Morishita, Tsutsui et al. 2002). The *rad60-1* mutant shows

hypersensitivity to MMS, UV and IR and is epistatic with *rhp51-d* (Morishita, Tsutsui et al. 2002). In addition, when irradiated with IR to induce DSBs, *rad60-1* cells are unable to repair fragmented chromosomes, suggesting a role for Rad60 in the repair of DSBs via HR (Morishita, Tsutsui et al. 2002).

The observations that the *rad60-1* mutant is synthetically lethal with *smc6-X*, and that the MMS sensitivity of *smc6-X* cells can be partially suppressed by the over-expression of the Rad60 protein, implies a genetic interaction between the two genes (Morishita, Tsutsui et al. 2002). Like *rad60-1*, a *rad60-3* mutant is synthetically lethal with *smc6-X* and like *smc6-X*, *rad60-3* is synthetically lethal with *brc1-d*, *mus81-d* and *rqh1-d* (Morishita, Tsutsui et al. 2002; Boddy, Shanahan et al. 2003). Although Rad60 is not part of the Smc5/6 complex, it has been shown to interact with ~2% and ~0.5% of Smc5 and Smc6 respectively, suggesting that Rad60 is loosely or transiently associated with the complex and may act co-dependently with the complex in a cell cycle specific manner (Boddy, Shanahan et al. 2003).

In addition to the physical interaction identified with the Smc5/6 complex, Rad60 interacts with the checkpoint kinase Cds1 in an FHA-domain specific manner (Boddy, Shanahan et al. 2003). In response to HU treatment, Rad60 is hyperphosphorylated in a Cds1-dependent manner, concomitant with its delocalisation from the nucleus (Boddy, Shanahan et al. 2003). Cds1 is able to phosphorylate Rad60 on multiple N-terminal sites. T72 has been identified as the mediator of the Cds1-Rad60 interaction and phosphorylation of S32 and S34 has a critical role in the survival of the activities of the recombinational repair factors Rqh1 and Mus81-Eme1 (Raffa, Wohlschlegel et al. 2006). Interestingly, Rad60 S32 and S34 are found within a putative SXS SUMO-binding motif (Section 1.7.7), which is conserved in other RENi family members including Esc2 and Nip45.

The *rad60-4* mutant (T72A, I232S, Q250R, K312N), that is unable to interact with Cds1, is defective in survival of replication arrest induced by HU, and proficient for survival of DNA damage caused by UV (Boddy, Shanahan et al. 2003). This strongly suggests that interaction with Cds1 is not required for the role of Rad60 in DSB repair but that Cds1-

mediated phosphorylation and nuclear delocalisation is important for the survival of replication fork arrest (Boddy, Shanahan et al. 2003). Unlike *rad60-4*, *rad60-1* cells are proficient in Cds1-dependent mitotic arrest in response to HU. However, after release from HU, *rad60-1* cells enter aberrant mitosis in which septation occurs without proper chromosome segregation (Miyabe, Morishita et al. 2006). This suggests that Rad60 function is required after release from replication arrest. The lethality of a *rad60-1 rqh1-d* double mutant can be suppressed by the deletion of *rhp51* or *rhp55* (Miyabe, Morishita et al. 2006). In addition, Rhp51-dependent DNA structures that cannot activate the mitotic checkpoints accumulate in *rad60-1* cells suggesting that *rad60* is required at a step downstream of *rhp51* (Miyabe, Morishita et al. 2006). A similar phenomenon has been observed for *smc6* mutants, suggesting that Rad60 re-enters the nucleus upon HU arrest to carry out a late repair role in concert with the Smc5/6 complex (Ampatzidou, Irmisch et al. 2006; Miyabe, Morishita et al. 2006).

Rad60 has recently been identified as a potential target of the Slx8-Rfp SUMO-targeted ubiquitin ligase (Section 1.8.8). A robust interaction between Rfp1 and the Rad60 SLDs has been detected *in vitro* and shown to be dependent on the Rfp1 SBMs (Prudden *et al,* 2007). *In vivo,* both full-length Rad60 and the SLDs have been shown to interact with Slx8 (Prudden *et al,* 2007). During the course of this project, Rad60 has been classified as a member of the RENi protein family, having two SUMO-like domains in its C-terminus (Novatchkova, *et al* 2005). It has been suggested, that STUbLs may recognise SUMO-like domains as well as SUMO-conjugated species. (Prudden *et al* 2007). The C-terminal region of Rad60, encompassing the SUMO-like domains, is required and sufficient for Rad60 homodimerisation (Raffa *et al*, 2006). Three putative SUMO-binding motifs (Section 1.8.7) contribute to Rad60 dimerisation (Raffa, Wohlschlegel et al. 2006). This suggests that dimerisation of Rad60 may be the result of SUMO-binding motifs in one molecule interacting with a SUMO-like domain of another.

1.10 Aims

The aim of this project was to undertake an investigation into the functional roles of the two Rad60 SUMO-like domains. First, I wanted to create SUMO-like domain-deletion

mutants to identify whether or not the SUMO-like domains are required for the essential role of Rad60, and if not whether they are required for the role of Rad60 in the DNA damage response. The second aim of this project was to undertake sequence comparisons and molecular modelling of the SLDs to initiate a structure-function study of the Rad60 SUMO-like domains. Since Rad60 is a target of STUbL activity and is associated with the Smc5/6 complex, which includes the E3 SUMO ligase Nse2, the final aim of this project was to investigate whether or not Rad60 is itself a target of sumoylation.

CHAPTER 2
MATERIALS AND METHODS

2.1 YEAST METHODS

Standard fission yeast techniques and media were employed (Moreno, Klar et al. 1991)

2.1.1 *S. pombe* Media

2.1.1.1 Rich media

Yeast Extract (YE)

5 g/l	Yeast extract (Formedium)
20 g/l	Glucose
200 mg/l	Adenine
100 mg/l	Leucine, uracil, histidine, arginine

For solid YE media, 25 g/l DIFCO agar was added.

2.1.1.2 Selective media

Yeast Nitrogen Base (YNB)

1.9 g/l	YNB (Formedium)
4 g/l	Ammonium sulphate
20 g/l	Glucose

For solid YNB media, 30 g/l DIFCO Bactoagar and 0.2 ml/l 10 M NaOH were added to liquid YNB.

Edinburgh Minimal Media (EMM2)

50 ml/l	20 X EMM2 salts
25 ml/l	20% NH_4Cl
25 ml/l	0.4 M Na_2HPO_4
12.5 ml/l	40% Glucose
1 ml/l	1000 x Vitamins
100 μl/l	10,000 x Trace elements

For solid EMM2 media, 30 g/l DIFCO Bactoagar was added.

20 x EMM2 Salts

61.2 g/l	Potassium hydrogen phthalate
20 g/l	KCl
21.4 g/l	$MgCl_2.6H_2O$
0.20 g/l	Na_2SO_4
0.26 g/l	$CaCl_2.2H_2O$

10,000 x Trace elements

5 g/l	H_3BO_3
4 g/l	$MnSO_4$
4 g/l	$ZnSO_4.7H_2O$
2 g/l	$FeCl_3.6H_2O$
1.5 g/l	Na_2MoO_4
1 g/l	KI
0.4 g/l	$CuSO_4.5H_2O$
10 g/l	Citric acid

1000 x Vitamins

1 g/l	Pantothenic acid
10 g/l	Nicotinic acid
10 g/l	Inositol
10 mg/l	Biotin

2.1.1.3 Sporulation media

Extra low nitrogen (ELN)

27.3 g/l	EMM Broth (Formedium)
0.05 g/l	Ammonium chloride
200 mg/l	Adenine
100 mg/l	Leucine, uracil, histidine, arginine
30 g/l	Bactoagar

2.1.1.4 *S. pombe* media supplements

The wild-type *S. pombe* strain used in this study has the genotype; *ade6-704, leu1-32, ura4-D18* and can not grow unless in the presence of adenine, leucine and uracil. Therefore, when grown in selective media the media must be supplemented. Strains containing markers (e.g. a *LEU2* gene) can be selected for by using selective media restricted for a particular supplement (e.g. leucine). Supplementing media with 5-fluoroorotic-acid (5FOA) can counterselect for strains containing an ura^+ gene. Similarly, strains marked with an antibiotic resistance gene, e.g. $kanamycin^r$ can be selected for by growing cells in the presence of that particular antibiotic. The same principles can be applied when selecting for plasmid containing cells. PhloxinB can be added to media to stain dead cells/diploids. Table 2.1 lists the supplements used in this study and the concentrations at which they are used.

2.1.2 *S. pombe* strains

Table 2.2 indicates the *S. pombe* strains used during this study. All *S. pombe* strains were stored in 50% glycerol stocks and maintained at –80^{o}C.

Table 2.1: Supplements for *S. pombe* media

Supplement	Stock Concentration	Working Concentration	Storage
Adenine hydrochloride	100 mg/ml in water	100 μg/ml	Room temperature
L-leucine	100 mg/ml in water	100 μg/ml	Room temperature
Uracil	50 mg/ml in water	100 μg/ml	Room temperature
Thiamine	10 mg/ml water	10 μg/ml	4^{o}C, store in dark
G418	100 mg/ml in water	100 μg/ml	-20^{o}C
5-FOA		1 mg/ml	Dissolve powder directly in warm media
PhloxinB	20 mg/ml in water	5 μg/ml	4^{o}C, store in dark

Table 2.2: *S. pombe* strains used in this study

Strain	Common name	Genotype
sp.011	wild-type h-	*ade6-704, leu1-32, ura4-D18, h*$^{-}$
sp.012	wild-type h+	*ade6-704, leu1-32, ura4-D18, h*$^{+}$
sp.226	*rhp51-d*	*rhp51-d::ura4, ade6-704, leu1-32, ura4-D18, h*$^{-}$
sp.418	*chk1-d*	*cds1-d::ura4, ade6-704, leu1-32, ura4-D18, h*$^{-}$
sp.437	*cds1-d*	*cds1-d::ura4, ade6-704, leu1-32, ura4-D18, h*$^{+}$
sp.481	*brc1-d*	*brc1-d::Leu2, ade6-704, leu1-32, ura4-D18, h*$^{+}$
sp.557	*rad3-d*	*rad3-d::ura4, ade6-704, leu1-32, ura4-D18, h*$^{+}$
sp.715	*pli1-d*	*pli1-d::ura4, ade6-704, leu1-32, ura4-D18, h*$^{-}$
sp.1124	*nse2-SA*	*nse2-SA:ura4, ade6-704, leu1-32, ura4-D18, h*$^{+}$
sp.1125	*smc6-X*	*smc6-X, leu1-32, ura4-D18, h*$^{+}$
sp.1126	*smc6-74*	*smc6-74, ade6-704, leu1-32, ura4-D18, h*$^{-}$
sp.1174	*rad60-ct*	*rad60-ct:G418*$^{+}$*, ade6-704, leu1-32, ura4-D18, h*$^{-}$
sp.1175	*rad60-FL*	*rad60-FL:G418*$^{+}$*, ade6-704, leu1-32, ura4-D18, h*$^{-}$
sp.1178	*crb2-T215A*	*crb2-T215A, ade6-704, leu1-32, ura4-D18, h*$^{+}$
sp.1179	*rad60-1*	*rad60-1, ade6-704, leu1-32, ura4-D18, h*$^{-}$
sp.1303	*rqh1-d*	*rqh1-d::ura4, ade6-704, leu1-32, ura4-D18, h*$^{+}$
sp.1305	*rad60-ct nse2-SA*	*rad60-ct:G418*$^{+}$*, nse2.SA:ura4, ade6-704, leu1-32, ura4-D18*
sp.1371	*rad60-FL-GFP*	*rad60-FLGFP:G418*$^{+}$*, ade6-704, leu1-32, ura4-D18, h*$^{-}$
sp.1372	*rad60-ct-GFP*	*rad60-ctGFP:G418*$^{+}$*, ade6-704, leu1-32, ura4-D18, h*$^{-}$
sp.1327	*rad60-ct chk1-d*	*rad60.ct:G418*$^{+}$*, chk1-d::ura4, ade6-704, leu1-32, ura4-D18*
sp.1328	*rad60-ct cds1-d*	*rad60-ct:G418*$^{+}$*, cds1-d::ura4, ade6-704, leu1-32, ura4-D18*
sp.1330	*rad60-ct rad3-d*	*rad60-ct:G418*$^{+}$*, rad3-d::ura4, ade6-704, leu1-32, ura4-D18*
sp.1372	*rad60-ct rhp51-d*	*rad60-ct:G418*$^{+}$*, rhp51-d::ura4, ade6-704, leu1-32, ura4-D18*
sp.1384	*rad60-ct-GFP chk1-d*	*rad60-ctGFP:G418*$^{+}$*, chk1-d::ura4, ade6-704, leu1-32, ura4-D18*
sp.1385	*rad60-FL-GFP chk1-d*	*rad60-FLGFP:G418*$^{+}$*, chk1-d::ura4, ade6-704, leu1-32, ura4-D18*
sp.1386	*rad60-ct-GFP cds1-d*	*rad60-ctGFP:G418*$^{+}$*, cds1-d::ura4, ade6-704, leu1-32, ura4-D18*
sp.1387	*rad60-FL-GFP cds1-d*	*rad60-FLGFP:G418*$^{+}$*, cds1-d::ura4, ade6-704, leu1-32, ura4-D18*
sp.1388	*rad60-ct crb2T215A*	*rad60-ct:G418*$^{+}$*, crb2-T215A, ade6-704, leu1-32, ura4-D18*
sp.1409	*top1-d*	*top1-d::Leu2, leu1-32, h*$^{+}$
sp.1482	*GFP rad60-FL*	*GFPrad60-FL:G418*$^{+}$*, ade6-704, leu1-32, ura4-D18, h*$^{-}$
sp.1483	*GFP-rad60-ct*	*GFPrad60-ct::G418*$^{+}$*, ade6-704, leu1-32, ura4-D18, h*$^{-}$
sp.1701	*rad60* base	*rad60:ura4*$^{+}$*, ade6-704, leu1-32, ura4-D18 h*$^{-}$
sp.1702	*rad60 wt a*	*ade6-704, leu1-32, ura4-D18, h*$^{-}$
sp.1703	*rad60 wt b*	*ade6-704, leu1-32, ura4-D18, h*$^{-}$
sp.1704	*rad60-SBM2 a*	*rad60-SBM2a, ade6-704, leu1-32, ura4-D18, h*$^{-}$
sp.1705	*rad60-SBM2 b*	*rad60-SBM2b, ade6-704, leu1-32, ura4-D18, h*$^{-}$
sp.1706	*rad60-L348V a*	*rad60-L348V, ade6-704, leu1-32, ura4-D18, h*$^{-}$
sp1707	*rad60-L348V b*	*rad60-L348V, ade6-704, leu1-32, ura4-D18, h*$^{-}$
sp.1708	*rad60-L348G a*	*rad60-L348G,, ade6-704, leu1-32, ura4-D18, h*$^{-}$
sp.1709	*rad60-L348G b*	*rad60-L348G, ade6-704, leu1-32, ura4-D18, h*$^{-}$
sp.1710	*rad60-L338V a*	*rad60-L338V, ade6-704, leu1-32, ura4-D18, h*$^{-}$

sp.1711	*rad60-L338V b*	*rad60-L338V, ade6-704, leu1-32, ura4-D18, h*$^{-}$
sp.1712	*rad60-I350L a*	*rad60-I350L, ade6-704, leu1-32, ura4-D18, h*$^{-}$
sp.1713	*rad60-I350L b*	*rad60-I350L, ade6-704, leu1-32, ura4-D18, h*$^{-}$
sp.1714	*rad60-I350G a*	*rad60-I350G, ade6-704, leu1-32, ura4-D18, h*$^{-}$
sp.1715	*rad60-I350G b*	*rad60-I350G, ade6-704, leu1-32, ura4-D18, h*$^{-}$
sp.1716	*rad60-I334L a*	*rad60-I334L, ade6-704, leu1-32, ura4-D18, h*$^{-}$
sp.1717	*rad60-I334L b*	*rad60-I334L, ade6-704, leu1-32, ura4-D18, h*$^{-}$
sp.1718	*rad60-I334G a*	*rad60-I334G, ade6-704, leu1-32, ura4-D18, h*$^{-}$
sp.1719	*rad60-I334G b*	*rad60-I334G, ade6-704, leu1-32, ura4-D18, h*$^{-}$
sp.1778	*rad60-SBM1 a*	*rad60-SBM1ade6-704, leu1-32, ura4-D18, h*$^{-}$
sp.1779	*rad60-SBM1 b*	*rad60-SBM1 ade6-704, leu1-32, ura4-D18, h*$^{-}$
sp.1780	*rad60-SBM3 a*	*rad60-SBM3 ade6-704, leu1-32, ura4-D18, h*$^{-}$
sp.1781	*rad60-SBM3 b*	*rad60-SBM3 ade6-704, leu1-32, ura4-D18, h*$^{-}$
sp.1782	*rad60-L336V a*	*rad60-L336V ade6-704, leu1-32, ura4-D18, h*$^{-}$
sp.1783	*rad60-L336V b*	*rad60-L336V ade6-704, leu1-32, ura4-D18, h*$^{-}$
sp.1784	*rad60-L336G a*	*rad60-L336G ade6-704, leu1-32, ura4-D18, h*$^{-}$
sp.1785	*rad60-L336G b*	*rad60-L336G ade6-704, leu1-32, ura4-D18, h*$^{-}$
sp.1786	*rad60-Y363F a*	*rad60-Y363F ade6-704, leu1-32, ura4-D18, h*$^{-}$
sp.1787	*rad60-Y363F b*	*rad60-Y363F ade6-704, leu1-32, ura4-D18, h*$^{-}$
sp.1788	*rad60-Y363G a*	*rad60-Y363G ade6-704, leu1-32, ura4-D18, h*$^{-}$
sp.1789	*rad60-Y363G b*	*rad60-Y363G ade6-704, leu1-32, ura4-D18, h*$^{-}$
sp.1790	*rad60-L359V a*	*rad60-Y359V ade6-704, leu1-32, ura4-D18, h*$^{-}$
sp.1791	*rad60-L359V b*	*rad60-Y359V ade6-704, leu1-32, ura4-D18, h*$^{-}$
sp.1792	*rad60- L359G a*	*rad60-Y359G ade6-704, leu1-32, ura4-D18, h*$^{-}$
sp.1793	*rad60-L359G b*	*rad60-Y359G ade6-704, leu1-32, ura4-D18, h*$^{-}$
sp.1794	*rad60-L346V a*	*rad60-Y346V ade6-704, leu1-32, ura4-D18, h*$^{-}$
sp.1795	*rad60-L346V b*	*rad60-Y346V ade6-704, leu1-32, ura4-D18, h*$^{-}$
sp.1796	*rad60-L346G a*	*rad60-Y346G ade6-704, leu1-32, ura4-D18, h*$^{-}$
sp.1797	*rad60-L346G b*	*rad60-Y346G ade6-704, leu1-32, ura4-D18, h*$^{-}$
sp.1845	diploid *rad60* base	*rad60*$^{+}$ *rad60*$^{+}$*:ura4*$^{+}$*, ade6-M216 ade6-M210, leu1-32 leu1-32, ura4-D18 ura4-D18, h*$^{+}$ *h*$^{-}$
EH353	EH353	*ade6-M216, leu1-32, ura4-D18, h*$^{+}$
EH358	EH358	*ade6-M210, leu1-32, ura4-D18, h*$^{+}$
EH682	EH682	*ade*$^{+}$*, leu1-32, ura4-D18, h*$^{+}$

2.1.3 *S. pombe* vectors

2.1.3.1 pREP41 and pREP42

pREP41 and pREP42 are derivatives of the *S. pombe* expression vectors pREP1 and pREP2 respectively (Maundrell 1993). The pREP vectors contain a thiamine repressible *nmt1* (no message in thiamine) promoter. The pREP41/42 vectors contain a T4 mutation in the *nmt1* promoter resulting in a weaker promoter than pREP1 and pREP2. pREP81 and pREP82 contain a T81 mutation in the promoter, resulting in a weaker promoter than pREP41/42. pREP41 contains the *S. cerevisiae LEU2+* gene and pREP42 contains a *ura4+* gene allowing selection of plasmid containing cells. The tagged pREP vectors pREP41HA and pREP42MH were also used in this study. These vectors allow the protein of interest to be N-terminally tagged with HA_3 and Myc_2-His_6 tags respectively. The pREP41EGFP(C) vector was used to C-terminally tag the protein of interest with an EGFP tag allowing visualisation of the protein within the cell.

2.1.3.2 pFA6 vectors- PCR based gene targeting

The pFA6a series of plasmids (Bahler, Wu et al. 1998) contain the heterologous selectable marker *kanMX6* and are designed to be used as templates for PCR-based gene targeting in *S. pombe* as described by Bahler *et al*, 1998. The pFA6 series includes plasmids containing a number of different markers, for example; 3 copies of the influenza virus hemaglutinin (HA) epitope, 13 copies of the human *c-myc* epitope and a copy of the *Aequorea victoria* jellyfish gene encoding green fluorescent protein (GFP). Through PCR amplification of the heterologous module with primers flanked with 80 bp of sequence homologous to target sequences within the *S. pombe* genome, epitopes can be introduced at gene loci via homologous integration.

2.1.3.3 pGEM-EGFP- N-terminal tagging

The pGEM-EGFP vector is a derivative of the pGEM3zf cloning vector (Pharmacia Biotech) and was devised for use in the 'simple Cre-*loxP* method for chromosomal N-terminal tagging' system (Werler, Hartsuiker et al. 2003). pGEM-EGFP has two *loxP* sites separated by a copy of the *sup3-5* cassette, which suppresses the *ade6-704* non-sense

mutation. The sequence encoding the EGFP tag has been cloned immediately before the first *loxP* site and an *nmt* promoter has been placed following the *sup3-5* cassette. Primers flanked with 80 bp of sequence homologous to target sequences within the *S. pombe* genome are used to PCR amplify the tagging construct. Fusion PCR of this tagging construct with fragments amplified from genomic DNA containing a) 500 base pairs of sequence immediately upstream of the ATG of the targeted gene, and b) 500 base pairs of the coding sequence including the ATG result in a targeting construct for integration into the genome. Following integration of the construct in an *ade6-704* background, ade^+ transformants, in which the gene is under the control of the *nmt* promoter, can be selected. Transformation with a plasmid containing the *Cre* recombinase allows excision of the both the promoter and the *sup3-5* cassette located between the two *loxP* sites thus leaving the newly tagged gene under the control of its native promoter. Other N-terminal tagging plasmids exist, in which the EGFP of the pGEM-EGFP vector has been replaced with another tag, e.g. TAP tag.

2.1.3.4 pAW vectors- Recombinase-mediated cassette exchange system

The pAW series of vectors are for use in the 'recombinase-mediated cassette exchange (RCME) system'(Watson, Garcia et al. 2008)pAW11 and pAW12 are used as PCR templates for generating a '*rad60* base strain' in which a 'loxP-*rad60*-$ura4^+$-loxM3' cassette has been introduced into the *S. pombe* genome. Creating the *rad60* base strain is a two-step process; first the loxP site is integrated ~300 bases upstream of the ATG and then the $ura4^+$ gene is integrated immediately downstream of the *rad60* coding sequence.

pAW11 contains a *sup3-5* cassette flanked by 2 loxP sites. Through PCR amplification of the heterologous module, with primers flanked with 80bp of sequence homologous to target sequences within the *S. pombe* genome, the cassette is introduced via homologous integration ~300 base pairs upstream of the *rad60* start codon. Ade^+ transformants are selected and transformed with the Cre-expressing plasmid pAW8 to excise the sup3-5 cassette leaving a single lox-P site upstream of the *rad60* coding sequence.

pAW12 contains a *ura4*$^+$ gene followed by a loxM3 site. Through PCR amplification of the heterologous module, with primers flanked with 80bp of sequence homologous to target sequences within the *S. pombe* genome, the *ura4*$^+$-loxM3 cassette is introduced via homologous integration immediately downstream of the *rad60* coding sequence. *Ura4*$^+$ transformants are selected.

pAW8 contains the *S. cerevisiae LEU2+* gene and is a Cre-expression plasmid When the *rad60* coding sequence is cloned into the pAW8 plasmid it is consequnectly flanked by loxP and loxM3 sites. Site-directed mutagenesis on this pAW8 cassette (pAW8p*rad60*) followed by cassette exchange between this plasmid cassette and the chromosomal cassette allows a simple method for integrating point mutations into the *rad60* gene.

2.1.4 *S. pombe* transformation

2.1.4.1 *S. pombe* plasmid transformation- standard LiAc method

S. pombe cells were grown overnight in YE until they were in mid-log phase. 10 ml (~1 x 10^8) cells were used per transformation. Cells were harvested at 3,000 rpm for 5 minutes. The cells were than washed with 1 ml distilled water, followed by 1 ml freshly prepared LiAc/EDTA. The cell pellet was then re-suspended in 100 μl LiAc/EDTA and ~1 μg plasmid DNA was added. The sample was incubated at room temperature for 5 minutes before adding 300 μl fresh PEG/EDTA/LiAc. The sample was then incubated for 30-45 minutes at 30^{o}C with shaking. The cells were then heat shocked at 42^{o}C for 15 minutes and centrifuged at 3,000 rpm for 5 minutes. The cell pellet was washed in 1 ml water and re-suspended in 100 μl distilled water before being plated on appropriate selective media. Plates were incubated at 30^{o}C for 3 days, or until transformants appeared.

LiAc/EDTA

0.1 M	LiAc, pH4.9
1 mM	EDTA

PEG/EDTA/LiAc

40%	PEG 4000 (filter sterilised)
0.1 M	LiAc, pH 4.9
1 mM	EDTA

2.1.4.2 *S. pombe* transformation- Bahler method (Bahler, Wu et al. 1998)

S. pombe cells were grown overnight in YE until the cell density was ~1 x 10^7 cells/ml. 10 ml (~1 x 10^8) cells were used per transformation. Cells were harvested at 3,000 rpm for 5 minutes and washed with 1 ml distilled water, followed by 1 wash with 1 ml freshly prepared LiAc/EDTA. The cell pellet was then re-suspended in 100 µl LiAc/EDTA and ~ 15 µg DNA was added with 2 µl 10 mg/ml sheared herring testes DNA. The sample was incubated at room temperature for 10 minutes before adding 260 µl fresh PEG/EDTA/LiAc. The sample was then incubated for a 30-45 minutes at 30^{o}C with shaking. 43 µl DMSO was added to the sample before heat shocking at 42^{o}C for 5 minutes. The cells were then centrifuged at 3,000 rpm for 5 minutes and the cell pellet was re-suspended in 500 µl distilled water. The transformation sample was plated between three YEA plates. Plates were incubated at 30^{o}C overnight before being replica plated onto appropriate selective plates. These plates were incubated for a further 3 days at 30^{o}C or until transformants appeared.

LiAc/EDTA

0.1 M	LiAc, pH7 .5
1mM	EDTA

PEG/EDTA/LiAc

40%	PEG 4000 (filter sterilised)
0.1 M	LiAc, pH 7.5
1 mM	EDTA

2.1.5 Recombination-mediated cassette exchange (Watson, Garcia et al. 2008)

A pAW8 vector containing the sequence for exchange was transformed into the base strain as described in section 2.1.4.1. Following transformation, cells were plated directly onto EMM containing adenine and thiamine to repress transcription of the Cre-recombinase from the *nmt* promoter. When transformants appeared after ~72 hours, colonies were re-streaked onto fresh EMM (plus adenine, plus thiamine) plates. The transformants were grown to saturation in 10 ml YE for ~36 hours at 30°C. Cells were counted and 1 $x10^5$, 1 $x10^4$ and 1 $x10^3$ cells were plated onto YEA plates containing 5FOA at a concentration of 1 mg/ml. Following incubation at 30°C for ~72 hours, 5FOA resistant colonies were re-streaked onto fresh YEA plates containing 5FOA for further analysis.

2.1.6 Genomic DNA extraction from *S. pombe*

Genomic DNA extraction from *S. pombe* (Moreno, Klar et al. 1991)

A 10 ml *S. pombe* culture was grown overnight in YEP until the cells reached stationary phase. The cells were harvested at 3,000 rpm for 5 minutes and washed once with 2 ml SP1 buffer. The cell pellet was then re-suspended in 2 ml SP1 buffer containing 2 mg/ml zymolyase (T 20,000) and incubated at 37°C for 45-60 minutes until ~80% cell lysis was observed. Spheroplasting was checked by removing 10 μl of sample onto a microscope slide with 1 μl 10% SDS and viewing by a light microscope. Once the cells were sufficiently lysed the protoplasts were harvested at 3,000 rpm for 5 minutes. The pellet was re-suspended in 900 μl 5x TE and 100 μl 10% SDS was added. The sample was incubated for 5 minutes at room temperature before 300 μl KAc was added to the sample. The sample was then incubated for 10 minutes on ice and then centrifuged at 4,500 rpm for 15 minutes. The supernatant was transferred to a clean falcon tube and one volume (~2 ml) of isoproponol was added. After centrifuging at 4,500 rpm for 15 minutes the pellet was washed with 500 μl 70% ethanol. The pellet was air dried and re-suspended in 250 μl 1 x TE.

SP1 Buffer:

1.2 M	Sorbitol
50 mM	Sodium citrate
50 mM	Sodium phosphate
40 mM	EDTA

Buffer was adjusted to pH 5.6 with NaOH

5x TE

50 mM	Tris, pH 8.0
5 mM	EDTA

2.1.6.2 Genomic DNA extraction from *S. pombe* (for use in Southern blots)

Genomic DNA was extracted as detailed in section 2.1.5.1. After re-suspending the DNA pellet in 250 µl 1 x TE, 4 µl RNase (10 mg/ml) was added and incubated for 20 minutes at 37°C. 4 µl proteinase K (20 mg/ml) was then added and the sample incubated overnight at 30°C. An equal volume of phenol chloroform was added and the DNA sample was spun for 10 minutes at 4,500 rpm. The supernatant was transferred into two new micro-centrifuge tubes. After 625 µl 100% EtOH plus 25 µl 3 M NaOAc was added to each tube, the samples were placed at –20°C for 1 hour. Following a 10-minute spin at 13,000 rpm the supernatant was discarded and the pellet washed with 500 µl 70% EtOH. Following a 5 minute spin at 13,000 rpm each pellet was air dried before being re-suspended in 25 µl 1 x TE. The two tubes were combined and 5 µl was checked on a 0.8% TBE gel.

2.1.7 Colony PCR

Colonies identified as successfully growing on the appropriate selective media were streaked onto the selective media and grown for a further 3 days at 30°C. A small loop of cells was used inoculate 100 µl water. The sample was boiled for 7 minutes and then cooled on ice for 5 minutes. 10 µl of this boiled sample was added to a master mix containing; 0.25 µl forward primer (100 µM), 0.25 µl reverse primer (100 µM), 2.5 µl 2.5 mM dNTPs, 2.5 µl 10 x PicoMax buffer (Stratagene), 0.25 µl *Taq* polymerase (Abgene) and 9.25 µl dH_2O. The PCR programme consisted of 45 cycles of; 94° C for 10 seconds,

54°C for 15 seconds and 72°C for 1 minute. 10 μl PCR product was analysed on a 1% TBE gel.

2.1.8 *S. pombe* genetic mating crosses

S. pombe crosses were set up by mixing two strains of opposite mating types on extra low nitrogen (ELN) media. The plates were incubated for 3 days at 25°C until spore-containing asci could be observed by a light microscope.

2.1.8.1 Random spore analysis

For mating crosses between strains with different selectable markers random spore analysis was used to select for double mutants. 1 ml of water, with 1 μl helicase (S.P.P. *Helix pomatia* juice) was inoculated with a loop of mating mixture. The sample was incubated on a rotating wheel overnight at room temperature. Serial dilutions of the spores were plated onto YEA and incubated at 30°C for 3 days. Colonies were then replica-plated onto selective media plates and double mutants selected.

2.1.8.2 Tetrad analysis

For mating crosses between strains without different selectable markers tetrad dissection analysis was used to select for double mutants. Following sporulation, a small loop of cells was streaked on one side of a YEA plate and incubated at 30°C for ~3 hours to allow the ascus wall to break down. Each ascus was then micro-manipulated to separate the four individual spores on the YEA plate. The spores were incubated for 3-4 days at 30°C until colonies formed. Depending on the phenotype of the individual mutant strains, double mutants were identified by replica plating onto suitable selection plates and/or exposing to UV radiation following replica plating onto phloxine B plates and the progeny analysed.

2.1.9 Survival analysis

2.1.9.1 UV survival analysis

Cells were grown in appropriate media overnight to exponential phase and diluted to $5x10^3$ cells/ml (or a dilution suitable for the strain). To test UV sensitivity, 100 μl cells (~500

cells) were plated in duplicate onto yeast extract agar (YEA) plates and irradiated at a dose of 25 Jm^{-2} /min for doses ranging between (0 and 200 Jm^{-2}). Colonies were counted following incubation for 72 hours at 30^{o}C and percentage survival calculated with reference to the non-irradiated sample.

2.1.9.2 Ionising radiation (IR) survival analysis

Cells were grown in appropriate media overnight to exponential phase and diluted to $5x10^{3}$ cells/ml (or a dilution suitable for the strain). To test γ sensitivity, cells were irradiated with γ rays from a ^{137}Cs source at a dose of 10 Gy/min for doses ranging from 0-1,000 Gy. 100 μl cells (~500 cells) were plated in duplicate onto yeast extract agar (YEA) plates. Colonies were counted following incubation for 72 hours at 30^{o}C and percentage survival calculated with reference to the non-irradiated sample.

2.1.9.3 Sensitivity to genotoxins

To determine the sensitivity of cells to DNA damaging agents by spot tests, exponentially growing cultures were adjusted to an equal cell density and four successive tenfold dilutions were spotted onto YEA or YEA plates containing hydroxyurea (HU), thiabendazole (TBZ), 4-nitroquinoline-1-oxide or methyl methanesulfonate (MMS). Plates were incubated at 30^{o}C for 3 days. Table 2.3 lists the genotoxins used in this study.

2.1.10 Microscopy

Cells were observed using an Applied Precision Deltavision Spectris microscope using deconvolution software.

2.1.10.1 Live cell imaging

1 ml of exponentially growing cells was harvested for 1 minute at 3,000 rpm and the supernatant removed. The cells were washed with 1 ml PBS and re-suspended in 100 μl EMM2 media supplemented with the appropriate amino acids and containing Hoechst 33442. 5 μl of the cell suspension was placed on a microscope slide. A coverslip was placed on top and the cells visualised.

Table 2.3: Genotoxins used in this study

Genotoxin	Stock Concentration	Working Concentration	Storage
HU	3 M in water	4-6 mM (plates) 20 mM (liquid culture)	-20°C
MMS	/	0.005- 0.01%	Added directly to media
TBZ	20 mg/ml in DMSO	15-20 μg/ml	-20°C
4NQO	1mM in DMSO	0.0μM	-20°C

2.1.10.2 DAPI staining of *S. pombe* cells

1 ml of exponentially growing cells was harvested for 1 minute at 3,000 rpm and the supernatant removed. The cells were washed with 1 ml PBS and resuspended in 1 ml cold methanol. Following centrifugation for 1 minute at 3,000 rpm, the supernatant was discarded and the cells were re-suspended in 100 μl mounting mix. 5 μl of the cell suspension was placed on a microscope slide. Once the sample was dry a small drop of vectashield (Vecta) was added to the slide and covered with a coverslip. The coverslip was sealed with clear nail varnish and the cells visualised.

Mounting Mix

0.5 μg/ml	DAPI
2.5 μg/ml	Calcofluor
In PBS	

2.1.10.3 <u>Immunofluorescence</u> (Hagan 1998)

Cells were grown in appropriate media to A_{595} 0.125. 5.5 ml 30% paraformaldehyde was added to 40 ml cells and the sample was incubated at room temperature on a rotating wheel for 10 minutes. The cells were harvested at 2,000 rpm for 2 minutes and the supernatant discarded. The cells were washed briefly in 10 ml PBS, followed by 1 wash in 1 ml PEM solution and 1 wash in 1 ml PEMS solution with spins between washes at 3,000 rpm for 1 minute. The cell pellet was re-suspended in 1 ml PEMS containing 1.25 mg/ml zymolyase T 20,000 and incubated at 37^{o}C for 70 minutes or until the cells wall had become digested. The sample was centrifuged at 3,000 rpm for 1 minute and the supernatant discarded. The cells were washed gently in 1x 1 ml PEMS, 1 x 1 ml PEMS containing 1% triton, 2 x 1ml PEM and finally 2 x 1 ml PEMBAL. The cell pellet was re-suspended in 1 ml PEMBAL and incubated at room temperature for 1 hour on a rotating wheel. 1 μl primary antibody was added to 100 μl of cells and left overnight at room temperature on a rotating wheel. The following day, the cells were washed 3 x 1ml PEMBAL with spins at 3,000 rpm for 1 minute in-between washes. The cell pellet was then re-suspended in 1 ml PEMBAL and incubated for 20 minutes at room temperature on a rotating wheel. The cells were then centrifuged for 1 minute at 3,000 rpm and the cell pellet re-suspended in 100 μl PEMBAL.

1 µl secondary antibody (1:100) was then added and the sample was wrapped in foil and incubated at room temperature for 3 hours on a rotating wheel. The cells were washed in 1 ml 1 x PEM and 1x PBS and re-suspended in 100 µl PBS. The cells were incubated at room temperature for 10 minutes on the rotating wheel. The cells were then centrifuged for 1 minute at 3,000 rpm and the cell pellet re-suspended in 100 µl PBS containing DAPI (0.5 µg/ml) 5 µl cells were spotted onto polylysine coverslips. Once dried, a small drop of vectashield (Vecta) was added to the slide and covered with the coverslip. The coverslip was sealed with clear nail varnish and when dry the slide visualised under a microscope.

30 % Paraformaldehyde

15 g paraformaldehyde was dissolved in 50 ml PEM solution. To aid dissolving the mixture was heated to 65^{o}C for 5 minutes and 300 µl 10 M NaOH was added. The mixture was heated for a further 20 mins at 65^{o}C. When the paraformaldehyde was fully dissolved, the solution was neutralized with 100 µl conc. HCl. The paraformaldehyde solution was cooled before use.

PEM Solution

100 mM	PIPES
1 mM	EGTA
1 mM	$MgCl_2$

Solution was adjusted to pH 6.9 with NaOH and filter sterilised

PEMS Solution

100 mM	PIPES
1 mM	EGTA
1 mM	$MgCl_2$
1.2 M	Sorbitol

Solution was adjusted to pH 6.9 with NaOH and filter sterilized.

PEMBAL Solution

100 mM	PIPES
1 mM	EGTA
1 mM	$MgCl_2$
1 %	BSA
0.1 %	NaN_3
100 mM	Lysine

Solution was adjusted to pH 6.9 with NaOH and filter sterilised

2.2 BACTERIAL METHODS

2.2.1 Bacterial media

L-Broth (LB)

10 g/l	Tryptone
5 g/l	Yeast extract
5 g/l	NaCl

For solid LA media 8 g/l agar was added.

2.2.2 Antibiotics

To select for plasmids containing a resistance marker, antibiotics were added to media prior to use. All antibiotics were stored at -20^{o}C.

Antibiotic	Stock Concentration	Working Concentration
Ampicillin	100 mg/ml in water	100 μg/ml
Chloramphenicol	34 mg/ml in ethanol	34 μg/ml

2.2.3 Blue-white selection

For blue-white selection using insertional activation of the LacZ gene, IPTG and X-Gal were added to media containing the appropriate selective antibiotic. Both IPTG and X-Gal were stored at -20^{o}C.

Additive	Stock Concentration	Working Concentration
IPTG	20 mg/ml in water	40 μg/ml
X-Gal	20 mg/ml in dimethylformamide	100 μg/ml

2.2.4 *E.coli* strains

The *E. coli* strains used in this study are listed in table 2.4.

2.2.5 Bacterial cloning vectors

pGEM-T Easy (Promega) and pTOPO (Invitrogen)

The pGEM-T Easy and pTOPO cloning vectors are high copy number plasmids that can be used for the cloning of PCR products. The vectors have a 3′ terminal thymidine at both ends providing a compatible overhang for PCR products generated by polymerases, which add single deoxyadenosine, to the 3′-ends of the amplified fragments. The vectors contain both T7 and SP6 RNA polymerase promoters in addition to the α-peptide coding region of the enzyme β-galactosidase. Insertional inactivation of the α-peptide allows selection of recombinant clones by blue-white screening.

2.2.6 Bacterial expression vectors

The bacterial expression vectors used in this study are under the control of the T7 promoter, which is activated by the T7 polymerase. The bacterial expression strain BL21 is a λDE3 lysogen containing an integrated copy of the T7 polymerase gene, which is under the control of the *lacZ* promoter. Expression of the T7 polymerase, and therefore the protein of interest, is induced by the addition of IPTG.

Table 2.4: ***E. coli*** **strains used in this study**

Strain	Genotype	Additional selection
NM522	F^- lacI^qD(lacZ)*M15*, *pro*A+B+ / *supE*, *thiD*, (lac-*proAB*)*D*, (*hsdMS-mcrB*)5.	-
BL21	(λDE3 lysogen/pLysS) F^- *ompT* r_B^- m_B^-	Chloramphenicol

pET-15B (Novagen)

The pET-15B vector carries a $_6$His-tag allowing affinity purification of N-terminally tagged proteins on Ni^{2+} agarose beads. A thrombin cleavage site allows cleavage of the tag following purification. An Amp^r gene allows selection of the plasmid.

pGEX (Pharmacia Biotech)

The pGEX vector encodes a 26 kDa GST tag allowing purification of the N-terminally tagged proteins on glutathione sepharose beads. A thrombin cleavage site allows cleavage of the tag following purification. An Amp^r gene allows selection of the plasmid.

pEPEX

The pEPEX vector contains a T7 promoter and is a good vector for use in the *In vitro* transcription dependant translation reaction (Section 2.4.13). An Amp^r gene allows selection of the plasmid. The pEPEXHA vector places a single HA tag at the N-terminus of the expressed protein.

2.2.7 Preparation of competent *E.coli* cells

Competant cells were prepared based on a modified version of a protocol by D. Hanahan (Hanahan 1983).

A single colony was used to inoculate 5 ml LB and grown overnight in a 37^{o}C shaker. The 5 ml pre-culture was used to inoculate 1 litre pre-warmed LB and grown at 37^{o}C with shaking for 2-4 hours until the OD_{550} reached 0.5-0.6. The cells were chilled on ice for 1 hour and centrifuged at 5,000 rpm for 5 minutes at 4^{o}C. The supernatant was discarded and the cell pellet re-suspended in 25 ml ice-cold TRNS 1 solution. The sample was centrifuged at 3,000 rpm for 5 minutes at 4^{o}C. The supernatant was again discarded and the cell pellet re-suspended in 25 ml TRNS 1 solution. After incubating on ice for 5 minutes, the sample was centrifuged at 3,000 rpm for 5 minutes at 4^{o}C. The supernatant was discarded and the cell pellet re-suspended in 6 ml ice cold TRNS 2. The sample was incubated on ice for 10 minutes before aliquoting into volumes of 300 μl. The cells were then snap-frozen in liquid nitrogen and stored at –80^{o}C.

TRNS 1 Solution

12.1 g/l	RbCl
9.6 g/l	$MnCl_2$
1.48 g/l	$CaCl_2$
2.88 g/l	CH_3COONa
66 ml/l	Glycerol

Solution adjusted to pH 5.8 with acetic acid, and then filter sterilized.

TRNS 2 Solution

1.2 g/l	RbCl
11 g/l	$CaCl_2$
2.1 g/l	MOPS
66 ml/l	Glycerol

Solution adjusted to pH 6.8 with acetic acid, and then filter sterilized.

2.2.8 ***E. coli* transformation**

Competent *E. coli* cells were thawed on ice for 15 minutes. Approximately 0.5 μg of plasmid DNA was added to 100 μl cells. The sample was incubated on ice for 15 minutes before being 'heat shocked' at 37°C for 2 minutes. The cells were then incubated on ice for a further 5 minutes. 0.5 ml L-Broth was added and the sample incubated for 45 minutes at 37°C. After incubation, the cells were spun at 3,000 rpm for 5 minutes and the supernatant poured off. The cell pellet was re-suspended in 100 μl LB and the cells plated onto LB agar plates supplemented with the appropriate selective antibiotic. Plates were incubated at 37°C for ~16 hours.

2.3 DNA METHODS

2.3.1 Agarose gel electrophoresis

Typically, 200 ml 0.8% agarose gels were used to analyse DNA samples, although occasionally, a 1% agarose gel was used to analyse small (<500bp) DNA fragments. Agarose (Melford) was dissolved, by heating, in 1 x TBE buffer. Prior to pouring in a pre-

prepared agarose gel cast, ethidium bromide was added to a final concentration of 0.25 μg/ml. Once set, the gel was submerged in a gel tank containing 1 x TBE buffer. Typically, DNA samples were loaded as a 20 μl volume with one-tenth volume of 10 x loading buffer and were run against 1 μl of a 1 kb ladder (Invitrogen). Electrophoresis was carried out at 150 V for ~ 45 minutes or until DNA bands were well separated. The DNA was visualised using a UV transilluminator.

10 x TBE Buffer

108 g/l	Tris base
55 g/l	Boric acid
0.2 M	EDTA, pH 8.

10 x Loading Buffer

0.1%	SDS
40%	Sucrose
1 mM	EDTA
1 mM	Tris, pH 7.5
0.25 %	Bromophenol blue

2.3.2 PCR-Amplifying DNA fragments

PCR was generally carried out using the DNA polymerase, *Expand* (Roche). Approximately 50 ng template DNA was used per 100 μl reaction containing; 1 μl forward primer (10 μM), 1 μl reverse primer (10 μM), 10 μl 10 x *Expand* buffer, 5 μl 2.5 mM dNTPs, 10 μl 10 X BSA and 1 μl *Expand* enzyme, which was added last. The PCR programme consisted of 18 cycles of; 94^{o}C for 1 minute, X^{o}C for 30 seconds and 68^{o}C for Y minutes where X, the annealing temperature, is dependent of the melting temperature of the primer pair, and Y, the elongation time, is dependent on the length of desired product. Typically, the extension time was calculated as 2 minutes per kb product. 5 μl of the PCR product was analysed on a 0.8% TBE agarose gel.

2.3.3 PCR- Site-directed mutagenesis

Site-directed mutagenesis was carried out based on the 'QuickChange site-directed mutagenesis' technique (Stratagene). Complementary primer pairs were designed to contain the DNA sequence encoding the mutation of choice flanked either side by ~ 12 bases that will hybridise to the original DNA sequence. *PfuTurbo* (Stratagene) was used to amplify the entire template plasmid. Approximately 50 ng template DNA was used per 50 µl reaction containing; 1 µl forward primer (1 µM), 1 µl reverse primer (1 µM), 5 µl 10 x *Pfu* buffer, 3 µl 2.5 mM dNTPs, and 1 µl *PfuTurbo* enzyme, which was added last. The PCR programme consisted of 18 cycles of; 94^{o} C for 1 minute, X^{o}C for 30 seconds and 72^{o}C for Y minutes where X (the annealing temperature) is dependent of the melting temperature of the primer pair, and Y (the elongation time) is dependent on the length of desired product. 5 µl of the PCR product was analysed on a 0.8% TBE agarose gel. The remaining PCR product was digested with 1 µl *DpnI* (Stratagene), which digested the methylated parental DNA template, leaving only the newly amplified 'mutagenic' DNA product. 20 µl of the mutagenic PCR product was transformed into *E. coli* NM522 cells and the DNA extracted using a QIAGEN miniprep kit as according to the manufacturer's instructions. The presence of the desired mutation was confirmed by sequencing (Section 2.3.11).

2.3.4 Fusion PCR for N-terminal tagging

Approximately 400 ng tagging construct, 150 ng of PCR fragment containing the upstream region of the gene and 150 ng of PCR fragment containing the downstream region of the gene were fused in a two step PCR reaction. In the first 'fusion' step the PCR reaction mixture consisted of template DNA at the aforementioned concentrations, 5 µl of 10 x *KOD* buffer, 5 µl 2.5 mM dNTPs, 2.5 µl DMSO, 8 µl $MgSO_4$ and 1 µl *KOD* polymerase in a total volume of 50 µl. The PCR programme consisted of 5 cycles of; 95^{o} C for 5 minute, 55^{o}C for 1 minute and 68^{o}C for 4 minutes followed by 10 minutes at 68^{o} C. In the second 'amplification' step the PCR reaction mixture consisted of 50 µl product from the 'fusion' step, 5 µl of 10 x *KOD* buffer, 5 µl 2.5 mM dNTPs, 2.5 µl DMSO, 4 µl $MgSO_4$, 1.5 µl forward primer (10 µM), 1.5 µl reverse primer (10 µM) and 1 µl *KOD* polymerase in a total volume of 100 µl. The PCR mixture was heated at 95^{o} C for 2 minutes followed by 24

cycles of; 95° C for 30 seconds, 55°C for seconds and 68°C for 4 minutes followed by 10 minutes at 68°C. 5 µl of the fusion PCR product was analysed on a 0.8% TBE gel.

2.3.5 PCR purification

PCR products were purified using a QIAGEN PCR purification column according to the manufacturer's guidelines.

2.3.6 Ethanol precipitation

2.5 x sample volumes EtOH (100%) was added to the DNA sample with 1/10th volume 3 M NaOAc. Samples were incubated at –20°C for ~ 1 hour and then spun at 13,000 rpm for 10 minutes at 4°C. The supernatant was removed and the DNA pellet washed with 500 µl EtOH. The supernatant was removed and the DNA pellet was dried for ~ 10 minutes before being re-suspended in 50 µl (or desired volume) 1 x TE.

2.3.7 Restriction enzyme digests

Typically, 1 µg of DNA was digested in a total volume of 30 µl. Restriction enzymes (New England Biolabs) were used as according to the manufacturers guidelines with 1 µl restriction enzyme, 3 µl of the relevant 10 x restriction enzyme buffer, and if required 3 µl of 10 x BSA. Digests were incubated at 37°C for 2 hours. For double digests, where the enzyme buffers were not compatible the DNA was cleaned, following the first enzyme digest, using a QIAGEN PCR purification column as according to the manufacturer's guidelines.

2.3.8 Purification of DNA fragments

DNA fragments were isolated by electrophoresis. Typically on a 0.8% TBE gel. For DNA fragments less than 500 base pairs, a 1% TBE gel was used. The DNA fragments were analysed using a UV transilluminator. The DNA band was excised using a clean scalpel and purified from the gel using a QIAGEN gel purification kit, according to the manufacturer's instructions.

2.3.9 Ligations

Ligations were carried out using T4 DNA ligase (Roche) according to the manufacturer's guidelines. Typically, the vector and insert were ligated in a 1:3 molar ratio with 2 μl 10 x T4 ligase reaction buffer (Roche) and 1 μl T4 DNA ligase (Roche) (1 unit/μl) in a final reaction volume of 20 μl. The ligation mixture was incubated at room temperature for a minimum of 4 hours before being transformed into NM522 cells.

2.3.10 Amplifying plasmid DNA

2.3.10.1 DISH minipreps

A 2 ml L-Broth culture, supplemented with the appropriate selective antibiotic was inoculated with a single colony and grown for ~4 hours at 37^{o}C, with shaking. 1 ml of the cell culture was harvested at 13,000 rpm for 5 minutes and the supernatant discarded. The cell pellet was re-suspended in 100 μl DISH I solution. 200 μl DISH II was added and the sample mixed by inversion. 150 μl ice cold DISH III was added and the sample mixed by inversion. 200 μl phenol chloroform was added and the sample vortexed. The sample was then spun at 13,000 rpm for 15 minutes and the top aqueous layer removed to a clean microcentrifuge tube containing 750 μl 100% ethanol. The sample was spun for a further 5 minutes at 13,000 rpm and the supernatant removed. The DNA pellet was dried for approximately 10 minutes in a dessicator before being re-suspended in 40 μl 1x TE containing 20 μg/ml RNase. 5 μl of the DNA sample was analysed on an agarose gel.

DISH I

9 g/L	Glucose
3 g/L	Tris-base
3.72g/L	EDTA

DISH II

0.2 M	NaOH
1%	SDS

DISH III

3 M	KOAc
11.5%	Glacial acetic acid

Phenol/chloroform

24 Volumes	Equilibrated phenol
25 Volumes	Chloroform
1 Volume	Isoamyl alcohol.

Phenol equilibration

Phenol (Pre-equilibrated with 10 mM Tris-HCl, pH 8, 1 mM EDTA) (Sigma-Aldrich) was adjusted to pH 7.9 by incubating overnight at room temperature with equilibration buffer as according to manufacturer's guidelines.

2.3.10.2 Qiagen minipreps

If the DNA was to be sequenced, minipreps were carried out using a QIAGEN miniprep kit according to the manufacturer's guidelines.

2.3.10.3 Midipreps

Midipreps were carried out using a QIAGEN midiprep kit according to the manufacturers' guidelines.

2.3.11 Sequencing

2.3.11.1 In-house sequencing

Sequencing was carried out using the BigDye Terminator v1.1 kit (Applied biosciences). Approximately 500 ng of the DNA to be sequenced was used per 20 μl sequencing reaction. 5 μl reaction buffer, 3 μl primer (10 μM), and 2 μl enzyme mix were added to the template DNA in a 20 μl final volume. The PCR programme and subsequent ethanol precipitation of the PCR product was carried out as according to the manufacturers

guidelines. The sample was re-suspended in 25 μl highly deionised formamyde and heated to 95°C for 2 minutes before analysis by an ABI PRISM 310 Genetic Analyser.

2.3.11.2 Sequencing by GATC

DNA samples and sequencing primers were sent to GATC for sequencing. 30 μl DNA (30-100 ng/μl) and 30 μl corresponding primer (30 pmol/μl) were required.

2.3.12 Southern blot

Genomic DNA was extracted and the DNA fragment of interest was isolated by restriction enzyme digest. 5 μg DNA was digested with *Bcl*I in a reaction volume of 30 μl. The digested DNA was run on a 0.8% TBE gel. The gel was then washed for 30 minutes in depurination buffer, 30 minutes in denaturation buffer and finally 30 minutes in neutralisation buffer with gentle shaking at room temperature. The gel was blotted onto a genescreen (PerkinElmer) membrane overnight in 20 x SSC buffer. Following blotting, the DNA was crosslinked to the membrane by exposure to 1200 μJ. To prehybridise the membrane, the membrane was incubated for 30 minutes in 80 ml hybridisation buffer with 266 μl 30 % BSA added. The membrane was then incubated overnight at 65°C in 20 ml hybridisation buffer containing 50 μl DNA probe (Section 2.3.13). Following hybridisation, the membrane was washed in 500 ml wash buffer 1 for 15 minutes at 65°C, followed by 2 x 20 minutes in 500 ml wash buffer 2 at 42°C. The membrane was then exposed to a phosphocassette overnight. The signal was detected by a phosphoimager.

Depurination Buffer

0.25 M	HCl

Denaturation Buffer

0.5 M	NaOH
1.5 M	NaCl

Neutralisation Buffer

1 M	Tris/HCl
1 M	NaCl.

Adjusted to pH 7.4

20 x SSC

3 M	NaCl
0.3 M	Sodium citrate

Adjusted to pH 7

Hybridisation Buffer (100 ml)

30 ml	20x SSC buffer
1 ml	Denhardt's solution
3.33 ml	30 % N-Lauryl sarcosine salt solution

Denhardt's Solution (100x)

20 g/l	Ficoll
20 g/l	Polyvinylpyrrolidone
20 g/l	BSA

Wash Buffer 1 (500 ml)

50 ml	20x SSC
50 ml	SDS (10%)

Wash Buffer 2 (1 litre)

5 ml	20x SSC
10 ml	SDS (10%)

2.3.13 Labelling DNA Probe

The *ura4*$^{+}$ DNA probe was isolated from the pKSUra plasmid as a *Hind*III fragment. 100 ng DNA probe was labelled with ^{32}P using the *Radprime Labeling* kit (Sigma-Aldrich) according to the manufacturer's guidelines.

2.3.14 Primers

Table 2.5 indicates the primers used during this study. All primers were diluted in water to a concentration of 10 μM and stored at -20^{o}C.

2.4 PROTEIN METHODS

2.4.1 SDS polyacrylamide gel electrophoresis (SDS-PAGE)

SDS PAGE gel electrophoresis was carried out using *Biorad Mini Protean II* kits. Protein samples were resolved on 7.5, 10 or 12.5% separating gels. Polymerisation was achieved by the addition of 10% ammonium persulphate (APS) and TEMED to the separating buffer. The pre-polymerised gel solution was poured between glass plates separated with 0.75 mm plastic spacers and left to set for approximately 30 minutes with a layer of distilled water on top to achieve a level surface. Once set, the water layer was poured off and the plates dried with *Whatman* paper. The stacking gel (3%) was poured on top of the separating gel and the gel comb positioned. After approximately 30 minutes the comb was removed and the gel kit assembled. Protein samples were mixed with 5 x sample buffer and denatured at 95^{o}C for 5 minutes. 10-25 μl of sample were loaded into each well. 8 μl of benchmark protein ladder (Invitrogen) was loaded into the end lane as a size indicator. Gels were run in 1 x SDS running buffer at 150 V for approximately 1 hour or until the dye front reached the bottom of the gel.

Table 2.5: Primers used in this study

Primer	Forward /reverse	Primer sequence (5' to 3')
L17	F	GTGCTATCTCCTGTGTAA
L18	F	GTTCTCCAGTTAGCCGTA
L19	F	GTTATCCTCGGTAACTGA
L26	F	TCAAAAGAATAAAAGAATTGGAAGTGGAAAAGTTATCCTCGGTAACT GAAGATTCAACTGCTCAAACGTGTAAACTTTAACGGATCCCCGGGTTA ATTAA
L27	R	CGTGATCATTCTATAAAAGTATTATGGCGGTAATTAAATATAAGAAAG AACAATGGTAAAAGTAAGAGCCAAATATCCTTGAATTCGAGCTCGTTT AAAC
L28	F	GTGAATGGTTAGATCCCAACGATCAAGTGCAAAGCACGGAACTTGAA GATGAAGATCAAGTTAGTGTTGTTTTGGATTAACGGATCCCCGGGTTA ATTAA
L31	F	GTTTGGTTGTGCATGCCTACTGTCACTCGG
L33	F	CACTCAAAAGAATAAAAGAATTGGAAGTGGAAAAGTTATCCTCGGTA ACTGAAGATTCAACTGCTCAAACGTGTAAACTTCGGATCCCCGGGTTA ATTAA
L34	F	GAAGTGAATGGTTAGATCCCAACGATCAAGTGCAAAGCACGGAACTT GAAGATGAAGATCAAGTTAGTGTTGTTTTGGATCGGATCCCCGGGTTA ATTAA
L35	R	GCAGTGTACGAACAAGCAATAATGCC
L37	F	GCTTTTGCGTTCGAGTAGGAGTGAGGATCTTCG
L38	R	CGAAGATCCTCACTCCTACTCGAACGCAAAAGC
L40	R	GGTAAAAGTAAGAGCCAAATGTCGACTTAATCCAAAACAACAC
L41	F	CCGTAATTGCTAAAACTCGCCATATGGACAACCTAGATGAAGATG
L45	F	GCCTAGGTAAAATTGGGTACCTTCCTTAGAATC
L56	F	CCGTCGATTTCACTGTTAGAGATTTGATTAAGAG
L57	R	CTATTAATCAAATCTCTAACAGTCAAATCGACGG
L58	F	CACTGTTAAAGATTTGATTAGGAGATATTGTACTG
L59	R	CAGTACAATATCTCCTAATCAAATCTTTAACAGTG
L60	F	GTACTGAAGTAAGGATTAGTTTTCATGAACGC
L61	R	GCGTTCATGAAAACTAATCCTTACTTCAGTAC
L63	F	GCTTTTGCGTTCGAGTAAGAGTGAGGATCTTCG
L64	R	CGAAGATCCTCACTCTTACTCGAACGCAAAAGC
L65	F	GTACTGAAGTAAAGATTAGTTTTCATGAACGC
L66	R	GCGTTCATGAAAACTAATTCTTACTTCAGTAC
L68	F	GCGTACTCTGAACATATGAAAGTAGATAACG
L72	F	ACATTATACGAAGTTATCGGGCGGCGGGGGTGGTATGGACAACCTAGA TGAAGATGAC
L73	R	CGTGTGAATTTGTACATCCATATCAC
L74	R	TTCCGCGGCCGCTATGGCCGACGTCGACCCTACCTTCCTCTTCTTCTTC GGAAGTTTACACGTTTGAGC
L75	F	GGAATATCGGCTGATTAAACC
L78	F	CGTACTCTGAAAGAAGAAGAGTAGATAACG
L79	R	CGTTATCTACTCTTCTTCTTTCAGAGTACG
L80	R	CAGTGAATAATTCTTCACCTTTAGACATTTGGCGAGTTTTAGCAATTAC GG
L88	R	GCAACGTTATTTATTTACACGTTTGAGC
L91	R	ACCACCCCCGCCGCCCGATAACTT

L94	F	ATGTCTAAAGGTGAATTATTCACTG
L96	R	TTAATTAACCCGGGGATCCG
L109	F	CAAAGCCTATTAGAAGGCCTCCATTAAACTATGCC
L110	R	GGCATAGTTTAATGGAGGCCTTCTAATAGGCTTTC
L111	F	GGTATGCTTAGAGTCGATACCCG
L112	R	CGGGTATCGACTCTAAGCATACC
L113	F	GCTCAAACGTGTAGACTTATAACGTTGC 3’
L114	R	GCAACGTTATAAGTCTACACGTTTGAGC
L117	F	GACGCGTCGACATGTCTGAATCACCAGCAAAC
L118	R	CGCGGATCCCTAAGGCATAGATGGGTGCAACC
L125	F	CCAGTTATTTCCGCCGCTCTCCAGTTAGCCG
L126	R	CGGCTAACTGGAGAGCGGCGGAAATAACTGG
L127	F	GTAGATAACGTTGCTCTTGCATTTCAAAATTC
L128	R	GAATTTTGAAATGCAAGAGCAACGTTATCTAC
L129	F	GAAGATCAAGCTAGTGCTGTTTTGGATTAA
L130	R	TTAATCCAAAACAGCACTAGCTTGATCTTC
L140	F	GGTGAATGGTTAGATCCCAACGATCAAGTGCAAAGCACGGAACTTGA AGATGAAGATCAAGTTAGTGTTGTTTTGGATTAAAAGCTTAGCTACAA ATCCCA
L141	R	CGTGATCATTCTATAAAAGTATTATGGCGGTAATTAAATATAAGAAAG AACAATGGTAAAAGTAAGAGCCAAATATCCTTGAATTCGAGCTCGTTT AAAC
L142	R	TGGGATTTGTAGCTAAGCTT
L143	F	ATGGACGGACGCAATGTAGCCGTCGTAAGGTGAGCCAATGTCATTGAA ATTCATCAAACCTAATGTCTCAGTACAAGAAGTAGAATACTCAAGCTT GGAC
L144	R	ACCCGATCTTGTCCACTTAGCAAACAGATTTAAGTCTATAGAATTTCAT TTTTTAGGTTAAGTAATTTGAAAACTCTTTGTTCACCACCCCCGCCGCC CG
L150	F	ACAAATTATGAATGGCAGTAATGGACGGACGCAATGTAGCCGTCGTAA GGTGAGCCAATGTCATTGAAATTCATCAAACCTAATGTCTCAGTACAA GAAGTAGAATACTC AAGCTTGGAC
L151	R	AGTTTGTTTACTTACGCAAAACCCGATCTTGTCCACTTAGCAAACAGAT TTAAGTCTATAGAATTTCATTTTTTAGGTTAAGTAATTTGAAAACTCTT TGTTCACCACCCCCGCCGCCCG
L156	F	GTACAAATTCACACGCATAGGAGAGAAATTGAAGAAGACG
L157	R	CGTCTTCTTCAATTTCTCTCCTATGCGTGTGAATTTG TAC
L158	F	CGCTGTATCACTCCAGATCGGAATTCTCAAC
L159	R	GTTGAGAATTCCGATCTGGAGTGATACAGCG
L170	F	GTACCTGAATAGTCTACTACTG
L172	R	GCGACACACCTTAAACTAGG
L179	R	TCAGTTACCGAGGATAAC
L202	F	CAGTTTCGTCGTGGCAGAATAGCGTACTCT
L210	F	CAAACG TGTAAACTTATAACGGTGCTTTTGCGTTCGAG
L211	R	CTCGAACGCAAAAGCACCGTTATAAGTTTACACGT TTG
L212	F	CAAACGTGTAAACTTATAACGGGGCTTTTGCGTTCGAG
L213	R	CTCGAACGCAAAAGCCCCGTTATAAGTTTACACGT TTG
L214	F	GTGAGGATCTTCGTGTCTCAATACCCGTCG
L215	R	CGACGGGTAT TGAGACACGAAGATCCTCAC
L216	F	GTGAGGATCTTCGTGGCTCAATACCCGTCG
L217	R	CGACGGGTATTGAGCCACGAAGATCCTCAC
L219	F	CGATTTCACTGTTAAAGATGTGATTAAGAGATATTGTACTG
L220	R	CAGTACAATATCTCTTAATCACATCTTTAACAGTGAAATGG
L221	F	CGATTTCACTGTTAAAGATGGGATTAAGAGATATTGTACTG

L222	R	CAGTACAATATCTCTTAATCCCATCTTTAACAGTGAAATGG
L223	F	GATTTGATTAAGAGATTTTGTACTGAAGTAAAG
L224	R	CTTTACTTCAGTACAAAATCTCTTAATCAAATC
L225	F	GATTTGATTAAGAGAGGTTGTACTGAAGTAAAG
L226	R	CTTTACTTCAGTACAACCTCTCTTAATCAAATC
L227	F	CGTGTATAACGTTGCTTGTGCGTTCG AGTAAGAG
L228	R	CTCTTACTCGAACGCACAAGCAACGTTATACACG
L229	F	CGTGTATAACGTTGCTTGGGCGTTCGAGTAAGAG
L230	R	CTCTTACTCGAACGCCCAAGCAACGTTATACACG
L231	F	GTAAGAGTGAGGATGTTCGTCTCTCAATACC
L232	R	GGTATTGAGAGACGAACATCCTCACTCTTAC
L233	F	GTAAGAGTGAGGATGGTCGTCTCTCAATACC
L234	R	GGTATTGAGAGACGACCATCTCACTCTTAC
L235	F	CTTCGTCTCTCACTACCCGTCGATTTCAC
L236	R	GTGAAATCGACGGGTAGTGAGAGACGAAG
L237	F	CTTCGTCTCTCAGGACCCGTCGATTTCAC
L238	R	GTGAAATCGACGGGTCCTGAGAGACGAAG
L239	F	GCTCAAACGTGTAAACTTTTAACGTTGCTTTTGCG
L240	R	CGCAAAAGCAACGTTAAAAGTTTACACGTTTGAGC
L241	F	GCTCAAACGTGTAAACTTGGAACGTTGCTTTTGCG
L242	R	CGCAAAAGCAACGTTCCAAGTTTACACGTTTGAGC
L245	F	CATCAAACCTAATGTCTCATATGGAGCTCCAAAGAGTTTTCAAATTACTTAACC
L254	F	GAGAGATATTGCTGTTTGGCTCGAGAATTCTCTGTCC
L255	R	GGATTTTATATCACTCCTCGAGAAAAGAATAAAAGAATTGG
L256	F	CCAATTCTTTTATTCTTTTCTCGAGGAGTGATATAAAATCC

Separating gels: (To make 2 mini gels)

Separating Gel		**7.5%**	**10%**	**12.5%**
Protogel	(ml)	2.5	3.3	4.2
4x separating buffer	(ml)	2.5	2.5	2.5
Distilled water	(ml)	5.0	4.2	3.3
10% APS	(µl)	100	100	100
TEMED	(µl)	10	10	10

Stacking gels: (To make 2 mini gels)

Stacking Gel		**3%**	**6%**
Protogel	(ml)	0.5	1.0
4x stacking buffer	(ml)	1.3	1.3
Distilled water	(ml)	3.3	2.8
10% APS	(µl)	50	50
TEMED	(µl)	10	10

4 x Separating Buffer

1.5 M	Tris HCl, pH 8.8
0.4%	SDS

4 x Stacking Buffer

0.5 M	Tris HCl, pH 8.8
0.4%	SDS

5 x Sample Buffer

60 mM	Tris HCl, pH 6.8
25%	Glycerol
2%	SDS
14.4 mM	β-mercaptoethanol
10%	Bromophenol blue

10 x SDS-PAGE Buffer

25 mM	Tris HCl, pH 8.3
192 mM	Glycine
0.1%	SDS

2.4.2 Coomassie Brilliant Blue Staining

An SDS-PAGE gel was placed in Coomassie gel stain at room temperature for ~ 1 hour with gentle shaking. The gel was then briefly washed in water and then placed in destain solution overnight with gentle shaking. To dry the SDS-PAGE gel, the gel was placed on Whatman 3 MM paper and dried for 1 hour on a gel dryer.

Coomassie Gel Stain

1 g/l	Coomassie Brilliant Blue (Sigma)
45%	Methanol
10%	Glacial acetic acid

Destain Solution

10%	Methanol
10%	Glacial acetic acid

2.4.3 Western Blotting

Twelve pieces of Whatman 3 MM paper and one piece of PVDF membrane (millipore) were cut to the same size as the SDS-PAGE protein gel. The Whatman 3MM papers were soaked in blotting buffer and 6 pieces were stacking on top of each other and placed on the Electroblotter (Biorad). The PVDF membrane soaked in methanol and then placed on top of the 6 Whatman sheets. The protein gel was laid on top of the membrane and the remaining 6 soaked Whatman papers placed on top. Bubbles were removed by rolling a thick marker pan over the stack. The electroblotter was run at 100 mA for 35 minutes per gel. Following blotting the PVDF membrane was transferred to a container containing 4% milk (in PBS) and was blocked for at least 30 minutes at room temperature or overnight at $4^{o}C$ with gentle shaking.

Semi-Dry Transfer Buffer

48 Mm	Tris-Base
39 mM	Glycine
0.04%	SDS
Methanol	20%

2.4.4 Incubation of PVDF membrane with antibodies

Following blocking in 4% milk (in PBS), the PVDF membrane was incubated in 10 ml milk containing the primary antibody. Primary antibodies were typically used at a 1:2,000 dilution in 4% milk (in PBS) and incubated overnight at 4^{o}C with gentle shaking. Alterations to this general protocol were made depending on the efficiency of the particular antibody. The blot was washed with 3 x 10 minute washes in PBS containing 0.1% Tween 20 and 1 x minute wash with PBS. Following washing, 10 ml 4% milk (in PBS) was added to the membrane and an HRP-conjugated secondary antibody was added to a final dilution of 1:2,000. The blot was left to incubate at room temperature for approximately 90 minutes with gentle shaking. The previous 10-minute wash steps were repeated (3 x PBS with 0.1% Tween, 1 X PBS) and the proteins detected by ECL (Section 2.4.5).

2.4.5 Enhanced Chemi-Luminescence (ECL)

The washed membrane was placed in 10 ml of 100 mM Tris-HCl, pH 8.5 with 3 μl hydrogen peroxide, 50 μl 250 mM luminol and 25 μl 90 mM p-coomaric acid. The blot was incubated for ~1 minute with slight agitation before being removed from solution and wrapped in Saran wrap. In a dark room, the membrane was exposed to X-ray film (Kodak) for varying lengths of time depending on the intensity of the signal.

2.4.6 Determining protein expression and solubility

A single BL21(DE3) colony, carrying the appropriate expression vector, was used to inoculate 2 ml of L-broth media containing chloramphenicol and the appropriate selective antibiotic. The culture was grown overnight at 37^{o}C with shaking. The following morning 1 ml of this pre-culture was used to inoculate 10 ml of media. The cells were incubated at 37^{o}C, with shaking until an A_{595} reading of ~0.6 was reached. At this point 1 ml of each

culture (non-induced) was removed and placed in a fresh tube. Cells in the remaining 9 ml culture were induced with an appropriate concentration of IPTG and grown with the non-induced samples for either a further 1 or 3 hours at 37°C. 1 ml of cells was harvested at 13,000 rpm for 5 minutes and the pellet re-suspended in X ml (X = A_{595} reading/ 4) of an appropriate buffer (NETN (section 2.4.8) for GST-fusion proteins). The sample was sonicated for 15 seconds on ice and then spun at 13,000 rpm for 5 minutes. The supernatant was transferred to a fresh microcentrifuge tube and one-fifth 5 x sample buffer added. The pellet was re-suspended in X ml 5 x sample buffer. Samples were boiled for 5 minutes and analysed by SDS-PAGE (Section 2.4.1) followed by Coomassie staining (Section 2.4.2).

2.4.7 Bradford assay

To determine protein concentration of a sample the Bradford assay reagent (Biorad) was diluted 1 in 5 with water. 1-5 μl protein sample was added to 1 ml of the diluted Bradford reagent. The OD A_{595} was measured as compared to a 1 ml reagent only 'blank'. The protein concentration of the sample was determined by comparing the sample reading against a BSA standard curve.

2.4.8 GST-tagged protein purification

2.4.8.1 GST-tagged protein purification

A single BL21(DE3) colony, carrying the appropriate expression vector, was used to inoculate 2 ml of L-broth containing chloramphenicol and the selective antibiotic (amp). This pre-culture was grown at 37°C with shaking for ~8 hours. 1 ml of this was used to inoculate 100 ml pre-warmed media, which was grown overnight at 37°C. The following day this 100 ml pre-culture was used to inoculate a 1-litre pre warmed culture. When an A_{595} reading of 0.6 was reached, the cells were induced with IPTG at a final concentration of 5mM. After incubating for a further 3 hours at 37°C with shaking cells were harvested at 5,000 rpm for 10 minutes at 4°C and the supernatant discarded. The cell pellet was re-suspended in 10 ml ice cold NETN (freshly supplemented with PMSF to 0.1 mM, and 1 complete protease inhibitor cocktail tablet (Roche) per 50 ml buffer). The cells were sonicated on ice 3 times for 15 seconds with 1-minute intervals on ice. The cell extract was

cleared by centrifugation at 14,000 rpm for 15 minutes at 4°C. The supernatant was then added to 100 µl pre-washed glutathione-sepharose beads (Amersham) equilibrated with NETN. The beads were incubated for 2 hours at 4°C on a rotating wheel. The beads were washed 7 times in total (3 x 1 ml NETN, followed by 3 x 1 ml wash buffer and 1 x PBS). Washing was carried with a brief spin at 13,000 rpm to pellet the beads. Following this spin, the supernatant was discarded and the beads were incubated with 1 ml of the appropriate buffer on a rotating wheel for 5 minutes at 4°C. Protein was collected either by glutathione elution of the GST-fusion protein or thrombin cleavage of the protein from the GST bound to the beads.

NETN Buffer

0.5%	NP40
1 mM	EDTA
20 mM	Tris-HCl, pH 8.0
100 mM	NaCl
freshly supplemented with:	
0.1 mM	PMSF
1	protease inhibitor cocktail tablet (Roche) per 50 ml buffer

Wash Buffer

100 mM	Tris-HCl, pH 8.0
100 mM	NaCl
1 mM	EDTA

2.4.8.2 Glutathione elution of GST-tagged protein

Following the final PBS wash step in the GST-tagged protein purification protocol (Section 2.4.8.1) the GST-fusion protein was eluted from the beads by adding 250 µl of elution buffer and incubating on a rotating wheel for 30 minutes at 4°C. After a 15 second spin at 2,500 rpm the supernatant was kept. This elution step was repeated a further two times and

5-10 µl of the elution samples were analysed by SDS-PAGE (Section 2.4.1) followed by Coomassie staining (Section 2.4.2).

Elution Buffer	
100 mM	Tris-HCl, pH 8.0
120 mM	NaCl
20 mM	Glutathione

2.4.8.3 Thrombin cleavage

Following the final PBS wash step in the GST-tagged protein purification protocol (Section 2.4.8.1). The beads were re-suspended in 200 µl PBS and thrombin (Sigma) added to a concentration of ~1 unit/mg protein. The sample was incubated on a rotating wheel for 1 hour at room temperature. The beads were pelletted by centrifuging at 2,000 rpm for 30 seconds and the supernatant removed to a clean microcentrifuge tube. To ensure all beads were removed the sample was centrifuged again at 2,000 rpm for 30 seconds and the supernatant transferred to a clean tube. 5-10 µl of the protein sample was then analysed by SDS-PAGE (Section 2.4.1) followed by Coomassie staining (Section 2.4.2).

2.4.9 His-tagged protein purification

A 10 ml culture of the BL21 strain carrying the appropriate expression vector was grown overnight at 37^{o}C in L-broth containing chloroamphenicol and the selective antibiotic. The pre-culture was used to inoculate a 1-litre culture of pre-warmed L-broth, containing the appropriate selective antibiotic. The culture was incubated at 37^{o}C for ~4 hours until the OD_{550} reached 0.6-0.8. IPTG was added to a final concentration of 1 mM and the cells incubated for a further 4 hours at 37^{o}C. The cells were harvested at 5,000 rpm for 5 minutes and the supernatant discarded. The cell pellet was placed at –20^{o}C for at least an hour, before being re-suspended in 20 ml ice-cold binding buffer freshly supplemented with 0.1 mM PMSF. The cells were sonicated on ice for 5x 15 seconds, with 30 second intervals on ice. The cell extract was cleared by centrifugation at 14,000 rpm for 15 minutes at 4^{o}C. The supernatant was gradually applied to a 10 ml column containing pre-washed Ni^{2+}-agarose beads equilibrated with binding buffer at 4^{o}C. Once the supernatant has passed through the

column by gravity, the column was washed with 10 column volumes of binding buffer, freshly supplemented with PMSF, followed by 10 column volumes of wash buffer containing PMSF. Elution buffer was added to the column and 0.5 ml fractions were collected on ice. The protein concentration of each elution was obtained by Bradford assay and ~5 μg protein was analysed by SDS-PAGE.

Binding Buffer

5 mM	Imidazole
0.5 M	NaCl
20 mM	Tris HCl, pH 7.5

Wash Buffer

20 mM	Imidazole
0.5 M	NaCl
20 mM	Tris HCl, pH 7.5

Elution Buffer

500 mM	Imidazole
0.5 M	NaCl
20 mM	Tris HCl, pH 7.5

2.4.10 Affinity purification of crude anti-sera

2.4.10.1 Preparation of the Rad60 affinity column

Affinity purification of crude anti-sera was carried out using the AminoLink®Plus Coupling Gel kit (PIERCE Biotechnology). A column containing 3 ml AminoLink®Plus Coupling Gel was equilibrated with 3 column volumes of Coupling Buffer, pH 10. Purified protein (His-tagged Rad60) was diluted in a 1:3 ratio with coupling buffer, pH 10. The diluted protein sample (final concentration of 1-20 mg/ml) was added to the column. The column was sealed and mixed by gentle end-over-end rocking for 4 hours at 4^{o}C. The column was then washed with 3 column volumes of Coupling Buffer, pH 7.2. 1 column volume of

Coupling Buffer, pH 7.2 and 0.02 column volumes of cyanoborohydride solution was added to the column. The column was sealed and mixed overnight by gentle end-over-end rocking at 4^{o}C. The column was allowed to drain and the flow through collected. Protein content was checked by Bradford assay to ensure protein had been bound. To block the remaining active sites, the column was first washed with 2 column volumes of Quenching Buffer, and then 1 column volume of Quenching Buffer with 0.02 column volumes of cyanoborohydride solution. The column was sealed and mixed gently by end-over-end rocking for 30 minutes. The column was allowed to drain before being washed with 20 column volumes of Wash Solution. To check that the protein would not be immobilised in the elution step, the column was washed with 100 mM glycine, pH 2.3. The flow through was collected and the protein content determined by Bradford assay. To re-equilibrate, the column was washed with 10 column volumes of Quenching buffer followed by 10 volumes of Wash buffer. The column was then washed with 10 column volumes of PBS.

2.4.10.2 Affinity purification of crude anti-sera

6 ml crude anti-sera was diluted in one-tenth volume of 10x PBS and added to the column. The column was sealed and incubated at 4^{o}C overnight on an end-over-end rocker. The column was drained and the flow-through collected. The column was then washed with 10 column volumes of PBS. Bound antibody was eluted with 1 column volume of 100 mM glycine, pH 2.3 and the flow through collected in 1 ml fractions. The antibody fractions were neutralised by adding 100 µl 1 M Tris-HCl, pH 7.5. The antibody concentration was analysed by Bradford assay and the purity checked by SDS-PAGE (Section 2.4.1).

2.4.10.3 Regenerating and storing the affinity column

Following elution with glycine, the column was washed extensively with PBS. PBS containing 0.05% sodium azide was added and the column sealed. The column was stored upright at 4^{o}C for future use. To regenerate the column for affinity purification, the column was washed extensively with PBS, followed by 10 column volumes of Quenching buffer, 10 volumes of Wash buffer and 10 volumes of PBS. At this stage the column is ready for the anti-sera to be added.

Coupling Buffer, pH 10

0.1 M	Sodium citrate
0.05 M	Sodium carbonate

Solution adjusted to pH 10 and then filter sterilized

Coupling Buffer, pH 7.2

0.1 M	Sodium phosphate
0.15 M	NaCl

Solution adjusted to pH 7.2 and then filter sterilized

Quenching Buffer

1 M	Tris-HCl

Solution adjusted to pH 7.4 and then filter sterilized.

Cyanoborohydride Solution

Supplied by PIERCE

Wash Solution:

1 M	NaCl

2.4.11 Concentrating protein samples

Proteins were concentrated using a vivaspin column (Sartorius), according to the manufacturer's guidelines.

2.4.12 Total Cell Extracts

S. pombe cells were grown in 10 ml appropriate medium overnight. 1 x 10^8 cells were harvested at 3,000 rpm for 5 minutes and washed in 1 ml 20% (w/v) trichloro-acetic acid (TCA). The cell pellet was re-suspended in 200 µl 20% TCA, transferred to a screw cap ribolyser tube and an equal volume of glass beads was added. The cells were broken to ~50% lysis by ribolysing for 3 x 15 seconds, with 1 minute intervals on ice. 400 µl 5% (w/v) TCA was added and the bottom of the screw-capped tube was punctured with a hot

needle. The cell extract was spun into a clean microcentrifuge tube at 3,000 rpm for 5 minutes. The extract was then spun for a further 5 minutes at 13,000 rpm. The supernatant was discarded and the pellet re-suspended in 200 μl TCA sample buffer. The sample was then boiled and analysed by SDS-PAGE (Section 2.4.1).

TCA Sample Buffer	
250 mM	Tris HCl, pH 8.0
5%	Glycerol
0.4%	SDS
2.9 mM	β-mercaptoethanol
2%	Bromophenol blue

2.4.11 Ni $^{2+}$ agarose His_6-affinity purification from *S.pombe*

S. pombe cells transformed with pREP constructs were grown for ~6 hours in 10 ml minimal media, supplemented with the appropriate amino acids and containing thiamine (30 μM) to inhibit expression of the gene of interest from the *nmt* promoter of the pREP vector. The cells were washed of thiamine to induce protein expression by harvesting at 3,000 rpm for 5 minutes and washing twice with the appropriate selective minimal media, lacking thiamine. The cells were then re-suspended in 1 ml of the selective media and used to inoculate 100 ml of the same media. Protein expression was de-repressed by incubating the cells at 30^{o}C, with shaking for ~16 hours in the absence of thiamine. 60 OD units (A_{595}) of exponentially growing cells were harvested at 3,000 rpm for 5 minutes and washed in 1 ml binding buffer. The cell pellet was re-suspended in 500 μl binding buffer and an equal volume of glass beads was added. The cells were broken to ~50% lysis by ribolysing for 3x 15 seconds, with 1 minute intervals on ice. The lysed cells were diluted with the addition of another 500 μl of binding buffer and centrifuged for 13,000 rpm for 5 minutes. The supernatant was then added to a new micro centrifuge tube. 120 μl of charged Ni^{2+} beads (50% slurry) were washed four times in 1 ml binding buffer and re-suspended in 60 μl binding buffer (~60 μl beads, 60 μl binding buffer). 120 μl prepared beads were then added to the supernatant. The sample was then incubated on a rotating wheel at room temperature for 1 hour. The beads were pelleted at 3,000 rpm for 5 seconds and the supernatant was

discarded. The beads were washed three times with 1 ml binding buffer, three times with 1 ml wash buffer A, three times with 1 ml wash buffer B and twice with 1 ml PBS. His tagged protein was eluted from the Ni^{2+} beads by boiling the beads with 50 µl 5x sample buffer. The sample was then analysed by SDS-PAGE (Section 2.4.1).

Binding Buffer:

6 M	Guanidinium hydrochloride
0.1 M	NaH_2PO_4
10 mM	Tris HCl

Solution adjusted to pH 8.0 and then filter sterilized

Wash Buffer A:

8 M	Urea
0.1 M	NaH_2PO_4
10 mM	Tris HCl

Solution adjusted to pH 8.0 and then filter sterilized

Wash Buffer B:

8 M	Urea
0.1 M	NaH_2PO_4
10 mM	Tris HCl

Solution adjusted to pH 6.2 and then filter sterilized

2.4.12 ^{35}S-labelled *in vitro* transcription/translation

In vitro transcription-coupled translation of a protein of interest from a T7 promoter-containing plasmid was achieved using a TNT T7 coupled rabbit reticulocyte lysate system (Promega). In a typical reaction, 1 µg plasmid DNA was incubated with 2 µl ^{35}S-labelled methionine and TNT T7 Quick master mix to a a final volume of 40 µl. the reaction was incubated at 30^{o}C for 2 hours and the efficiency of the translation was checked by analysing 2 µl of the reaction by SDS-PAGE (Section 2.4.1). The protein gel was fixed in Fix solution for 30 minutes and then incubated in Destain (Section 2.4.2) for 10 minutes

before drying the gel. The dried gel was then exposed to a phosphoimager screen overnight and the results detected by a phosphoimager.

Fix Solution

50%	Methanol
10%	Acetic acid

2.4.13 *In vitro* sumoylation assay

An *in vitro* sumoylation assay as described previously (Ho, Warr et al. 2001)was used to test the sumoylation status of a protein *in vitro*. The protein of interest was radiolabelled with [^{35}S] methionine using the T7 TnT coupled rabbit reticulocyte lysate system (Promega) (Section 2.4.12). Typically, 2 μl of translated protein was incubated with 2 μl 10x *in vitro* assay buffer, 3 μg Hus5, 0.5 μg GST-Rad31/GST-Fub1, 0.12 U inorganic pyrophosphatase and 0.7 U creatine phosphokinase, with or without 10 μg His-Pmt3. The reaction was made to a final volume of 20 μl with dH_2O. The reactions incubated at 30 ^oC for 2 hours and analysed by SDS-PAGE (Section 2.4.1). The protein gel was fixed in Fix solution (Section 2.4.12) for 30 minutes and then incubated in Destain (Section 2.4.2) for 10 minutes before drying the gel. The dried gel was then exposed to a phosphoimager screen overnight and the results detected by a phosphoimager.

10x *in vitro* assay buffer

500 mM	Tris-HCl, pH7.5
50 mM	$MgCl_2$
50 mM	ATP
100 mM	Creatine phosphate

2.4.14 *In vitro* GST-pull down assay

A 100 ml culture of a BL21 strain carrying the GST-expression construct of choice was grown at 37^oC, with shaking until A_{595} 0.6 was reached. Cells were then induced with 1 mM IPTG and grown for a further 3 hours at 37^oC, with shaking. Cells were harvested at 5,000 rpm for 5 minutes at 4^oC and the supernatant discarded. The cell pellet was re-

suspended in 1 ml binding buffer freshly supplemented with a protease inhibitor cocktail tablet (Roche). The cells were sonicated on ice for 3 x 15 seconds with 1-minute intervals on ice. The cell debris was cleared at 13,000 rpm for 3 minutes at 4°C. The supernatant was transferred to a new microcentrifuge tube. 20 µl of this supernatant was added to 180 µl binding buffer and incubated for 1 hour at 4°C with 30 µl glutathione-sepharose beads that had been pre-equilibrated in binding buffer. The beads were then harvested at 3,000 rpm for 5 seconds and washed twice with 1 ml binding buffer containing protease inhibitors. 5 µl ^{35}S- labelled protein was added to fresh binding buffer containing 1 mM ATP, 50 mM creatine phosphate and 1 U creatine phosphokinase in a 200 µl total volume (the input). This 200 µl sample was then added to the pre-bound glutathione beads and incubated on a rotating wheel for 1 hour at 4°C. The beads were harvested at 3,000 rpm for 5 seconds and a 10 µl sample of the supernatant was taken (unbound fraction). The rest of the supernatant was discarded and the beads were washed for 15 minutes in wash buffer 1, followed by 15 minutes in wash buffer 2. The protein was eluted by boiling in 30 µl 5 x sample buffer (bound fraction). The input, unbound and bound fraction were analysed by SDS-PAGE (Section 2.4.1) and detected using a phosphoimager and Western blotting (Section 2.4.3) with anti-GST antibody (1:2,000).

Binding Buffer

25 mM	HEPES, pH 7.8
150 mM	KCl
0.4 mM	EDTA
2 mM	EGTA
3 mM	$MgCl_2$
8%	Glycerol
0.1%	NP-40
0.5 mM	PMSF
0.2 mM	DTT

Wash Buffer 1

25 mM	HEPES, pH 7.8
200 mM	KCl
0.4 mM	EDTA
2 mM	EGTA
3 mM	$MgCl_2$
8%	Glycerol
0.1%	NP-40
0.5 mM	PMSF
0.2 mM	DTT

Wash Buffer 2

25 mM	HEPES, pH 7.8
100 mM	KCl
0.4 mM	EDTA
2 mM	EGTA
3 mM	$MgCl_2$
8%	Glycerol
0.1%	NP-40
0.5 mM	PMSF
0.2 mM	DTT

CHAPTER 3

The *S. pombe* Rad60 SUMO-like domain 2 is required for the DNA damage response

3.1 Introduction

The *rad60* gene was first identified in a screen designed to identify novel *S. pombe* genes involved in recombinational repair (Morishita, Tsutsui et al. 2002). Based on the observation that strains with mutations in recombination genes are often synthetically lethal with *rad2-d,* mutants both hypersensitive to MMS and synthetically lethal with *rad2-d* were isolated. The *rad60-1* mutant is hypersensitive to both MMS and IR, implicating *rad60* in the repair of DSBs. Rad60 is essential for viability (Morishita, Tsutsui et al. 2002). When Morishita *et al* carried out a search using the SSEARCH program of DDBJ no proteins homologous to Rad60 were identified. However, when searching for amino-acid sequence motifs in the PROSITE profile library, a match between amino acids 336 and 406 of Rad60 and the ubiquitin-2 motif was identified (Morishita, Tsutsui et al. 2002) During the course of this study, Rad60 was identified as a member of a novel family of proteins termed the RENi family, after its best-studied members *S. pombe* Rad60, *S. cerevisiae* Esc2 and *M. musculus* Nip45 (Novatchkova, Bachmair et al. 2005). With the exception of the plant members, proteins belonging to the RENi family share the unique feature of containing two C-terminal SUMO-like domains. Plant members contain only one SUMO-like domain. Since the biological functions of the RENi family members appear to be so different, the precise role of the SUMO-like domains remains unclear.

In this study I have begun an investigation into the importance of the two SUMO-like domains for Rad60 function. To analyse the importance of the Rad60 SLDs, I have created domain deletion mutants and analysed their phenotypes.

3.2 Rad60 has two SUMO-like domains

A ClustalW (http://www.ebi.ac.uk/tools/clustalw2/index.html) alignment of the Rad60 protein sequence (NCBI accession number NP_595995.1) against the *H. sapiens* SUMO-1 (AAC50996) and *S. pombe* Pmt3 (NP_596035.1) sequences identified two potential SUMO-like domains (Figures 3.1 A, B). The first alignment (Figure 3.1A) shows ~14%

Figure 3.1: The C-terminal region of Rad60 has two SUMO-like domains

(A, B) A ClustalW sequence alignment of Rad60 (NCBI accession number NP_595995.1) against *H. sapiens* SUMO-1 (AAC50996) and *S. pombe* Pmt3 (NP_596035.1) identifies two potential SUMO-like domains (underlined).* identical residues, **:** conserved substitutions, **.** semi-conservative substitutions. **(C)** Schematic to illustrate the position of Rad60 SLD1 and SLD2.

A

```
Hs_SUMO-1       ----------MSDQEAKPSTEDLGD------KKEGEYIKLKVIGQDSSE-IHFKVKMTTH  43
Sp_Pmt3         --MSESPSANISDADKSAITPTTGDTSQQDVKPSTEHINLKVVGQDNNE-VFFKIKKTTE  57
Sp_Rad60_SLD1   HSKSDHSTLYHSKSEFSTNEPVISVVLQLAVIGQRIPNSNISLPRDWEAPLFFKVKSNQQ 251
                          *. : ..     .         .    .   : :* .  :.**:* . .

Hs_SUMO-1       LKKLKESYCQRQGVPMNSLRFLFEGQRIADNHTPKELGMEEEDVIEVYQEQTGGHSTV-- 101
Sp_Pmt3         FSKLMKIYCARQGKSMNSLRFLVDGERIRPDQTPAELDMEDGDQIEAVLEQLGGCTHLCL 117
Sp_Rad60_SLD1   FRRVRIAYSER--KKVDNVVLVFQNQRLWDYGTPKGAGMLKVDTRLVVHAYCHSDFIS-- 307
                : ::   *. *    ::.: ::.:.:*:    **   .* . *   .      .
```

B

```
Hs_SUMO-1       --------MSDQEAKPSTEDLGD------KKEGEYIKLKVIGQDSSEIHFKVKMTTHLKK  46
Sp_Pmt3         MSESPSANISDADKSAITPTTGDTSQQDVKPSTEHINLKVVGQDNNEVFFKIKKTTEFSK  60
Sp_rad60_SLD2   AYCHSDFISLKRIKELEVEKLSSVTEDSTAQTCKLITLLLRSSKSEDLRLSIPVDFTVKD 358
                                              *.* : .....:: :.:     ...

Hs_SUMO-1       LKESYCQRQGVPMNS-LRFLFEGQRIADNHTPKELGMEEEDVIEVYQEQTGGHSTV--   101
Sp_Pmt3         LMKIYCARQGKSMNS-LRFLVDGERIRPDQTPAELDMEDGDQIEAVLEQLGGCTHLCL   117
Sp_Rad60_SLD2   LIKRYCTEVKISFHERIRLEFEGEWLDPNDQVQSTELEDEDQVSVVLD----------   406
                * : ** .   .::. :*: .:*: :  :.   .  :*: * :..  :
```

C

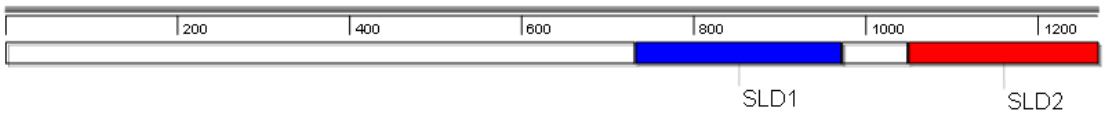

Figure 3.1: The C-terminal region of Rad60 has two SUMO-like domains

sequence identity between amino acid residues 228-307 of Rad60, Pmt3 and SUMO-1. Comparing the amino acid sequence of only Rad60 (228-307) and Pmt3, ~16% sequence identity was observed, whilst the sequence identity of SUMO-1 and Pmt3 is ~48%. The second alignment (Figure 3.1B) shows ~13% sequence identity between amino acid residues 334-406 of Rad60, Pmt3 and SUMO-1. Comparing the amino-acid sequence of only residues 334-406 of Rad60 and *S. pombe* Pmt3, ~21% sequence identity was observed. Although, by protein standards the sequence identity is low, it is important to note that SUMO-1 and ubiquitin share only ~18% sequence identity and, although functionally different, the two proteins share the same core structure consisting of a ββαββαβ fold. When we look more closely at the alignments between Rad60 and SUMO-1/Pmt3 there is significant conservation of the biochemical character of the side-chains. For example, residues with hydrophobic side chains (I, L, V) are substituted for one another. This suggests that the Rad60 SLDs may share a similar fold to that of SUMO/Pmt3. Unlike ubiquitin, SUMO contains an N-terminal flexible tail that protrudes from the hydrophobic core (Bayer, Arndt et al. 1998). The N-terminal tail is poorly conserved across SUMO species and is not required for sumoylating activity (Bylebyl, Belichenko et al. 2003). In the SUMO/Pmt3/Rad60 alignment, only the sequence relating to the core 'ubiquitin' fold of SUMO is conserved with the Rad60 SUMO-like domains. Unlike SUMO-1/Pmt3, the Rad60 SLDs do not contain the C-terminal diglycine motif required for covalent attachment to target proteins. Further analysis of the Rad60 SLDs is discussed in Chapter 6.

To analyse the importance of the two C-terminal SLDs I have created domain deletion mutants and analysed their phenotypes.

3.3 Rad60 SLD2 is not required for the essential function of Rad60.

Having identified two 'SUMO-like' domains in Rad60, the importance of SLD2 for Rad60 function was first tested. To investigate the role of this domain an *S. pombe* strain was created in which the C-terminal 73 amino acids were deleted (334-406). The C-terminal truncation of the essential *rad60* gene was introduced into the *S. pombe* genome by a one-step PCR-based gene disruption method (Bahler, Wu et al. 1998). The one-step PCR-based gene disruption method uses long primers containing 80 nucleotides of gene-specific

sequence and 20 nucleotides of sequence homologous to the pFA6a-kanMX6 template plasmid. The gene-specific sequence of forward primer L26 corresponded to 77 bases upstream of, and including, codon 333 of *rad60,* followed by a stop codon (TAA). In the reverse primer, L27, the gene-specific sequence corresponded to 80 bases immediately downstream from the *rad60* stop codon. Primers L26 and L27 were used to amplify a ~1.6 kb heterologous kanMX module from the pFA6a-kanMX6 plasmid. The products of 5 PCRs were pooled (~20 μg) and gel extracted to a volume of 20 μl. The DNA was transformed directly into haploid wild-type cells (*sp.011*) using the Bahler transformation protocol (Bahler *et al*, 1998). Cells were plated onto YEA plates and grown for 24 hours at 30^{o}C before being replica plated onto YEA plates containing 100 μg/ml G418. The replica plates were incubated at 30^{o}C for 72 hours and large colonies were re-streaked onto fresh YEA plates containing G418. Colony PCR, with primers L17 and L96, was used to screen transformants for successful integration (Figure 3.2B). Primer L17 anneals within the *rad60* gene and reverse primer L96 anneals within the kanMX6 cassette to give a PCR product of ~710 bp for colonies with the truncated copy of *rad60.* A wild-type strain, with no G418 resistance gene integrated was used as a negative control and gave no bands in the colony PCR (Figure 3.2C). The resulting C-terminal truncated Rad60 *S. pombe* strain was termed *rad60-ct* (*sp.1174*).

As a control for the integration of the kanMX6 cassette, a control strain (*rad60-FL (sp.1175)*) was created in which the G418 resistance gene was incorporated at the 3' end of the full-length *rad60* gene. Primers L28 and L27 were used to amplify the kanMX6 module and following integration, the presence of a ~940 bp colony PCR product, with primers L17 and L96, verified correct integration of the cassette (Figure 3.2C).

Although the colony PCR confirmed that the G418 resistance gene had been incorporated at the 3' end of the C-terminally truncated/full-length copy of the *rad60* gene, sequencing across the integration junction was required. Genomic DNA was extracted from the positive colonies and the region surrounding the junction site was PCR amplified from the genomic DNA using primers L41 and L96. Sequencing with primers L18 confirmed correct integration of the G418 resistance gene in the *rad60-ct* and *rad60-FL* strains. The presence

Figure 3.2: Cells deleted for Rad60 SLD2 are viable

(A) A copy of *rad60* deleted for SLD2 was introduced into the *S. pombe* genome by a one-step PCR based gene disruption method. (i) Long primers were used to amplify a heterologous kanMX6 module from the pFA6a-kanMX6 plasmid. (ii) The DNA was transformed directly into haploid wild-type cells (iii) A copy of the truncated *rad60* gene is incorporated via homologous recombination between the cassette and the genomic DNA. (iv) Positive transformants were identified by G418 (kan) resistance. **(B, C)** Colony PCR with primers L17/L96 confirmed the truncated copy of *rad60* had been incorporated in the *rad60-ct* cells. Wild-type cells, used as a negative control gave no band in the PCR, the *rad60-FL* control strain gave a PCR product of 940 bp and the *rad60-ct* cells gave a PCR product of ~710 bp (indicated with arrow).

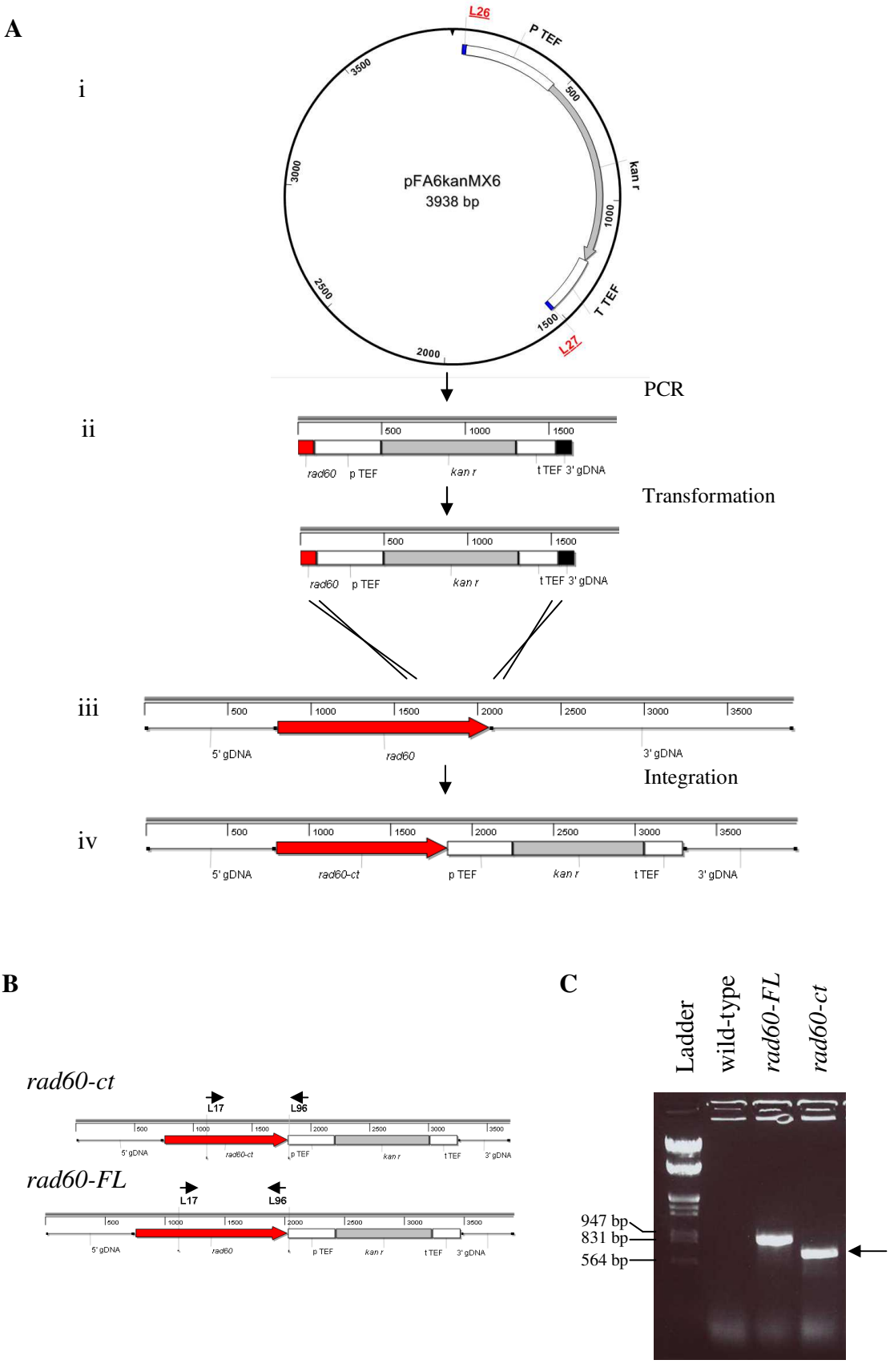

Figure 3.2: Cells deleted for Rad60 SLD2 are viable

of viable *rad60-ct* colonies indicates that the C-terminal SLD2 is not essential for *S. pombe* viability and is therefore not required for the essential role of Rad60.

3.4 The phenotype of *rad60-ct*

The previously published *rad60-1* (K263E) mutant is temperature sensitive for growth at 36°C but grows normally at 26°C (Morishita, Tsutsui et al. 2002). The *rad60-3* (F272V) and *rad60-4* (T72A, I232S, Q250R, K312N) mutants are temperature sensitive, growing best at 25°C. The ability of *rad60-ct* to grow at different temperatures was therefore assessed. Single colonies were streaked on YEA, and grown at 25, 30 and 36°C for ~72 hours. *rad60-ct* grows in a wild-type manner at 25°C and 30°C and like *rad60-1*, is temperature sensitive for growth at 36°C (Figure 3.3A). Wild-type and *rad60-FL* cells were streaked out as a control and, as expected, both grew well at all three temperatures. This suggests that the temperature sensitivity observed for *rad60-ct* is the direct result of deleting SLD2 and is not a consequence of the integrated G418 resistance gene.

Visualisation of *rad60-ct* cells under the microscope showed a phenotype reminiscent of the *smc6* mutants (Lehmann, Walicka et al. 1995; Verkade, Bugg et al. 1999). The cells were elongated, compared to wild-type and *rad60-FL* cells, with some cells having multiple septa (Figure 3.3B), suggesting a problem in DNA replication.

3.4.1 Rad60 SLD2 is required for the DNA damage response.

rad60 has been implicated in the response to DNA damage, in association with the Smc5/6 complex (Morishita, Tsutsui et al. 2002). To characterise the DNA damage response of *rad60-ct* cells to UV and IR, survival analysis was carried out. *rad60-ct* cells show ~15% survival after high doses of UV (200 J/m^2) and IR (1,000 Gy) (Figure 3.4A, B). This level of survival is comparable to that shown by *rad60-1* cells. Although *rad60-ct* cells are sensitive to UV and IR when compared to wild-type cells, they are less sensitive than the *smc6-X* mutant cells. Interestingly, like the *smc6-X* cells, *rad60-ct* cells grow more slowly than wild-type cells after exposure to UV irradiation, suggesting that they have a DNA repair phenotype. The sensitivity of *rad60-FL* cells was tested and, as anticipated, the sensitivity of the *rad60-FL* strain to UV and IR is similar to that of the wild-type *S. pombe*

Figure 3.3: Initial characterization of *rad60-ct*

(A) *rad60-ct* cells are temperature sensitive at 36^{o}C, but not at 25 and 30^{o}C. Cells were streaked on YEA and incubated at the indicated temperature for ~72 hours before being imaged. **(B)** *rad60-ct* cells are morphologically similar to *smc6* mutants. Cells were grown at 30^{o}C to exponential phase in YE medium and imaged using the Applied Precision Deltavision Spectris microscope.

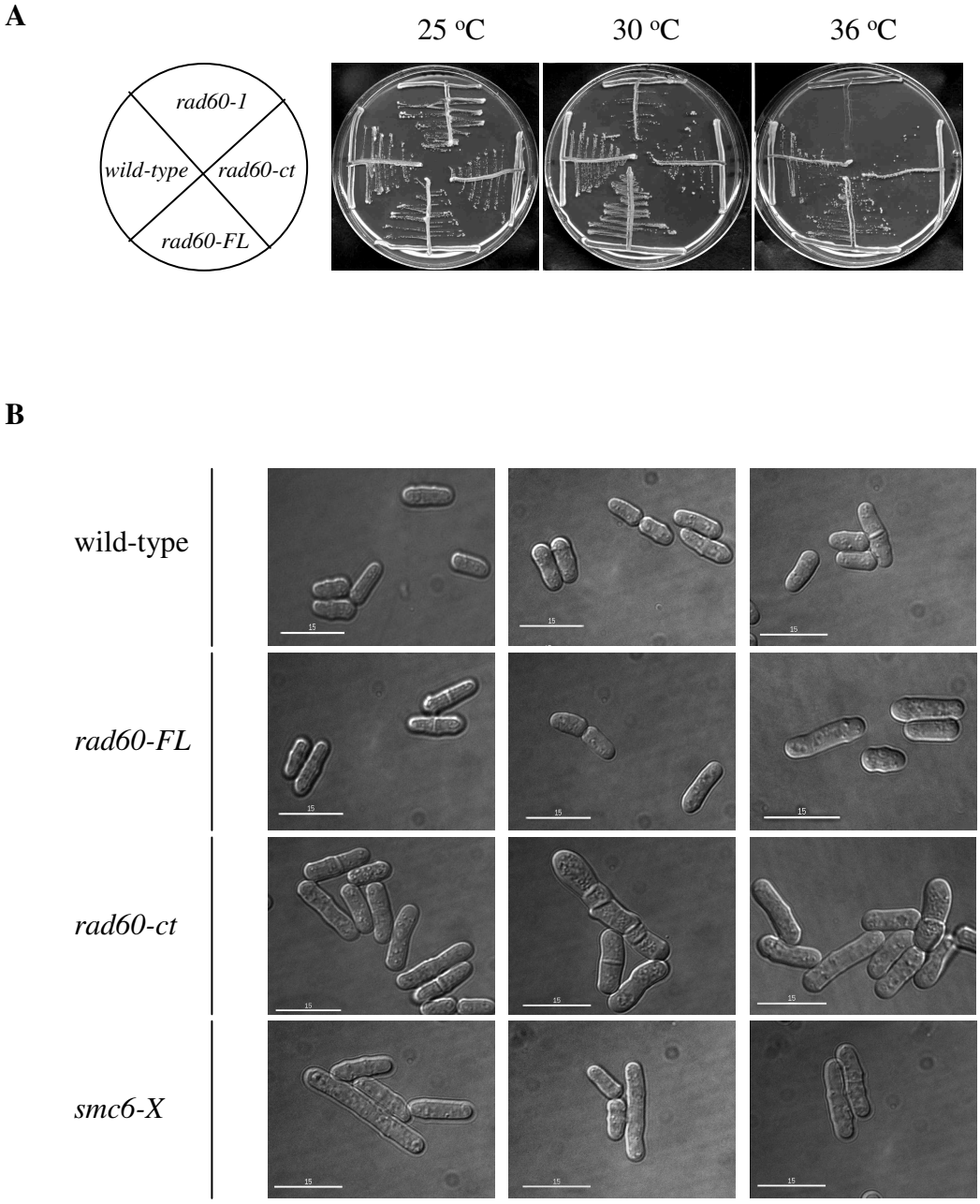

Figure 3.3: Initial characterisation of *rad60-ct*

Figure 3.4: Rad60 SLD2 is required for the DNA damage response

(A, B) *rad60-ct* cells are sensitive to UV and γ irradiation. Cells were grown at 30°C in YE medium to mid-exponential phase and irradiated with UV (A) or γ (B) rays at the indicated doses. Cells were plated on YEA and grown at 30°C for ~72 hours. Colonies were counted and % survival was calculated. **(C)** *rad60-ct* cells are sensitive to HU, MMS and 4NQO. Cells were grown at 30°C in YE mediium to mid-exponential phase. 10 μl of 10 fold serial dilutions were spotted onto YEA plates containing supplements at the indicated doses. Plates were incubated at 30°C for 72 hours and photographed.

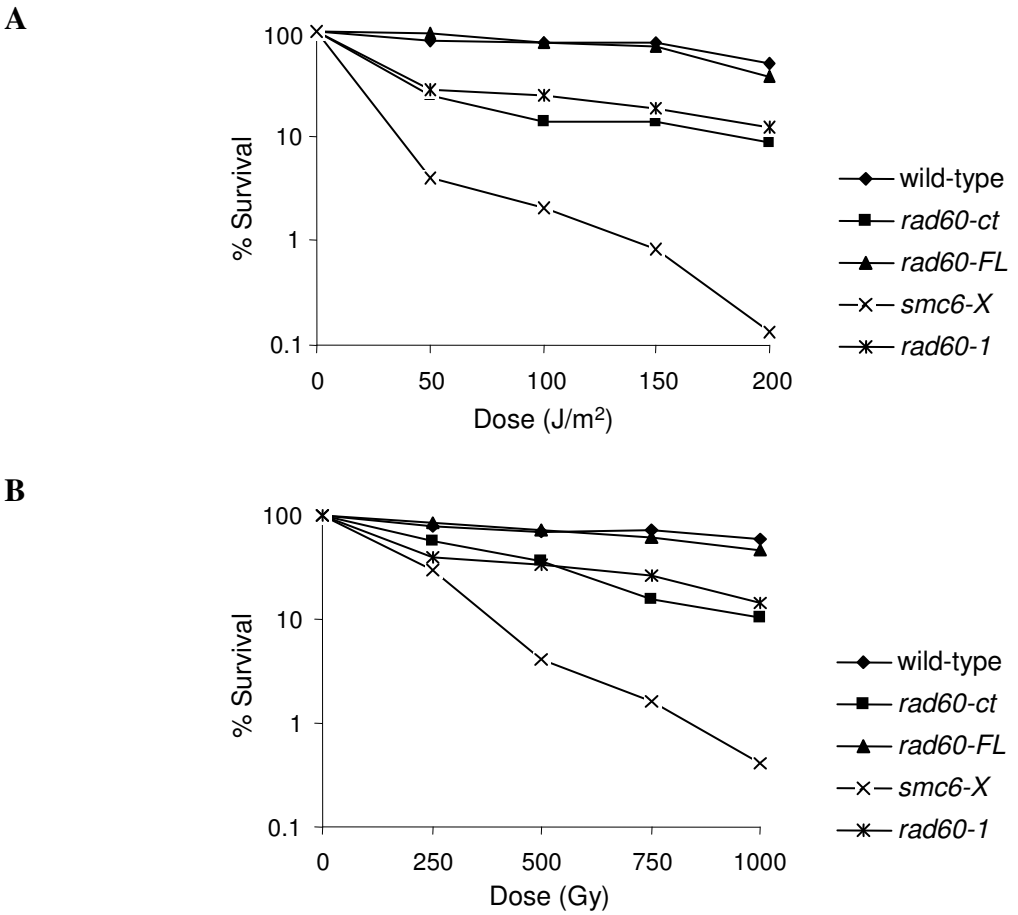

Figure 3.4: Rad60 SLD2 is required for the DNA damage response

cells (Figure 3.4A, B). This observation eliminates the possibility that the *rad60-ct* phenotype may be an indirect result of inserting the G418 resistance gene into the genome and suggests that the sensitivity shown by *rad60-ct* cells is the direct effect of deleting SLD2.

To further characterise the phenotype of the *rad60-ct* strain, spot tests were carried out. As expected, the sensitivity of the *rad60-FL* strain to the genotoxins; hydroxyurea (HU), thiabendazole (TBZ), 4-nitroquinoline-1-oxide (4NQO) and methyl methanesulfonate (MMS) is identical to that of the wild-type *S. pombe* cells (Figure 3.4C). In contrast, *rad60-ct* cells are hypersensitive to both MMS and HU, and to a lesser extent the UV mimetic 4NQO. Interestingly, the sensitivity of *rad60-ct* is comparable to that of *rad60-1* in response to MMS but not to HU and 4NQO. The *rad60-ct* cells are slightly more sensitive to HU and significantly more sensitive to 4NQO than the *rad60-1* cells. *rad60-ct* cells are less sensitive than the *smc6-X* to MMS, HU and 4NQO. The sensitivity of the *rad60-ct* cells to IR, MMS and HU suggests a defect in DSB repair. *rad60-ct* cells show no significant sensitivity to the microtubule inhibitor TBZ.

To examine whether the sensitivity of the *rad60-ct* strain can be complemented by *rad60*$^{+}$, cells were transformed with pREP41HA-*rad60*. To obtain this, the *rad60* cDNA was amplified by PCR from a cDNA library (gift from Jan Palecek, University of Sussex) using primers L41 and L40, which were designed to introduce an *Nde*I restriction site at the 5' end of the coding sequence and a *Sal*I site at the 3' end. The PCR product was cleaned up by gel extraction and ligated into the pTOPO vector (Invitrogen). A pTOPO-*rad60* clone was sequenced and found to contain a silent mutation changing the E150 codon from GAA to GAG. The *rad60* sequence was subsequently sub-cloned as an *Nde*I/*Sal*I fragment into pREP41HA. The sequence corresponding to the C-terminally truncated *rad60* gene (*rad60-ct*) was also cloned. The *rad60-ct* sequence *(*Rad60 aa 1-333*)* was amplified by PCR from the pREP41HA-*rad60* construct using primers L41 and L52. Primer L52 was designed to incorporate a stop codon (TAA) immediately after codon 233, followed by a *Sal*I restriction site. The PCR product was digested with *Nde*I/*Sal*I and ligated directly into pREP41HA to create the pREP41HA-*rad60-ct* construct.

To look at the effect of over-expressing *rad60* and *rad60-ct,* cells were transformed with the pREP41HA constructs. Expression from the *nmt1* promoter was de-repressed by growing cells for ~16 hours in the absence of thiamine. Wild-type and *rad60-ct* cells transformed with the 'empty' pREP41HA vector, have similar sensitivities to those previously observed (Figure 3.5). Over-expression of *rad60* in a *rad60-ct* background, results in a reversal of phenotype, with wild-type sensitivity to HU and MMS observed. Expression of *rad60-ct* in the mutant cells is unable to rescue cells to the same extent. This confirms that the *rad60-ct* phenotype is not an indirect consequence of secondary mutations that may act as extragenic sensitisers. Expression of *rad60-ct* in the wild-type background does not have a dominant negative effect.

3.4.2 *rad60-ct* epistasis analysis

To investigate the genetic interactions of *rad60-ct*, epistasis analysis was carried out. Since Rad60 is known to associate with the Smc5/6 complex, analysis was first carried out with mutants defective in this complex. Like *rad60-1*, *rad60-3, nse2-SA*, and *nse4-1* (Morishita, Tsutsui et al. 2002; Boddy, Shanahan et al. 2003; Morikawa, Morishita et al. 2004; Andrews, Palecek et al. 2005), tetrad analysis suggests that the double mutant of *rad60-ct* with *smc6-X* is synthetically lethal. In addition, a *rad60-ct smc6-74* double mutant is also synthetically lethal. In contrast, a double mutant of *rad60-ct* and *nse2-SA* is viable and *rad60-ct* and *nse2-SA* are epistatic in their response to both UV and IR. After exposure to UV and IR, the double mutant is no more sensitive than the most sensitive single mutant (Figure 3.6A). Like *smc6-X, smc6-74, nse2-SA and nse4-1* (Verkade, Bugg et al. 1999; Morikawa, Morishita et al. 2004; Andrews, Palecek et al. 2005), *rad60-ct* is synthetically lethal with *brc1-d*. Brc1 is a multi-copy suppressor of *smc6-74* (Verkade, Bugg et al. 1999).

HR is a major pathway for the repair of radiation-induced DSBs in *S. pom*be and Rhp51 (*H. sapiens* Rad51 homologue) is a key player in this pathway. Mutants of the Smc5/6 complex including *smc6-X*, *nse2-SA*, *nse2-1* and *nse4-1* (Lehmann, Walicka et al. 1995; McDonald, Pavlova et al. 2003; Morikawa, Morishita et al. 2004; Andrews, Palecek et al. 2005) are all epistatic with *rhp51-d*. *rad60-1* is also epistatic to the *rhp51-d* mutant (Morishita, Tsutsui

Figure 3.5: ***rad60-ct*** **can be suppressed by over-expressing** ***rad60***

Cells carrying the pREP41HA multicopy plasmid (pEV) or the pREP41HA containing *rad60* or *rad60-ct* (p*rad60*/p*rad60-ct*) were grown at 30^{o}C in YNB medium supplemented with adenine and uracil to mid-exponential phase. 10 μl of 10 fold serial dilutions were spotted onto YNB plates supplemented with adenine and uracil and containing supplements at the indicated doses. Plates were incubated at 30^{o}C for 72 hours and photographed

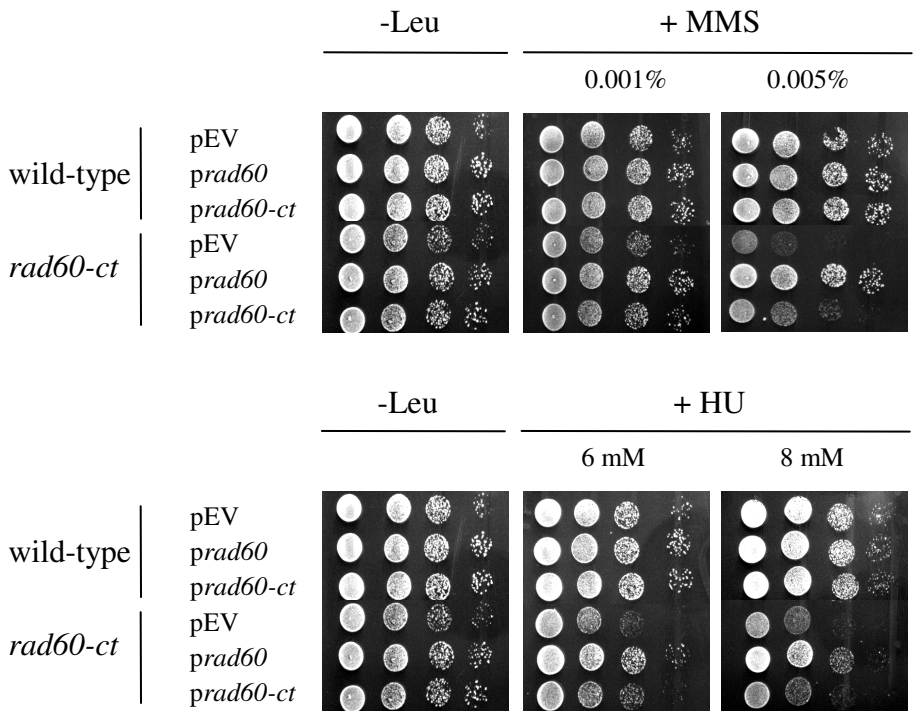

Figure 3.5: ***rad60-ct*** **can be suppressed by over-expressing** ***rad60***

Figure 3.6: *rad60-ct* epitasis analysis

Cells were grown at 30^{o}C in rich medium to mid-exponential phase and irradiated with UV or γ rays at the indicated doses. Cells were plated on rich medium and grown at 30^{o}C for 72 hours. Colonies were counted and % survival was calculated. *rad60-ct* is epistatic with *nse2-SA* **(A)** and *rhp51-d* **(B)** in response to both UV and γ irradiation and epistatic with *cds1-d* **(C)** in response to γ irradiation but not UV. *rad60-ct* is not epistatic to *chk1-d* **(D)**, *crb2-T215A* **(E)** or *top1-d* **(F)**.

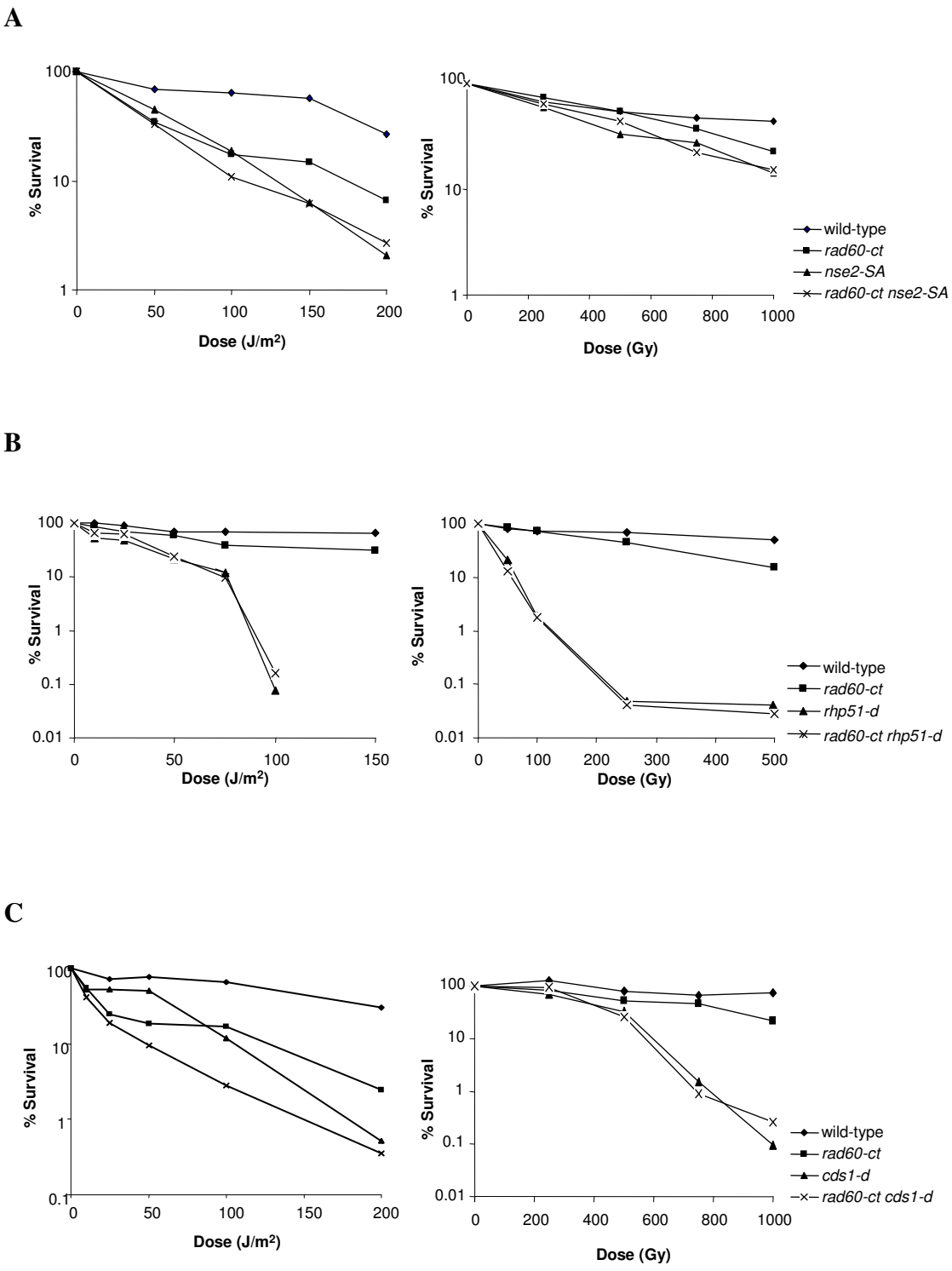

Figure 3.6i: *rad60-ct* epitasis analysis

D

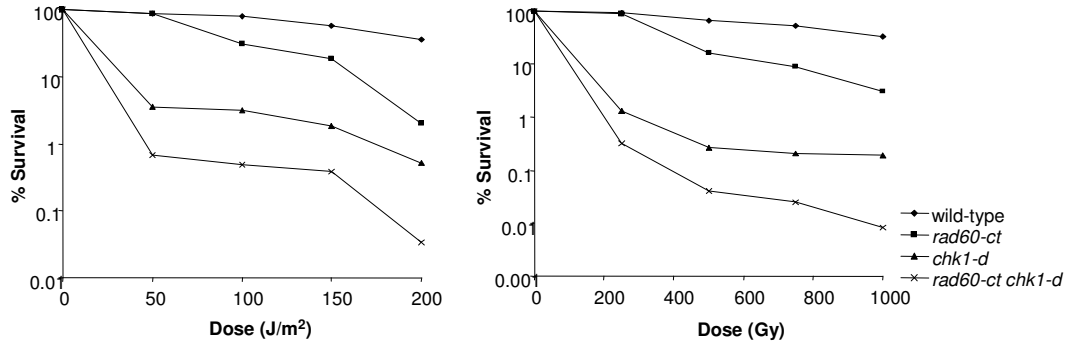

E

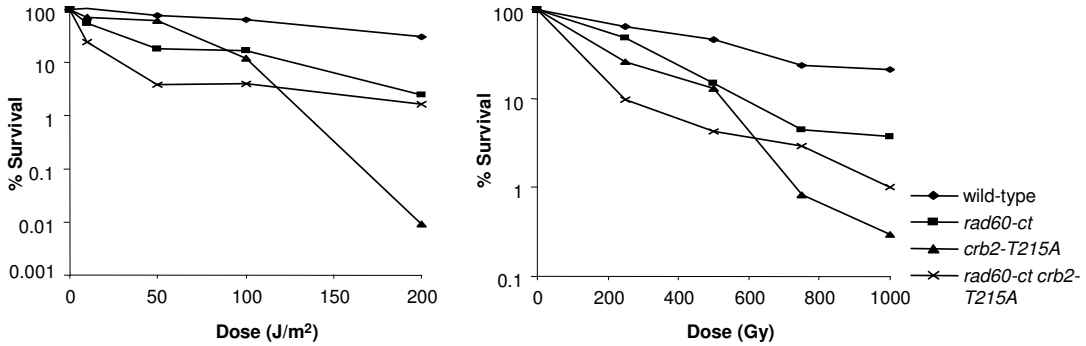

F

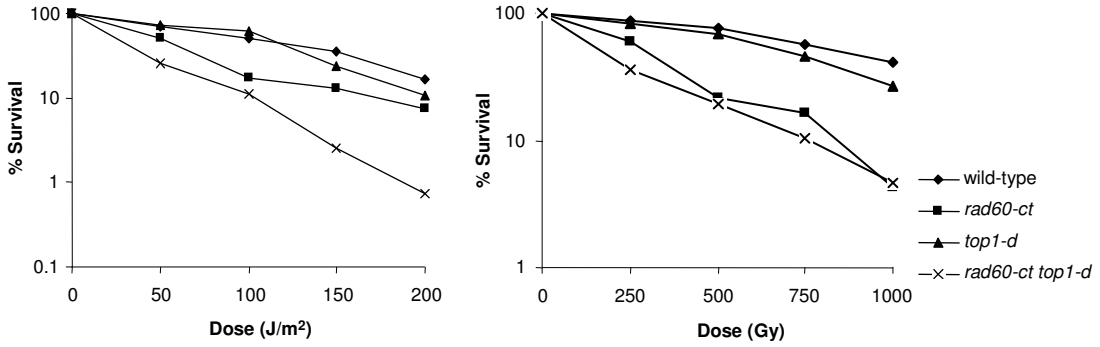

Figure 3.6ii: *rad60-ct* epitasis analysis

et al. 2002), suggesting a relationship between *rad60* and *rhp51*. The same relationship was tested for the *rad60-ct* mutant with *rhp51-d*. *rhp51-d* is more sensitive to both UV and IR than the *rad60-ct* mutant but the double mutant is no more sensitive than the single *rhp51-d* mutant after UV and IR treatment, suggesting that *rad60-ct* is epistatic to *rhp51-d* (Figure 3.6B).

In addition to the physical interaction identified with the Smc5/6 complex, Rad60 interacts with the checkpoint kinase Cds1 in an FHA-domain specific manner (Boddy, Shanahan et al. 2003). *cds1-d* is more sensitive to both UV and IR than the *rad60-ct* mutant but in response to IR, the *cds1-d rad60-ct* double mutant is no more sensitive than the single mutants. In response to UV the *cds1-d rad60-ct* double mutant is more sensitive than either of the single mutants at low doses (Figure 3.6C). This suggests that *rad60* and *cds1* are epistatic in response to IR but not UV. Epistasis analysis was carried out with *chk1-d*, a strain defective for the other *S. pombe* checkpoint kinase, Chk1. *rad60-ct* is not epistatic to the *chk1.d* strain in response to UV or IR (Figure 3.6D).

Crb2 is required for checkpoint arrest and is required for Rad3-dependent activation of Chk1 (Saka, Esashi et al. 1997). Crb2 is also required for the regulation of HR in G2 by regulating the activity of the Rqh1 helicase (Caspari, Murray et al. 2002). T215 phosphorylation by Cdc2-cyclin B occurs at mid-mitosis and allows further phosphorylation of Crb2 by Rad3. Since Rad60 has been implicated in HR and is synthetically lethal with *rqh1-d*, the relationship between *rad60* and *crb2* was tested. A *rad60-ct crb2-T215A* double mutant is more sensitive to UV and IR at low doses than either of the single mutants suggesting that Rad60 and Crb2 do not act in the same pathway (Figure3.6E).

smc6-X, *nse2-SA*, *nse4-1*, *rad60-1* and *rad60-3* (Lehmann, Walicka et al. 1995; Morishita, Tsutsui et al. 2002; Boddy, Shanahan et al. 2003; McDonald, Pavlova et al. 2003; Morikawa, Morishita et al. 2004) are synthetically lethal with *rqh1-d*. Like these mutants, *rad60-ct* is also synthetically lethal with *rqh1-d*. Rqh1 is a member of the RecQ family of helicases and has been implicated in the maintenance of replication forks and prevention of

illegitimate recombination (Doe, Ahn et al. 2002; Laursen, Ampatzidou et al. 2003). This is consistent with a model in which Rad60 is required for recombinational repair of fork breaks that acquire in an *rqh1-d* background (Boddy, Shanahan et al. 2003).

During the course of this project, the *S. cerevisiae* RENi protein, Esc2 was shown to be synthetically lethal with Sgs1 (*S. pombe* Rqh1) and Mus81. This suggests that like Rad60, Esc2 may play have a role in the maintenance of replication forks. Esc2 is also synthetically lethal with the topoisomerase1 mutant, *top1-d*. The relationship between *rad60* and *top1* was therefore tested. The *rad60-ct top1-d* double mutant is more sensitive to UV than either single mutant, implying that they are not epistatic in their response to UV (Figure 3.6F).

3.4.3 Rescue of *Smc6-X* sensitivity by Rad60 is dependent on SLD2

When the *rad60* gene is expressed from a multicopy plasmid in the *smc6-X* background, the MMS hypersensitivity of the *smc6-X* mutant can be partially suppressed (Morishita, Tsutsui et al. 2002). To test whether the Rad60 SLD2 is required for this suppression, *rad60* and *rad60-ct* were expressed from the pREP41HA plasmid in *smc6-X* cells. As reported by Morishita *et al*, expression of *rad60* in the mutant background is able to suppress the sensitivity of *smc6-X* cells to 0.001% MMS (Figure 3.7A). In contrast, expression of *rad60-ct* is unable to suppress the MMS sensitivity of *smc6-X* cells. Neither *rad60* nor *rad60-ct* is able to suppress the sensitivity of the *smc6-X* cells to HU. This suggests the Rad60 SLD2 is required to overcome the damage caused by MMS in *smc6-X* cells. The same phenomenon was tested in the *smc6-74* background. Unlike in the *smc6-X* background, expression of either *rad60* or *rad60-ct* is unable to suppress the sensitivity of the *smc6-74* cells to MMS or HU (Figure 3.7A).

Given that *nse2-SA* and *rad60-ct* are epistatic in their response to IR and MMS (Section 3.4.2), the ability of *rad60* to suppress the sensitivity of *nse2-SA* cells was assessed. The sensitivity of *nse2-SA* cells to HU and MMS can be suppressed by the expression of *rad60* and *rad60-ct* (Figure 3.7B). This suggests that the suppression of the *nse2-SA* HU and MMS by *rad60* is not dependent on the Rad60 SLD2.

Figure 3.7 Rescue of *Smc6-X* sensitivity by Rad60 is dependent on SLD2

(A) Over-expression of *rad60* but not *rad60-ct* can suppress the sensitivity of *smc6-X,* but not *smc6-74* to 0.001% MMS. **(B)** Over-expression of *rad60* and *rad60.ct* can suppress the sensitivity of *nse2-.SA* to HU and MMS. Cells carrying the pREP41HA multicopy plasmid (pEV) or pREP41HA containing *rad60* or *rad60-ct* (p*rad60/*p*rad60-ct*) were grown at 30^{o}C in YNB medium supplemented with adenine and uracil to mid-exponential phase. 10 μl of 10 fold serial dilutions were spotted onto YNB plates supplemented with adenine and uracil and containing supplements at the indicated doses. Plates were incubated at 30^{o}C for 72 hours and photographed.

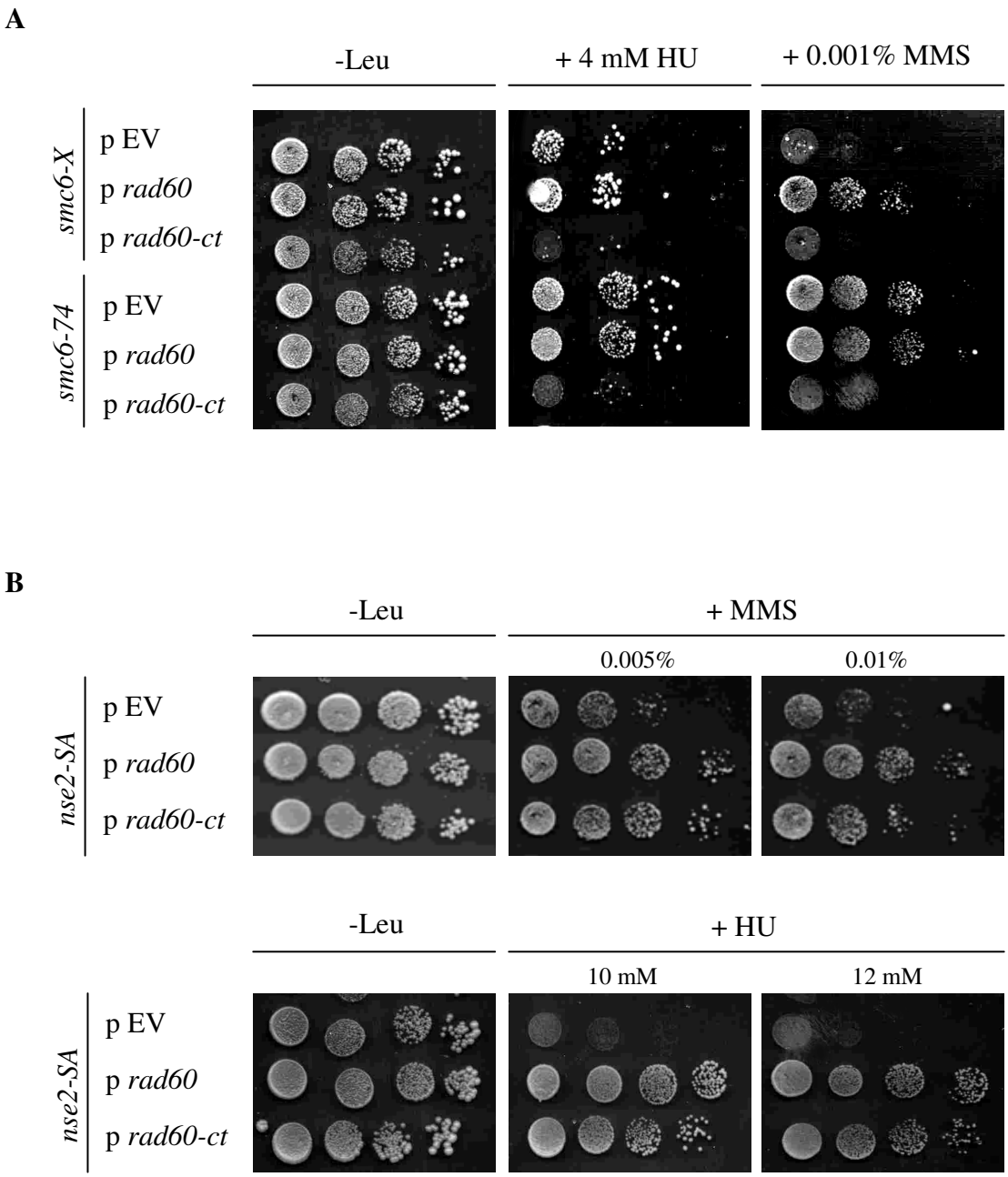

Figure 3.7: Rescue of *Smc6-X* sensitivity by Rad60 is dependent on SLD2

3.4.4 Rad60 can suppress the sensitivity of *rhp51-d* and *rad9-T225C*

Since *rad60-ct* and *rhp51-d* are epistatic in their response to UV and IR (Section 3.4.2), the ability of *rad60* to suppress the sensitivity of *rhp51-d* cells was tested. Expressing *rad60* from the pREP41HA plasmid is able to suppress the sensitivity of the *rhp51-d* cells to both HU and MMS (Figure 3.8A). In contrast, expression of *rad60-ct* is unable to suppress the *rhp51-d* phenotype, suggesting the SLD2 of Rad60 is required for the suppression of *rhp51-d* sensitivity to HU and MMS by *rad60.*

Expression of *rad60* in an *rqh1-d* background is unable to rescue the HU and MMS sensitivity of *rqh1-d* cells. Unlike the expression of *rad60*, expression of *rad60-ct* in the *rqh1-d* mutant cells has a dominant negative effect, enhancing the sensitivity of the *rqh1-d* cells to HU and MMS (Figure 3.8B).

Rad9 is one of the proteins that make up the 9-1-1 complex that is required for the DNA damage checkpoint. Rad9 Thr225 is required for phosphorylation of Rad9 on replication fork collapse and concomitant inhibition of recombination (Furuya, Poitelea et al. 2004; Kai, Furuya et al. 2007). The sensitivity of the *rad9-T225C* mutant to MMS and HU is partially suppressed by the expression of *rad60.* Expression of *rad60-ct* cannot suppress the sensitivity of the *rad9-T225C* cells (Figure 3.8C).

3.4.5 Suppression of *rad60-ct*

To determine whether the sensitivity of the *rad60-ct* mutant to HU and MMS can be suppressed by the expression of any genes of interest, wild-type and *rad60-ct* cells were transformed with pREP41HA constructs containing the gene of interest. Since the HA tag affects Brc1 function (Murray, unpublished data) *brc1* was transformed on a pREP41 vector, lacking the HA tag. The sensitivity of cells was assessed by spot tests (Figure 3.9).

Given the emerging relationship between *nse2* and *rad60*, the ability of *nse2* to suppress *rad60* was assessed. Expression of the *nse2* gene is not able to suppress the HU and MMS sensitivity of the *rad60-ct* cells. Expression of *rad60* can partially suppress the sensitivity

Figure 3.8 *rad60* can suppress *rhp51-d* and *rad9-T225C*

(A) Over-expression of *rad60* but not *rad60-ct* can suppress the sensitivity of *rhp51-d* **(B)** Over-expression of *rad60* cannot suppress the sensitivity of *rqh1-d* cells. **(C)** Over-expression of *rad60* can partially suppress the sensitivity of *rad9-T225C* cells. Cells carrying the pREP41HA multicopy plasmid (pEV) or pREP41HA containing *rad60* or *rad60-ct* (p*rad60*/p*rad60-ct*) were grown at 30^{o}C in YNB medium supplemented with adenine and uracil to mid-exponential phase. 10 μl of 10 fold serial dilutions were spotted onto YNB plates supplemented with adenine and uracil and containing supplements at the indicated doses. Plates were incubated at 30^{o}C for 72 hours and photographed

Figure 3.8: ***rad60*** **can suppress** ***rhp51-d*** **and** ***rad9-T225C***

Figure 3.9 Suppression of *rad60-ct*

Wild-type and *rad60-ct* carrying the pREP41HA multicopy plasmid (pEV) or pREP41HA containing the gene of interest were grown at 30^{o}C in YNB medium supplemented with adenine and uracil to mid-exponential phase. 10 μl of 10 fold serial dilutions were spotted onto YNB plates supplemented with adenine and uracil and containing supplements at the indicated doses. Plates were incubated at 30^{o}C for 72 hours and photographed

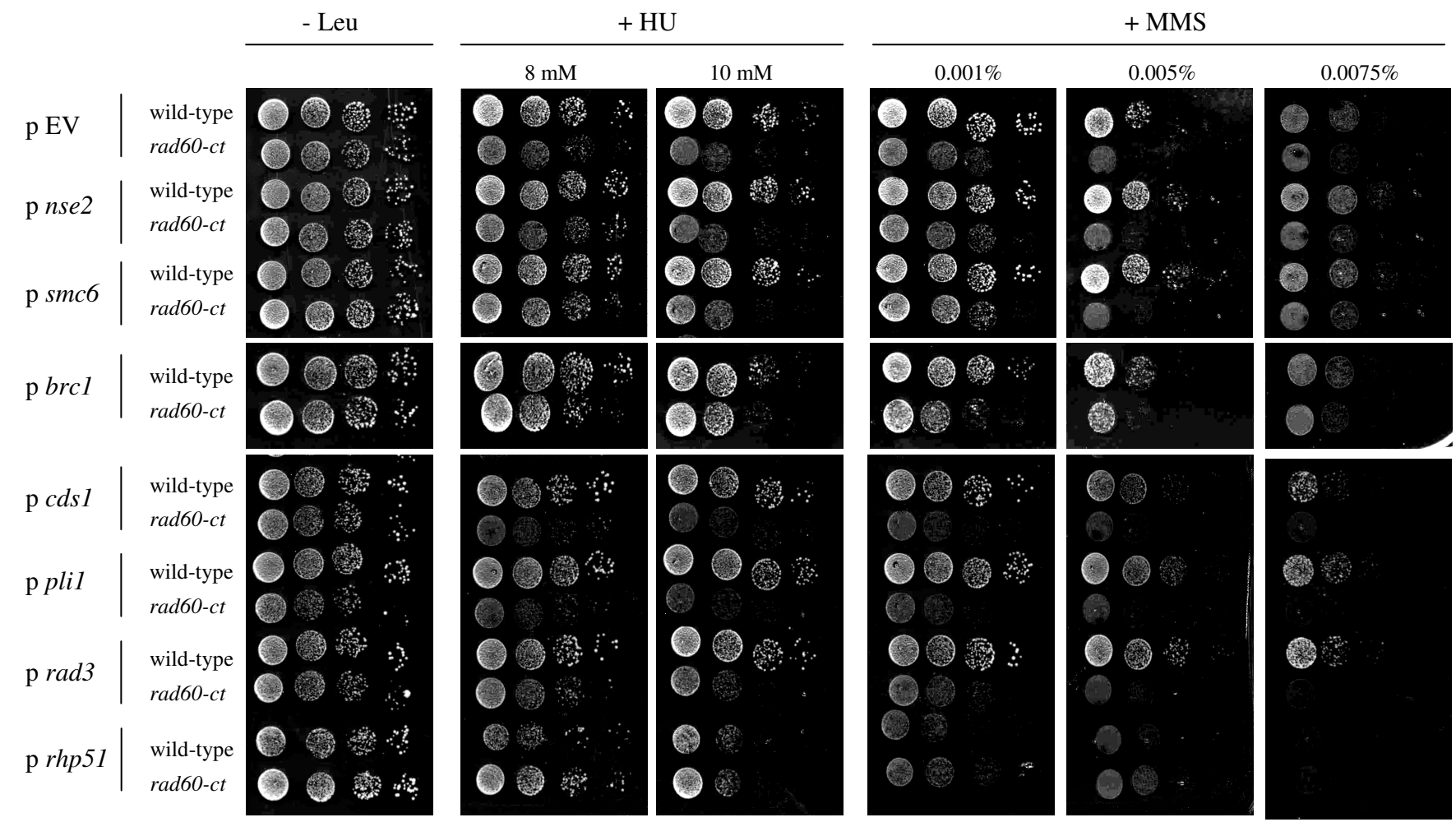

Figure 3.9: Suppression of *rad60-ct*

of *smc6-X* cells (Section 3.4.3 and (Morishita, Tsutsui et al. 2002)). However, the expression of *smc6* is unable to complement the sensitivity of *rad60-ct* cells, suggesting that whilst *rad60* may be able to functionally compensate for loss of *smc6* function in *smc6-X* cells, *smc6* cannot compensate for loss of *rad60* function. *brc1* is a multicopy suppressor of *smc6-74* (Verkade *et al*, 1999). *brc1* is unable to suppress the MMS and HU sensitivity of *rad60-ct* cells. Expression of the genes coding for Rad3, Rhp51, Cds1 and Pli1 are also unable to suppress the MMS and HU sensitivity of *rad60-ct* cells.

3.5 Rad60 SLD1 is essential for viability.

Three previously characterised mutants, *rad60-1* (K263E), *rad60-3* (F272V) and *rad60-4* (T72A, I232S, Q250R, K312N) contain point mutations that lie within the predicted SLD1, suggesting that this domain may be of key importance for Rad60 function (Morishita, Tsutsui et al. 2002; Boddy, Shanahan et al. 2003). To test the importance of SLD1 for Rad60 function, a method for replacing the genomic copy of *rad60* with a copy of *rad60* deleted for SLD1 was required. For this reason the 'recombinase-mediated cassette exchange (RMCE) system'(Watson, Garcia et al. 2008) was utilised. The RMCE is a novel system, in which Cre/lox site-specific recombination is utilised to allow an efficient method for gene tagging and/or gene replacement. For gene replacement a 'cassette' is integrated into the *S. pombe* genome at the gene locus of choice. The 'cassette' consists of the *S. pombe ura4*$^+$ selectable marker flanked by a wild-type loxP site at one end and a modified heterospecific lox site (loxM3) at the other side of the gene to be replaced. Exchange is achieved by introducing a Cre-recombinase expression plasmid containing an equivalent 'cassette' containing the desired copy of the gene and lacking the *ura4*$^+$ marker. Recombinants can be selected by uracil prototrophy on plates containing 5-flouroorotic acid (5-FOA).

3.5.1 Creating a '*rad60* base strain' for RMCE

To use the RMCE system a '*rad60* base strain', containing the loxP-*rad60-ura4*$^+$-loxM3 cassette, was first created. Since *rad60* is an essential gene, the construction of the base strain was a two-step process requiring two homologous integration steps. First the loxP site is placed ~300 bp upstream of the *rad60* coding sequence so as to leave the *rad60*

promoter region intact, and secondly the *ura4*$^+$ marker and loxM3 site are placed immediately downstream from the gene sequence (Figure 3.10A, B)

Firstly, primers L143 and L144 were used to amplify by PCR the ~600 bp loxP-*Sup3-5*-loxP cassette from the template plasmid pAW11 (Figure 3.10A). Primers L143 and L144 contain 20 base pairs of sequence homology to the pAW11 plasmid and 80 base pairs of sequence homologous to the target sequence within the *S. pombe* genome (~300 bases upstream of the *rad60* start codon). The product of 5 PCRs were pooled and ethanol precipitated to a final volume of 25 μl and transformed into a wild-type haploid strain (*sp.011*) using the Bahler transformation procedure. Cells were plated on EMM2 medium supplemented with uracil and leucine and grown for 3 days at 30^{o}C. The loxP-*sup3-5*-loxP cassette was introduced into the genome via homologous integration and *ade*$^+$ transformants were selected. To check that integration had occurred at the correct locus colony PCR was carried out with primer L170 hybridising upstream of the *sup3-5* integration site and L172 hybridising downstream of the integrated *sup3-5* site and upstream of the *rad60* coding sequence. A PCR product of ~1.1 kb was observed (data not shown). The positive transformant was then transformed with the Cre-expressing plasmid pAW8 to excise the *sup3-5* cassette and leave a single lox-P site upstream of the *rad60* coding sequence. Transformants were plated on EMM2 plates containing uracil and adenine (10 μg/ml), to allow red/white selection of colonies. Red colonies were picked and streaked to rich medium to promote loss of the pAW8 plasmid.

Once the loxP site was correctly integrated into the *S. pombe* genome, the *ura4*$^+$ gene was placed immediately downstream of the *rad60* coding sequence (Figure 3.10B). Primers L140 and L141 were used to amplify by PCR the 1.9 kb *ura4*$^+$-loxM3 cassette from the template plasmid pAW12. Primer L140 and L141 contain 20 base pairs of sequence homology to the pAW12 plasmid and 80 base pairs of sequence homologous to the target sequence within the *S. pombe* genome. The product of 5 PCRs were pooled and ethanol precipitated to a final volume of 25 μl and transformed into the cells containing the loxP site. Cells were plated on EMM2 medium supplemented with adenine and leucine and *ura*$^+$ transformants were selected. To check for integration at the correct locus colony PCR was

Figure 3.10 Creating a *rad60* base strain for RMCE

(A) Integration of a loxP site ~300 bases upstream, of *rad60* coding sequence. Long primers L143 and L144 were used to amplify by PCR the loxP-*sup3-5*-loxP cassette from the pAW11 plasmid. The DNA was transformed directly into haploid wild-type cells. The loxP-*sup3-5*-loxP cassette was introduced into the genome via homologous integration. Positive transformants were transformed with the Cre-expressing plasmid pAW8 to excise the *sup3-5* cassette, leaving a single lox-P site upstream of the *rad60* coding sequence. **(B)** Integration of a *ura4*$^{+}$ immediately downstream of the *rad60* coding sequence. Long primers L140 and L141 were used to amplify by PCR the *ura4*$^{+}$-loxM3 cassette from the pAW12 plasmid. The DNA was transformed directly into haploid cells containing the loxP site ~300 bases upstream of *rad60* coding sequence. The *ura4*$^{+}$-loxM3 cassette was introduced into the genome via homologous integration to form the *rad60* base strain. **(C, D)** A Southern blot confirmed the presence of a single copy of the *ura4*$^{+}$ marker in the *rad60* base strain. Genomic DNA was extracted from the *rad60* base strain. A *Bcl*I digest was used to isolate a ~3.7 kb fragment containing the *ura4*$^{+}$ marker and a fragment of the *rad60* gene (Seen in C). The digested DNA was run on a 0.8% TBE gel and Southern blotted overnight. Following incubation with a ^{32}P labelled *ura4*$^{+}$ DNA probe, the membrane was exposed to a phosphocassette and the signal detected by a phosphoimager (Seen in D). DNA extracted from wild-type and Nse2-SA cells was used as negative and positive controls, respectively.

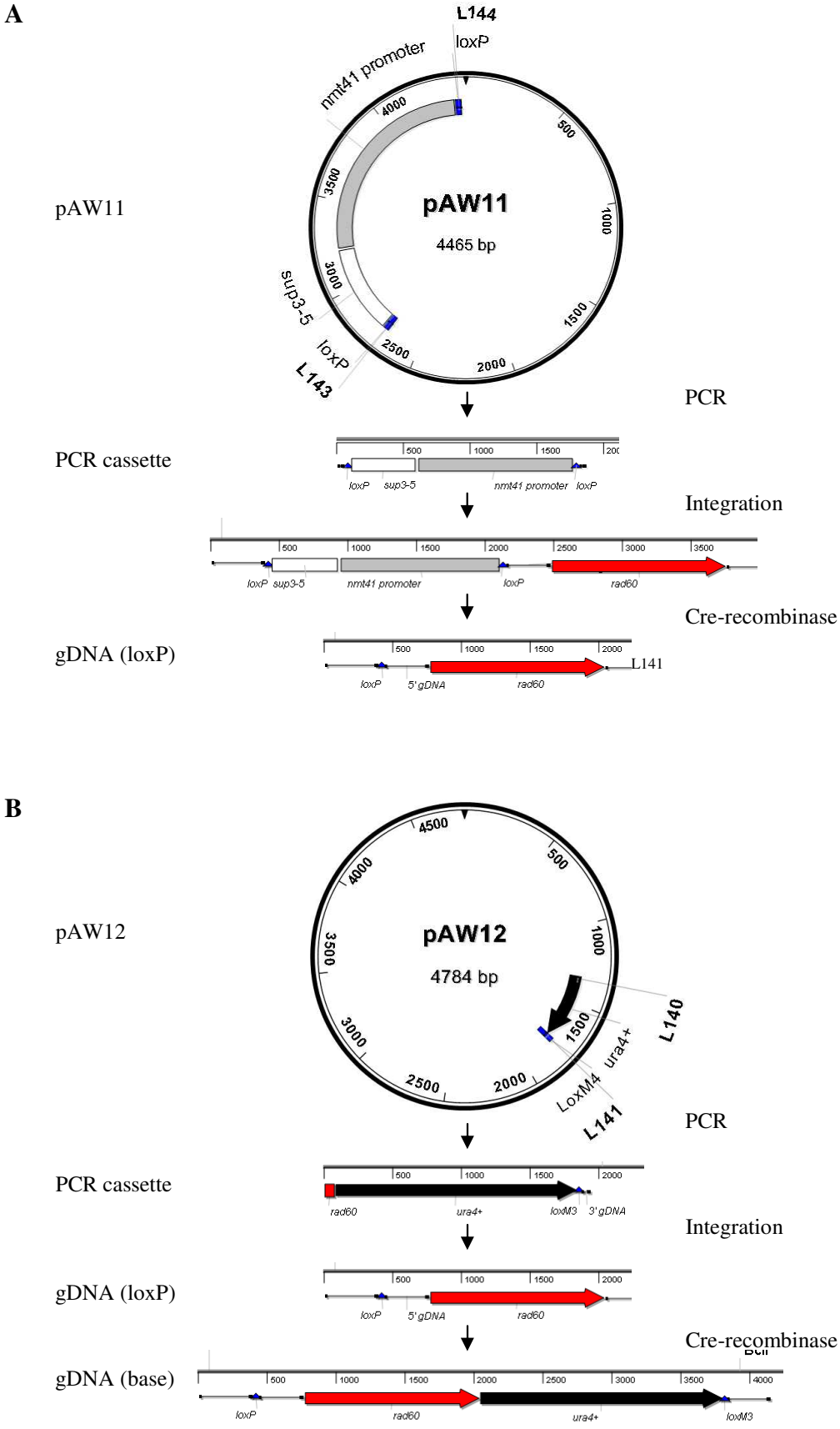

Figure 3.10i: Creating a *rad60* base strain for RMCE

C

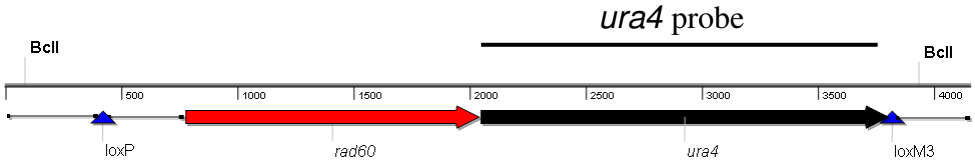

D

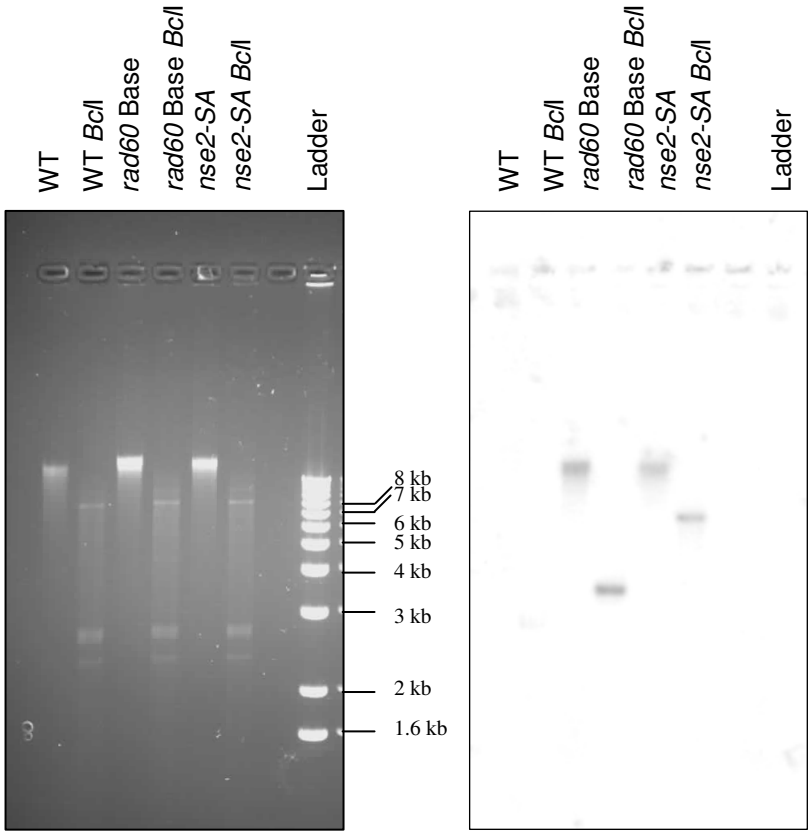

Figure 3.10ii: Creating a *rad60* base strain for RMCE

carried out with primer L142, hybridising to the newly integrated cassette and L17 hybridising within the *rad60* gene sequence. A PCR product of ~710 bp was observed (data not shown).

Although colony PCR confirmed integration at each stage, sequencing across the integration sites was necessary to confirm that integration had occurred at the correct sites. For this reason, following integration of both the lox P and *ura4*$^{+}$-loxM3 cassettes, genomic DNA was extracted from two positive colonies and the loxP-*rad60*-*ura4*$^{+}$-loxM3 cassette was amplified from the genomic DNA with primers L170 and L35. Sequencing of the PCR product with primers L170, L17, L18, L19 and L35 confirmed integration had occurred at the correct locus.

The RMCE system relies on loss of the *ura4*$^{+}$ marker from the genome. A Southern blot confirmed that only one *ura4*$^{+}$ marker had been incorporated into the genome of the *rad60* base strain. Genomic DNA was extracted from the *rad60* base strain and a *Bcl*I digest was used to isolate a ~3.7 kb fragment containing the *ura4*+ marker and a fragment of the *rad60* gene (Figure 3.10C). For both isolates, a Southern blot probed with a ^{32}P *ura4*$^{+}$ DNA probe detected only one ~3.7 kb fragment in the digested samples. (Figure 3.10D). gDNA from *nse2-SA* (*ura4*$^{+}$ integrated immediately downstream of the *nse2-SA* allele) was used as a positive control. Following *Bcl*I digestion a fragment containing *ura4*$^{+}$ was observed at the expected size of ~7500 bp. A wild-type DNA control showed no signal, suggesting the signal detected for the *rad60* base strain is not an artefact.

3.5.2 Testing the '*rad60* base strain' in the RMCE system

The RMCE system requires exchange between the genomic copy of the loxP-*rad60*-*ura4*$^{+}$-loxM3 'cassette' in the *rad60* base strain and an equivalent loxP-*rad60*-loxM3 'cassette' on the Cre-expression plasmid pAW8 (Figure 3.11A). To create such a construct the sequence equivalent to that flanked by the loxP and loxM3 sites in the *rad60* base strain was amplified by PCR from genomic DNA using primers L245 and L40. Primers L245 and L40 introduced a *Sac*I restriction site at the 5' end of the ~1.5 kb PCR fragment and a *Sal*I restriction site at the 3' end of the PCR fragment respectively enabling ligation of the PCR

Figure 3.11 Testing the *rad60* RMCE system

(A) Recombinase-mediated cassette exchange. The RMCE system relies upon exchange between the genomic copy of the loxP-*rad60*-*ura4*$^{+}$-loxM3 'cassette' in the *rad60* base strain (ii) and an equivalent loxP-*rad60*-loxM3 'cassette' on the Cre-expression plasmid pAW8 (i). Following RMCE, the *rad60*-*ura4*$^{+}$ copy in the base strain is replaced with the *rad60* copy on the pAW8 plasmid (iii). **(B)** The *rad60* base strain has wild-type phenotype. Cells were grown at 30^{o}C in YE medium to mid-exponential phase. 10 μl of 10 fold serial dilutions were spotted onto YEA plates containing supplements at the indicated doses. Plates were incubated at 30^{o}C for 72 hours and photographed.

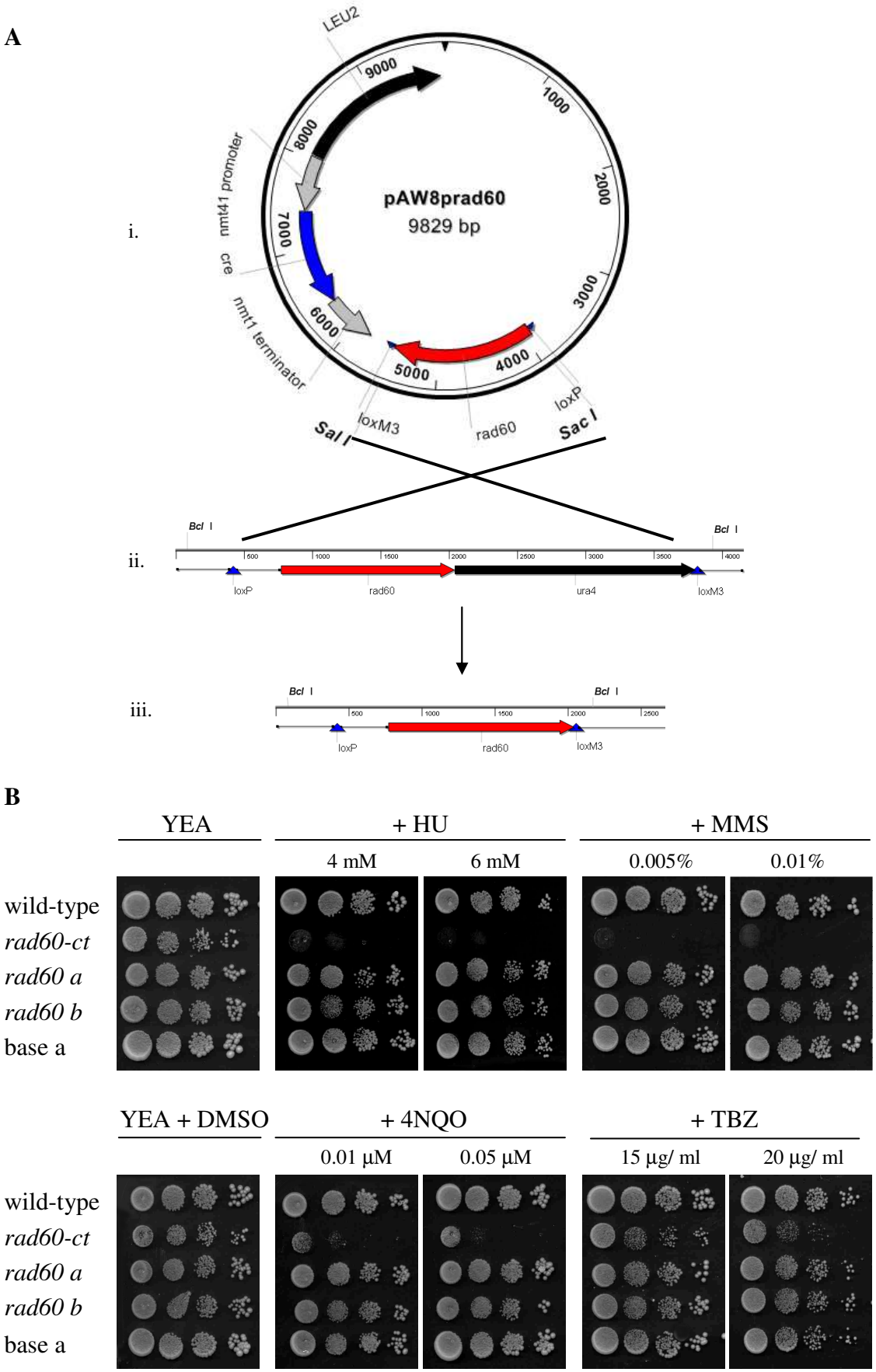

Figure 3.11: Testing the *rad60* RMCE system

fragment into the multiple cloning site of pAW8. The Cre-expression plasmid pAW8 contains the *S. cerevisiae LEU2*$^{+}$ gene. When the *rad60* coding sequence is cloned into the pAW8 plasmid it is consequently flanked by loxP and loxM3 sites. Since the loxP site in the *rad60* base strain was placed ~300 bases upstream of the ATG, the sequence amplified contained the equivalent promoter region as well as the coding sequence. The resulting construct was therefore referred to as pAW8p*rad60.* Site-directed mutagenesis on pAW8p*rad60* followed by Cre-recombinase-mediated cassette exchange allows a simple method for integrating point mutations into the genomic copy of *rad60*.

Before introducing mutations into the *rad60* locus, the RMCE system was tested by replacing the copy of *rad60-ura4*$^{+}$ in the base strain with wild-type *rad60* from the pAW8p*rad60* construct. RMCE was achieved as described in Section 2.1.5. Two 5FOA (*ura4*$^{-}$) colonies were selected (*rad60a* and *rad60b*) and their phenotype tested. Spot tests were carried out. The sensitivity of the two isolates was compared to the *rad60* base strain, wild-type and *rad60-ct* cells. As would be expected for a functional *rad60*, the *rad60a* and *rad60b* had similar responses to HU, MMS, TBZ and 4NQO as observed for the wild-type and *rad60* base strain cells (Figure 3.11B). This indicates that the presence of the loxP and loxM3 sites flanking the *rad60* gene does not confer a mutant phenotype. The *rad60* base-strain could therefore be used for RMCE.

3.5.3 Rad60 SUMO-like domain 1 is essential for viability

To test whether the Rad60 SLD1 is required for Rad60 function, the *rad60* RMCE system was used to replace the wild-type copy of *rad60* with a copy of the *rad60* gene, lacking SLD1 (amino acids 228-307). In two consecutive site-directed mutagenesis reactions, primer pairs L243/L254 and L255/L256 were used to introduce *Xho*I sites into the pAW8p*rad60* construct immediately prior to codon 228, and immediately after codon 307 of *rad60* respectively. The resulting construct was digested with *Xho*I and re-ligated to give a pAW8p*rad60-SLD1Δ* construct (Figure 3.12A). Sequencing of pAW8p*rad60-SLD1Δ* with primer L17 and L179 confirmed that SLD1 (aa 228-307) had been deleted and the remaining sequence (SLD2) was in frame with the N-terminus. Although the previously published *rad60-1*, *rad60-3* and *rad60-4* strains, carrying mutations within SLD1, are

Figure 3.12 Rad60 SLD1 is essential for viability

(A) Creating a pAW8p*rad60-SLD1Δ* construct. *Xho*I sites were introduced into the pAW8p*rad60* construct immediately prior to codon 228, and immediately after codon 307 of *rad60*. The resulting construct was digested with *Xho*I and re-ligated to give a pAW8p*rad60-SLD1Δ* construct. **(B)** A heterozygous diploid *rad60* base strain was transformed with pAW8p*rad60-SLD1Δ* and RMCE was achieved. Colony PCR, with primers L17 and L40, was used to confirm the presence of the *rad60-SLD1Δ* allele (i). Colony PCR reaction with primers L202 and L35 was used to confirm the presence of the wild-type *rad60* allele (ii). Haploid wild-type cells were used as a control. **(C)** The heterozygous *rad60-SLD1Δ* cells were sporulated and a dozen asci dissected. Each tetrad produced only two viable spores. **(D)** Viable spores carry the wild-type *rad60* allele**.** The viable spores from four different tetrads (1-8 boxed in red in (D)) were subjected to colony PCR with primers L17/L40. All viable spores gave a PCR product consistent with a wild-type (wt) *rad60* allele. Heterozygous diploid *rad60-SLD1Δ* cells (Δ) were used as a control.

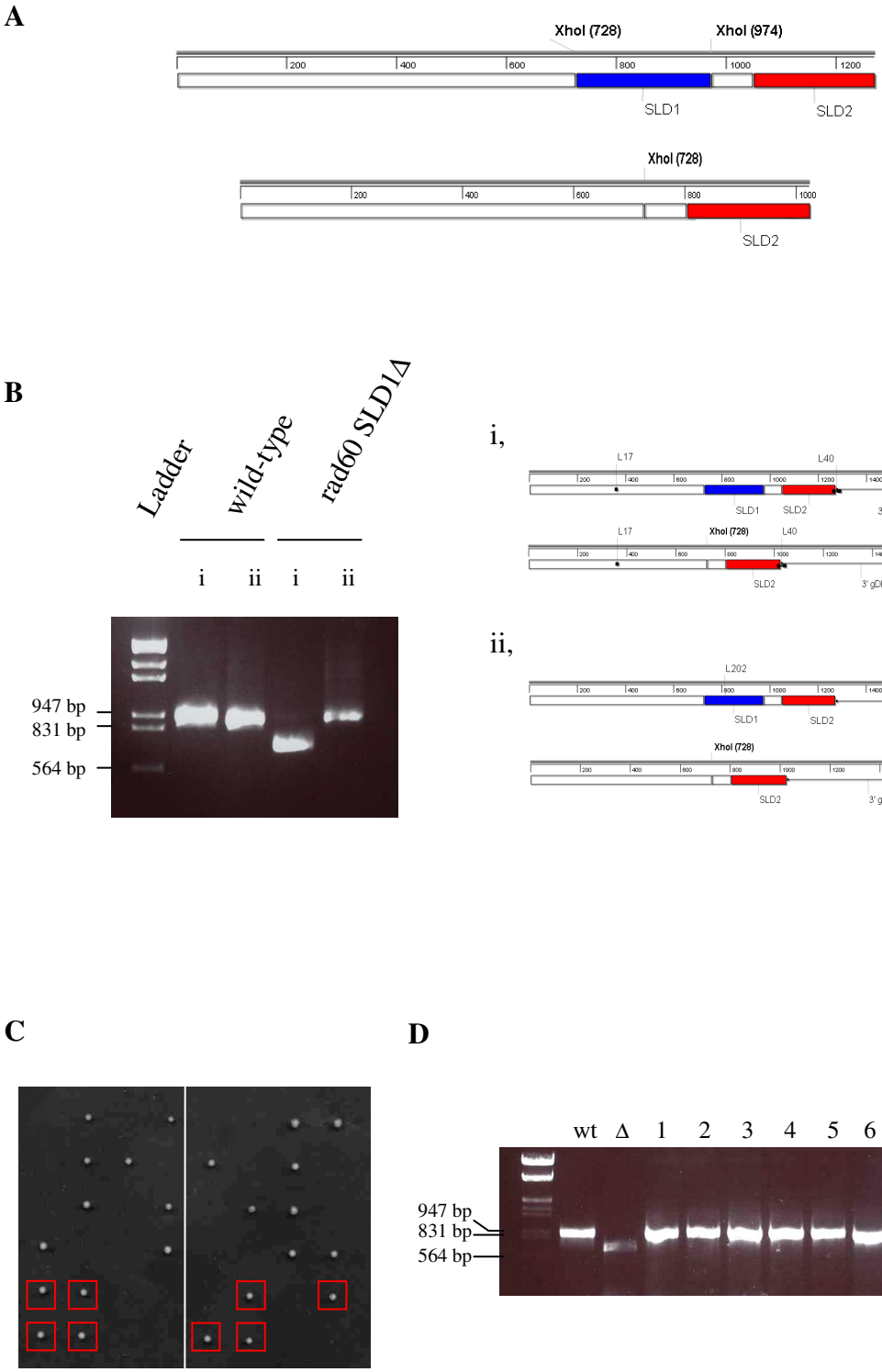

Figure 3.12: Rad60 SLD1 is essential for viability.

viable, it was possible that deletion of the entire domain would prove to be lethal for cells. For this reason, the pAW8p*rad60-SLD1Δ* construct was transformed into a heterozygous diploid *rad60* base strain.

To create a diploid base strain the haploid *rad60* base strain (*ade6-704, leu1-32,* h^-) was first crossed with the haploid strain EH682 (*leu1-32, ura4-D18,* h^+) to cross out the *ade6-704* mutation. Following random spore analysis ade^+, $ura4^+$ colonies were selected. An h^- colony was then crossed to the haploid strain EH358 (*ade6-M210, leu1-32, ura4-D18,* h^+) and ade^-, $ura4^+$ colonies were selected. An h^- colony was selected and crossed with the haploid strain EH353 (*ade6-M216, leu1-32, ura4-D18,* h^+). Complementation of the *ade6-M210* and *ade6-M216* alleles allowed diploid cells to produce white colonies on minimal medium containing leucine and adenine at a low concentration (10 μg/ml). ade^+, $ura4^+$ colonies were selected as the heterozygous diploid *rad60* base-strain (*sp.1845*).

The heterozygous diploid base-strain was transformed with pAW8p*rad60-SLD1Δ* and RMCE was achieved as described in section 2.1.5. To ensure the base strain remained diploid throughout the RMCE process, transformed cells were maintained on minimal medium containing adenine at a low concentration (10 μg/ml) plus thiamine allowing 'white' diploid cells to be distinguished from 'red' haploid cells. Instead of growing cells for 24 hours in YE medium, cells were grown in minimal medium containing adenine (10 μg/ml) plus leucine to promote loss of the plasmid. Cells were plated on minimal medium containing adenine (10 μg/ml), leucine, uracil, and 5FOA to select for cells lacking a copy of the $ura4^+$ gene.

Colony PCR, with primers L17 and L40, was used to confirm the presence of the *rad60-SLD1Δ* allele. Following colony PCR of the heterozygous diploid, I expected to observe two PCR products, a band of ~900 bp corresponding to the wild-type *rad60* allele and a band of ~650 bp corresponding to the *rad60-SLD1Δ* allele. However, all colonies screened produced one dominant band of ~650 bp suggesting a single copy of the *rad60-SLD1Δ* allele was present. If this were true, the colonies screened must have become haploid, suggesting that deletion of *rad60* SLD1 is not lethal. To investigate this, cells were streaked

to single colonies on YEA (-adenine) plates to identify between white (*ade*$^{+}$) and red (*ade*$^{-}$) cells. Only diploid cells, containing both copies of the *ade6-M210* and *ade6-M216* alleles should be white. As a control, cells from a haploid wild-type strain were also streaked on the YEA (-adenine) medium. As expected, the haploid strain grew 'red' but surprisingly, the *rad60-SLD1Δ* cells grew white, like the diploid base strain (data not shown). For further characterisation the cells were streaked onto phloxin-B plates. On the phloxin-B plates the haploid cells grew as light pink colonies and the *rad60-SLD1Δ* cells, like the diploid base strain grew as dark pink colonies (data not shown). Together, this suggests that the *rad60-SLD1Δ* cells are still diploid. To confirm the presence of both the wild-type *rad60* and the *rad60-SLD1Δ* alleles, colony PCR with L17/L40 was repeated. Wild-type haploid cells were used as a control. The wild-type cells gave a PCR product of ~900 bp, corresponding to a wild-type copy of the *rad60* gene (Figure 3.12B). As seen previously, and consistent with the *rad60-SLD1Δ* allele, a PCR product of ~650 bp was observed in the *rad60-SLD1Δ* cells. A very faint band equivalent to the wild-type product could also be detected (Figure 3.12B). In parallel, a second colony PCR with primers L202 and L35 was carried out. Primer L202 was designed to anneal within SLD1 whilst L35 anneals ~500 bp downstream of the *rad60* stop codon. In this reaction, a PCR product of ~900 bp, corresponding to a wild-type copy of the *rad60* gene, was observed for both the wild-type cells and the *rad60-SLD1Δ* cells (Figure 3.12B). If the *rad60-SLD1Δ* cells were haploid as originally believed, this PCR would yield no product. Together, this suggests that the *rad60-SLD1Δ* cells are in fact heterozygous diploid and that the PCR with L17/L40 preferentially amplifies the smaller DNA fragment from the *rad60-SLD1Δ* allele. 1 μl of this small PCR product was sequenced with primer L17 to confirm that SLD1 (aa 228-307) had been deleted and that the remaining sequencing was in frame.

To determine whether the *rad60-SLD1Δ* allele was lethal, the heterozygous *rad60-SLD1Δ* cells were placed on ELN medium for ~72 hours at 25^{o}C to induce sporulation. Unlike the diploid base-strain cells, which almost all sporulated, the *rad60SLD1Δ* cells showed a severely reduced sporulation frequency (~<1%), suggesting a defect in meiosis. A dozen asci were dissected and each tetrad produced only two viable spores (Figure 3.12C). Colony PCR (L17/L40) of the viable spores from four different tetrads confirmed that each

spore contained a wild-type copy of the *rad60* gene (Figure 3.12D). This implies that deletion of the *rad60* SLD1 is lethal.

3.6 Discussion

In this chapter, I have identified two potential SUMO-like domains in the C-terminal region of Rad60. During the course of this project Rad60 has been characterised as a member of the RENi family of proteins, which include the *S. pombe* Rad60, *S. cerevisiae* Esc2 and *M. musculus* Nip45 proteins amongst others. Rad60, Esc2 and Nip45 are all ~400 amino acids in length and share 2 C-terminal SUMO-like domains. Unlike SUMO, the SUMO-like domains of the RENi proteins do not share the C-terminal diglycine motif required for covalent attachment to target proteins, suggesting that the SUMO-like domain of these proteins is likely to function as a protein-protein interface and is not conjugated to other proteins. In this chapter I have created SUMO-domain deletion mutants to analyse the importance of the SLDs for Rad60 function.

A Rad60 SLD2 deletion mutant (*rad60-ct*) is viable, suggesting Rad60 SLD2 is not required for the essential function of Rad60. Like the *rad60-1* (K263E) mutant, *rad60-ct* cells grow well at 25^{o}C and are temperature sensitive at 36^{o}C. Unlike the *rad60-1* cells, *rad60-ct* grows well at 30^{o}C. *rad60-ct* cells are sensitive to DNA damaging agents UV, IR, MMS, 4NQO. These defects are similar to, but not as severe as, the previously characterised *smc6-X* mutant (Lehmann, Walicka et al. 1995). Like other mutants defective in the Smc5/6 complex, *rad60-ct* is epistatic with *rhp51-d*, implying a role for *rad60* in homologous recombination that is dependent on SUMO-like domain 2. As is the case with the *smc6-X* and *smc6-74* mutants, *rad60-ct* cells are elongated, suggesting a defect in replication that is activating a checkpoint (Lehmann, Walicka et al. 1995; Verkade, Bugg et al. 1999). This is consistent with *rad60-ct* cells showing sensitivity to the replication inhibitor HU.

Rad60 is known to associate with the Smc5/6 complex (Morishita, Tsutsui et al. 2002; Boddy, Shanahan et al. 2003). Like the other *rad60* mutants, *rad60-1* and *rad60-3, rad60-ct* is synthetically lethal with *smc6-X* and is also synthetically lethal with *smc6-74*

(Morishita, Tsutsui et al. 2002; Boddy, Shanahan et al. 2003). The point mutations in *rad60-1* (K263E) and *rad60-3* (F272V) are located in SLD1 of Rad60. This suggests that either, the genetic interaction of *rad60* with *smc6* is not SLD2-dependent, or, that mutations in SLD1 disrupt the structure and/or function of SLD2. Additionally, expression of *rad60* but not *rad60-ct* in an *smc6-74* background can suppress the sensitivity of *smc6-74* to HU and MMS, suggesting that suppression is dependent on the SLD2 of Rad60.

Nse2 is a member of the Smc5/6 complex and has E3 SUMO ligase activity (Andrews, Palecek et al. 2005). The *nse2-SA* allele encodes a ligase-dead version of the Nse2 protein (Andrews, Palecek et al. 2005). *rad60-ct* and *nse2-SA* are epistatic in their response to both UV and IR, suggesting that *rad60* and *nse2* act in the same repair pathway. Interestingly, expression of *rad60* and *rad60-ct* in an *nse2-SA* background can suppress the sensitivity of *nse2-SA* cells to HU and MMS. One possible explanation for the genetic interaction between *rad60* and *nse2* is that Nse2-dependent sumoylation of Rad60 could help establish the transient interaction with the Smc5/6 complex. Sumoylation of rad60 is discussed in chapter 4.

Although initially the functions of the RENi family proteins do not seem well conserved, there is evidence to suggest that *rad60* and *esc2* may share some genetic interactions and hence may be functional homologues. The *S. pombe rad60* gene was first identified through its synthetic lethal interaction with *rad2* (Morishita, Tsutsui et al. 2002). Unlike *rad60, esc2* is not essential but an *esc2-d* strain has been shown to be synthetically lethal with mutations of the *rad27* (*rad2* homologue) gene (Tong, Evangelista et al. 2001). In addition, *esc2-d* is synthetically lethal with *sgs1-d*, (*rqh1* homologue). Like *rad60-1 and rad60-3* (Morishita, Tsutsui et al. 2002; Boddy, Shanahan et al. 2003). I have shown *rad60-ct* to be synthetically lethal with *rqh1-d.* This implies that the SUMO-like domains may be required for a conserved function of the RENi protein family. Unlike *esc2-d*, which is synthetically lethal with *top1-d*, a *rad60-ct top1-d* double mutant is viable. *rad60-ct* and *top1-d* are not epistatic, suggesting that the relationship between Esc2 and Top1 is not conserved with Rad60.

Integrating a Rad60 SLD1 deletion mutant into the *S. pombe* genome is lethal. The *rad60-SLD1Δ* allele can be maintained as a heterozygous diploid. The *rad60-SLD1Δ* heterozygous diploid is defective in meiosis. This suggests that the Rad60 SLD1 is essential for Rad60 function and may be required for a role in meiosis.

CHAPTER 4

Rad60 is sumoylated in a manner dependent on the C-terminus

4.1 Introduction

Rad60 interacts both functionally and genetically with the Smc5/6 complex (Morishita, Tsutsui et al. 2002; Boddy, Shanahan et al. 2003). Recently Nse2, a component of the Smc5/6 complex, has been identified as an E3 SUMO ligase (Andrews, Palecek et al. 2005). The Smc5/6 complex proteins Smc6, Nse2, Nse3, and Nse4 are sumoylated in an Nse2-dependent manner *in vitro*. Smc5 and Nse1 have been tested but are not targets of sumoylation *in vitro* (Andrews, Palecek et al. 2005). In chapter 3, I have shown that *rad60-ct* and *nse2-SA* are epistatic in response to both UV and IR. The *nse2-SA* allele encodes a ligase-dead version of the Nse2 protein. In addition, the expression of either *rad60* or *rad60-ct* in the *nse2-SA* background can suppress the sensitivity of *nse2-SA* cells to HU and MMS. Based on these observations it is possible that Rad60 may be a target of Nse2-dependent sumoylation. In this chapter I have tested Rad60 to determine whether it is sumoylated, and if so if this is dependent on Nse2.

4.2 Rad60 is sumoylated *in vitro*

To determine whether Rad60 can be modified by SUMO, Rad60 was tested as a potential substrate in the *in vitro* sumoylation assay (Ho, Warr et al. 2001). Rad60 was labelled with [^{35}S]-methionine by *in vitro* transcription-coupled translation. The *in vitro* transcription-coupled translation requires the gene of interest to be under the control of a T7 promoter. For this reason, *rad60* was sub-cloned from the pTOPO*rad60* construct (Section 3.4.1) into the pEPEXHA vector as an *Nde*I/*Sal*I fragment. 2 μl of the [^{35}S]-labelled Rad60 was incubated with the *in vitro* assay components with (Figure 4.1A, lane 2) and without (Figure 4.1, lane 1) the addition of the mature form of SUMO (Pmt3-GG). Rad60 has a predicted molecular weight of 46 kDa, but consistently runs at a mass of ~60 kDa when analysed by SDS-PAGE. The pEPEXHA vector places a single HA tag at the N-terminus of the expressed protein. Since the HA tag is 1.1 kDa, the increase in mass observed is unlikely to be the result of the HA tag. In the presence of SUMO (Figure 4.1A, lane 2), two slower migrating forms of Rad60 are observed at ~80 and ~100 kDa. SUMO has a

Figure 4.1: Rad60 is sumoylated *in vitro*

(A) Rad60 was tested as a potential substrate in the *in vitro* sumoylation assay. Incubation of ^{35}S-labelled Rad60 with the SAE heterodimer, Hus5 and the mature form of SUMO (Pmt3-GG) resulted in the appearance of two slower migrating forms with sizes consistent with sumoylated forms of Rad60. The products were separated by 7.5% SDS-PAGE and detected with a phosphoimager. **(B)** Schematic to show the relative positions of the 27 lysine residues of Rad60. Lysines are indicated by *.

A

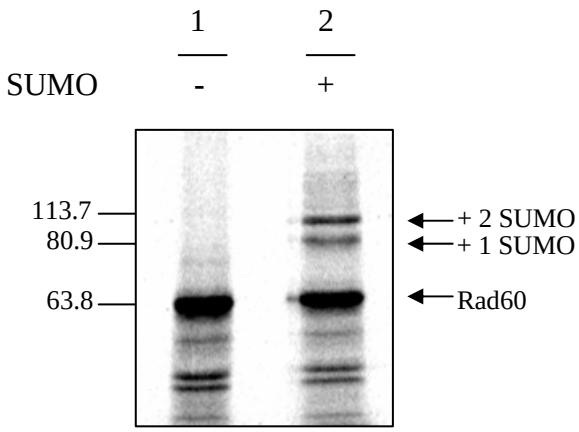

B

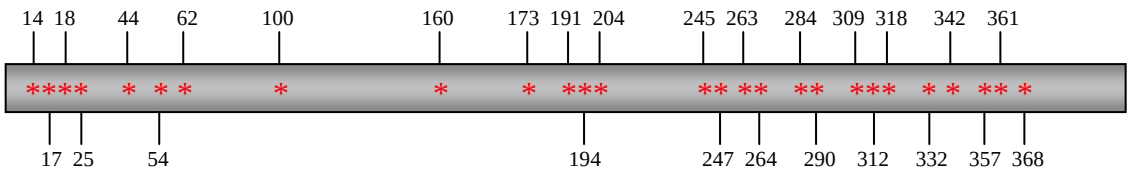

Figure 4.1: Rad60 is sumoylated *in vitro*

predicted molecular weight of ~11 kDa but when analysed by SDS-PAGE proteins appears much larger. SUMO modification adds ~20 kDa to the apparent molecular weight of most substrates. The bands observed for Rad60 modification are therefore consistent with sumoylated forms of Rad60. The Rad60 protein consists of 27 lysines, each of which could act as an acceptor for SUMO-modification (Figure 4.1B). The two modified forms of Rad60 may have arisen due to the use of more than one SUMO acceptor site or to the production of a SUMO chain on one lysine.

4.3 Sumoylation of Rad60 *in vitro* is enhanced by the E3 ligase Pli1, but not Nse2

To test the possibility that Rad60 sumoylation is enhanced by the SUMO E3 ligase Nse2, [^{35}S]-Rad60 was tested as a substrate in the *in vitro* sumoylation assay. 3 μg Hus5 is typically used in standard *in vitro* sumoylation assays. However, to determine whether sumoylation of Rad60 could be enhanced by the SUMO ligase Nse2, the level of Hus5 was reduced in the assay to 0.3 μg. In figure 4.2A, the SUMO activator and ATP-regenerating system are present in all lanes (1-5). In lane 1, the assay mix loaded includes the typical amount of Hus5 (3 μg) and 10 μg His-Pmt3 as a control for Rad60 sumoylation. As previously observed, two slower migrating forms of Rad60 were observed at ~80 and ~100 kDa consistent with SUMO-modified forms of Rad60. In lanes 2-5, the Hus5 concentration was dropped to 0.3 μg/reaction. In the presence of SUMO (lane 3), no modified forms of Rad60 could be observed, as compared to lane 1 (positive control) and lane 2 (negative control with no SUMO). In lane 4, 4 μg Nse2 was added to the sumoylation assay. No modified forms of Rad60 were observed. In contrast, when 4 μg Pli1, the only other known *S. pombe* SUMO ligase, was added to the assay mix, the modified forms of Rad60 were observed at ~80 and ~100 kDa (lane 5). This suggests that Pli1, but not Nse2, can enhance the levels of Rad60 sumoylation *in vitro*.

To test the genetic interactions of *pli1* and *rad60,* the *pli1-d* strain was crossed with *rad60-ct.* Following tetrad dissection, spores containing the *rad60-ct pli1-d* double mutant were not viable. This suggests that *pli1-d* and *rad60-ct* are synthetically lethal. To further test this relationship, *rad60* and *rad60-ct* were expressed from the pREP41HA plasmid in the *pli1-d* background. *pli1-d* cells exhibit a sensitivity to DNA damaging agents similar to

Figure 4.2 Sumoylation of Rad60 *in vitro* is enhanced by the E3 ligase Pli1

(A) 2 μl ^{35}S-labelled Rad60 was incubated with the SAE heterodimer, Hus5 and the mature form of SUMO (Pmt3-GG). To determine whether sumoylation could be enhanced by the SUMO ligases, the Hus5 concentration was reduced from 3 μg (lane 1 (++)) to 0.3 μg per reaction (lanes 2-5 (+)). 4 μg Nse2 (lane 4) or Pli1 (lane 5) were tested in the assay. The products were separated by 7.5% SDS-PAGE and detected with a phosphoimager. (Andi Skilton, University of Sussex, generated this particular image) **(B)** Over-expression of *rad60* but not *rad60-ct* can enhance the sensitivity of *pli1-d* to HU and MMS. Cells carrying the pREP41HA multicopy plasmid (pEV) or pREP41HA containing *rad60* or *rad60-ct* (p*rad60/*p*rad60-ct*) were grown at 30^{o}C in YNB medium supplemented with adenine and uracil to mid-exponential phase. 10 μl of 10 fold serial dilutions were spotted onto YNB plates supplemented with adenine and uracil and containing supplements at the indicated doses. Plates were incubated at 30^{o}C for 72 hours and photographed.

A

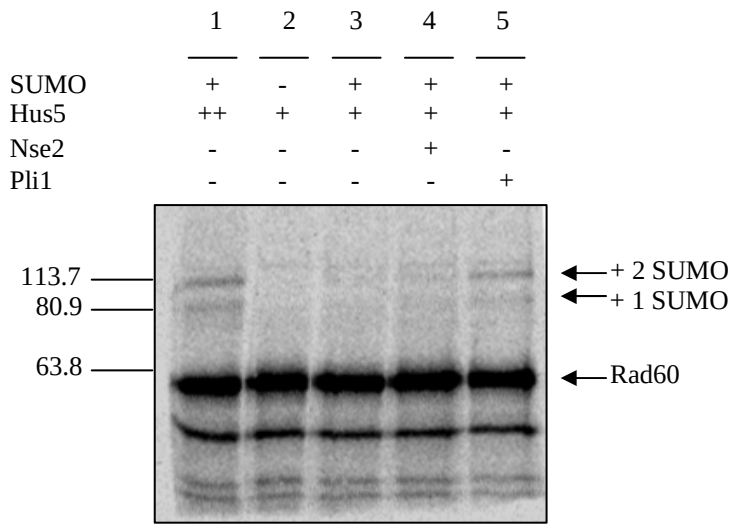

B

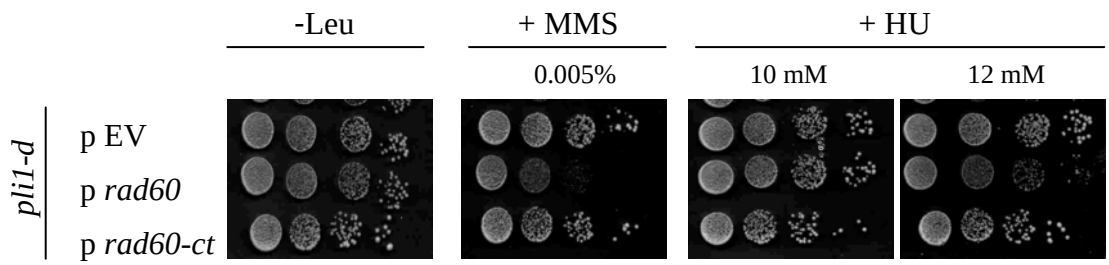

Figure 4.2: Sumoylation of Rad60 *in vitro* is enhanced by the E3 ligase Pli1

that observed for wild-type cells. However, when *rad60* is expressed in the *pli1-d* background, the *pli1-d* cells are hypersensitive to both HU and MMS (Figure 4.2B). This is not observed when *rad60-ct* is expressed in the *pli1-d* background, suggesting that the dominant negative effect of over-expressing *rad60* in *pli1-d* cells is SLD2 dependent.

4.4 Rad60 is sumoylated in a manner dependent on the C-terminus

To investigate the biological significance of Rad60 sumoylation, attempts were made to identify the site, or sites, of SUMO-modification. Rad60 has 27 lysine residues that could act as a SUMO-acceptor site. A systematic approach was therefore needed. One approach was to test truncated fragments of Rad60 in the *in vitro* sumoylation assay. Since a C-terminally truncated version of *rad60* (encoding aa 1-333) was already cloned into pREP41HA (Section 3.4.1), the coding sequence was subcloned into the pEPEX HA vector as an *Nde*I/*Sal*I fragment and tested in the *in vitro* sumoylation assay (Figure 4.3A). The C-terminally truncated form of Rad60 (Rad60-ct) runs at ~50 kDa. In contrast to Rad60, in the presence of SUMO no slower migrating forms of the Rad60-ct were observed (Figure 4.3B). This suggests that SUMO-modification of the Rad60 protein is dependent on the C-terminal 73 amino acids.

The C-terminal region contains four lysine residues that may act as potential sites of SUMO conjugation (Figure 4.4A). Of these four lysine residues, K342 is the only residue that conforms to the φKXE SUMO consensus motif with the localised environment of SKSE. To try to identify the site of SUMO-modification, site-directed mutagenesis was used to introduce lysine (AAA/AAG) to arginine (AGA/AGG) substitutions for each of the four lysines coded for in the *rad60* gene. The mutagenic primers used are described in Table 4.1. Sequencing of pEPEXHA*rad60*, with the T7, L17, L18 and L19 primers was necessary to confirm the lysine to arginine substitutions.

When tested in the *in vitro* sumoylation assay, the Rad60 K342R mutant showed a similar sumoylation pattern to that previously seen for the wild-type Rad60 protein (Figure 4.4B). This suggests that either K342 is not the site of Rad60 sumoylation, or that it is not the only site of Rad60 sumoylation. Rad60 protein with individual K357R, K361R and K368R

Figure 4.3: Rad60 is sumoylated *in vitro*, in a manner dependent on the C-terminus

(A) Schematic to illustrate the C-terminal truncation of Rad60-ct. **(B)** Rad60-ct was tested as a potential substrate in the *in vitro* sumoylation assay. 2 μl ^{35}S-labelled Rad60 and Rad60-ct were incubated with the SAE heterodimer, Hus5 and the mature form of SUMO (Pmt3-GG). The products were separated by 7.5% SDS-PAGE and detected with a phosphoimager.

A

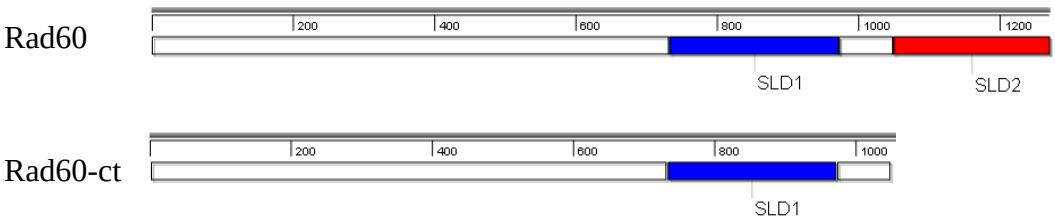

B

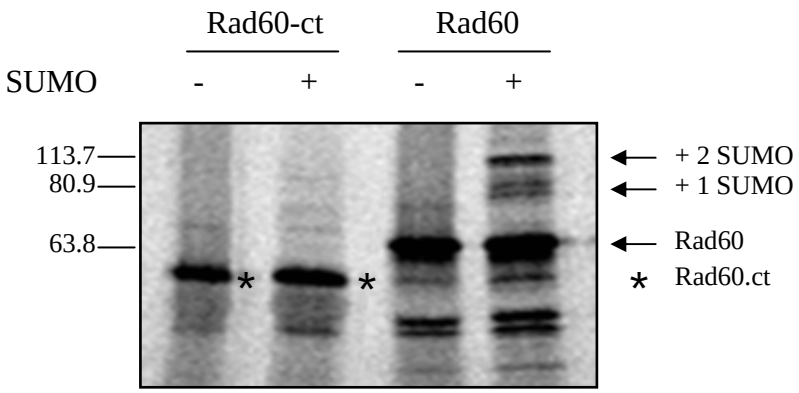

Figure 4.3: Rad60 is sumoylated *in vitro* in a manner dependent on the C-terminus

Figure 4.4: The Rad60 quadruple mutant is still sumoylated *in vitro*

(A) The C-terminal region of Rad60 contains four lysine residues. K342 (boxed in red) conforms to the φKXE SUMO consensus motif. **(B, C)** Rad60 K342R (C) and Rad60 K342/357/361/368R mutants (D) were tested in the *in vitro* sumoylation assay. 2 μl ^{35}S-labelled mutant Rad60 was incubated with the SAE heterodimer, Hus5 and the mature form of SUMO (Pmt3-GG). The products were separated by 7.5% SDS-PAGE and detected with a phosphoimager.

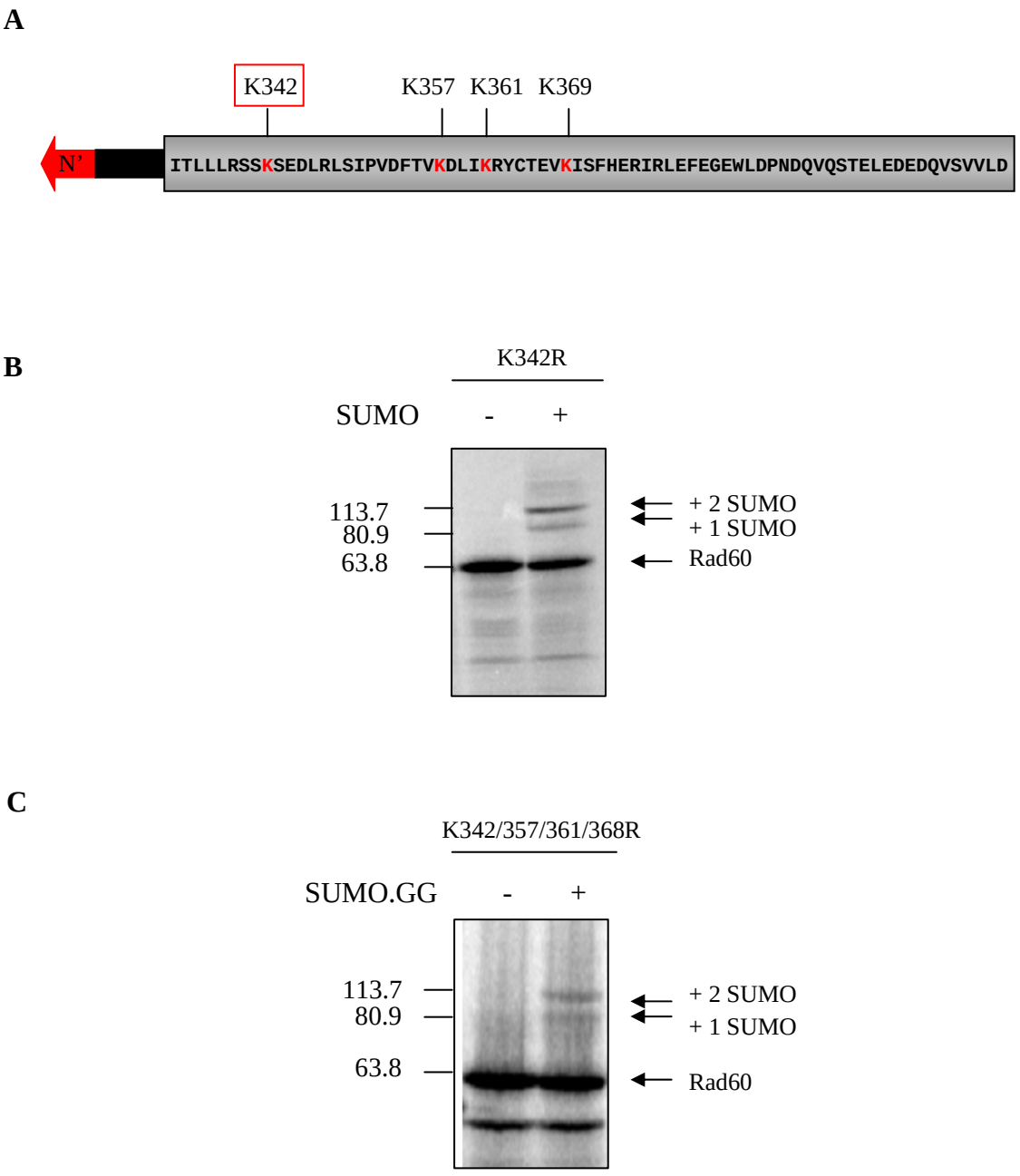

Figure 4.4: The Rad60 quadruple mutant is still sumoylated *in vitro*

Table 4.1: Mutagenic primer sequences for mutating potential sumoylation sites of Rad60

Mutation	Primer	Primer sequence (5' to 3')
K17/18R	L109 L110	F-CAAAGCCTATTAGAAGGCCTCCATTAAACTATGCC R-GGCATAGTTTAATGGAGGCCTTCTAATAGGCTTTC
K173	L156 L157	F-GTACAAATTCACACGCATAGGAGAGAAATTGAAGAAGACG R-CGTCTTCTTCAATTTCTCTCCTATGCGTGTGAATTTGTAC
K204	L158 L159	F -CGCTGTATCACTCCAGATCGGAATTCTCAAC R-GTTGAGAATTCCGATCTGGAGTGATACAGCG
K263/264R	L78 L79	F-CGTACTCTGAAAGAAGAAGAGTAGATAACG R-CGTTATCTACTCTTCTTCTTTCAGAGTACG
K290	L111 L112	F-GGTATGCTTAGAGTCGATACCCG R-CGGGTATCGACTCTAAGCATACC
K332R	L113 L114	F-GCTCAAACGTGTAGACTTATAACGTTGC R-GCAACGTTATAAGTCTACACGTTTGAGC
K342R	L37 L38	F-GCTTTTGCGTTCGAGTAGGAGTGAGGATCTTCG R-CGAAGATCCTCACTCCTACTCGAACGCAAAAGC
K357R	L56 L57	F-CCGTCGATTTCACTGTTAGAGATTTGATTAAGAG R-CTATTAATCAAATCTCTAACAGTCAAATCGACGG
K361R	L58 L59	F-CACTGTTAAAGATTTGATTAGGAGATATTGTACTG R-CAGTACAATATCTCCTAATCAAATCTTTAACAGTG
K368R	L60 L61	F-GTACTGAAGTAAGGATTAGTTTTCATGAACGC R-GCGTTCATGAAAACTAATCCTTACTTCAGTAC

mutations also showed the same wild-type sumoylation pattern when tested (data not shown). Since two modified forms of Rad60 can be identified by the SUMO assay, it is possible that by knocking out single lysine residues, other lysine residues can still be modified by SUMO. Further rounds of site-directed mutagenesis on the mutant pEPEXHA*rad60* constructs were therefore undertaken to produce combinations of double and triple mutants. Like the single mutants, the double and triple mutants produced the same sumoylation pattern as wild-type Rad60 when tested in the *in vitro* sumoylation assay (data not shown). Since the region truncated in the Rad60-ct protein, which showed a loss of SUMO-modification, contains only four lysine residues, a Rad60 K342/357/361/368R quadruple mutant was tested. Surprisingly, in the presence of SUMO, the wild-type Rad60 sumoylation pattern was still observed (Figure 4.4C). This suggests that the site of Rad60 SUMO-modification, *in vitro*, is not within the C-terminal 73 amino acids, but that SUMO modification of Rad60 is dependent on the C-terminus. The site at which Rad60 was truncated to create Rad60-ct lies between L333 and I334 in the CKLITL peptide sequence. This raises the possibility that, if the site of Rad60 modification is K332, the truncation may have altered the local environment of the lysine in such a way that it cannot be modified. To test this a K332R mutation was created and tested in the *in vitro* sumoylation assay. In the presence of SUMO, the wild-type Rad60 sumoylation pattern was still observed for the K332R mutation (Figure 4.5B).

4.5 Mutating possible sumoylation sites in Rad60 does not disrupt sumoylation *in vitro*

To identify possible sites of SUMO modification, the Rad60 protein sequence was submitted to the SUMOplot (http://www.abgent.com/tool/sumoplot) and SUMOsp (http://bioinformatics.lcd-ustc/org/sumosp) prediction software. Predicted sites of Rad60 SUMO-modification are shown in figure 4.5A. The *rad60-1* mutant carries a K263E mutation in its *rad60* coding sequence. Since K263 has been identified as a possible site of SUMO-modification, it is possible that the phenotype observed for *rad60-1* cells may be a consequence of loss of sumoylation. To test this *in vitro*, site-directed mutagenesis was used to create the double K263/264R mutation in the pEPEXHA*rad60* construct. Since K263 is immediately followed by another lysine, K264, a double mutant was created with a

Figure 4.5: Mutating possible sumoylation sites in Rad60 does not disrupt sumoylation *in vitro*

(A) Table to illustrate the possible Rad60 sumoyltaion sites predicted by SUMOplot (http://www.abgent.com/tool/sumoplot) and SUMOsp (http://bioinformatics.lcd-ustc/org/sumosp). **(B)** Lysines within the predicted motifs were mutated to arginine and tested in the *in vitro* sumoylation assay. 2 μl ^{35}S-labelled mutant Rad60 was incubated with the SAE heterodimer, Hus5 and the mature form of SUMO (Pmt3-GG). The products were separated by 7.5% SDS-PAGE and detected with a phosphoimager.

A

SUMOplot	SUMOsp	Context
K17		IKKPP
K18		IKKPP
K173	K173	HKRE
	K204	SKSE
K263		ERKKV
K290	K290	LKVD
	K342	SKSE

B

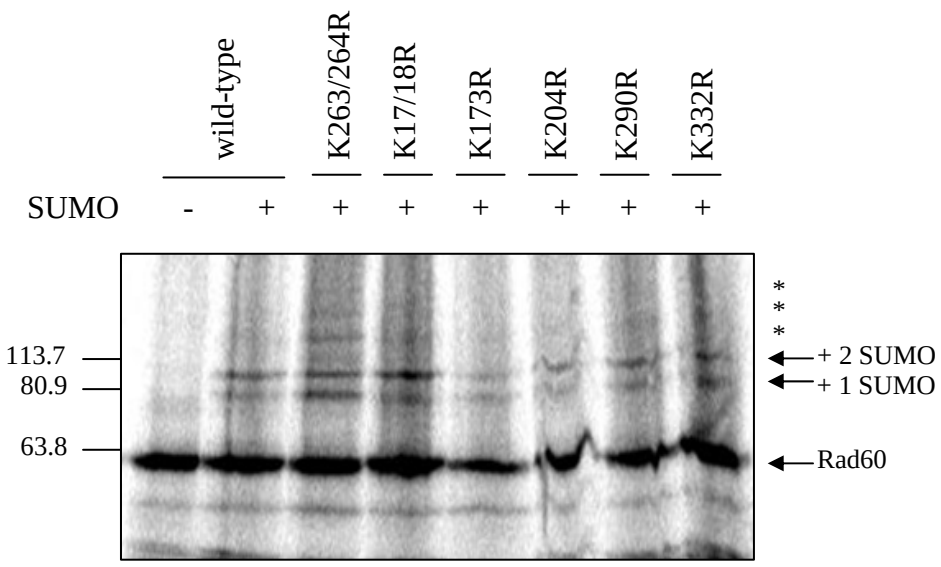

Figure 4.5: Mutating possible sumoylation sites in Rad60 does not disrupt sumoylation *in vitro*

single primer pair. The mutagenic primers used are described in Table 4.1. Sequencing of pEPEXHA*rad60*, with the T7, L17, L18 and L19 primers was necessary to confirm the lysine to arginine substitutions. When tested in the *in vitro* sumoylation assay, the Rad60 K263/264R mutant showed a similar sumoylation pattern to that previously seen for the wild-type Rad60 protein (Figure 4.5B). Other predicted sumoylation sites were tested in a similar manner. Rad60 carrying K17/18R, K204R, K263R and K290R mutations all produced a similar SUMO-modification pattern to that of the wild-type protein when tested in the *in vitro* sumoylation assay (Figure 4.5B). This suggests that either Rad60 is not modified on one of the predicted sumoylation sites, or, if it is, when that site is no longer available for modification, SUMO can be conjugated to another lysine residue. To explore this further, double and triple mutants would have to be made and tested. Due to time constraints this was not undertaken.

4.6 Rad60-ct does not interact with Hus5 *in vitro*

During the process of SUMO conjugation, the target protein forms a thiolester linkage with the SUMO conjugator (Johnson and Blobel 1997). Since Rad60 is sumoylated *in vitro*, it is therefore predicted that it would interact with the *S. pombe* SUMO conjugator, Hus5. To test this, an *in vitro* GST pull-down assay was carried out. Glutathione-sepharose beads were incubated with lysate from cells expressing either GST-Hus5 or GST as a control. ^{35}S-labelled Rad60 was incubated with the pre-bound beads. Figure 4.6A shows GST-Hus5 (lane 5 ~40 kDa, lower panel) and a GST control (lane 4 ~26 kDa, lower panel) bound to the glutathione-sepharose beads. In the GST-Hus5 lane (lane 5), a small portion of the GST has become cleaved from the Hus5 protein producing a faint band at ~26 kDa. When incubated with the pre-bound GST-Hus5 beads, a strong band of ^{35}S-labelled Rad60 (~60 kDa) was detected in the bound fraction (lane 5, upper panel), with substantially less in the unbound fraction (lane 6, upper panel). When ^{35}S-labelled Rad60 was incubated with control GST beads, Rad60 was detected in the unbound fraction (lane 3) but not the bound fraction (lane 4). This suggests that Rad60 can interact with Hus5 *in vitro*, supporting the results obtained from the *in vitro* sumoylation assay.

The C-terminally truncated Rad60-ct protein is not SUMO-modified *in vitro* (Section 4.2). To determine if the Rad60-ct protein can interact with the Hus5 SUMO conjugator, Rad60-

Figure 4.6: Hus5 interacts with Rad60, but not Rad60-ct, *in vitro*

(A) An *in vitro* GST pull-down assay was carried out. Glutathione-sepharose beads were incubated with lysate (L) from cells expressing either GST-Hus5 or GST as a control. ^{35}S-labelled Rad60 (Input (I)) was incubated with the pre-bound beads in the presence of ATP, CPK and CP for 1 hour. Beads were washed and the unbound (U) fraction was collected. The beads were boiled in 30 ml 5x sample buffer and 15 μl of the bound proteins (B) were separated by 10% SDS-PAGE. The gels were analysed by a phosphoimager and Western blotting with anti-GST antibody. **(B)** ^{35}S-labelled Rad60-ct was tested in the *in vitro* GST pull-down assay.

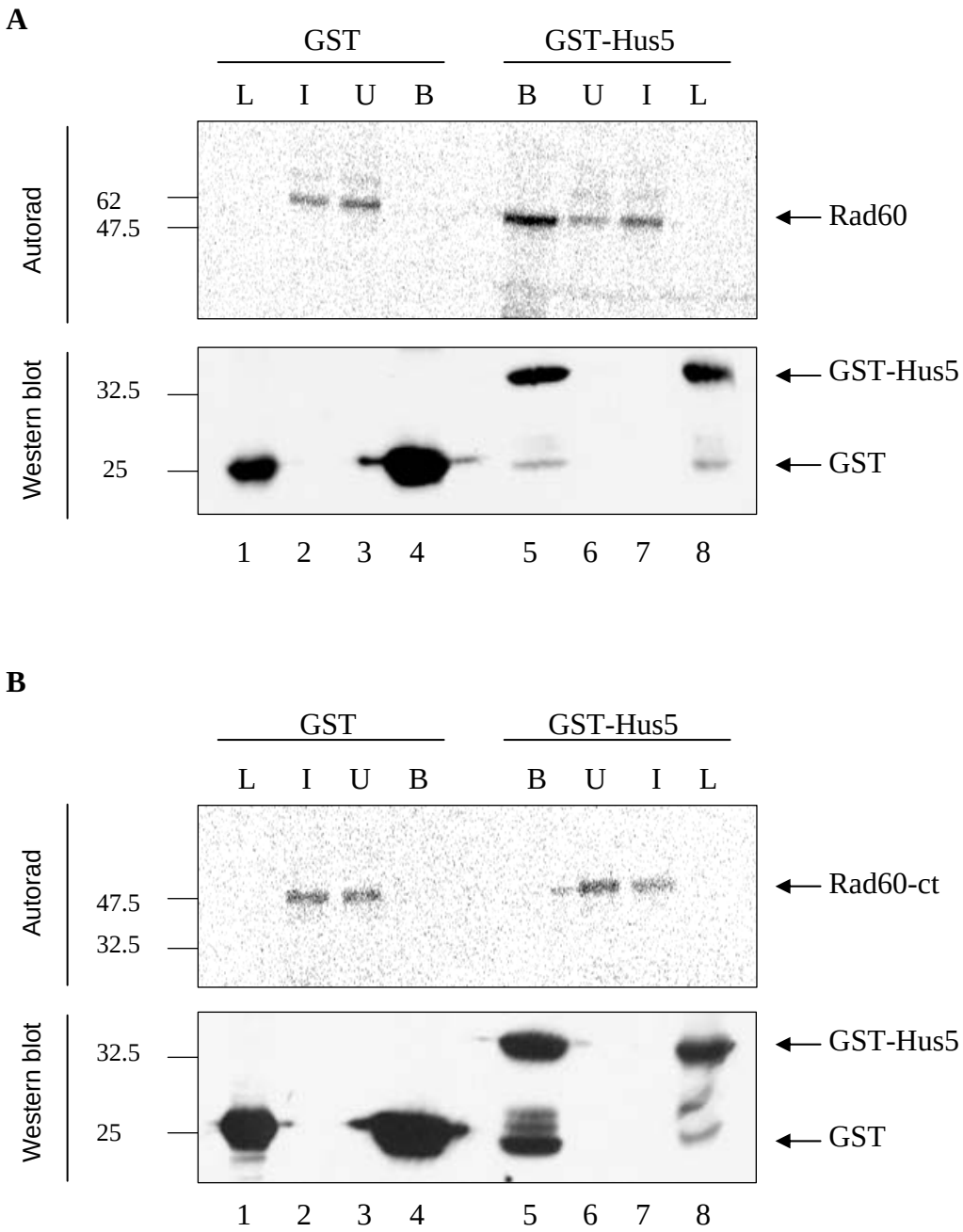

Figure 4.6: Hus5 interacts with Rad60, but not Rad60-ct, *in vitro*

ct was tested in the *in vitro* GST pull-down assay (Figure 4.6B). As is observed with the control GST beads (lane 4), the pre-bound GST-Hus5 beads do not pull down ^{35}S-labelled Rad60-ct (lane 5). All Rad60-ct protein remains in the unbound fraction (lane 6). This observation that Rad60-ct cannot interact with Hus5 *in vitro*, suggests that this is why Rad60-ct is not modified in the *in vitro* sumoylation assay.

In parallel with Rad60 and Rad60-ct, Smc6 and Nse2 were tested in the *in vitro* GST pull-down assay. Smc6 has previously been shown to be sumoylated both *in vitro* and *in vivo* and shown to interact with Hus5 *in vitro* (Andrews, Palecek et al. 2005) (Andrews, E, thesis) and was therefore tested as a positive control for the Rad60 and Rad60-ct *in vitro* GST pull-down assay. Figure 4.7A shows that when incubated with the pre-bound GST-Hus5 beads, a strong band of ^{35}S-labelled Smc6 (~130 kDa) was detected in the bound fraction (lane 5), as compared to the unbound fraction (lane 6). When incubated with the control GST beads, Smc6 was detected only in the unbound fraction (lane 3). In contrast, when the E3 SUMO ligase, Nse2, was incubated with the GST-Hus5 beads (Figure 4.7B) no ^{35}S-labelled Nse2 was detected in the bound fraction (lane 5). All Nse2 protein remained in the unbound fraction (lane 6). This suggests that Nse2 does not interact with Hus5 *in vitro*.

4.7 High molecular weight forms of Rad60, with sizes consistent for sumoylated species, can be identified *in vivo*

Since sumoylation of Rad60 had been shown *in vitro,* the next step was to try to confirm that Rad60 is also sumoylated *in vivo*. Ni^{2+}pulldown experiments were therefore carried out. myc-His-tagged SUMO (MH-SUMO) and HA-tagged Rad60 (HA-Rad60) were co-expressed by transforming wild-type *S. pombe* cells with pREP42MH*pmt3-GG* and pREP41HA*rad60*. As controls, cells were also transformed with the empty pREP vectors. Expression of the SUMO and Rad60 proteins from the pREP vectors was de-repressed by growing cells without thiamine for ~16 hours. Cells were lysed and MH-SUMO was pulled down using Ni^{2+} agarose beads under denaturing conditions. TCA total cell extracts were carried out in parallel as a control for protein expression.

Figure 4.7: Hus5 interacts with Smc6, but not Nse2, *in vitro*

A) An *in vitro* GST pull-down assay was carried out. Glutathione-sepharose beads were incubated with lysate (L) from cells expressing either GST-Hus5 or GST as a control. ^{35}S-labelled Smc6 (Input (I)) was incubated with the pre-bound beads in the presence of ATP, CPK and CP for 1 hour. Beads were washed and the unbound (U) fraction was collected. The beads were boiled in 30 ml 5x sample buffer and 15 μl of the bound proteins (B) were separated by 10% SDS-PAGE. The gels were analysed by a phosphoimager and Western blotting with anti-GST antibody. **(B)** ^{35}S-labelled Nse2 was tested in the *in vitro* GST pull-down assay.

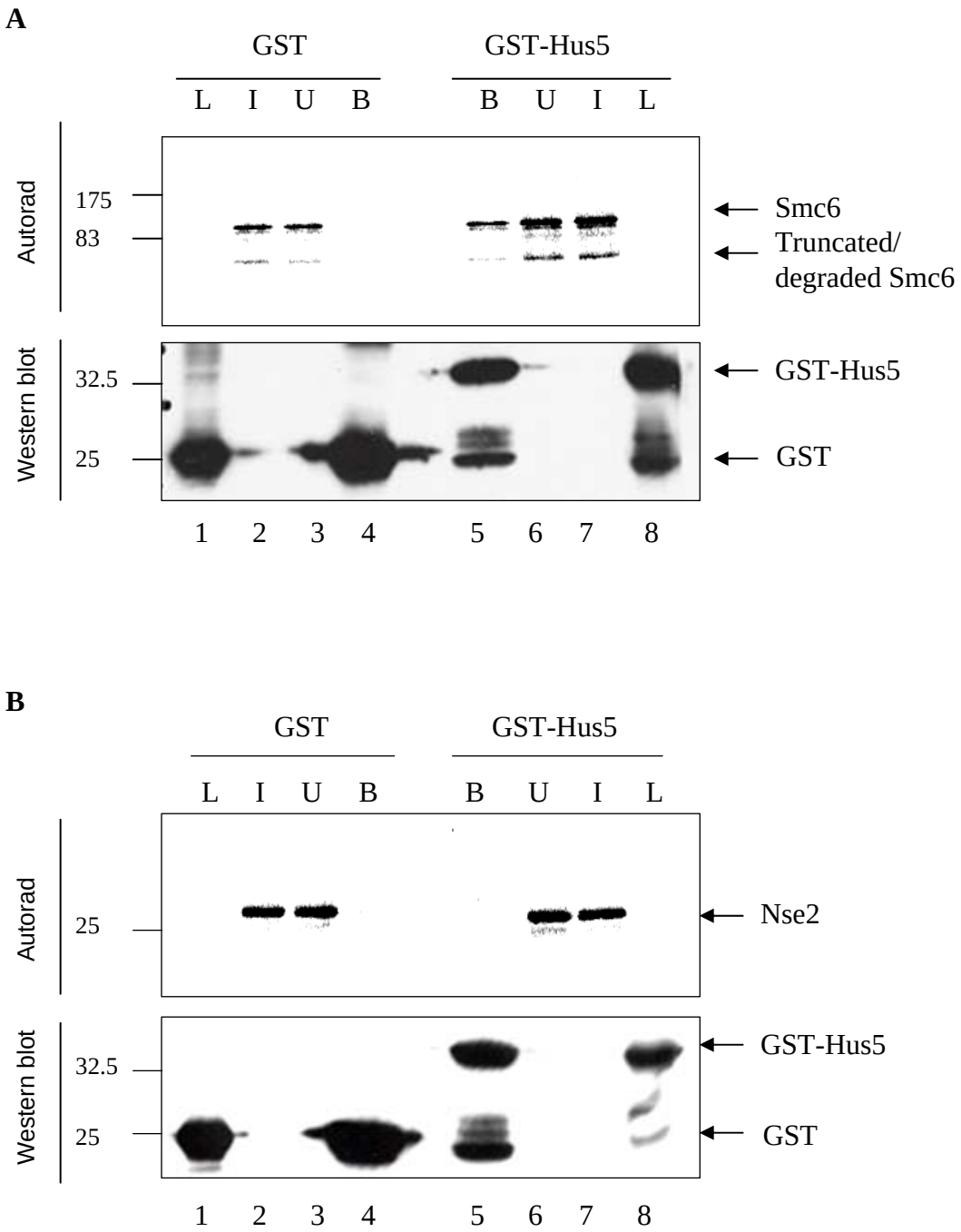

Figure 4.7: Hus5 interacts with Smc6, but not Nse2, *in vitro*

Figure 4.8 shows results of the Ni^{2+} pull-downs and corresponding TCA blots. In lane 1, cells were transformed with empty pREP41HA and pREP42MH vectors. The anti-myc and anti-HA antibodies therefore detected no signal in this sample. In lane 2 cells were transformed with pREP41HArad60 and empty pREP42MH vector. When probed with anti-HA, a strong band at ~60 kDa, corresponding to HA-tagged Rad60 was observed in the TCA extract. Above the Rad60 band is a smear that may correspond to a ladder of modified forms of Rad60. As expected, the anti-myc antibodies detected no signal. When the same cells were used for the Ni^{2+} pull-down (lane 2), a weak signal, corresponding to the size expected for Rad60, was detected by the anti-HA antibodies. Since only His-tagged species should bind to the Ni^{2+} beads, no signal should be detected. This suggests that Rad60 can bind non-specifically to the Ni^{2+} beads. In lane 3, when cells were transformed with pREP42MH*pmt3.GG* and empty pREP41HA vector, a ladder of SUMO-modified species was observed for both the Ni^{2+} pull-down and the TCA extract when probed with anti-myc antibody. As expected, no signal was observed when probed with anti-HA. In lanes 4, 5, 6, and 7 cells were transformed with pREP42MH*pmt3.GG* and pREP41HA*rad60* constructs. In lane 4, a ladder of SUMO-modified species was observed for both the Ni^{2+} pull-down and the TCA extract when probed with anti-myc antibody. When probed with anti-HA, a strong band of ~60 kDa, corresponding to HA-tagged Rad60 was observed in the TCA extracts. As in lane 2, a smear above Rad60 can be observed. This smear may correspond to a ladder of modified Rad60 forms. The HA signals observed in lane 2 and 4 are comparable for the TCA extracts. This indicates that cells are expressing Rad60 at a similar level. When the same cells were used for the Ni^{2+} pull-down (lane 4), a strong signal, corresponding to the size expected for Rad60, was detected by the anti-HA antibodies. In addition, the slower migrating forms of Rad60 are more discrete than observed in the TCA samples. Slower migrating bands can be identified. The first two bands correspond to a size of ~80 and ~100 kDa, consistent with the sizes expected for Rad60 modified with one and two SUMO molecules respectively. Unfortunately in the Ni^{2+} pull-downs, the signal for the unmodified form of Rad60 is also increased in lanes 4 to 7 relative to that of lane 2. It is therefore difficult to say with certainty that these bands are SUMO-dependent. It is possible that the increase in signal for the unmodified form of Rad60 is the result of modified forms losing their conjugated SUMO species prior to being analysed by SDS-PAGE. In lanes 5,

Figure 4.8: High molecular weight forms of Rad60, with sizes consistent for sumoylated species, can be identified *in vivo*

Wild-type *S. pombe* cells were transformed with pRE42MH*pmt3.GG* and pREP41HA*rad60* constructs. As controls, cells were also transformed with empty pREP vectors. Expression of the SUMO and Rad60 proteins from the pREP vectors was de-repressed by growing cells without thiamine for ~16 hours. Cells were exposed to 250 Gy, 0.01% MMS or 20 mM HU as indicated. 60 OD units of cells were lysed and MH-SUMO was pulled down using Ni^{2+} agarose beads under denaturing conditions. TCA total cell extracts were carried out in parallel. Proteins were separated by 7.5% SDS-PAGE. The gels were analysed by Western blotting with anti-myc or anti-HA antibody as indicated.

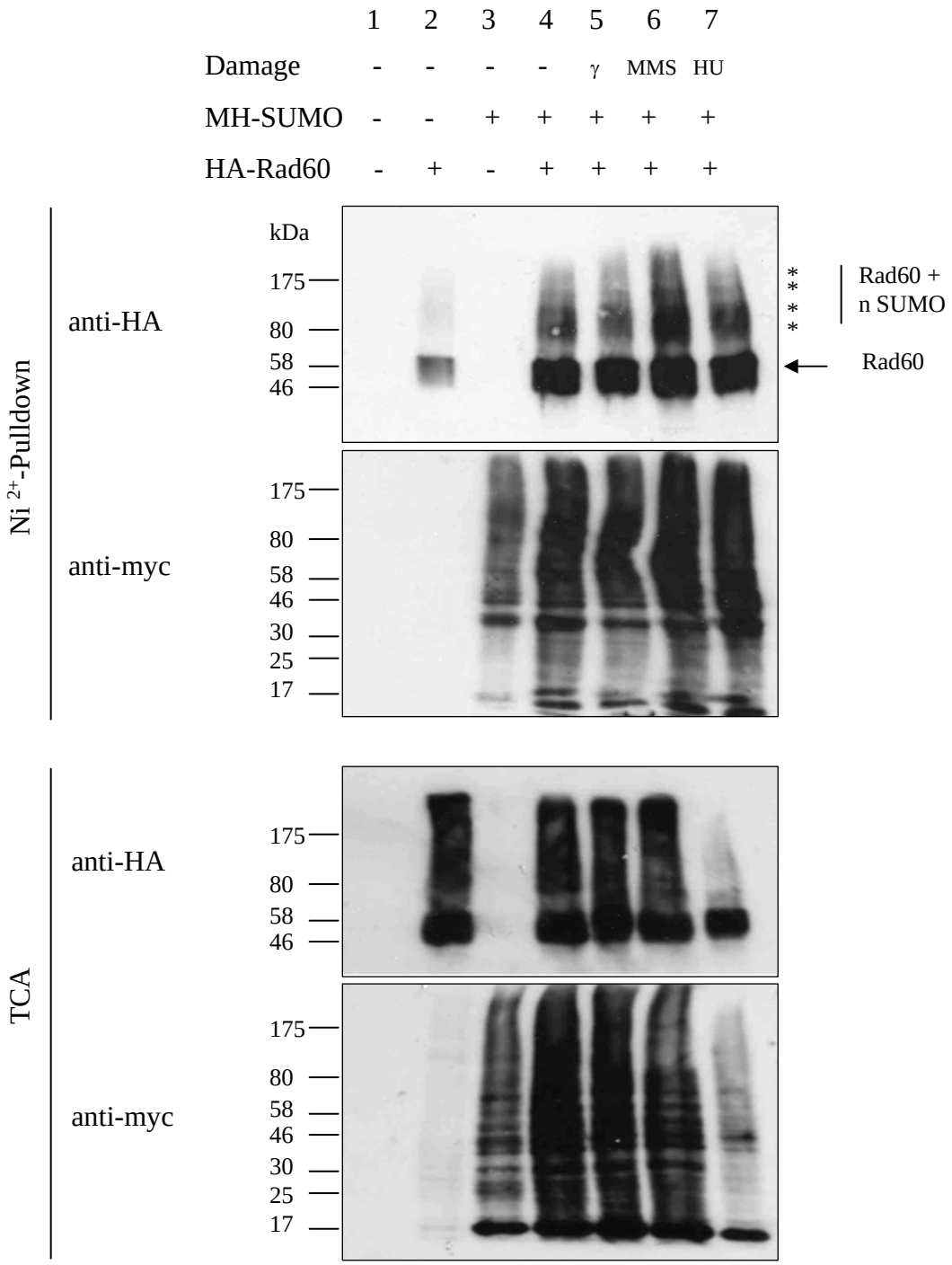

Figure 4.8: High molecular weight forms of Rad60, with sizes consistent for sumoylated species, can be identified *in vivo*

6, and 7, cells were treated exposed to IR and treated with MMS and HU respectively. A similar pattern of modification was observed in all three lanes. Treatment with 0.01% MMS (lane 6), resulted in a stronger signal for the modified forms. This is reminiscent of Smc6, which shows an increased level of sumoylation following treatment with MMS (Andrews, Palecek et al. 2005).

Slower migrating forms of Rad60, consistent with sumoylation, were consistently observed in TCAs and Ni^{2+} pull-down experiments. Due to the time constraints and the fact that Rad60 binds non-specifically to the Ni^{2+} beads, further investigation into the *in vivo* sumoylation of Rad60 was not carried out.

4.8 Discussion

In this chapter I have tested Rad60 as a potential substrate of sumoylation. When tested in the *in vitro* sumoylation assay, two slower migrating forms of Rad60 were observed with sizes consistent with that expected for SUMO-modified forms. The two modified forms may have arisen as a result of the use of more than one SUMO-acceptor site, or the production of a SUMO chain on one target lysine. In the case of Rad60, it is likely that modification is occurring on two separate lysine residues. This is because the lower band corresponding to Rad60 modified with a single SUMO is consistently less discreet than the upper band. In fact, in figure 4.3, two discrete bands can be identified within the lower band, suggesting that SUMO-modification on the two different lysine residues results in a slightly different mobility when analysed on SDS-PAGE.

To investigate the biological significance of Rad60 sumoylation, attempts were made to identify the site(s) of SUMO-modification. A C-terminally truncated form of Rad60 (aa 1-333) is not modified *in vitro*. The C-terminal region contains four lysine residues, one of which, K342, conforms to the φKXE consensus motif. When tested in the *in vitro* sumoylation assay, the K342R mutant showed a similar modification pattern to that previously seen for the wild-type Rad60 protein. A K342/357/361/368R quadruple mutant also shows a modification pattern similar to the wild-type Rad60 protein. This suggests that although the site(s) of sumoylation are not within the C-terminal 73 amino acids, SUMO

modification of Rad60 is dependent on the C-terminus. There are a few possibilities as to why Rad60-ct is not sumoylated, but the quadruple mutant is. Firstly, the truncated form of the protein may have altered the conformation of the protein in such a manner that the protein cannot be sumoylated. Secondly, the site at which *rad60* was truncated is in close proximity to K332. This raises the possibility that if K332 is the site of SUMO-modification, the truncation may have altered the local environment of the residue in such a way that it can longer be modified. This possibility can be discounted since the K332R mutant can still be modified *in vitro*. A third possibility is that the SUMO conjugator cannot bind the truncated Rad60-ct protein. For sumoylation to occur, the conjugator must bind Rad60. This possibility is supported by the fact that in an *in vitro* GST pull-down assay, Rad60 but not Rad60-ct is able to bind the Hus5 conjugator.

Despite the genetic interaction of Rad60 and Nse2 (Section 3.4), sumoylation of Rad60 *in vitro* is not enhanced by the Nse2 SUMO ligase. This is in contrast to the situation with some of the other proteins of the Smc5/6 complex (Andrews, Palecek et al. 2005). It is possible however, that Nse2-dependent sumoylation of Rad60 may require the rest of the Smc5/6 complex. Instead sumoylation of Rad60 *in vitro* can be enhanced by the Pli1 SUMO ligase. A *rad60-ct pli1-d* double mutant is synthetically lethal. In addition, expression of *rad60* but not *rad60-ct* can enhance the sensitivity of *pli1-d* cells to HU and MMS. One possible explanation for this is that Pli1-dependent sumoylation of Rad60 is necessary for Rad60 function. In this scenario, in the absence of Pli1, the unmodified from of Rad60 has a dominant negative effect. This is consistent with the loss of SUMO-modification observed for the truncated Rad60-ct protein. The *rad60-ct* mutant is sensitive to HU and MMS (Section 3.4).

Attempts to identify the site(s) of SUMO-modification were made by mutating lysines within motifs predicted to be possible sites of sumoylation. All mutants tested were still modified *in vitro*. Before being able to investigate the biological significance of Rad60 sumoylation, the site(s) of sumoylation must be identified and sumoylation verified *in vivo*. Since Rad60 appears to be modified on two separate sites, further mutagenesis is required to mutate more than one residue at a time. Due to time constraints this was not carried out.

Slower migrating forms of Rad60, consistent with sumoylation, were consistently observed when Rad60 and SUMO were over-expressed in wild-type cells. As previously observed for Smc6 (Andrews, Palecek et al. 2005), modified forms of Rad60 were enhanced after treatment of cells with MMS. Due to time constraints further investigation into the *in vivo* sumoylation of Rad60 was not carried out.

CHAPTER 5

SUMO-like domain 2 is required for the correct localisation of the *S. pombe* Rad60 protein

5.1 Introduction

Rad60 is a nuclear protein that exits the nucleus upon treatment of cells with HU (Morishita, Tsutsui et al. 2002; Boddy, Shanahan et al. 2003). HU is an S-phase inhibitor that inhibits ribonucleotide reductase, thereby depleting dNTP pools and causing replication fork arrest. HU-induced fork stalling triggers a replication checkpoint response that leads to the activation of the effector protein kinase Cds1 (*H. sapiens* Chk2 homologue). Cds1 interacts with a number of DNA replication and repair factors, including Rad60. Interaction with Cds1 results in hyperphosphorylation and concomitant delocalisation of Rad60 from the nucleus (Boddy, Shanahan et al. 2003). A *rad60-4* (T72A, I232S, Q250R, K312N) mutant is proficient for survival of UV-induced DNA damage but is uncoupled from Cds1 regulation, therefore unable to delocalise from the nucleus following HU treatment (Boddy, Shanahan et al. 2003). This suggests that Rad60 performs its DSB repair role in the nucleus and that phosphorylation by Cds1 acts to inhibit this activity by delocalising Rad60 from the nucleus. It has been suggested that the role of this delocalisation may be to prevent homologous recombination of unfavourable substrates e.g. stalled replication forks (Boddy, Shanahan et al. 2003).

I have previously created a *rad60-ct* strain in which the C-terminal SLD has been deleted. Like *rad60-1* (K236E), *rad60-ct* is hypersensitive to DNA damage caused by IR and UV and also to treatment with the DNA damaging agents MMS and HU. In this chapter I will investigate the localisation of the Rad60 protein in the *rad60-ct* mutant strain. For simplicity, I will refer to the C-terminally truncated Rad60 protein in this strain as 'Rad60-ct'.

5.2 Deletion of the C-terminal 73 amino acids results in mis-localisation of the Rad60 protein.

5.2.1 Creating C-terminally GFP-tagged Rad60 and Rad60-ct strains

To determine whether deletion of SLD2 affects the localisation of this protein, C-terminally GFP-tagged *rad60* and *rad60-ct* strains were constructed using the one-step PCR-based gene disruption method (Bahler, Wu et al. 1998). The one-step PCR-based gene disruption method uses long primers containing 80 nucleotides of gene-specific sequence and 20 nucleotides of sequence homologous to the pFA6a-GFP(S65T)-kanMX6a template plasmid.

Primer pairs L34 and L27, and L33 and L27 were used to PCR out the gene specific cassette for the *rad60* and *rad60-ct* GFP-tagged strains respectively. The gene specific sequences of these forward primers L33 and L34 correspond to 80 nucleotides immediately upstream of the sites at which the tag is to be placed, omitting the stop codon. In the reverse primer, L27, the gene-specific sequence corresponds to 80 nucleotides immediately downstream of the *rad60* stop codon. The primer pairs were used to amplify an ~3.6 kb heterologous kanMX6 module from the pFA6a-GFP(S56T)-kanMX6 plasmid. The products of 5 PCRs were pooled (~20 μg) and gel extracted to a volume of 20 μl. The DNA was transformed directly into haploid wild-type cells (*sp.011*) using the Bahler transformation protocol (Bahler, Wu et al. 1998). Cells were plated onto YEA plates and grown for 24 hours at 30^{o}C before being replica plated onto YEA plates containing 100 μg/ml G418. The replica plates were incubated at 30^{o}C for 72 hours and large colonies were re-streaked onto fresh YEA plates containing G418. Colony PCR, with primers L17 and L96, was used to screen transformants for successful integration (Figure 5.1A). The forward primer, L17, anneals within the *rad60* gene and reverse primer, L96, anneals within the kanMX6 cassette to give a PCR product of ~940 bp and ~710 bp for colonies containing the full-length, and C-terminally truncated copy of the *rad60* gene respectively. Since the primer sequence of L96 includes the *Bam*HI and *Pac*I sites of the multiple cloning site of pFA6a, which is included at the 5' end of both the kanMX6 and GFP(S56T)-kanMX6 cassettes, colony PCRs with *rad60-FL* and *rad60*-ct strains were carried out as positive controls and with the wild-type strain as a negative control. As expected, no bands were amplified for wild-type cells. The C-terminally GFP-tagged strains were named *rad60-FL-GFP* (*sp.*1307) and *rad60-ct-GFP* (*sp.1306*).

Figure 5.1: Creating C-terminally GFP-tagged *rad60-ct and rad60-FL* strains

C-terminally GFP-tagged *rad60-FL* and *rad60-ct* strains were created using the one-step PCR based gene disruption method**. (A)** Colony PCR with primers L17/L96 confirmed integration of the kanMX6 cassette in the *rad60-FL-GFP* and *rad60-ct-GFP* cells. **(B)** TCA extracts from *rad60-FL-GFP* and *rad60-ct-GFP* were separated by 10% SDS-PAGE and analysed by Western blotting with anti-GFP antibody. **(C)** Comparison of the HU and MMS sensitivity of tagged and untagged *rad60-FL* and *rad60-ct* cells. Cells were grown at 30^{o}C in YE medium to mid-exponential phase. 10 μl of 10 fold serial dilutions were spotted onto YEA plates containing supplements at the indicated doses. Plates were incubated at 30^{o}C for 72 hours and photographed.

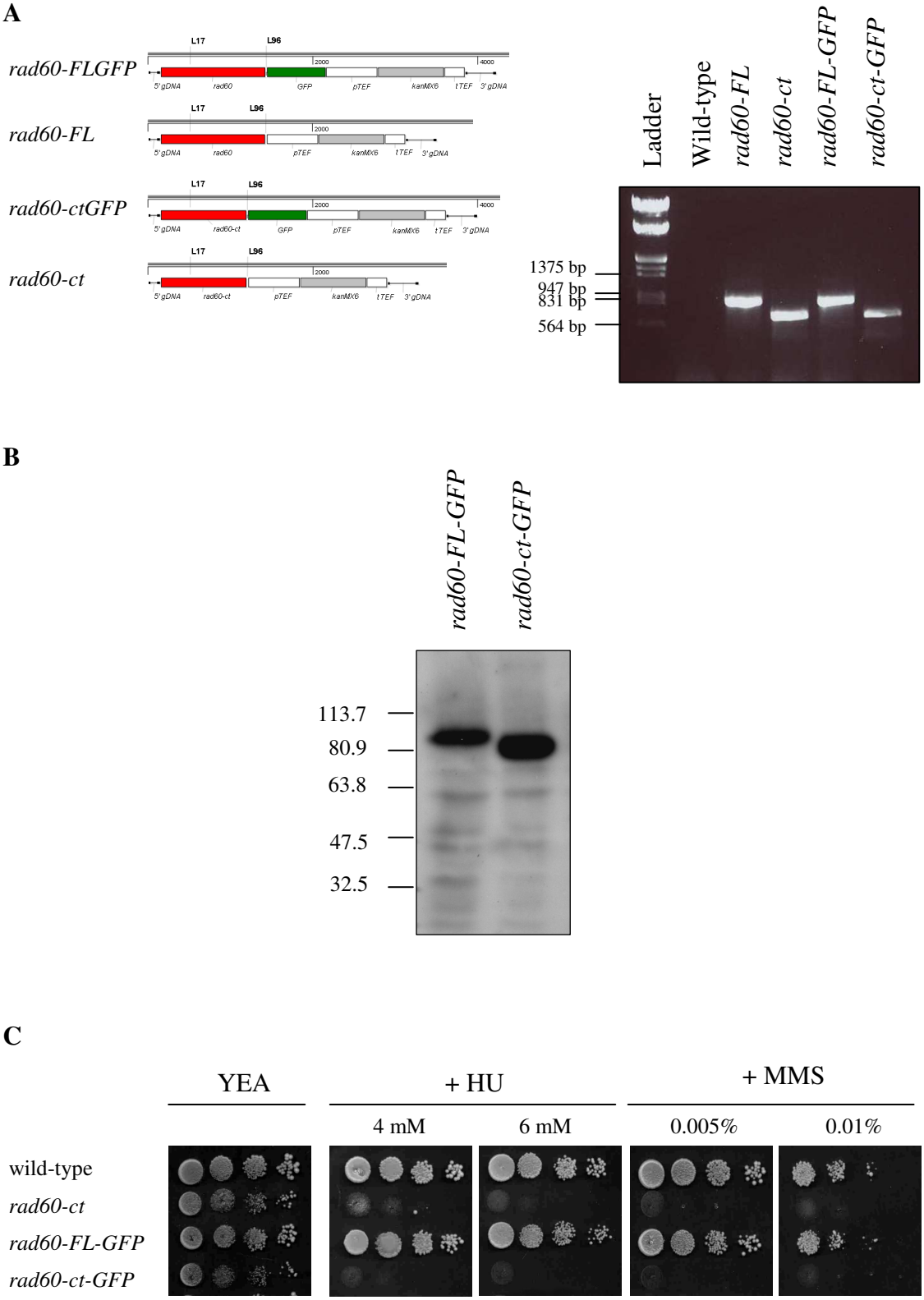

Figure 5.1: Creating C-terminally GFP-tagged *rad60-ct and rad60-FL* strains

To ensure that integration had occurred at the correct site and no mutations had been introduced, sequencing across the integration junction was required. Genomic DNA was extracted from the positive colonies and the region surrounding the junction site was amplified by PCR from the genomic DNA with primers L41 and L96. Sequencing with primers L18 confirmed correct integration of the GFP(S56T)-kanMX6 cassette in the *rad60-ct-GFP* and *rad60-FL-GFP* strains.

To confirm that the Rad60-GFP and Rad60-ct-GFP protein is stable, TCA extracts from *rad60-FL-GFP* and *rad60-ct-GFP* were Western blotted with anti-GFP antibody (Figure 5.1B). A band of ~95 kDa was observed for the full-length protein (Rad60-FL-GFP). Rad60 has a predicted molecular weight of 46 kDa, but consistently runs at a mass of ~60 kDa when separated by SDS-PAGE (Chapter 4). Since the GFP-tag is ~35 kDa, I would expect the Rad60-GFP protein to run at ~95 kDa. A smaller band of ~85 kDa was observed for the C-terminally truncated protein (Rad60-ct-GFP). Since the HA-tagged Rad60-ct expressed by TNT migrates with at mass of ~50 kDa (Chapter 4), I would expect the Rad60-ct-GFP protein to be ~80 kDa. The Rad60-ct-GFP and Rad60-FL-GFP proteins were expressed at similar levels. This suggests that both proteins are stable when C-terminally tagged with GFP.

To ensure C-terminal tagging does not affect the function of the Rad60/Rad60-ct protein, the sensitivities of *rad60-FL-GFP* and *rad60-ct-GFP* cells were tested and compared to those of both wild-type and *rad60-ct* cells (Figure 5.1C). The sensitivities of *rad60-FL-GFP* and *rad60-ct-GFP* cells to HU and MMS are similar to that seen for wild-type and *rad60-ct* cells respectively. This suggests that C-terminal tagging of Rad60 does not affect Rad60 protein function.

5.2.2 Rad60-ct is mis-localised

To compare the nuclear localisation of Rad60 and Rad60-ct, exponentially growing cells were fixed in methanol and stained with DAPI. Cells were visualised using the Deltavision microscope. A large proportion of the GFP signal co-localises with DAPI-stained chromosomal DNA (Figure 5.2). This suggests that the majority of the GFP-tagged Rad60

Figure 5.2: Deletion of the C-terminal 73 amino acids results in mis-localisation of the Rad60 protein

Comparison of Rad60 localisation in *rad60-FL-GFP* and *rad60-ct*-GFP cells. Cells were grown at 30^{o}C in EMM2 medium supplemented with adenine, leucine and uracil. 1 ml exponentially growing cells were fixed with methanol and stained with DAPI. Cells were observed using an Applied Precision Deltavision Spectris microscope using deconvolution software.

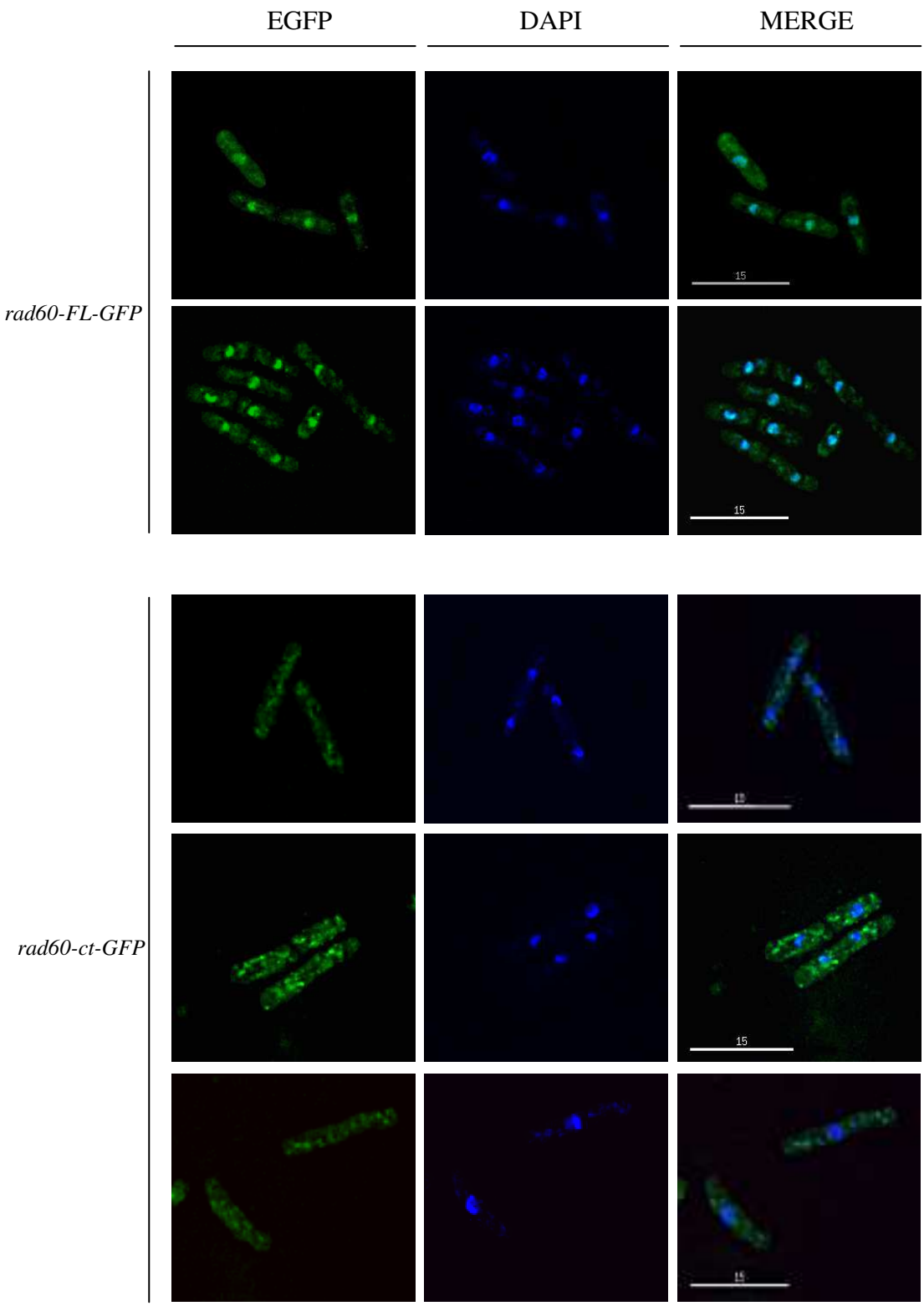

Figure 5.2: Deletion of the C-terminal 73 amino acids results in mis-localisation of the Rad60 protein.

protein is localised within the nucleus and is consistent with previous studies (Morishita, Tsutsui et al. 2002; Boddy, Shanahan et al. 2003). However, the GFP signal from the *rad60-ct-GFP* cells is pan-cellular (Figure 5.2). This suggests that deletion of the C-terminal 73 amino acids (SLD2) results in the mis-localisation of the Rad60 protein.

Rad60 exits the nucleus both upon treatment of cells with HU and by over-expressing *cds1* (Boddy, Shanahan et al. 2003). To confirm that the C-terminally GFP-tagged Rad60 protein behaves in the same way, exponentially growing cells were treated with 20 mM HU for 4 hours before being visualised under the microscope. Treatment of cells with HU results in the dispersal of Rad60 from the nucleus (Figure 5.3). This further suggests that C-terminally tagging Rad60 with GFP does not affect protein function.

5.3 N-terminal tagging Rad60 affects protein localisation

To eliminate the possibility that mis-localisation of the Rad60-ct protein is an artefact of the C-terminal GFP tagging, N-terminally GFP tagged *rad60-FL* and *rad60-ct* strains were generated using the Cre-loxP method (Werler, Hartsuiker et al. 2003). The Cre-loxP method allows essential genes to be N-terminally tagged at their genomic locus *and* under the control of their native promoter.

To integrate the tagged gene at the correct locus three PCRs were first carried out. Firstly a ~2.5 kb fragment containing the GFP tag and *sup3-5* marker upstream of the *nmt* promoter was amplified from the pGEM-EGFP template plasmid using primers L94/L91 (Figure 5.4A). A second PCR using primer pair L75/L80 amplified a fragment from gDNA with ~500 bp homology to the region immediately upstream of the *rad60* ATG and included a 24 bp region of homology to the 5' region of the ~2.5 kb fragment (Figure 5.4B). A third PCR using primer pairs L72/L73 and L72/L88 (for *rad60* and *rad60-ct* respectively) amplified a fragment from genomic DNA with at least 500 bp homology to the *rad60* gene and 24 bp homology to the 3' region of the ~2.5 kb fragment (Figure 5.4C). Primers L72/L73 were used to amplify a ~500 bp fragment starting from the *rad60* ATG. Primers L72/L88 were used to amplify a ~1kb fragment that includes codon 1-333 of *rad60*, followed by a stop codon to truncate the protein. The products of the three PCR reactions

Figure 5.3: Rad60-GFP is able to delocalise from the nucleus following replication stress

rad60-FL-GFP and *rad60-ct*-GFP were grown at 30^{o}C in EMM2 medium supplemented with adenine, leucine and uracil. Exponentially growing cells were treated with 20 mM HU for four hours. 1 ml cells were fixed in methanol and stained with DAPI. Cells were observed using an Applied Precision Deltavision Spectris microscope using deconvolution software.

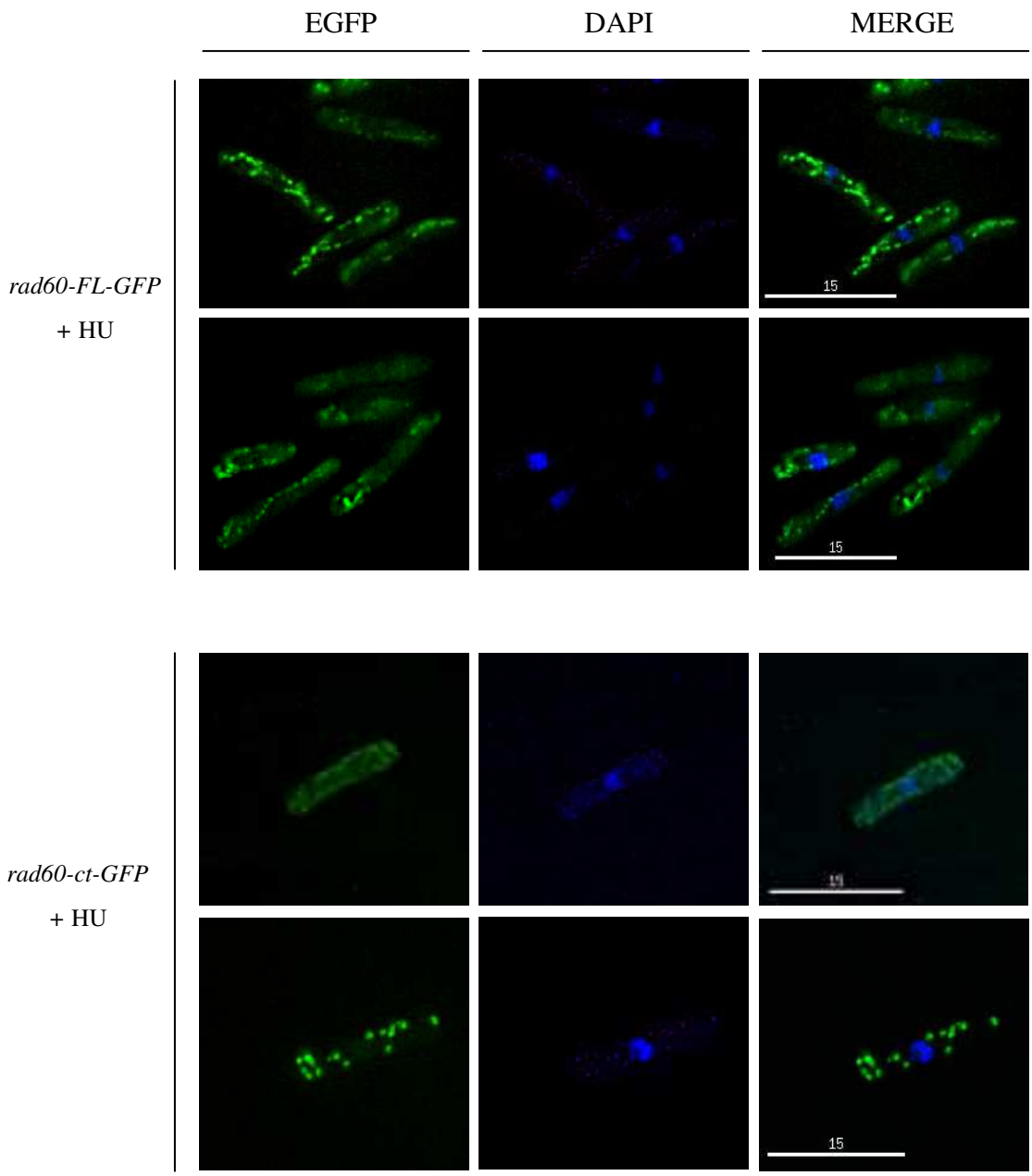

Figure 5.3: Rad60-GFP is able to delocalise from the nucleus following replication stress

Figure 5.4: N-terminal GFP-tagging of Rad60 and Rad60-ct

N-terminally GFP tagged *rad60-FL* and *rad60-ct* strains were generated using the Cre-loxP method (Werler *et al*, 2003). To integrate the tagged gene at the correct locus three PCRs were first carried out. **(A)** A ~2.5 kb fragment containing the GFP tag and *sup3-5* marker upstream of the *nmt1* promoter was amplified from the pGEM-EGFP template plasmid **(B)** A fragment with ~500 bp homology to the region immediately upstream of the *rad60* ATG and included a 24 bp region of homology to ~ 2.5 kb fragment was amplified from genomic DNA. **(C)** A fragment with ~500 bp homology to the *rad60* gene and 24 bp homology to the ~ 2.5 kb fragment was amplified from genomic DNA. **(D)** The PCR products were fused together in a fusion PCR to yield a linear gene-specific cassette. **(E)** The cassette was transformed into wild-type *S. pombe* cells allowing homologous integration to occur. Positive colonies were transformed with the pREP2-*Cre* recombinase plasmid (pPW7). The Cre-recombinase allows excision of the *nmt1* promoter between the two loxP sites, leaving the GFP tagged gene under the control of its native promoter. An arrow indicates PCR products of the correct sizes.

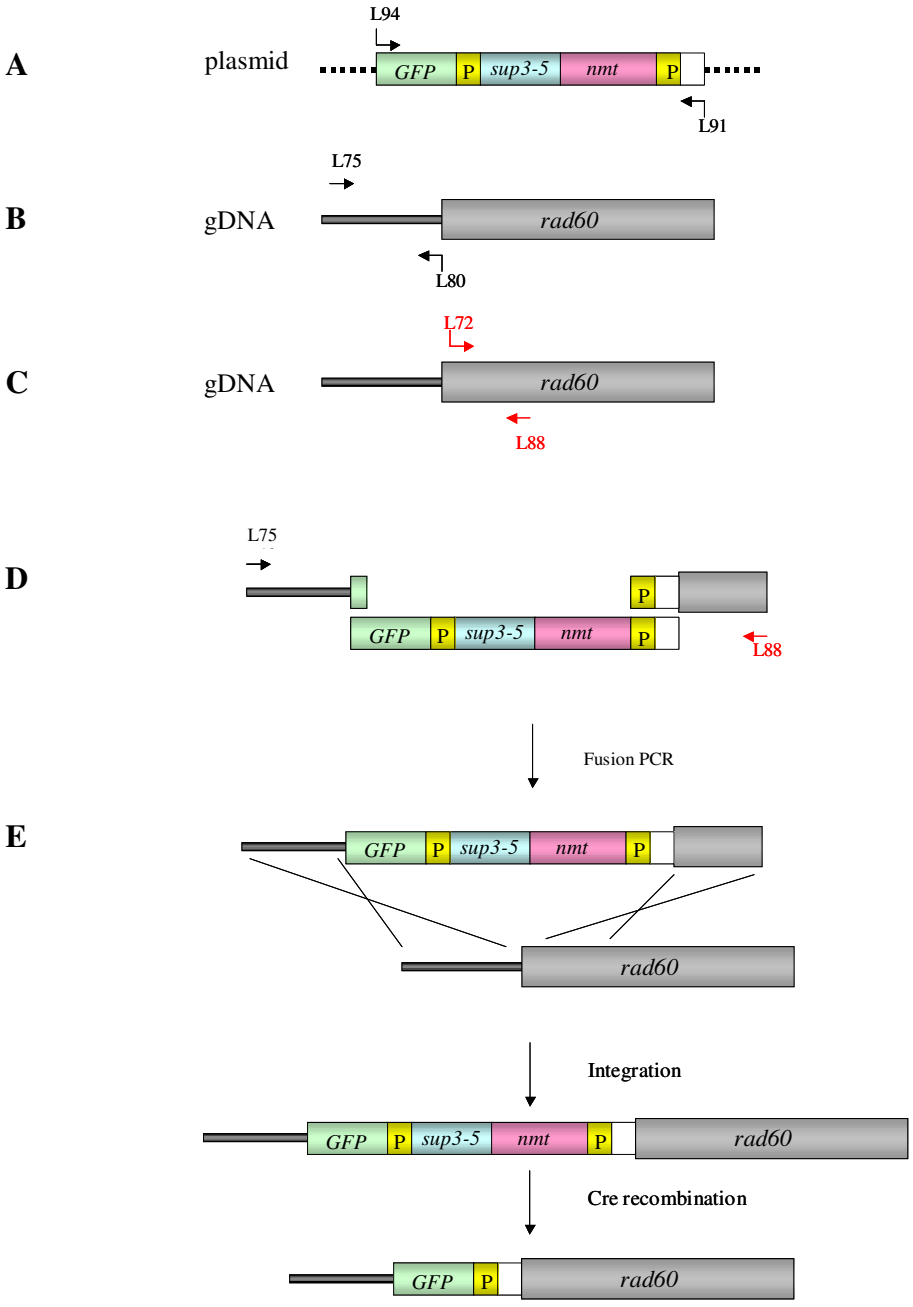

Figure 5.4: N-terminal GFP-tagging of Rad60 and Rad60-ct

were gel extracted to a final volume of 50 μl. The PCR products were use for fusion PCR to yield a linear gene-specific cassette for homologous integration into wild type *S. pombe.* Primers L75 and L73/L88 were used to amplify a ~3.5 kb/ ~4 kb linear product for *rad60* and *rad60-ct* respectively (Figure 5.4D).

The linear gene-specific cassette was transformed into wild-type *S. pombe* cells using the Bahler transformation protocol (Bahler, Wu et al. 1998). Since the *sup3-5* marker of the integrated cassette can suppress the *ade6-704* nonsense mutation in the wild-type *S. pombe* strain, positive transformants were grown on YNB medium supplemented with leucine and uracil and ade^+ transformants were selected. Colony PCR with primers L31 and L79 was used to screen transformants for successful homologous integration. The forward primer, L31, anneals upstream of the *rad60* start codon, and reverse primer, L79, anneals downstream of the *rad60* start codon. If the GFP tag failed to be incorporated a PCR product of ~0.8 kb was observed. A PCR product of ~3.3 kb indicated that the GFP tagging construct (~2.5 kb) had been successfully integrated upstream of the *rad60* start codon. Positive colonies were transformed with the pREP2-*Cre* recombinase plasmid (pPW7). Transformants were selected on YNB plus leucine and adenine (10 μg/ml). The YNB medium contained no thiamine to allow expression of the Cre Recombinase from the *nmt1* promoter of the pPW7 plasmid. The Cre-recombinase allows excision of the *nmt1* promoter between the two loxP sites, leaving the GFP-tagged gene under the control of its native promoter (Figure 5.4E). Red/white selection was used to select for loss of the *sup3-5* marker, which leads to the formation of red colonies. Red colonies were re-streaked on YEA plates to promote loss of the pPW7 plasmid. Genomic DNA was extracted from the positive colonies and the region surrounding the junction site was PCR amplified from the genomic DNA with primers L72 and L96. Sequencing with primers L177, L178 confirmed correct integration of the GFP tagging cassette in the GFP-*rad60-FL* and *GFP-rad60-ct* strains.

To ensure that N-terminal tagging does not affect the function of the Rad60/Rad60-ct proteins, the sensitivities of *GFP-rad60-FL* and *GFP-rad60-ct* cells were tested and compared to those of both wild-type and *rad60-ct* cells and to the C-terminally GFP-tagged

strains *rad60-FL-GFP* and *rad60-ct-GFP* (Figure 5.5A). Whilst lower doses of HU and MMS should havealso been tested, the sensitivity of *GFP-rad60-FL* and *GFP-rad60-ct* cells to HU and MMS is similar to that seen for wild-type and *rad60-ct* cells respectively. This suggests that N-terminal tagging of Rad60 does not affect Rad60 protein function. However, when the *GFP-rad60-FL* cells are visualised using the Deltavision microscope, Rad60 does not localise to the nucleus, as previously published (Morishita *et al*, 2002; Boddy *et al*, 2003). Instead, the GFP signal is dispersed throughout the cell (Figure 5.5B). Due to the observation that the *GFP-rad60-FL* cells have a wild-type phenotype in response to HU and MMS, it is possible that the GFP-tag is unstable and may be cleaved from the Rad60 protein, resulting in the pan cellular signal. To test this, TCA extracts taken from wild-type, *rad60-FL-GFP* and *GFP-rad60-FL* cells were Western blotted and probed with anti-GFP antibody (Figure 5.5C). In the negative control (w*ild-type*), no GFP signal was detected. In the positive control (*rad60-FL-GFP*) a band running at approximately 95 kDa was observed. Since Rad60 runs at approximately 60 kDa in yeast extracts and the GFP-tag is ~35 kDa this is the expected band size for Rad60 tagged with GFP. A band of the same size can be seen for the TCA extract taken from the GFP-*rad60-FL* cells. Therefore it can be assumed that, like the C-terminally tagged Rad60 protein, the N-terminally tagged Rad60 protein is stable. This does not explain the mis-localisation. Since the GFP-Rad60-FL protein does not show the correct localisation, N-terminally tagged Rad60-ct cannot be used to confirm the mis-localisation of the Rad60-ct protein.

5.4 Rad60 antibody production

To eliminate the possibility that the mis-localisation of the Rad60-ct protein is an artefact of the C-terminal GFP tagging an attempt to generate a Rad60-specific antibody was carried out. In addition to allowing visualisation of the untagged protein by immunofluorescence, a Rad60-specific antibody would allow more intricate biochemical studies to be undertaken. To obtain Rad60 antisera, ~600 μg of Rad60 antigen was required to inoculate two host rabbits. Prior to carrying out large-scale protein purification, the best conditions for Rad60 protein expression and solubility were determined.

Figure 5.5: N-terminal GFP-tagging of Rad60 gives a mutant phenotype

(A) N-terminally GFP-tagged cells do not show a DNA-damage sensitive phenotype. Cells were grown at 30^{o}C in YE medium to mid-exponential phase. 10 μl of 10 fold serial dilutions were spotted onto YEA plates containing supplements at the indicated doses. Plates were incubated at 30^{o}C for 72 hours and photographed. **(B)** N-terminally GFP-tagged Rad60 does not show nuclear localisation. *GFP-rad60-FL* cells were grown at 30^{o}C in EMM2 medium supplemented with adenine, leucine and uracil, with and without 20 mM HU. 1 ml of exponentially growing cells were harvested, washed and re-suspended in 100 μl EMM2 medium and stained with Hoechst. Cells were visualised using an Applied Precision Deltavision Spectris microscope using deconvolution software. **(C)**TCA extracts were taken from wild-type, *rad60-FL-GFP* and *GFP-rad60-FL* cells. Proteins were separated on a 10% SDS-PAGE gel and visualised by Western blotting with anti-GFP antibody

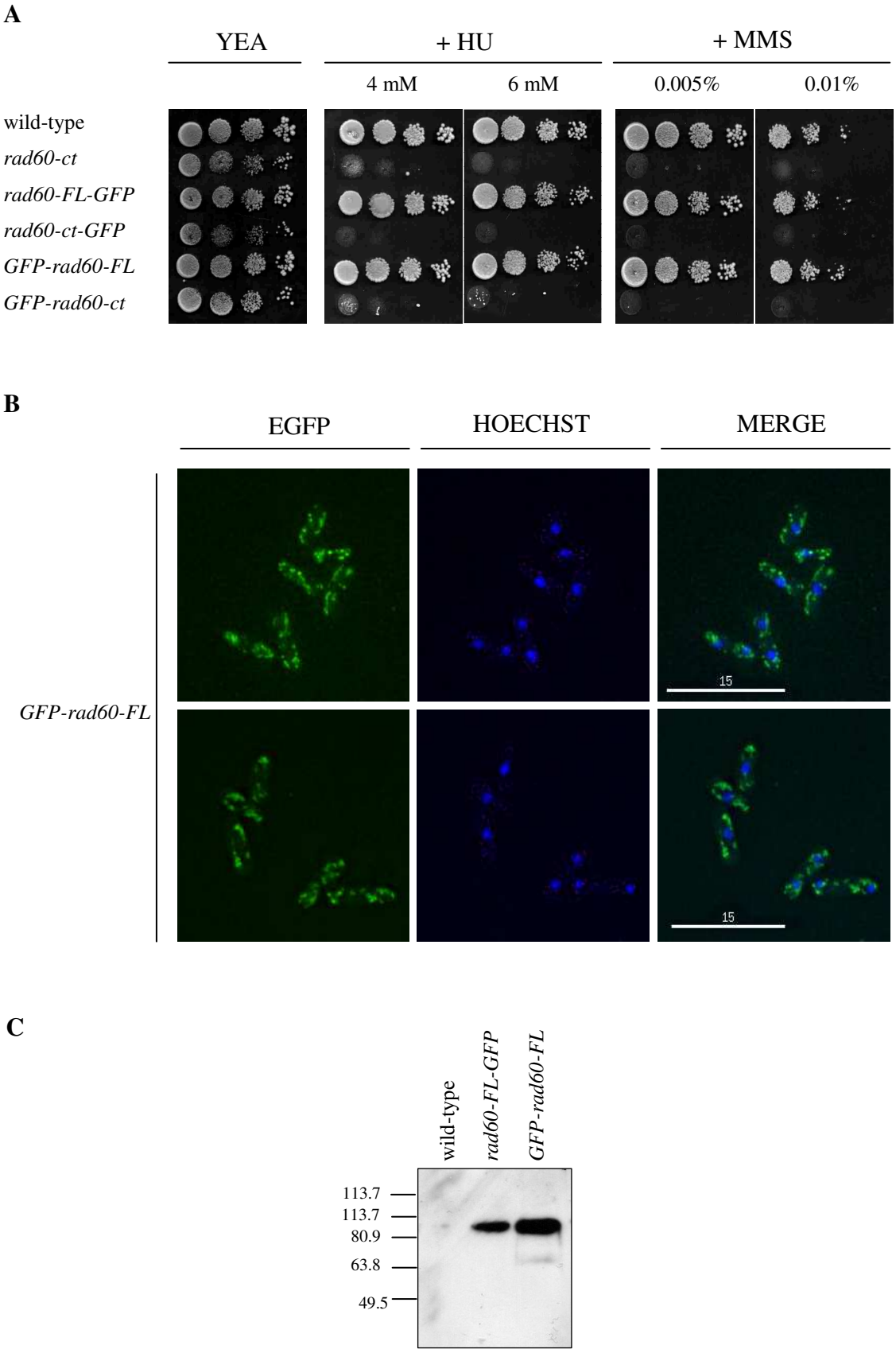

Figure 5.5: N-terminal GFP-tagging of Rad60 gives a mutant phenotype

5.4.1 Determining the optimum conditions for Rad60 protein expression and solubility

Rad60 protein was expressed from the pGEX-*rad60* construct (Gift from I. Miyabe, University of Sussex), which places a 26 kDa GST tag at the N-terminus of the protein. To test different conditions for expression of the GST-tagged fusion protein (GST-Rad60), the pGEX-*rad60* construct was transformed into *E. coli* BL21(DE3) cells. and 5 10 ml cultures were grown at 37^{o}C, with shaking until an A_{595} reading of ~0.6 was reached. At this point 1 ml of each culture (non-induced) was removed and placed in a fresh tube. Cells in the remaining 9 ml culture were induced with 0.3, 0.5 or 5 mM IPTG. The cultures were grown with the non-induced samples for a further 1 or 3 hours at 37^{o}C. 1 ml of each culture harvested and the soluble and insoluble fractions collected. Samples were analysed by 10% SDS-PAGE with Coomassie staining and Western blotting with anti-GST antibody. When protein expression is induced with 0.3 mM IPTG for 3 hours, a strong ~75 kDa band can be detected by Coomassie staining in the insoluble fraction (Figure 5.6A, bottom panel). This band is absent in the non-induced sample, suggesting that it corresponds to the GST-Rad60 protein. Rad60 has a predicted molecular weight of 46 kDa but runs at ~60 kDa in both *S. pombe* extracts and when translated using with the rabbit reticulocyte TNT kit (Chapter 4). I would therefore expect the GST-tagged Rad60 to run at ~86 kDa (~60 kDa + 26 kDa). Western blotting with anti-GST antibody confirms that the ~75 kDa band observed by Coomassie staining corresponds to the GST-Rad60 protein (Figure 5.6A, bottom panel). This suggests that in bacterial cells Rad60 migrates at its predicted size of ~46 kDa. The Rad60-GST expression level is not increased for cells induced with 3 mM IPTG for 1 hour compared with 3 hours. The effect of inducing cells with different IPTG concentrations on Rad60 expression was also tested. Induction of cells with 0.5 mM IPTG did not improve the Rad60 expression levels as compared to induction with 0.3 mM IPTG. However, following induction of cells with 5 mM IPTG, GST-Rad60 was found in both the soluble and insoluble fractions. Since the purification of proteins is much simpler to carry out from the soluble fraction, the induction conditions chosen for the large-scale protein purification were 3 hours induction with 5 mM IPTG.

Figure 5.6: Expression and purification of Rad60 antigen for production of Rad60 antibodies

(A) Determining the optimum conditions for Rad60 protein expression and solubility. BL21 (DE3) cultures carrying the pGEX-*rad60* vector were grown at 37^{o}C until an A_{595} reading of ~0.6 was reached. Cells were induced with IPTG at the indicated concentration and grown at 37^{o}C for one or three hours. Cells were harvested and the insoluble and soluble fractions were analysed by 10% SDS-PAGE with Coomassie staining (Lower panel) and Western blotting with anti-GST antibody (Upper panel). **(B and C)** Large-scale purification of Rad60. BL21(DE3) cells, carrying the pGEX*rad60* construct, were cultured at 37^{o}C until an A_{595} reading of ~0.6 was reached. Cells were induced with IPTG at a final concentration of 5mM for 3 hours. GST-Rad60 was purified on glutathione-sepharose beads. Following elution, the GST-tag was removed from the Rad60 protein by thrombin cleavage. (B) 5 μl of the protein sample was analysed by 10% SDS-PAGE (lane 1) as compared to a control purification from cells carrying the empty pGEX vector (lane 2). An arrow indicates Rad60. (B) The Rad60 protein sample was concentrated to a volume of ~500 μl and run on a large 10% SDS-PAGE gel alongside 10, 50 and 100 μg BSA standards (C). Following Coomassie staining the Rad60 gel bands were excised.

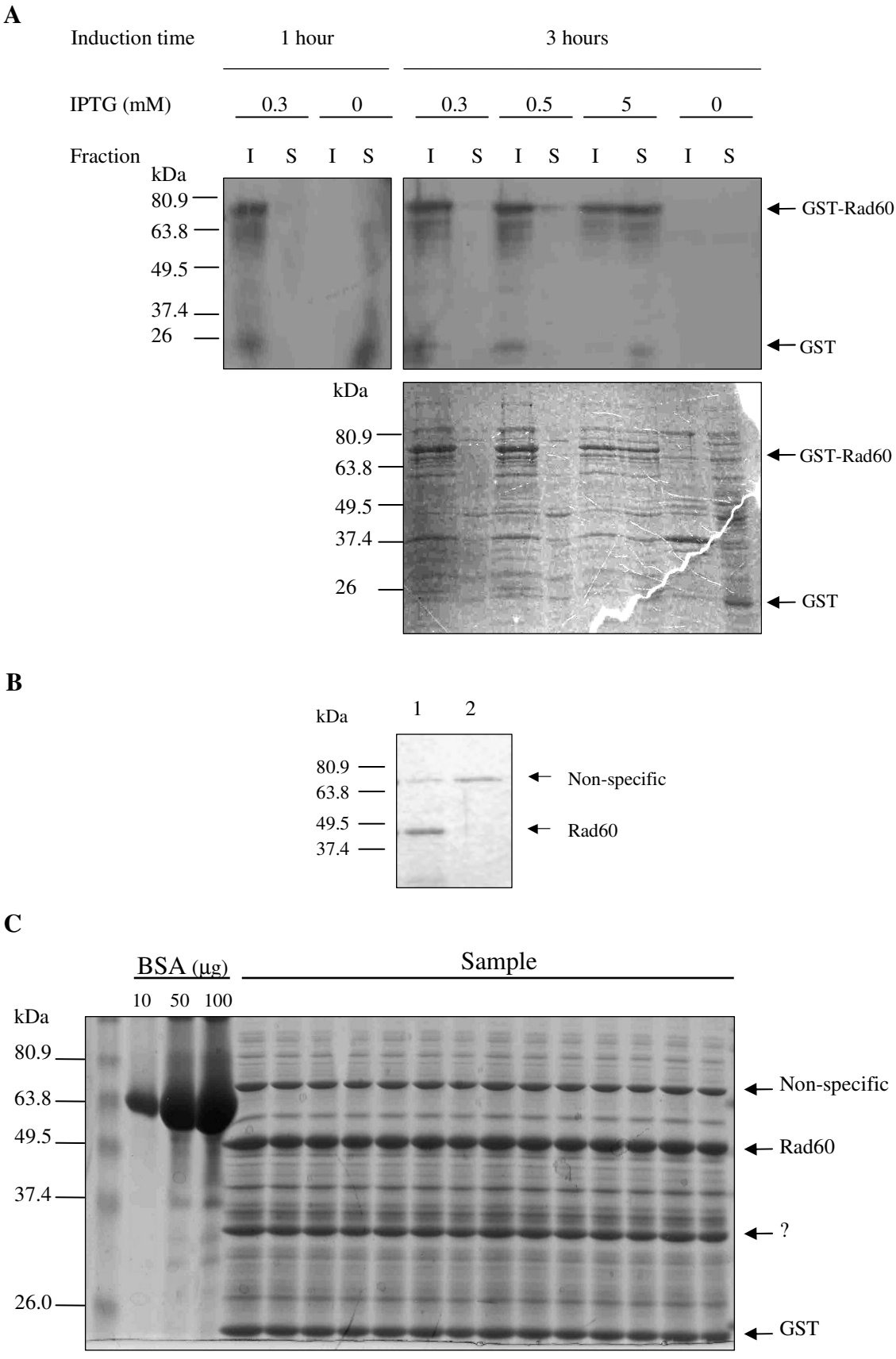

Figure 5.6: Expression and purification of Rad60 antigen for production of Rad60 antibodies

5.4.2 Large-scale purification of Rad60

Having identified the best conditions for expression of GST-Rad60, 6 litres of BL21(DE3) cells, carrying the pGEX*rad60* construct, were cultured at 37°C until an A_{595} reading of 0.6 was reached. The cells were induced with IPTG at a final concentration of 5mM and grown for a further 3 hours at 37°C. The GST-Rad60 protein was purified from the cell extract with glutathione-sepharose beads. GST-Rad60 was eluted from the beads with 3 x 250 μl elution buffer. Following elution, the GST-tag was removed from the Rad60 protein by thrombin cleavage. 5 μl of the protein sample was analysed by 10% SDS-PAGE (Figure 5.6B). When visualised by Coomassie staining two bands of ~45 and ~70 kDa were observed in the Rad60 protein sample (lane 1). The smaller band of ~45 kDa corresponds with the predicted size of the untagged Rad60 protein. In a control purification where cells were transformed with the empty pGEX vector (lane 2), only the larger ~70 kDa band is present. This suggests that this is a non-specific band from the *E. coli* cells. The Rad60 protein sample was concentrated to a volume of ~500 μl and loaded onto a large 10% SDS-PAGE gel (Figure 5.6C). To help determine Rad60 protein concentration, 10, 50 and 100 μg BSA standards were also loaded. Following Coomassie staining, four bands of strong intensity could be detected. These bands correspond to the Rad60 protein at ~45 kDa, the cleaved GST-tag at ~26 kDa and the non-specific *E. coli* band at ~70 kDa. The source of the fourth band at ~30 kDa is unknown. With reference to the BSA standard, ~150-200 μg Rad60 was purified from the 6 litre culture. To ensure enough protein for antibody production, a further 12 litre purification was carried out. The Rad60 bands were carefully excised from the gel and sent to Eurogentec for generation of the Rad60 antibody.

5.4.3 Testing and purifying the anti-Rad60 antisera

Over a three month period, two host rabbits were injected with ~100 μg Rad60 antigen on three separate occasions. Antisera were then collected and returned by Eurogentec. The ability of the crude antisera to recognise the Rad60 protein was tested. TCA extracts of wild-type cells transformed with the empty pREPHA41 vector and the pREPHA41*rad60* construct analysed on a 10% SDS-PAGE gel, Western blotted and probed with 1:100, 1:500 and 1:1000 dilutions of the crude anti-Rad60 antisera (Figure 5.7A). A strong signal at ~60 kDa was detected in the lanes containing TCA extracts taken from cells exogenously

Figure 5.7: Testing the anti-Rad60 antibodies

TCA extracts of wild-type cells carrying the empty pREPHA41 vector (-) and the pREPHA41*rad60* (+) construct were run on a 10% SDS-PAGE gel and analysed by Western blotting with 1:100, 1:500 and 1:1000 dilutions of the crude anti-Rad60 antisera and 1:2000 anti-His antibody. Rad60 is indicated with an arrow. **(B)** anti-Rad60 antisera were affinity-purified against His-Rad60. Purified His-Rad60 was run on a 10% SDS-PAGE gel and Western blotted with a 1:1000 dilution of the crude antisera (lane 1), 1:100 dilutions of the purified anti-Rad60 antibody fractions (lanes 2-7), and a 1:2000 dilution of the anti-His antibody (Lane 8). His-Rad60 is indicated with an arrow. **(C)** Wild-type cells were grown at 37^{o}C and fixed. Cells were stained with anti-Rad60 (1:100) and anti-tubulin (1:1000) primary antibodies which were detected with 1:100 swine anti-rabbit(TRITC) and 1:100 goat anti-mouse(FITC) secondary antibodies and then stained with DAPI. Cells were visualised using an Applied Precision Deltavision Spectris microscope using deconvolution software

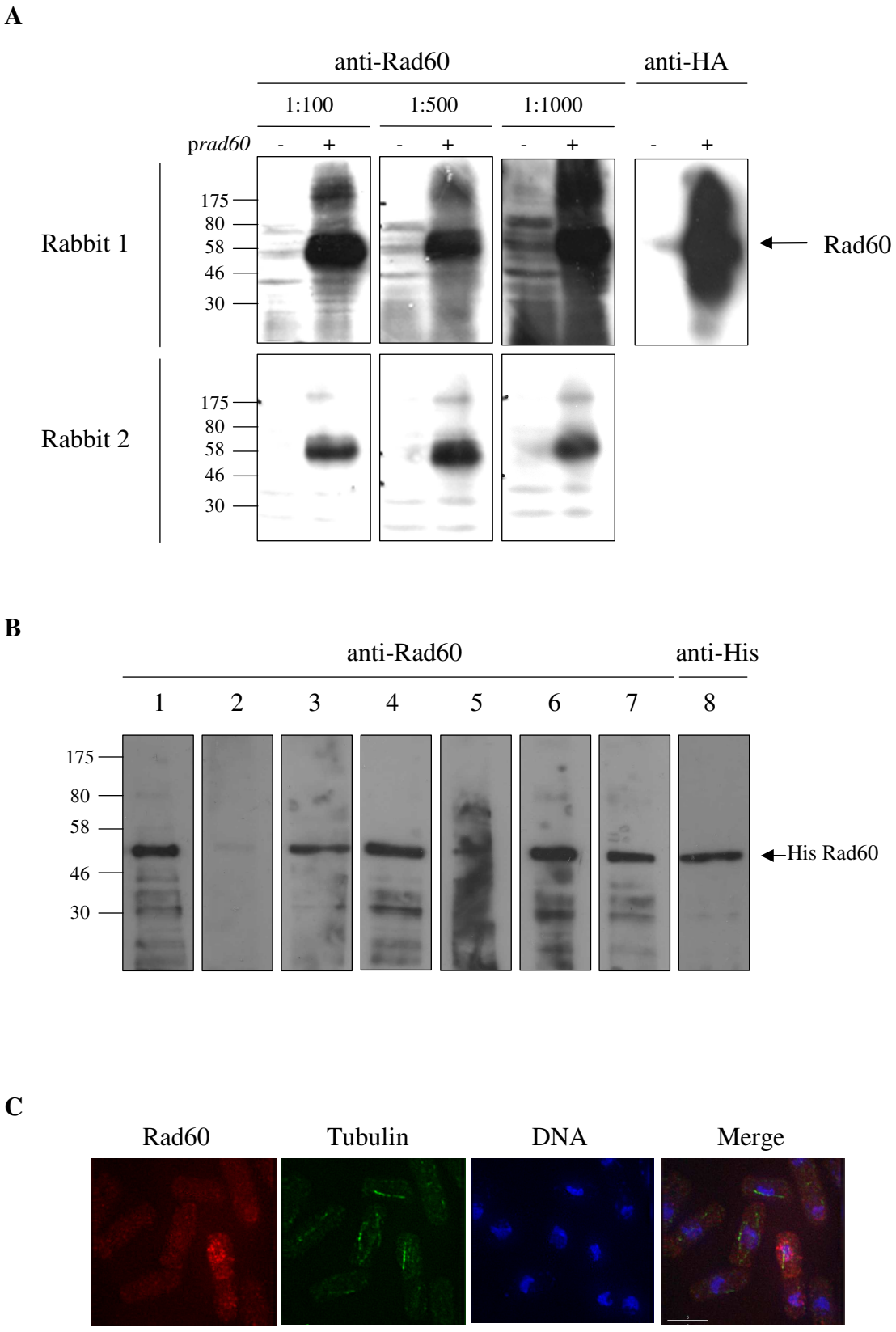

Figure 5.7: Testing the anti-Rad60 antibodies

expressing Rad60. The intensity of the signal was greater with the antisera from 'Rabbit 1' than 'Rabbit 2'. In lanes containing TCA extracts taken from cells expressing Rad60 at endogenous levels, only a very faint band can be detected at ~60 kDa by Rabbit 1. Antisera from Rabbit 2 were unable to detect this band.

Affinity purification was carried out in an attempt to increase the specificity of the anti-Rad60 antibody. Since the Rad60-antibody was made by injecting thrombin-cleaved GST-Rad60, purifying the antisera against His-Rad60 should enhance the level of purification as antibodies raised against the GST protein would not be purified. *rad60* was subcloned from the pREP41HA*rad60* construct into the pET15B vector, which places a His_6-tag at the N-terminus of the Rad60 protein. Since *Sal*I and *Xho*I restriction sites share compatible ends, *rad60* was subcloned as an *Nde*I/*Sal*I fragment into the *Nde*I/*Xho*I sites of pET15B. His-Rad60 protein (purified by F. Z. Watts, University of Sussex) was immobilised using the AminoLink®Plus Coupling Gel kit (PIERCE Biotechnology). Crude Rad60 antisera were incubated overnight on the His-Rad60 affinity column. Flow-through was analysed by Bradford assay to confirm the Rad60 antibody had bound to the column. After extensive washing, bound antibody was eluted with 100 mM glycine, pH 2.3 and 500 μl fractions were collected. Analysis of the collected fractions by Bradford assay identified six antibody-containing fractions. The purified anti-Rad60 antibody fractions were tested to assess their specificity. Purified His-Rad60 (F. Z. Watts, University of Sussex) was run on a 10% SDS-PAGE gel and Western blotted. When probed with the crude antisera (Figure 5.7B, lane 1), a strong signal was detected at ~50 kDa, corresponding to His-Rad60. This was confirmed by probing with an anti-His antibody (Lane 8). In addition, a number of faster migrating bands were observed. These may be non-specific bands of the anti-sera or may correspond to degradation products of the His-Rad60 protein. When the His-Rad60 blot was probed with the purified Rad60 antibody fractions (lanes 2-7), no signal was detected with antibody from fraction 1 (lane 2). The His-Rad60 was detected by antibody from fractions 2-6 (lanes 3-7) but the signal was not greater, nor more specific, than the signal seen for the crude antisera (pre-affinity purification). Given that the His-Rad60 protein had already been purified the number of non-specific bands to be detected should be low. The purified antibodies were therefore tested on TCA extracts from cells

expressing Rad60 at both endogenous and exogenous levels. As is the case for the crude antisera, the purified antibodies strongly detected the exogenously expressed protein and only a very faint band was observed at a size consistent with the endogenous protein (data not shown). However, when the antibodies were tested on TCA extracts taken from *rad60-ct* cells in which a truncated form of rad60 is expressed at endogenous levels, the band did not shift. This suggests that the band seen for the endogenously expressed Rad60 protein is non-specific. In addition, TCA extracts were taken from cells treated with either 20 mM HU, 0.01% MMS or 250 Gy and probed with the purified antibodies to test whether Rad60 expression is cell-cycle specific or DNA damage induced. No increase in signal was detected (data not shown). Together this suggests that the purified antibodies cannot be used to detect endogenous levels of Rad60 by Western blotting.

Since the primary reason for creating the anti-Rad60 antibodies was for use in immunofluorescence, their ability to be used to image cells was tested. Fractions 4, 6 and 7 were pooled and concentrated to ~100 μl. Exponentially growing wild-type cells were fixed and incubated overnight with primary anti-Rad60 (1:100) and anti-tubulin (1:1000) antibodies. Following extensive washing, cells were incubated with swine-anti-rabbit(TRITC) and goat-anti-mouse(FITC) secondary antibodies and then stained with DAPI. Cells were then visualised under the microscope (Figure 5.7C). Tubulin staining of the microtubules suggests that the immunofluorescence protocol worked. However, the signal from the anti-Rad60 antibody is dispersed throughout the cell and is not nuclear, as seen by the DAPI staining. This suggests that the purified Rad60 antibodies are unsuitable for use in immunofluorescence as well as Western blotting. Further purification of the anti-Rad60 antibodies is therefore required.

5.5 Mis-localisation of Rad60-ct is not the result of constitutive activation of Cds1

Activation of the S-phase checkpoint kinase Cds1 causes hyper-phosphorylation and concomitant delocalisation of Rad60 from the nucleus (Boddy, Shanahan et al. 2003). To determine whether the mis-localisation of the Rad60-ct protein is due to constitutive activation of Cds1 in *rad60-ct* cells, the localisation of the Rad60 and Rad60-ct protein was

observed in the absence of Cds1. *rad60-FL-GFP* and *rad60-ct-GFP* were therefore introduced into a *cds1-d* background. As anticipated, Rad60 is localised within the nucleus of the *cds1-d* cells (Figure 5.8). However, as seen for the *rad60-ct-GFP* cells, Rad60-ct is distributed throughout the cell in the *cds1-d* background (Figure 5.8). This suggests that the mis-localisation observed for Rad60-ct is not the result of constitutive activation of Cds1

The delocalisation of Rad60 from the nucleus is S-phase specific and is not observed in G2 cells treated with IR (Boddy, Shanahan et al. 2003). Inactivation of Rad60 leads to a Chk1 dependent checkpoint arrest (Boddy, Shanahan et al. 2003). Given that *rad60-ct* cells have a DNA damage sensitive phenotype, it is likely that the role of Rad60 in the DNA damage response is compromised (Chapter 3). Therefore, the localisation of Rad60 and Rad60-ct, was examined in a *chk1-d* background (Figure 5.9). Rad60-ct is distributed throughout the cell in the *chk1-d* background, suggesting that the mis-localisation of Rad60-ct in *rad60-ct* cells is not the result of constitutive activation of Chk1. Interestingly, in the *chk1-d* background, Rad60 is not nuclear. This may suggest that Chk1 has a role in maintaining Rad60 in the nucleus.

5.6 Provision of a nuclear localisation signal restores wild-type localisation to Rad60-ct but does not rescue the DNA damage sensitive phenotype

Having established that Rad60-ct mis-localisation is not due to a function of the checkpoint kinase Cds1, the question of what is causing the mis-localisation is posed. One possibility is that the main role of SLD2 is in localising Rad60 to the nucleus. If this theory is correct, by re-establishing nuclear localisation of Rad60, a wild-type DNA damage response should be restored. To test this possibility, a nuclear localisation signal (NLS) was incorporated at the C-terminus of the truncated Rad60-ct protein. The SV40 large T-antigen NLS, (PKKKRKV) has previously been shown to be functional in *S. pombe* and therefore must be recognised by the *S. pombe* importins (Shiozaki and Yanagida 1992). The nucleotide sequence encoding the SV40 NLS was incorporated at the 3' end of the *rad60-ct* coding sequence by PCR amplification from *S. pombe* gDNA using primers L41 and L74. The forward primer, L41, is designed to introduce an *Nde*I restriction site immediately before the ATG start codon. The reverse primer, L74, is designed to introduce the nucleotide

Figure 5.8: Mis-localisation of Rad60-ct is not the result of constitutive activation of Cds1

rad60-FL-GFP cds1-d and *rad60-ct*-GFP *cds1-d* were grown at 30^{o}C in EMM2 medium supplemented with adenine, leucine and uracil. 1 ml of exponentially growing cells were harvested, washed and re-suspended in 100 μl EMM2 media and stained with Hoechst. Cells were visualised using an Applied Precision Deltavision Spectris microscope using deconvolution software.

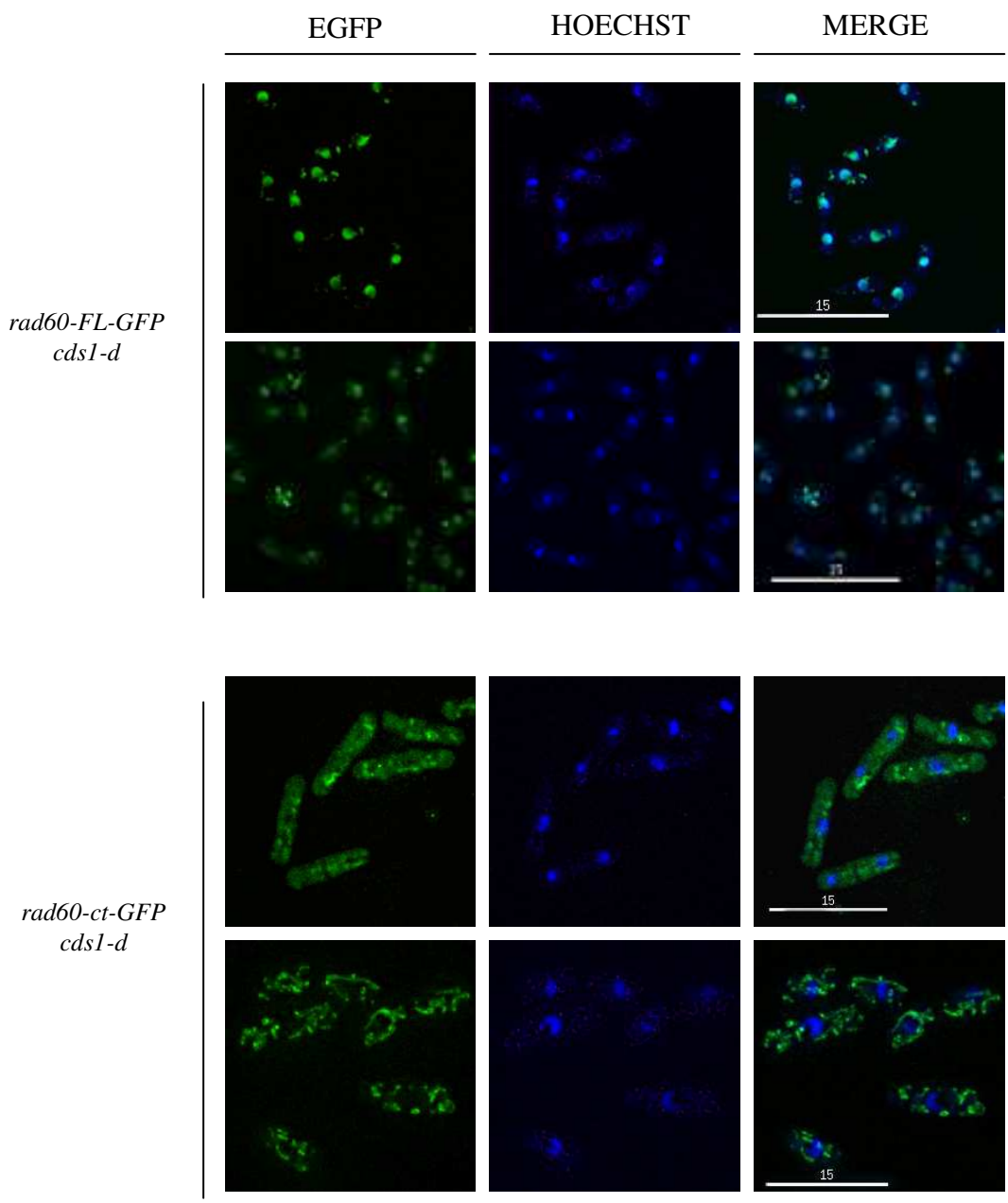

Figure 5.8: Mis-localisation of Rad60-ct is not the result of constitutive activation of Cds1

Figure 5.9: Mis-localisation of Rad60-ct is not the result of constitutive activation of Chk1

rad60-FL-GFP chk1-d and *rad60-ct*-GFP c*hk1-d* were grown at 30^{o}C in EMM2 medium supplemented with adenine, leucine and uracil. 1 ml of exponentially growing cells were harvested, washed and re-suspended in 100 μl EMM2 media and stained with Hoechst. Cells were visualised using an Applied Precision Deltavision Spectris microscope using deconvolution software.

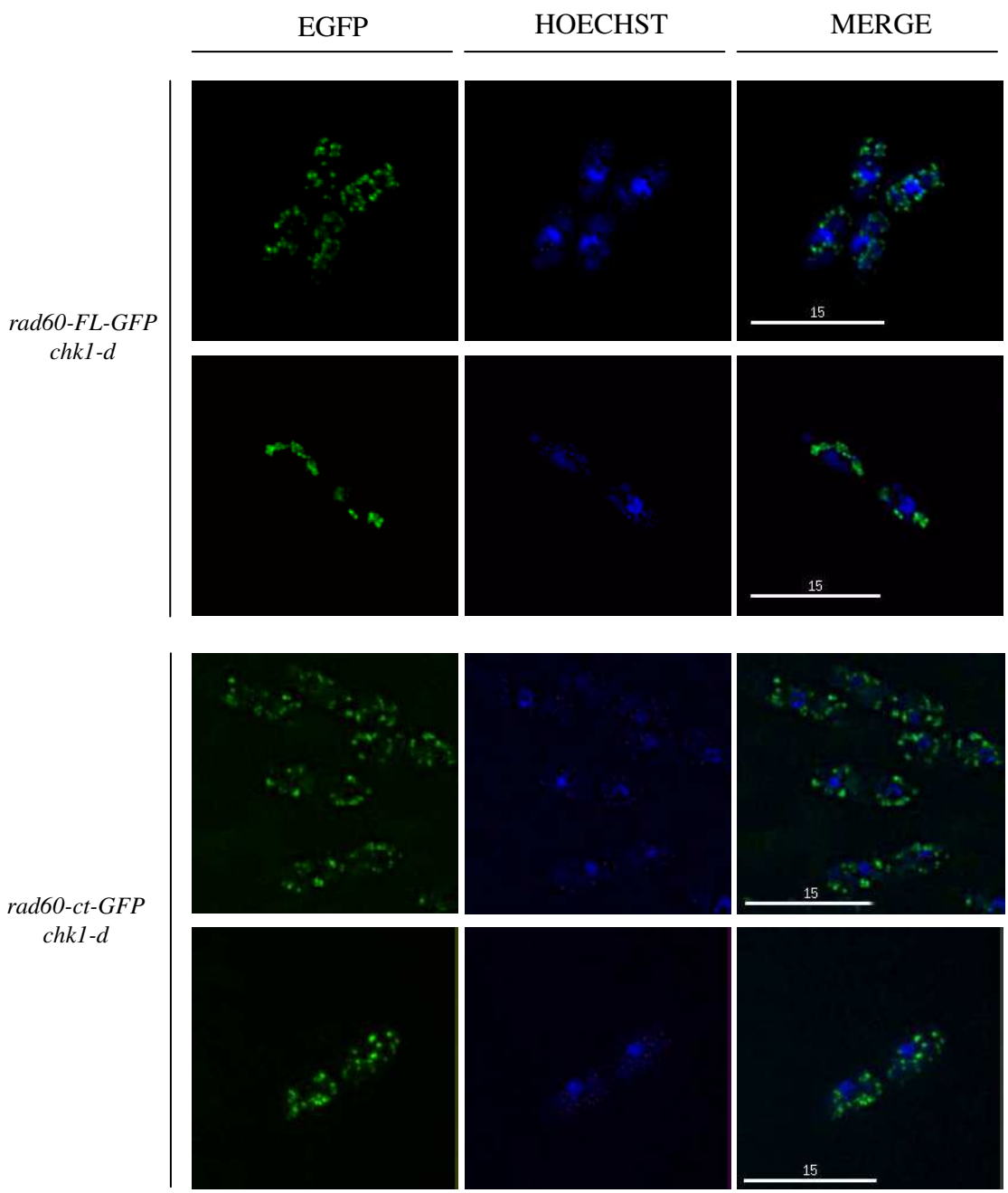

Figure 5.9: Mis-localisation of Rad60-ct is not the result of constitutive activation of Chk1

sequence encoding the SV40 NLS immediately after codon 333 of *rad60*, followed by a *Sal*I restriction site. The PCR product was digested and cloned directly into the pREP41EGFP(C) expression vector, as an *Nde*I/*Sal*I fragment. This places the EGFP tagging sequence downstream of the *rad60-ctNLS* fusion .

To examine the localisation of the Rad60-ctNLS protein, the pREP41EGFP(C)*rad60-ctNLS* construct was transformed into wild-type cells. Expression from the *nmt1* promoter was de-repressed by growing cells for ~16 hours in the absence of thiamine. Exponentially growing cells were visualised using the deltavision microscope. The Rad60-ctNLS protein is located within the nucleus (Figure 5.10). Nuclear localisation is confirmed by the co-localisation of the EGFP signal with the Hoechst signal. Wild-type cells were also transformed with pREP41 EGFP(C)*rad60,* pREP41 EGFP(C)*rad60-ct* and the empty pREP41EGFP(C) vector as controls. Similar to the cellular localisation pattern seen for Rad60 and Rad60-ct at endogenous levels (Section 5.2), exogenously over-expressed Rad60 is located in the nucleus while Rad60-ct is dispersed throughout the cell. However, it should be noted that the signal detected in the nucleus from the exogenously expressed Rad60 is much stronger than that of of the endogenously expressed Rad60. The pan-cellular localisation of the EGFP tag alone confirms that the nuclear localisation of the Rad60-ctNLS protein is not the result of the EGFP tag. To test whether the Rad60-ctNLS protein is able to delocalise from the nucleus under regulation of Cds1, exponentially growing cells were treated with 20 mM HU for 4 hours. Following HU treatment, the Rad60-ctNLS protein fails to delocalise from the nucleus (Figure 5.10). Unfortunately, unlike the endogenous Rad60 (Section 5.2.2), exogenously expressed Rad60 also failed to delocalise following HU treatment, highlighting a difference between the behaviour of endogenously and exogenously expressed Rad60 protein. For this reason it cannot be concluded whether the Rad60-ctNLS protein would be able to delocalise. The differences observed for endogenous and exogenous Rad60 suggest that studies using over-expression of the Rad60 protein may not be biologically significant. Studies at endogenous levels are, therefore, required todetremine if Rad60-ctNLS is capable of HU induced nuclear delocalisation.

Figure 5.10: Both the provision of a nuclear localisation signal and substitution of Rad60 SLD2 with authentic SUMO are capable of restoring wild-type localisation to Rad60-ct Wild-type cells expressing EGFP, Rad60, Rad60-ct, Rad60-ctNLS and Rad60-ctPmt3 from the pREP41EGFP(C) vector were grown at 30^{o}C in EMM2 medium supplemented with adenine, and leucine with and without 20 mM HU. 1 ml of exponentially growing cells were harvested, washed and re-suspended in 100 μl EMM2 medium and stained with Hoechst. Cells were visualised using an Applied Precision Deltavision Spectris microscope using deconvolution software

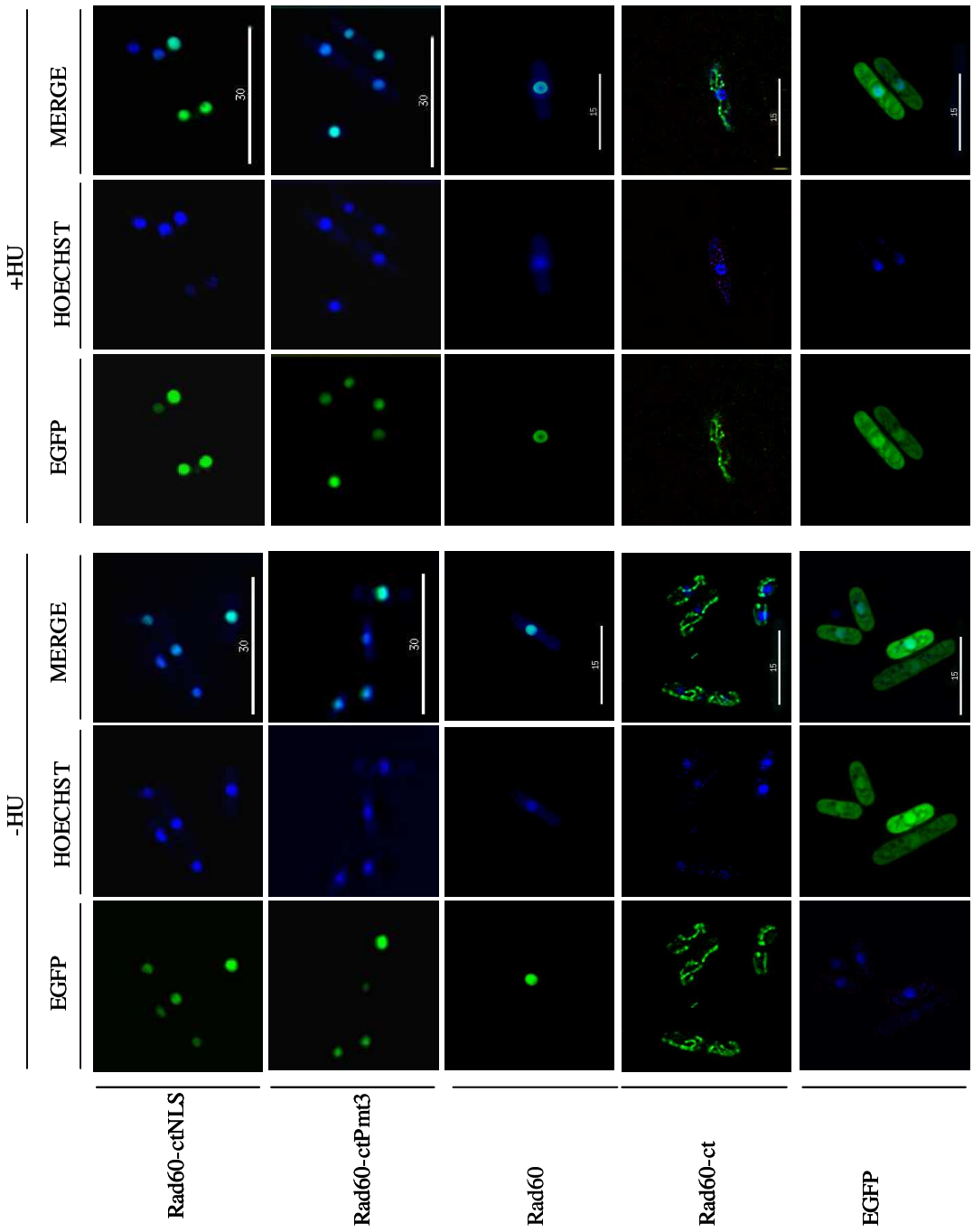

Figure 5.10: **Both the provision of a nuclear localisation signal and substitution of Rad60 SLD2 with authentic SUMO are capable of restoring wild-type localisation to Rad60-ct**

To test the hypothesis that by re-establishing nuclear localisation of Rad60, a wild-type DNA damage response should be restored, *rad60-ctNLS* was expressed in the *rad60-ct* background and the response to DNA damaging agents was tested (Figure 5.11). Wild-type and *rad60-ct* cells were transformed with the pREP41EGFP(C)*rad60* (p*rad60*), pREP41EGFP(C)*rad60-ct* (p*rad60-ct*) and pREP41EGFP(C)*rad60-ctNLS* (p*rad60-ctNLS*) constructs as well as the empty pREP41EGFP(C) vector (pEV) as a control. *rad60-ct* cells transformed with pEV, are sensitive to HU and MMS as compared to wild-type. The wild-type phenotype is seen when wild-type cells are transformed with the empty vector. The HU and MMS sensitivity of *rad60-ct* cells is complemented when *rad60-ct* cells are transformed with p*rad60*, but not p*rad60-ct.* When *rad60-ct* cells are transformed with p*rad60-ctNLS*, growth under normal conditions is impaired. In addition, *rad60-ct* cells expressing *rad60-ctNLS* are more sensitive to MMS and HU than *rad60-ct* cells transformed with pEV. This suggests that the expression of *rad60-ctNLS* has a dominant negative effect in *rad60-ct* cells. This dominant negative effect is also seen in wild-type cells, suggesting that the C-terminal 73 amino acids (SLD2) of Rad60 is not required just to localise Rad60 to the nucleus, but also for the DNA repair function of Rad60.

5.6.1 Rad60 SLD2 is not capable of targeting EGFP into the nucleus

Following the observation that the deletion of the C-terminal 73 amino acids results in the mis-localisation of Rad60 (Section 5.2), and that the addition of the SV40 NLS to the C-terminal of the truncated protein is able to restore nuclear localisation (Section 5.6), the question was raised as to whether Rad60, and in particular the C-terminal SUMO-like domain of the protein, contains an NLS. A variety of NLSs have been experimentally characterised and bioinformatics software packages can be used to predict potential NLSs within a peptide sequence. Typically, NLSs consist of a few short sequences of positively charged residues (K/R). No such regions in Rad60 could be identified by eye. When the Rad60 peptide sequence was submitted to predictNLS (http://cubic.bioc.columbia.edu/predictNLS), no NLS sequences were identified.

Given that the protein does not contain an NLS, it is possible that the C-terminal SLD2 of Rad60 is able to interact with proteins that facilitate nuclear import. The C-terminal region

Figure 5.11: Neither the provision of a nuclear localisation signal nor substitution of Rad60 SLD2 with authentic SUMO are capable of rescuing the DNA damage sensitive phenotype of *rad60-ct* cells.

The HU and MMS sensitivity of *rad60-ct* cells cannot be rescued by the expression of *rad60-ctNLS* or *rad60-ctpmt3*. Cells were grown at 30^{o}C in YE medium to mid-exponential phase. 10 μl of 10 fold serial dilutions were spotted onto YEA plates containing supplements at the indicated doses. Plates were incubated at 30^{o}C for 72 hours and photographed.

Figure 5.11: Neither the provision of a nuclear localisation signal nor substitution of Rad60 SLD2 with authentic SUMO are capable of rescuing the DNA damage sensitive phenotype of *rad60-ct* cells

of Rad60 was therefore tested for its ability to localise EGFP to the nucleus. Under normal conditions, EGFP is known to be found throughout the cell and localises to both the nucleus and the cytoplasm by fusion to NLSs and NESs (nuclear export signals) respectively. The nucleotide sequence encoding amino acids 264-406 of Rad60 was PCR amplified from genomic DNA with primers L68 and L40. L68 was designed to place an *Nde*I restriction site immediately upstream of codon 264. L40 was designed to introduce a *Sal*I restriction site immediately downstream of the Rad60 TAA stop codon. The *rad60(264-406*) nucleotide sequence was cloned directly into the pREP41EGFP(N) yeast expression vector as an *Nde*I/*Sal*I fragment, which places an EGFP-tag at the N-terminus of the protein coded for (Figure 5.12A). The empty pREP41EGFP(N) vector and the *rad60(264-406)* construct were transformed into wild type *S. pombe* cells and protein localisation was visualised using the Deltavision microscope (Figure 5.12B). In cells expressing the Rad60(264-400), EGFP signal was also detected throughout the cell, suggesting that the C-terminus of Rad60 is not capable of localising EGFP to the nucleus. Is it therefore unlikely that region has an NLS-like property.

5.7 Substitution of Rad60 SLD2 with authentic SUMO restores wild-type localisation to Rad60-ct but does not rescue the DNA damage sensitive phenotype of *rad60-ct* cells

Provison of the SV40 NLS to the C-terminal of the truncated Rad60-ct protein is able to restore nuclear localisation but not function of the Rad60 protein (Section 5.3). This suggests that SLD2 has a functional role in the DNA damage response. If Rad60 SLD2 really is SUMO-like in structure and function replacing Rad60 SLD2 with authentic SUMO (Pmt3) should restore both nuclear localisation and Rad60 function should remain intact. To test this, a pREP41EGFP(C)*rad60-ctpmt3* construct was created.

The pREP41EGFP(C)*rad60-ctpmt3* construct was created in a 5 step process. First, using pREPHA41*rad60* as a template, primers L150 and L151 were used to introduce a *Sal*I restriction site immediately after codon 333 of the *rad60* coding sequence by site-directed mutagenesis. Second, using pREPHA41*pmt3FL* (Watts lab, University of Sussex) as a template, primers L117 and L118 were used to PCR amplify *pmt3*. Primer L117 was

Figure 5.12: Rad60 SLD2 is not capable of targeting EGFP into the nucleus

(A) Schematic to illustrate the Rad60, Rad60-ct and Rad60-264 (aa 264-406) proteins. **(B)** Wild-type cells expressing EGFP, and Rad60-264 (aa 264-406) from the pREP41EGFP(C) constructs were grown at 30^{o}C in EMM2 medium supplemented with adenine and leucine. 1 ml of exponentially growing cells were harvested, washed and re-suspended in 100 μl EMM2 medium and stained with Hoechst. Cells were visualised using an Applied Precision Deltavision Spectris microscope using deconvolution software

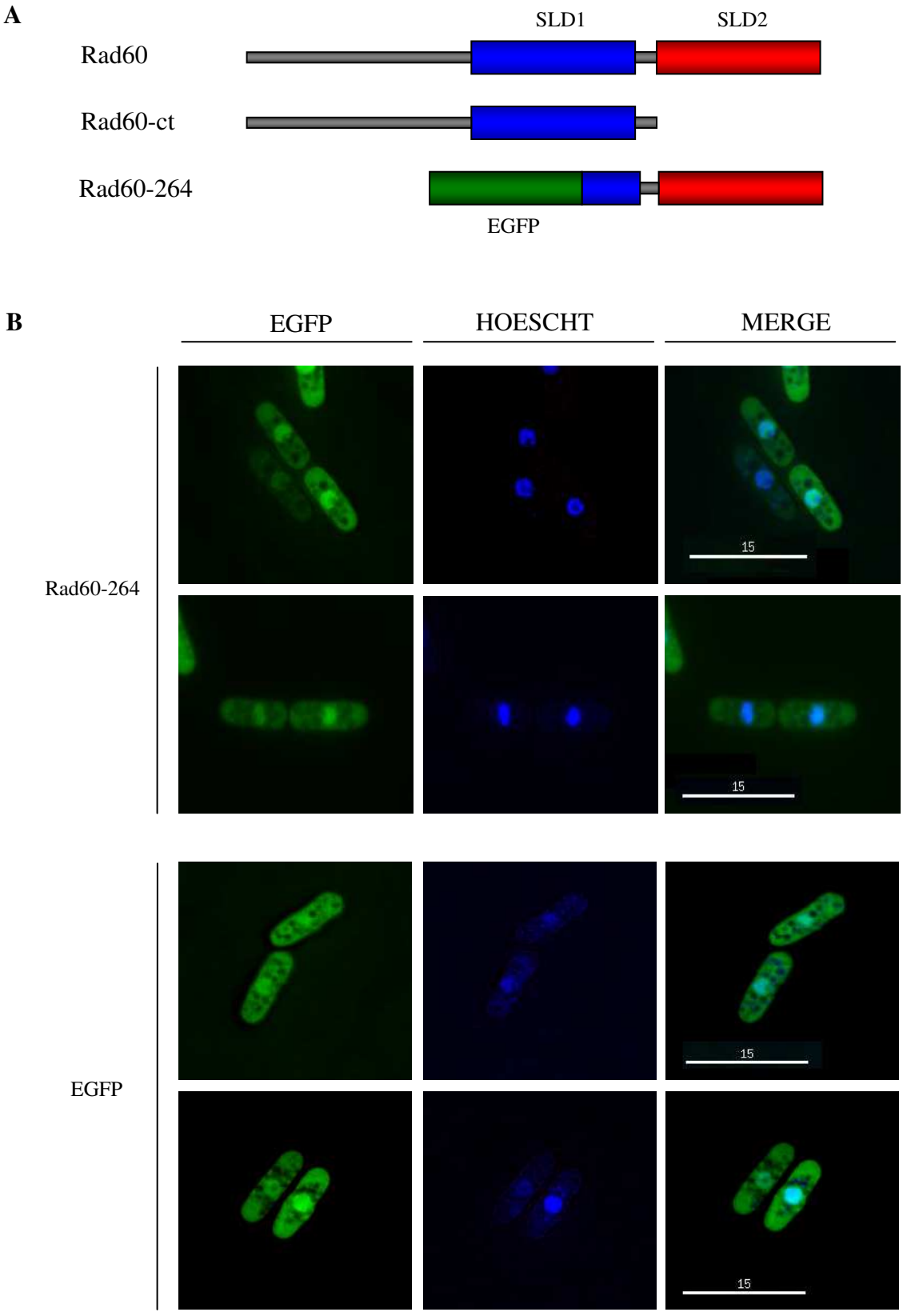

Figure 5.12: Rad60 SLD2 is not capable of targeting EGFP into the nucleus

designed to introduce a *Sal*I restriction site, immediately upstream of the ATG start codon. Primer L118 was designed to introduce a *Bam*HI restriction site immediately downstream of codon 99 and upstream of the diglycine coding sequence. The PCR product was ligated directly into the pGEM-T Easy cloning vector. Third, the pREPHA41*rad60(Sal*I) construct was digested with *Sal*I/*Bam*HI and the vector gel extracted. The *Sal*I/*Bam*HI digest excised the *rad60* nucleotide sequence upstream of the newly introduced *Sal*I restriction site. Fourth, the *pmt3* coding sequence was subcloned as a *Sal*I/*Bam*HI fragment from the pGEM-T Easy vector into the *Sal*I/*Bam*HI digested pREPHA41*rad60-ct* construct. Fifth, the *rad60-ctpmt3*coding sequence was subcloned as an *Nde*I/*Bam*HI fragment from pREPHA41 into the pREP41EGFP(C) vector, which places the EGFP tagging sequence downstream of the *rad60-ctpmt3* sequence.

To examine the localisation of the Rad60-ctPmt3 protein, the pREP41EGFP(C)*rad60-pmt3* construct was transformed into wild-type cells. Expression from the *nmt1* promoter was de-repressed by growing cells for ~16 hours in the absence of thiamine. Exponentially growing cells were imaged. The exogenously expressed Rad60-ctPmt3 protein is located within the nucleus (Figure 5.10). Nuclear localisation is confirmed by the co-localisation of the EGFP signal with Hoechst signal. Wild-type cells were also transformed with pREP41 EGFP(C)*rad60,* pREP41 EGFP(C)*rad60-ct* and the empty pREP41EGFP(C) vector as controls. Similar to the cellular localisation pattern seen by Rad60 and Rad60-ct at endogenous expression levels (Section 5.2), Rad60, which is exogenously over-expressed is located in the nucleus, whilst Rad60-ct is dispersed throughout the cell. However, the signal detected in the nucleus for the exogenously expressed Rad60 is much stronger than that of the endogenous protein. The pan-cellular localisation of EGFP confirms that the nuclear signal observed is not an artefact of the EGFP tag. To test whether the Rad60-ctPmt3 protein is able to delocalise from the nucleus under regulation of Cds1, exponentially growing cells were treated with 20 mM HU for 4 hours. Following HU treatment, the Rad60-ctPmt3 protein fails to delocalise from the nucleus (Figure 5.10). Unfortunately, unlike endogenous Rad60 (Section 5.2.2), exogenously expressed Rad60 failed to delocalise from the nucleus following HU treatment. This difference in the endogenously and exogenously expressed Rad60 suggests that studies using over-

expression of Rad60 may not be biologically significant, and for this reason it cannot be concluded whether the Rad60-ctPmt3 protein is proficient for regulation by Cds1. Studies at endogenous levels are, therefore, required to answer this question.

If Rad60 SLD2 is 'SUMO-like', replacing Rad60 SLD2 with authentic SUMO (Pmt3) should leave Rad60 function intact. To test this *rad60-ctpmt3* was expressed in the *rad60-ct* background and the response to DNA damaging agents was tested (Figure 5.11). Wild-type and *rad60-ct* cells were transformed with the pREP41EGFP(C)*rad60* (p*rad60*), pREP41EGFP(C)*rad60-ct* (p*rad60-ct*) and pREP41EGFP(C)*rad60-ctpmt3* (p*rad60-ctpmt3*) constructs, as well as the empty pREP41EGFP(C) vector (pEV) as a control. *rad60-ct* cells transformed with pEV, are sensitive to HU and MMS as compared to the wild-type cells transformed with the empty vector. As seen previously. the HU and MMS sensitivity of *rad60-ct* cells is complemented by expression of *rad60* but not *rad60-ct.* When *rad60-ct* cells are transformed with p*rad60-ctpmt3*, growth is impaired. In addition, *rad60-ct* cells expressing *rad60-ctpmt3* are more sensitive to MMS and HU than *rad60-ct* cells transformed with pEV. This suggests that expression of *rad60-ctpmt3* in *rad60-ct* cells has a dominant negative effect. This dominant negative effect is also seen in wild-type cells, suggesting that Pmt3 (SUMO) cannot functionally substitute for Rad60 SLD2. The dominant negative effect may be due to the inability of Rad60 to delocalise from the nucleus.

5.8 Discussion

Rad60 has been shown to be a nuclear protein (Morishita, Tsutsui et al. 2002; Boddy, Shanahan et al. 2003). Morishita *et al* first showed nuclear loaclisation of Rad60 by exogenously expressing an N-terminally tagged Rad60 from a modified *nmt*1 promoter on the pREP42 plasmid. However, when they attempted to express the N-terminally EGFP-tagged Rad60 from the Rad60 promoter no signal was seen (Morishita, Tsutsui et al. 2002). Boddy *et al* later confirmed that Rad60 was localised to the nucleus during all cell stages using an endogenously expressed C-terminally 13myc-tagged Rad60 and showed that the C-terminally 13myc-tagged Rad60 delocalises from the nucleus following HU treatment (Boddy, Shanahan et al. 2003).

In this chapter I have investigated the localisation of the C-terminally truncated Rad60-ct protein. For this purpose, *rad60-FLGFP* and *rad60-ctGFP* strains expressing C-terminally GFP-tagged full-length and C-terminally truncated Rad60 protein, repectively, were created. Visualisation of the C-terminally GFP-tagged Rad60 protein, confirms previous observations that Rad60 is a nuclear protein (Morishita, Tsutsui et al. 2002; Boddy, Shanahan et al. 2003). However, the C-terminally GFP tagged Rad60-ct protein is found dispersed throughout the cell. Although epitope tagging is a valuable tool for studying a protein of interest, one of the problems associated with attaching a tag to a protein is the possibility that it may lead to a mutant phenotype. This may be because the tag alters the protein conformation, or disrupts a protein-protein or protein/DNA interaction important for function. Comparison of the sensitivity of C-terminally GFP-tagged *rad60-FL* and *rad60-ct* strains to a range of DNA damaging agents showed no significant difference as compared to their untagged counterparts. However, it is not impossible that tagging of the protein has resulted in subtle phenotypic differences that cannot be detected by survival studies. To eliminate the possibility that the mis-localisation of the Rad60-ct protein is one such difference, N-terminally GFP-tagged *rad60-FL* and *rad60-ct* strains were created. Unfortunately, the full-length N-terminally GFP-tagged Rad60 protein failed to localise to the nucleus as previously reported (Morishita, Tsutsui et al. 2002; Boddy, Shanahan et al. 2003) and, as seen in this study for the C-terminally GFP-tagged Rad60. The mis-localisation of the C-terminally GFP-tagged Rad60-ct protein could, therefore, not be confirmed by N-terminal tagging. Interestingly, whilst Morishita *et al* were able to show nuclear localisation of exogenously expressed N-terminally tagged Rad60, no signal was seen when they attempted to express the N-terminally tagged protein from the Rad60 promoter (Morishita, Tsutsui et al. 2002). In a second attempt to eliminate the possibility that the mis-localisation of the Rad60-ct is an artefact of C-terminal GFP tagging, anti-Rad60 antibodies were produced. However, the specificity of the antibody was not high enough to be used for immunofluorescence.

Activation of the S-phase checkpoint kinase Cds1 causes hyper-phosphorylation and concomitant delocalisation of Rad60 from the nucleus (Boddy, Shanahan et al. 2003). In a *cds1-d* background Rad60-ct-GFP is observed throughout the cell. This suggests that mis-

localisation of Rad60-ct-GFP is not the result of constitutive activation of Cds1. With the same reasoning, the mis-localisation of Rad60-ct is not the result of constitutive activation of Chk1. Unlike in the *cds1-d* background, Rad60-FL-GFP is not localised within the nucleus of *chk1-d* cells. Since the delocalisation of Rad60 from the nucleus is S-phase specific, and is not observed in G2 cells treated with IR, (Boddy, Shanahan et al. 2003), this may suggest that Chk1 has a role in maintaining Rad60 in the nucleus.

Provision of a nuclear localisation signal to the Rad60-ct protein is capable of restoring wild-type localisation. However, expression of the Rad60-ctNLS protein in *rad60-ct* cells is unable to rescue the DNA damage sensitive phenotype of the *rad60-ct* cells and instead has a dominant negative effect in both wild-type and *rad60-ct* cells. Since a *rad60-4* mutant unable to delocalise from the nucleus is proficient for the survival of UV-induced DNA damage (Boddy, Shanahan et al. 2003), it is unlikely that the dominant-negative phenotype observed is purely a consequence of Rad60-ctNLS being unable to delocalise from the nucleus following replication stress. Rather, it would suggest that SLD2 is required not only to localise Rad60 to the nucleus for its role in the DNA damage response, but also for the DNA damage response itself. This hypothesis is strengthened by the observation that *rad60-ct* cells over-expressing the Rad60-ct protein do not show a dominant-negative phenotype. Unfortunately, HU treatment of cells expressing Rad60-ctNLS was unable to confirm that the Rad60-ctNLS protein is unable to delocalise from the nucleus following replication stress.

Since the Rad60 protein does not contain a recognised NLS it is possible that the C-terminal SLD2 of Rad60 is required to interact with proteins that facilitate nuclear import. However, the Rad60 SLD2 alone is not capable of targeting EGFP into the nucleus. This may suggest that although SLD2 is required for Rad60 nuclear localisation, localisation may be dependent on the correct folding of the entire protein.

Following the observation that provision of an NLS to the Rad60-ct protein is able to restore nuclear localisation but not function of the Rad60 protein it is likely that Rad60 SLD2 has a functional role in the DNA damage response. Provided Rad60 SLD2 really is

SUMO-like in structure and function, I would expect substitution of SLD2 with authentic SUMO (Pmt3) to restore both nuclear localisation and a wild-type response to DNA damaging agents. Similarly to the provision of an NLS to Rad60-ct, replacement of SLD2 with SUMO is able to restore wild-type localisation to Rad60-ct but unable to rescue the DNA damage sensitive phenotype of *rad60-ct* cells. In addition, expression of Rad60-ctPmt3 in both wild-type and *rad60-ct* cells has a dominant-negative effect. This suggests that once in the nucleus, SUMO (Pmt3) cannot functionally substitute for Rad60 SLD2.

It is important to note that the experiments in which either an NLS (Section 5.6) or Pmt3 (Section 5.7) were tethered to the C-terminus of the Rad60-ct protein were carried out using protein exogenously over-expressed from the *nmt1* promoter of the pREP41EGFP plasmid. As seen for endogenous levels of the protein (Section 5.2), Rad60 over-expressed exogenously is located in the nucleus whilst Rad60-ct is dispersed throughout the cell. However, the nuclear localisation of the exogenously expressed Rad60 is more discrete than that observed for the endogenous protein. Unfortunately, unlike endogenous Rad60 (Section 5.2.2)(Boddy, Shanahan et al. 2003), exogenously expressed Rad60 failed to delocalise from the nucleus following HU treatment. The differences observed for endogenous and exogenous Rad60 expression suggest that Rad60 over-expression studies may not be biologically significant. Studies at endogenous levels are, therefore, required to answer this question. During this study, attempts were made to create a haploid strain endogenously expressing a C-terminally tagged Rad60-ctNLS protein, using the Bahler method of integration. Unfortunately, when transformants were screened, no colonies contained the Rad60-ctNLS allele, suggesting that the provision of an NLS to the C-terminus of the Rad60-ct protein may be lethal. This is consistant with the dominant negative phenotype observed when Rad60-ctNLS is overexpressed in *rad60-ct* cells. Therefore, if further time were permitted, I would integrate the *rad60-ctNLS* allele as a single copy into a diploid strain to check whether cells are viable. Similarly, I would create a strain carrying the Rad60-ctpmt3 protein and assess localisation and phenotype.

CHAPTER 6

Further analysis of the Rad60 SUMO-like domains: sequence comparison, molecular modelling and preliminary structure-function studies

6.1 Introduction

Proteins containing at least one ubiquitin-like fold can be distinguished into two different categories; ubiquitin-like modifiers and ubiquitin-like domain proteins. As is the case with ubiquitin, ubiquitin-like modifiers are post-translational modifiers, which can be covalently attached to target proteins via lysine residues. Unlike ubiquitin, other modifiers do not directly target proteins for degradation but have a more diverse range of functions. For example, SUMO has been implicated in roles in regulating protein localisation, genomic integrity, and cell cycle control amongst others. In contrast to the ubiquitin-like modifiers, ubiquitin-like domain proteins lack the C-terminal diglycine motif required for conjugation to target molecules. Ubiquitin-like domain proteins are a heterogeneous class of proteins and are usually multi-domain proteins that are completely unrelated outside of their ubiquitin-like domains. Proteins such as Rad23 and Dsk2 have been extensively studied and have the unifying role of interacting with the proteosome (Funakoshi, Sasaki et al. 2002; Rao and Sastry 2002; Lambertson, Chen et al. 2003). This suggests that the ubiquitin-like domains fulfil their cellular role by functionally mimicking ubiquitination. The emergence of the RENi family of SUMO-like domain proteins suggests the existence of a group of proteins that may be able to functionally mimic the role of SUMO (Novatchkova *et al*, 2005). However, the precise role of these SUMO-like domains has yet to be determined.

In previous chapters, I have shown the C-terminal SLDs of Rad60 to be important for Rad60 function. A *rad60* mutant deleted for SLD1 (*rad60-SLD1Δ*) is not viable. A *rad60* mutant deleted for SLD2 (*rad60-ct*) is viable but is defective in the response to DNA damage (Chapter 3). The SLD2 of Rad60 is also important for the nuclear localisation of the Rad60 protein (Chapter 5). Despite the importance of the Rad60 SLDs for Rad60 function, little evidence exists to suggest the SLDs are in fact ‘SUMO-like’ in structure and function. To date, evidence is based only on a very low sequence identity between Rad60

and SUMO-1. In this chapter I have carried out preliminary structure-function studies of the Rad60 SUMO-like domains.

6.2 The phenotype of *rad60-ct* cells is not due to the loss of SBM3

The physiological consequence of SUMO modification is typically mediated by effector proteins that recognise SUMO through SUMO-binding motifs. Rad60 contains an SXS (Section 1.8.7) motif and three sequences conforming to the V/I-X-V/I-V/I motif (SBM1, 2 and 3) (Raffa, Wohlschlegel et al. 2006) (Figure 6.1.A). Both motifs have been shown to be SUMO-binding motifs (Minty, Dumont et al. 2000; Bi, Song et al. 2004; Song, Durrin et al. 2004). Unlike SUMO-consensus motifs that allow covalent attachment of SUMO to target proteins, SUMO-binding motifs mediate protein-protein interactions by allowing non-covalent binding to SUMO-conjugated proteins. The three V/I-X-V/I-V/I SBMs have been shown to be important for Rad60 self-association (Raffa, Wohlschlegel et al. 2006).

SBM3 (VSVVLD) is located at the very C-terminus of Rad60 (aa 401-406). This raises the possibility that the phenotype observed for the previously characterised *rad60-ct* mutant might be the result of losing SBM3 and not of losing SLD2 as believed. To investigate this, the RMCE system (Section 3.5) was used to disrupt SBM3. Site-directed mutagenesis of the pAW8*prad60* construct with primers L129/L130 was used to introduce V401A and V403A substitutions within the VSVVLD motif. (Figure 6.1B). SBM1 is located slightly upstream of SLD1, whilst SBM2 is located within SLD1 itself. Due to the importance of SLD1 for Rad60 viability (Section 3.5.3), mutant strains with a disrupted SBM1 and SBM2 were made in parallel to the SBM3 mutant. Primers L125/L126 were used to introduce V216A and V217A substitutions within the ISVV motif of SBM1 and primers L127/L128 were used to introduce V269A and V2671A substitutions within the VVLV motif of SMB2. (Figure 6.1B). RMCE between the mutated pAW8p*rad60* constructs and the *rad60* base strain was achieved as described in section 2.1.5. Two 5FOA resistant colonies were selected and their phenotype compared to the *rad60-ct* mutant. The *rad60-SBM1* and *rad60-SBM3* mutants showed no significant sensitivity to HU and MMS at either 30 or 36^{o}C (Figure 6.1C) and UV and IR (Figure 6.2A, B) as compared to wild-type cells. This suggests that the phenotype observed for the *rad60-ct* mutant is a consequence of deleting

Figure 6.1: The HU and MMS sensitivity of *rad60-ct* is not the consequence of loss of SBM3

(A) Rad60 has three SUMO-binding motifs (SBMs). Schematic to illustrate the relative positions of the Rad60 SBMs in relation to the C-terminal SUMO-like domains. **(B)** Table to illustrate the valine to alanine substitutions made in the *rad60*-SBM1, *rad60*-SMB2 and *rad60*-SBM3 mutants. **(C)** *rad60-SBM3* cells show a wild-type phenotype to HU and MMS. Cells were grown at 30^{o}C in YE medium to mid-exponential phase. 10 μl of 10 fold serial dilutions were spotted onto YEA plates containing supplements at the indicated doses. Plates were incubated at 30^{o}C for 72 hours and photographed.

A

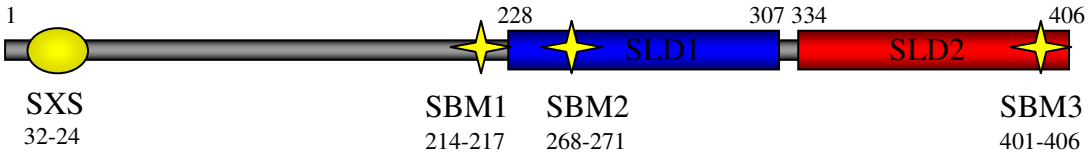

B

SBM1	SBM2	SBM3
ISVV	VVLV	VSVVLD
ISAA	VALA	ASAVLD

C

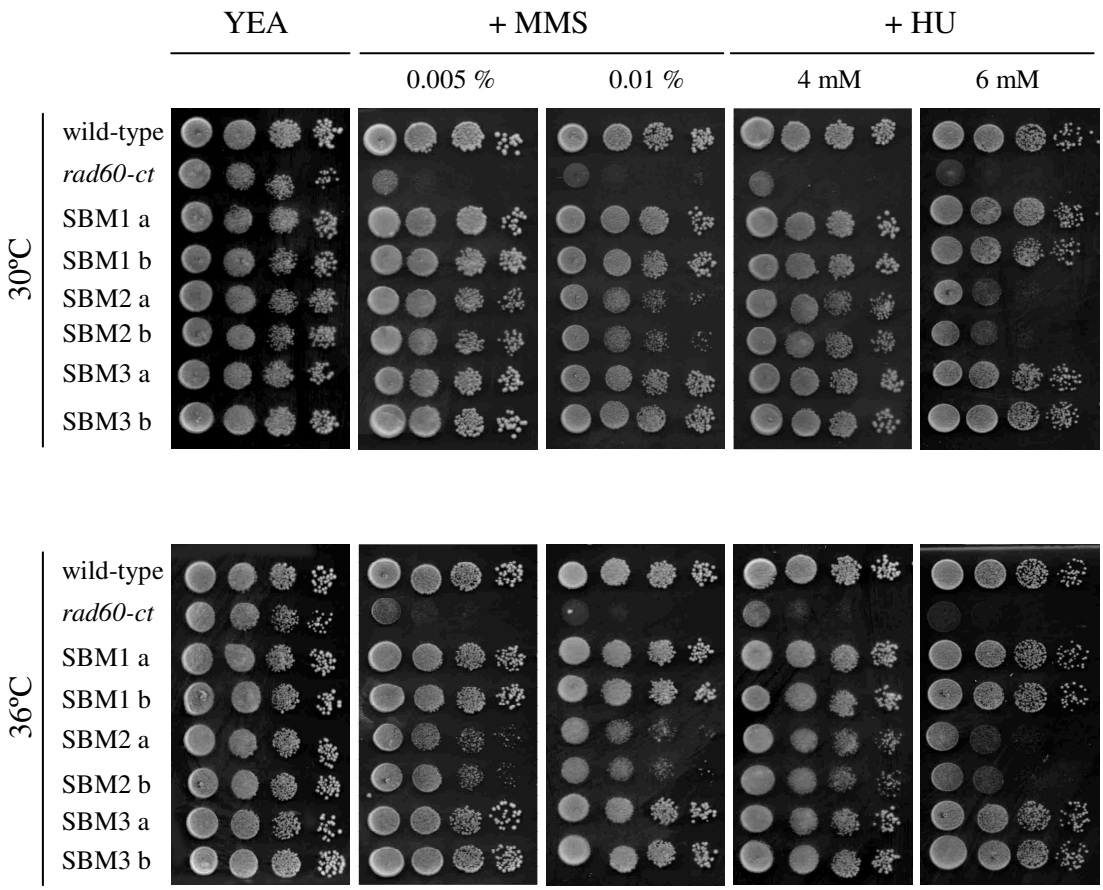

Figure 6.1: The HU and MMS sensitivity of *rad60-ct* is not the consequence of loss of SBM3

Figure 6.2: The UV and IR sensitivity of *rad60-ct* is not the consequence of loss of SBM3

(A, B) *rad60-SBM3* cells show a wild-type sensitivity to UV and γ irradiation. Cells were grown at 30^{o}C in YE medium to mid-exponential phase and irradiated with UV (A) or γ (B) rays at the indicated doses. Cells were plated on YEA and grown at 30^{o}C for ~72 hours. Colonies were counted and % survival was calculated.

A

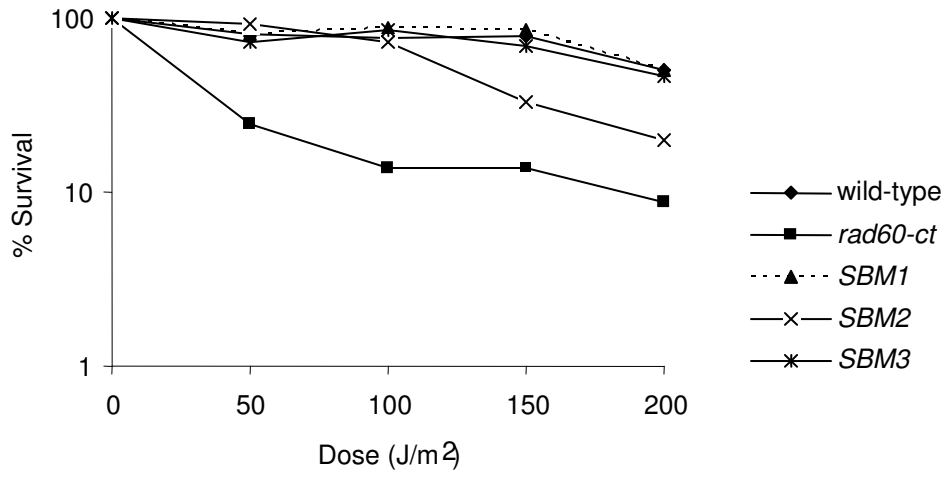

B

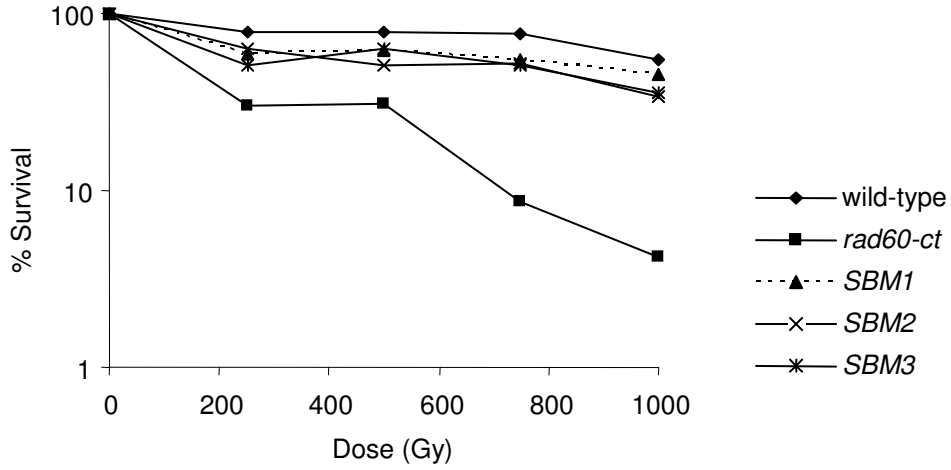

Figure 6.2: The UV and IR sensitivity of *rad60-ct* is not the consequence of loss of SBM3

more than SBM3. Interestingly, when compared to wild-type cells, the *rad60-SBM2* mutants are more sensitive to HU, MMS, UV and IR, but less sensitive than the *rad60-ct* mutant (Figures 6.1C; 6.2A, B). SBM2 is located in SLD1 of Rad60. Since the sensitivity of *rad60-ct* and *rad60-1* cells to HU, MMS, IR and UV is similar, *rad60-SBM2* cells are less sensitive than *rad60-1* (K263E) cells. The sensitivity to MMS and HU was no greater at 36^{o}C than 30^{o}C, suggesting this is not a temperature sensitive mutation.

6.3 Comparison of the amino-acid sequence of Rad60 SUMO-like domains with SUMO homologues

6.3.1 Comparison of SUMO-1 homologues identifies conserved features of SUMO molecules

In section 3.2, a ClustalW alignment of the Rad60 protein sequence against *H. sapiens* SUMO-1 and *S. pombe* Pmt3 identified two potential SUMO-like domains with low sequence identity. Despite the low sequence identity, there is significant conservation of the biochemical nature of the amino-acid side chains. However, Rad60 SLD2 was originally identified as a ubiquitin-like domain (Morishita, Tsutsui et al. 2002). Although SUMO and ubiquitin are functionally very different, they both share a conserved ββαββαβ fold. Ubiquitin and SUMO share only ~18% sequence identity but despite the low sequence identity, like SUMO and the SLDs, many of the amino-acid side chains of SUMO and ubiquitin are biochemically conserved. This raises the question of 'are we correct in assuming the SLDs are in fact SUMO-like, and not ubiquitin-like as first predicted?'. To attempt to answer this question, a search for features unique to SUMO, but not ubiquitin, was initiated. SUMO-1 homologues from *H. sapiens*, *C. elegans*, *S. cerevisiae*, *D. melanogastar*, and *S. pombe* were aligned using the online tool, ClustalW (http://www.ebi.ac.uk/tools/clustalw2/index.html). As a comparison, *H. sapiens* ubiquitin has been included. The alignment of proteins homologous to SUMO-1 highlights a number of residues conserved amongst the SUMO-1 homologues (Figure 6.3B). Of the conserved residues, only V26, G56, R63, G68, T76 and the C-terminal diglycine motif G96 G97 of SUMO-1 are conserved between both the SUMO-1 homologues and ubiquitin. Interestingly, when the residue conserved in the SUMO-1 homologues, but not in ubiquitin,

Figure 6.3: Amino acid sequence comparison of proteins homologous to SUMO-1

(A) A ClustalW alignment of the amino acid sequences of proteins homologous to SUMO-1 from *H. sapiens* (Hs_SUMO-1, Hs_SUMO-2, Hs_SUMO-3), *C. elegans* (Ce_Smt3), *S. cerevisiae* (Sc_Smt3), *D. melanogastar* (Dm_Smt3), *S. pombe* (Sp_Pmt3). As a comparison, *H. sapiens* ubiquitin (Hs_Ub1) has been aligned against the SUMO-1 homologues. Amino acid residues conserved in all SUMO-1 homologues and ubiquitin are highlighted in red, residues conserved in all SUMO-1 homologues but not ubiquitin are highlighted in yellow and residues conserved in at least 5 of the 7 SUMO-1 homologues are highlighted in blue. Residues shown to contribute to the overall stability of the SUMO-1 protein (Bayer *et al* 1998) are highlighted (*). Aligned underneath are the sequences for Rad60 SLD1 and Rad60 SLD2. **(B)** Table showing the conservation of Bayer residues in ubiquitin, Rad60 SLD1 and Rad60 SLD2. Bayer residues are highlighted in red.

A

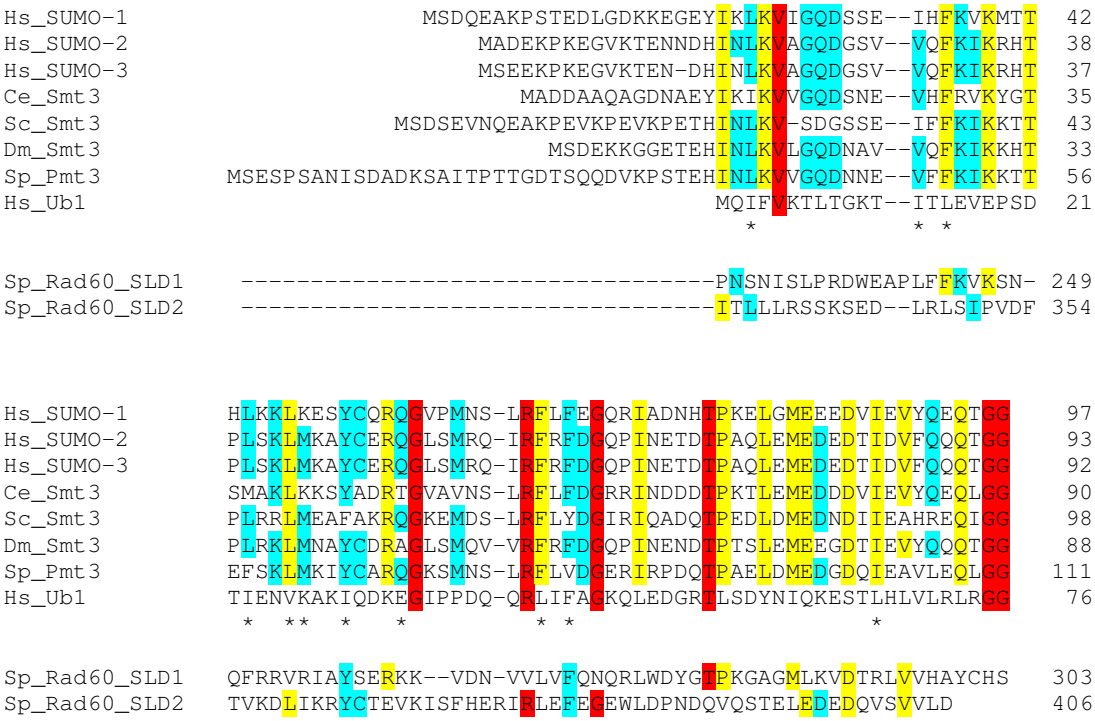

B

Position	SUMO-1	Ubiquitin	SLD1	SLD2
β-sheet	**L24**	I3	S230?	L336
β-sheet	**I34**	I13	L242	L346
β-sheet	**F36**	L15	F244	L348
β-sheet	**F64**	L43	L270	L377
β-sheet	**F66**	F45	F272	F379
β-sheet	**I88**	L67	R294	V401
α-helix	**L44**	I23	F252	V356
α-helix	**L47**	V26	V255	L359
α-helix	**K48**	K27	R256	I360
α-helix	**Y51**	I30	Y259	Y363
α-helix	Q53	D32	E261	T365
α-helix	**Q55**	E34	K263	V367

Figure 6.3: Amino acid sequence comparison of proteins homologous to SUMO-1

has a hydrophobic side chains (I/L/V), it is often substituted for another residue with the same hydrophobic properties (I/L/V). Aside from residues R54 and R63 of SUMO-1, no other charged residue is substituted with a like charge (K/R, H, E/D). When the SUMO-1 homologues are aligned with the amino acid sequence of Rad60 SLD1 and SLD2, very few residues are conserved with the SUMO-1 homologues (Figure 6.3A, B). The majority of those residues conserved differ for SLD1 and SLD2. As is the case for ubiquitin, many of the hydrophobic residues conserved amongst the SUMO-1 homologues are substituted for a residue with the same hydrophobic properties (I/L/V) in SLD1 and SLD2. These residues are likely to contribute to the hydrophobic core of SUMO/ubiquitin. Aside from *S. cerevisiae*, Y51 of SUMO-1 is conserved in all of the SUMO-1 homologues, but not ubiquitin Interestingly, SLD1 and SLD2 also have a tyrosine at this position. This may suggest a SUMO-specific residue.

One feature that strongly distinguishes SUMO homologues from other ubiquitin-like modifiers is the large cluster of negatively charged residues (aspartate, glutamate) close to the C-terminus (Figure 6.3B). This negative patch has been suggested to define an important interaction surface of SUMO (Bayer, Arndt et al. 1998). In SUMO-1 the negative surface is formed by E83, E84, E85 and D86. Of these residues, only the negative charge of E83 is conserved in ubiquitin. Interestingly, a large negative cluster is conserved at the C-terminus of Rad60 SLD2 (aa 394-399) but not SLD1. Unlike all SUMO homologues, the Rad60 SLDs lack the C-terminal diglycine motif required for conjugation to its substrate. This suggests that the domains are SUMO fusions that cannot conjugate to target proteins and must fulfil their SUMO-like role in some other manner.

6.3.2 Conservation of structurally important residues

The structure of SUMO-1 has been solved by NMR and X-ray crystallography (Bayer, Arndt et al. 1998; Song, Zhang et al. 2005). SUMO-1 consists of a ββαββαβ fold. With the exception of β4, which is twisted against the main plane, the β-sheets of SUMO-1 are aligned parallel to one another (Bayer, Arndt et al. 1998). Helix α1 is rotated approximately 45^{o} relative to β1. Contacts between the hydrophobic side chains of L24, I34, F36, F64, F66, I88 on the β-sheet and L44, L47, K48, Y51, Q53 and Q55 of the α1

helix have been identified at the helix-sheet interface in SUMO-1 (Bayer, Arndt et al. 1998). Despite the low sequence identity shared by SUMO-1 and ubiquitin, the two proteins share this same characteristic fold. With the exception of Q53 and Q55, the hydrophobic nature of residues forming the hydrophobic core is conserved in ubiquitin (Figure 6.3B). These residues are therefore thought to be of key importance in maintaining the ubiquitin fold (Bayer, Arndt et al. 1998). Of the residues identified to be of structural importance (Hereafter referred to as *Bayer* residues), the hydrophobic nature is better conserved in SLD2 than SLD1. Interestingly, the conserved tyrosine discussed in section 6.3.1 is listed as one of the residues of the α1 helix required make contacts at the helix-sheet interface in SUMO-1 (Bayer, Arndt et al. 1998). A tyrosine residue is found at the same position in both SLD1 and SLD2, but not ubiquitin, highlighting a possible SUMO-specific residue.

6.3.3 Comparison of the amino acid sequence of the RENi family protein members identifies conserved residues

The ubiquitin-like domains of proteins, including Rad23 and Dsk2, are believed to fulfil their cellular role by functionally mimicking ubiquitination (Funakoshi, Sasaki et al. 2002; Rao and Sastry 2002; Lambertson, Chen et al. 2003). With the discovery of the RENi family of SUMO-like domain proteins, it could be assumed that the SUMO-like domains are able to functionally mimic the role of SUMO (Novatchkova, Bachmair et al. 2005). However, the precise role of these domains has yet to be identified. If the SUMO-like domains do share a common function of mimicking SUMO, I would expect significant conservation between the SLDs of the RENi family. For this reason, a ClustalW (http://www.ebi.ac.uk/tools/clustalw2/index.html) alignment of RENi proteins against SUMO-1 was carried out (Figure 6.4).

In proteins of the RENi family, the C-terminal SLD2 shares several features discriminating SUMO proteins from other ubiquitin-like modifiers. Firstly, the large cluster of negatively charged residues (aa 394-399) is indicative of a SUMO-like protein rather than a ubiquitin-like protein. The negative surface patch formed by these residues has been suggested to form a SUMO-typical interaction surface (Bayer, Arndt et al. 1998). However, this

Figure 6.4: Multiple sequence alignment of the RENi protein family members

A ClustalW alignment of the amino acid sequences of members of the RENi protein family from *S. pombe* (Sp), *S. cerevisiae* (Sc), *M. musculus* (Mm), *H. sapiens* (Hs) and *C. elegans* (Ce_Smt3). The alignments show **(A)** SUMO-like domain 1 and **(B)** SUMO-like domain 2 of the RENi proteins. As a comparison, *H. sapiens* SUMO-1 has been aligned against the RENi proteins. The alignment is CLUSTALW coloured (Thompson *et al*, 1994). (All Gly (orange), Pro (yellow) are coloured. Other residues matching a frequent occurrence of a property in a column are coloured: hydrophobic = blue; hydrophobic tendency = light blue; basic = red; acidic = purple; hydrophilic = green; unconserved = white). Residues shown to contribute to the overall stability of the SUMO-1 protein (Bayer *et al* 1998) are highlighted (*).

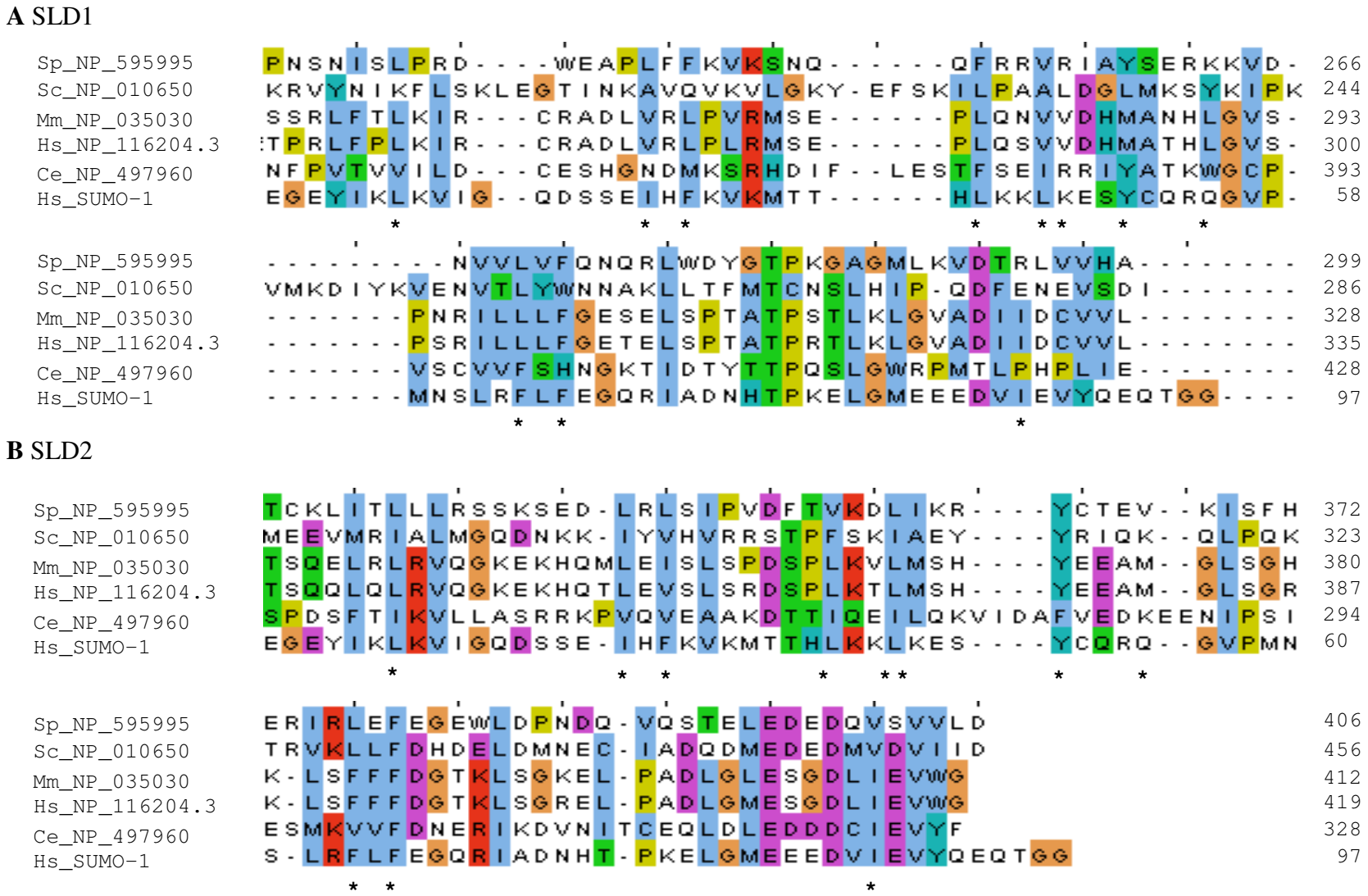

Figure 6.4: Multiple sequence alignment of the RENi protein family members

negative surface patch is absent in SLD1 of all RENi proteins. Although the sequence identity shared by proteins of the RENi family is low, the biochemical nature of the side chains is well conserved. When looking at the residues aligned to the structurally important 'Bayer' residues of SUMO-1, with the exception of Q55, it can be seen that the hydrophobic nature of these residues is conserved. This supports the hypothesis that the SUMO-like domains adopt a SUMO/ubiquitin-like fold. As in the case of the SUMO-1 homologues (Section 6.3.1) Y51 of SUMO-1 is conserved in SLD2 of most RENi proteins. This tyrosine is less well conserved in SLD1 of the RENi proteins, suggesting that the SLD2 of the RENi proteins more closely resembles SUMO-1 than SLD1.

6.3.4 Residues known to contribute to the SBM binding pocket of SUMO-1 are conserved in Rad60 SLD1 and SLD2

The biological importance of SUMO modification is often mediated by proteins that are able to recognise and interact with SUMO via their SBMs. The structure of SUMO-1 in complex with an SBM has identified an SBM binding surface of SUMO-1 (Song, Zhang et al. 2005). The SBM binding surface of SUMO-1 is formed by a deep groove that is lined with hydrophobic and aromatic patches consisting of residues I34, H35, F36, V38, L47 and Y51 (Song, Zhang et al. 2005). Within the SBM binding pocket, the peptide containing the SBM also contacts E33 of SUMO-1. With the exception of H35, the biochemical nature of the side chain of these residues is largely conserved in both SLD1 and SLD2 (Table 6.1). E33 of SUMO-1 is substituted with E239 and D345 in SLD1 and SLD2 respectively, maintaining a negatively charged residue at this site. The hydrophobic nature of the I34, F36, V38 and L47 side chains is maintained in both SLD1 and SLD2. Interestingly, of these residues, I34, F36, L47 and Y51 have been described as key residues of structural importance to SUMO-1 (Bayer, Arndt et al. 1998) and Y51 has been highlighted as a SUMO-specific residue (Section 6.3.1; 6.3.2). Y51 is conserved in both SLD1 and SLD2 of Rad60.

6.4 Comparative modelling of Rad60 SLD1 and SLD2 using MODELLER

Despite the low sequence identity between the SLDs, SUMO and ubiquitin (Section 3.2), there is significant conservation of the biochemical nature of the amino-acid side chains,

Table 6.1: Residues known to contribute to the SBM binding pocket of SUMO-1 are conserved in SLD1 and SLD2

SUMO-1	SLD1	SLD2
E33	E239	D345
I34	L242	L346
H35	F243	R347
F36	F244	L348
V38	V246	I348
L47	V255	L359
Y51	Y259	Y363

for example hydrophobic residues (I, L, V) are substituted for one another. To test whether the Rad60 SLDs can adopt the characteristic ββαββαβ fold of SUMO, a computer-modelling programme was used. In the absence of an experimentally determined structure, comparative or homology modelling can sometimes provide a useful 3D model for a target protein that is related to at least one known protein structure.

With the help of Dr. Darren Thompson (University of Sussex) the SUMO-like domains of Rad60 were modelled using MODELLER. MODELLER is a comparative modelling tool, which models protein structure by satisfaction of spatial restraints (Sali, Potterton et al. 1995; Sanchez and Sali 2000). MODELLER can be used in all stages of comparative modelling including template search, target-template alignment and model building (Sali, Potterton et al. 1995; Sanchez and Sali 2000). Since I wished to model the SUMO-like domains of Rad60 on SUMO, the template and target-template alignment were already known. In this instance, MODELLER was used only for model building. Since the X-ray crystal structure of the *S. pombe* Pmt3 (SUMO) structure has not yet been solved the structure of *H. sapiens* SUMO-1 was therefore used for comparative modelling. It is important to note that, unlike ubiquitin, SUMO has a flexible N-terminal tail but due to the packing constraints required for protein crystallisation only the structure of the ubiquitin-like fold of SUMO has been determined. The alignment of Rad60 SLD1 (aa 227-303) and SLD2 (aa 334-406) with *H. sapiens* SUMO-1 (aa 21-97) were submitted to MODELLER along with the pdb coordinates of SUMO-1 (2asq.pdb). Once a target-template alignment is obtained, the calculation of the 3D model of the target by MODELLER is completely automated. The program '*extracts atom-atom distance and dihedral angle restraints on the target from the template structure(s) and combines them with the general rules of protein structure such as bond length and angle preferences'* (Sanchez and Sali 2000). The program then uses an optimisation procedure that minimises violations of spatial restraints to calculate a model of the target protein (Sali, Potterton et al. 1995; Sanchez and Sali 2000). Due to the nature of the program, slight variations in the final model can be achieved with different rounds of comparative modelling. For this reason the data were submitted to MODELLER on three independent occasions. With the help of Dr. Darren

Thompson (University of Sussex), the model with the most likely positioning of side chains (least steric hindrance) was selected for analysis.

6.4.1 Comparative modelling suggests that Rad60 SLD1 and SLD2 can adopt a βαββαββ fold

The predicted structures of Rad60 SLD1 and Rad60 SLD2 were visualised using Swiss-Pdb Viewer and compared to the known structures of *H. sapiens* ubiquitin (1ubq.pdb) and *H. sapiens* SUMO-1 (2asq.pdb). Like SUMO-1 and ubiquitin, both Rad60 SLD1 and SLD2 are predicted to fold with the characteristic ββαββαβ fold (Figure 6.5A). The loops connecting the secondary structure elements in SUMO/ubiquitin are also similar in both SLD1 and SLD2. Recently, the structure of the *H. sapiens* Nip45 SLD2 has been solved (2jxx.pdb). Like SUMO-1 and ubiquitin, Nip45 SLD2 folds with a ββαββαβ fold (Figure 6.5A). Comparison of the solved Nip45 SLD2 structure with SUMO-1 strengthens the hypothesis that the SUMO-like domains of the RENi protein family fold to resemble SUMO.

As discussed in section 6.3.2, contacts between the hydrophobic side chains of L24, I34, F36, F64, F66, I88 on the β-sheet and L44, L47, K48, Y51, Q53 and Q55 of the α1 helix are thought to be of key importance in maintaining the ββαββαβ fold (Bayer, Arndt et al. 1998). Residues within SLD1 and SLD2, which align to the Bayer residues of SUMO-1, were visualised using Swiss-Pdb Viewer. With the exception of the residues aligning to Q53 of SUMO-1, the side-chains of the Bayer residues are orientated towards the core of the predicted structure (Figure 6.6). Q53 of SUMO-1 aligns to E261 and T365, of SLD1 and SLD2 respectively. These residues contribute part of the α1 helix and the side chains are orientated away from the core. This is also seen for residues of *H. sapiens* Nip45 SLD2, supporting the hypothesis that the Rad60 SLDs fold in a similar manner to SUMO.

6.4.2 Comparative modelling suggests that the surface charge of Rad60 SLD2, but not SLD1, resembles SUMO

Although structurally similar, SUMO and ubiquitin molecules have different surface charges. If the ββαββαβ fold were to be assumed for SLD1 and SLD2 of Rad60, the

Figure 6.5: Comparative modelling suggests that Rad60 SLD1 and SLD2 can adopt a βαββαββ fold

Comparative modelling of Rad60 SLD1 and SLD2 with SUMO-1 was carried out using MODELLER. *H. sapiens* ubiquitin (1ubq.pdb), *H. sapiens* SUMO-1 (2asq.pdb), *H. sapiens* NIP45 SLD2 (2jxx.pdb) and the predicted structures of *S. pombe* Rad60 SLD1 and Rad60 SLD2 were visualised with Swiss-Pdb Viewer. **(A)** Comparative modelling suggests that Rad60 SLD1 and SLD2 can adopt a βαββαββ fold. The tertiary folds of Rad60 SLD2 were compared with ubiquitin, SUMO-1 and Nip45. α-helices and β-sheets are coloured in red and blue respectively. **(B)** Comparative modelling suggests that the surface charge of Rad60 SLD2, but not SLD1, resembles SUMO. Negative and positive regions are shown in red and blue, respectively.

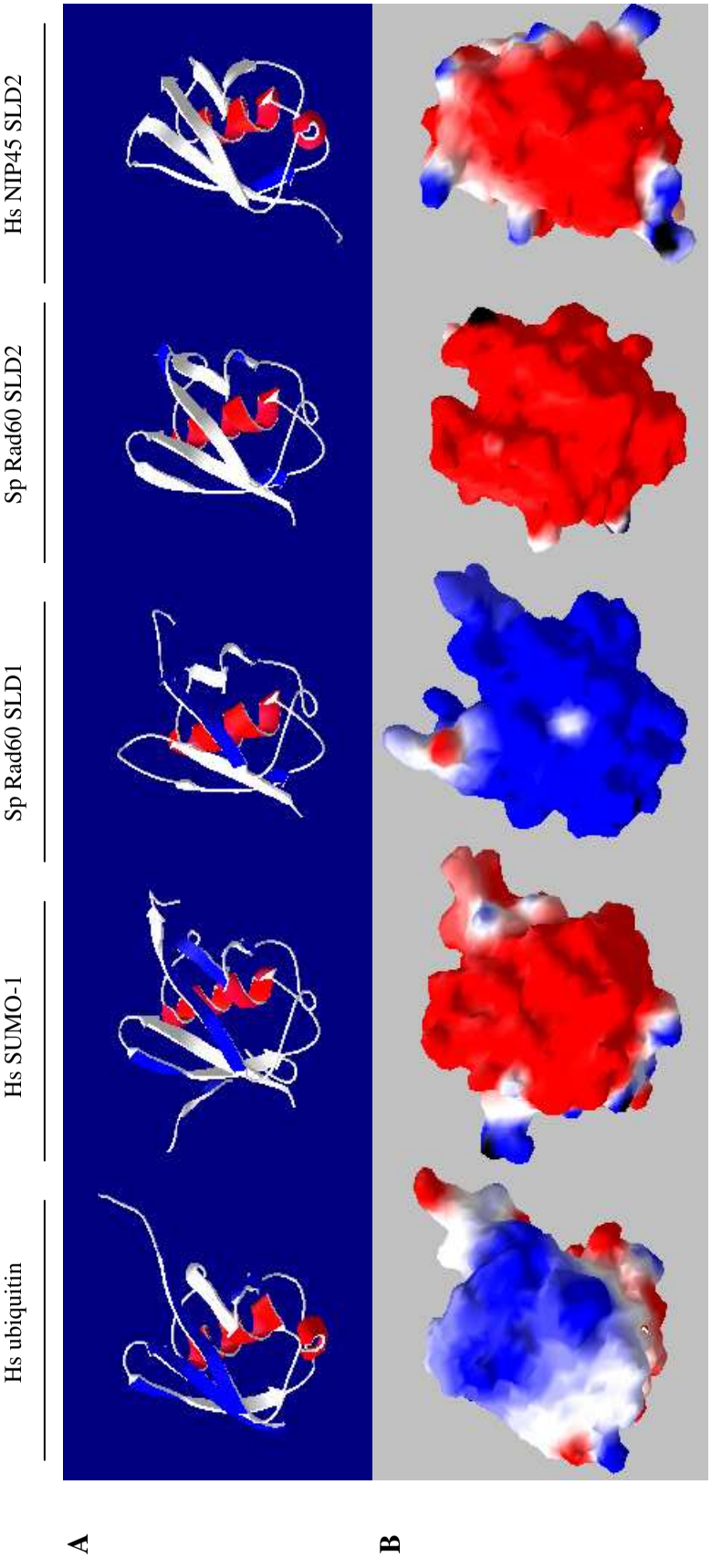

Figure 6.5: Comparative modelling suggests that Rad60 SLD1 and SLD2 can adopt a ββαββαβ fold

Figure 6.6: Comparing the position of Bayer residues within the predicted structures of Rad60 SLD1 and SLD2 highlights similarities with SUMO-1

Comparative modelling of Rad60 SLD1 and SLD2 with SUMO-1 was carried out using MODELLER. The position of Bayer residues within *H. sapiens* SUMO-1 (2asq.pdb), *H. sapiens* NIP45 SLD2 (2jxx.pdb) and the predicted structures for *S. pombe* Rad60 SLD1 and Rad60 SLD2 were visualised with Swiss-Pdb Viewer. α-helices and β-sheets are coloured in red and blue respectively. Amino acid side chains of the Bayer residues are shown in yellow. Side chains of residues aligning to Y51 of SUMO-1 are coloured in light blue.

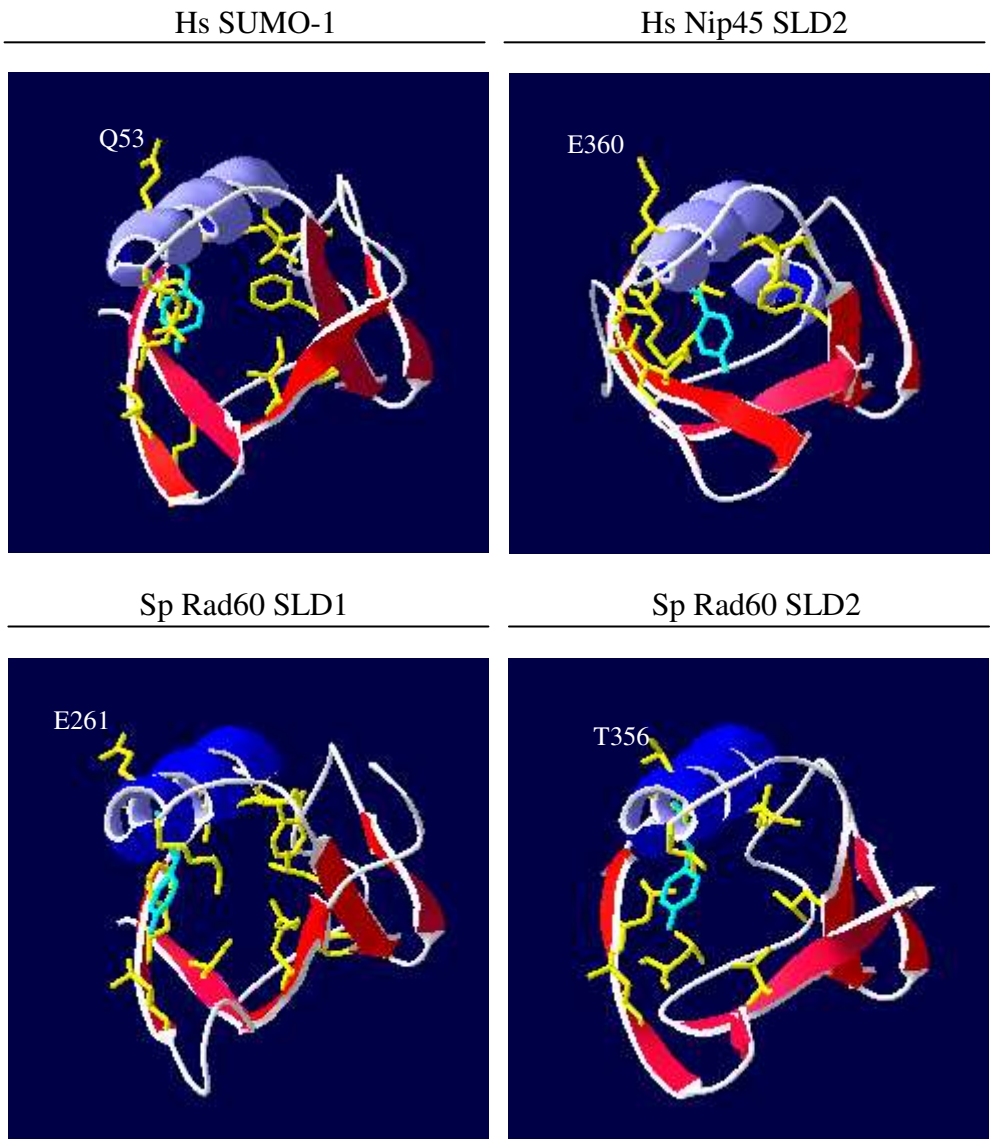

Figure 6.6: Comparing the position of Bayer residues within the predicted structures of Rad60 SLD1 and SLD2 highlights similarities with SUMO-1

surface charges of Rad60 SLD1 and SLD2 would differ (Figure 6.5B, lower panel). The overall surface charge of SLD2 is predominantly negatively charged and therefore more closely resembles that of SUMO than ubiquitin. In contrast the overall surface charge of SLD1 is largely positive and therefore shows more resemblance to ubiquitin than SUMO. This supports the observation that SLD1 of the RENI proteins lacks the large cluster of negatively charged residues at the C-terminus that is characteristic of SUMO-1 homologues (Section 6.3.3). This suggests that the two domains may have different biochemical functions.

6.5 Mutating residues, predicted to be of structural importance to SLD2, results in a DNA damage sensitive phenotype

Whilst the above data support the hypothesis that the Rad60 SLDs fold in a similar manner to SUMO, further structural evidence is required. In an attempt to support the *in silico* evidence, I have created a series of *S. pombe* strains carrying mutations in residues predicted to be important for maintaining the hydrophobic core of the ββαββαβ fold.

6.5.1 Selecting residues of structural importance in SLD2 for mutagenesis

SUMO and ubiquitin share the same ββαββαβ structure. The hydrophobic nature of residues shown to contribute to the hydrophobic core of SUMO is conserved in ubiquitin (Section 6.3.2) (Bayer, Arndt et al. 1998). Due to its extremely stable structure, ubiquitin was selected as a model protein for a study into 'stability-based selection' and the 'sequence requirements for packing in the hydrophobic core' (Finucane and Woolfson 1999). In the study by Finucane and Woolfson, ubiquitin was shown to become completely destabilised when seven core residues; I3, V5, I13, L15, V17, V26 and I30 were substituted with leucine. Leucine was selected on the basis that polyleucine cores are known to increase the conformational heterogeneity of proteins, thereby lowering their conformational specificity and stability (Finucane and Woolfson 1999). Further mutagenesis was carried out to introduce combinations of the five hydrophobic residues (I, L, V, F and M) to replace the 7 mutated residues on the sequence encoding the destabilised ubiquitin. Proteolysis based selection was used to recover protease resistant, and therefore stable, mutants. The proteins recovered revealed a strong consensus for near wild-type

sequences, indicating that the hydrophobic core of ubiquitin is naturally optimised for stability and plays an important role in the specification of the ubiquitin (ββαββαβ) fold. Given that this degree of core conservation extends to other proteins sharing the ββαββαβ fold, I have determined whether these residues were conserved in the SUMO-like domains of Rad60.

A ClustalW alignment of the Rad60 SLD1 and SLD2 protein sequence against the ubiquitin-like proteins *H. sapiens* ubiquitin, *S. pombe* ubiquitin, *H. sapiens* NEDD8, *H. sapiens* SUMO-1, and *S. pombe* SUMO (Pmt3) reveals that the hydrophobic nature of residues I3, V5, I13, L15, V17 and V26 is conserved between all proteins (Figure 6.7A). The hydrophobic nature of I30 is conserved amongst the ubiquitin and NEDD8 proteins, but in the SUMO proteins and SUMO-like domains is substituted for the 'SUMO-specific' tyrosine. The structure of the *H. sapiens* Nip45 SLD2 has recently been solved. When aligned with the proteins above, the same degree of conservation can be seen for Nip45 SLD2 as for SLD1 and SLD2 of Rad60 (Figure 6.7A). The position of the seven residues within the ββαββαβ fold of the predicted Rad60 SLD1 and SLD2 structures (Section 6.4) are conserved as compared to their position in the known structures of *H. sapiens* ubiquitin (1ubq.pdb), SUMO-1 (2asq.pdb) and Nip45 SLD2 (2jxx.pdb) (Figure 6.7B). Five of the seven residues mutated by Finucane and Woolfson (I3, I13, L15, V26, I30), align to positions identified by Bayer *et al* to be structurally important in SUMO-1 (L24, I34, F36, L47, Y51). Due to the fact that these residues contribute to the stability of the hydrophobic core, it is likely that they are important for hydrogen bonding (H-bonding). Using Swiss-Pdb Viewer to visualise H-bonding between residues in the ubiquitin structure, it can be seen that the residues selected by Finucane and Woolfson are important for H-bonding. With the exception of V17, these residues form H-bonds between each other (Figure 6.8A). V17 makes two H-bonds with M1. Finucane and Woolfson have shown that M1 (with I3, V5, I13, L15, V17, V26 and I30) forms part of a substructure in the hydrophobic core of ubiquitin. The conserved residues in SUMO-1, Rad60 SLD1 and SLD2 show the same bonding pattern. The H-bonding pairs of Rad60 SLD2 can be seen in figure 6.8A and are summarised in figure 6.8C. I have therefore selected to mutate residues in Rad60 SLD2 that

Figure 6.7: Residues required for the correct folding of ubiquitin are conserved in Rad60 SLD1 and SLD2

(A) A ClustalW alignment of the Rad60 SLD1 and SLD2 protein sequence against the ubiquitin-like proteins *H. sapiens* ubiquitin, *S. pombe* ubiquitin, *H. sapiens* NEDD8, *H. sapiens* SUMO-1, and *S. pombe* SUMO (Pmt3). Residues shown to disrupt the structure of ubiquitin when mutated (Finucane and Woolfson, 1998) are highlighted in yellow. Residues shown to contribute to the overall stability of the SUMO-1 protein (Bayer *et al* 1998) are highlighted (*).

A

```
Hs_Ubiquitin       ------------------------------------M---QIFVKTLTGKT-ITLEVEPSD  21
Sp_Ubiquitin       ------------------------------------M---QIFVKTLTGKT-ITLEVESSD  21
Hs_NEDD8           ---------------------------------------MIKVKTLTGKE-IEVDIEPTD  20
Hs_SUMO-1          --------MSDQEAKPSTEDLGD------KKEGEYI---KLKVIGQDSSE-IHFKVKMTT  42
Sp_SUMO            MSESPSANISDADKSAITPTTGDTSQQDVKPSTEHI---NLKVVGQDNNE-VFFKIKKTT  56
Hs_Nip45_SLD2      ---------------------------------TSQQL---QLRVQGKEKHQTLEVSLSRDS 359
Sp_Rad60_SLD1      ------------------------------------PNSNISLPRDWEAP-LFFKVKSN- 250
Sp_Rad60_SLD2      ------------------------------------I---TLLLRSSKSED-LRLSIPVDF 354
                                                       *          * *

Hs_Ubiquitin       TIENVKAKIQDKEGIPPDQ-QRLIFAGKQLEDGRTLSDYNIQKESTLHLVLRLRGG      76
Sp_Ubiquitin       TIDNVKSKIQDKEGIPPDQ-QRLIFAGKQLEDGRTLSDYNIQKESTLHLVLRLRGG      76
Hs_NEDD8           KVERIKERVEEKEGIPPQQ-QRLIYSGKQMNDEKTAADYKILGGSVLHLVLALRGG      75
Hs_SUMO-1          HLKKLKESYCQRQGVPMNS-LRFLFEGQRIADNHTPKELGMEEEDVIEVYQEQTGG      97
Sp_SUMO            EFSKLMKIYCARQGKSMNS-LRFLVDGERIRPDQTPAELDMEDGDQIEAVLEQLGG     111
Hs_Nip45_SLD2      PLKTLMSHYEEAMGLSGRK-LSFFFDGTKLSGRELPADLGMESGDLIEVW----G      419
Sp_Rad60_SLD1      QFRRVRIAYSERKK--VDN-VVLVFQNQRLWDYGTPKGAGMLKVDTRLVVHAYCHSD    303
Sp_rad60_SLD2      TVKDLIKRYCTEVKISFHERIRLEFEGEWLDPNDQVQSTELEDEDQVSVVLD         406
                    *  **  *   *         * *
```

B

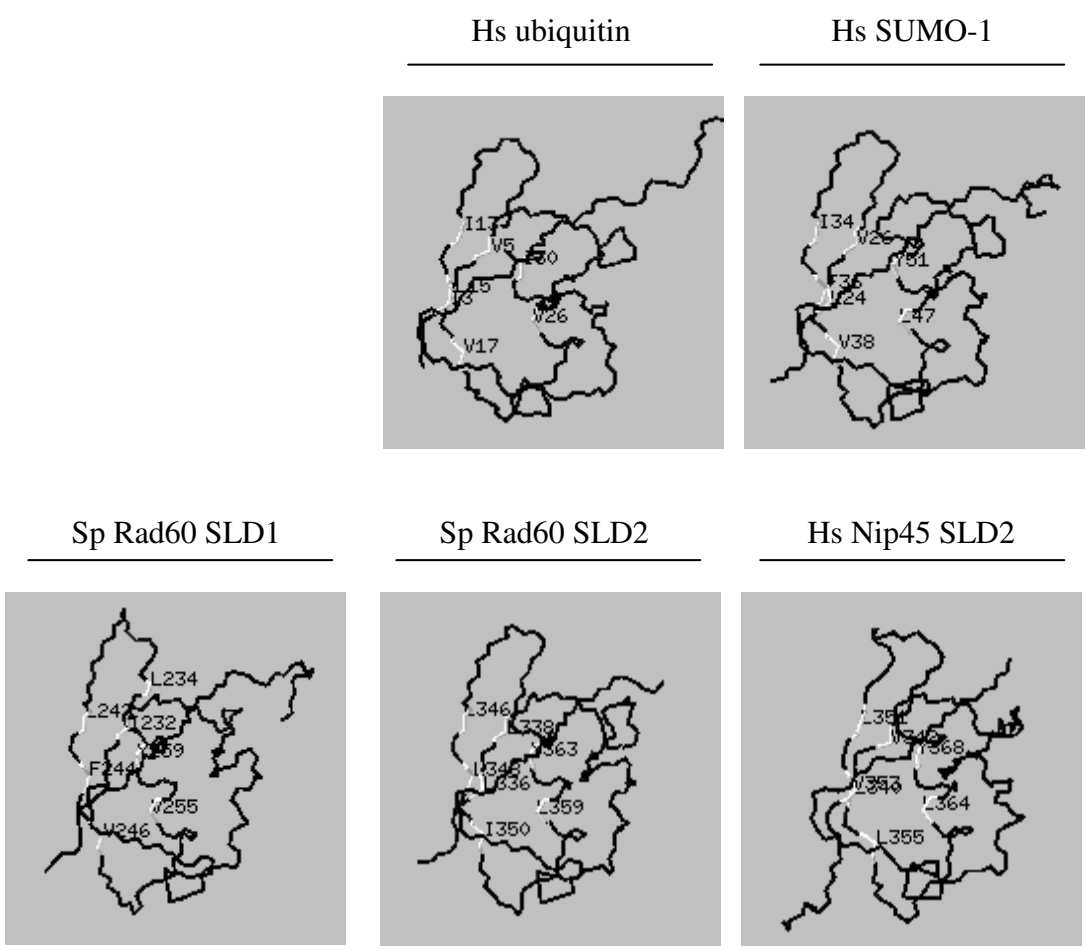

Figure 6.7: Residues required for the correct folding of ubiquitin are conserved in Rad60 SLD1 and SLD2

Figure 6.8: Selecting residues for mutagenesis of Rad60 SLD2

(A) Comparative modelling of Rad60 SLD2 with SUMO-1 was carried out using MODELLER. The hydrocarbon backbone of SUMO-1 and Rad60 SLD2 were visualised with Swiss-Pdb Viewer. The position of residues predicted to be of structural importance to SUMO-1 and Rad60 SLD2 are highlighted in red. Green lines indicate hydrogen bonding between the residues shown. **(B)** An example of a mutation designed to disrupt (L346G) and conserve (L346V) H-bonding between two residues (L346 and L338) in Rad60 SLD2. **(C)** Table summarising H-bonding between residues predicted to be of structural importance, and the mutations chosen to disrupt and conserve H-bonding.

A

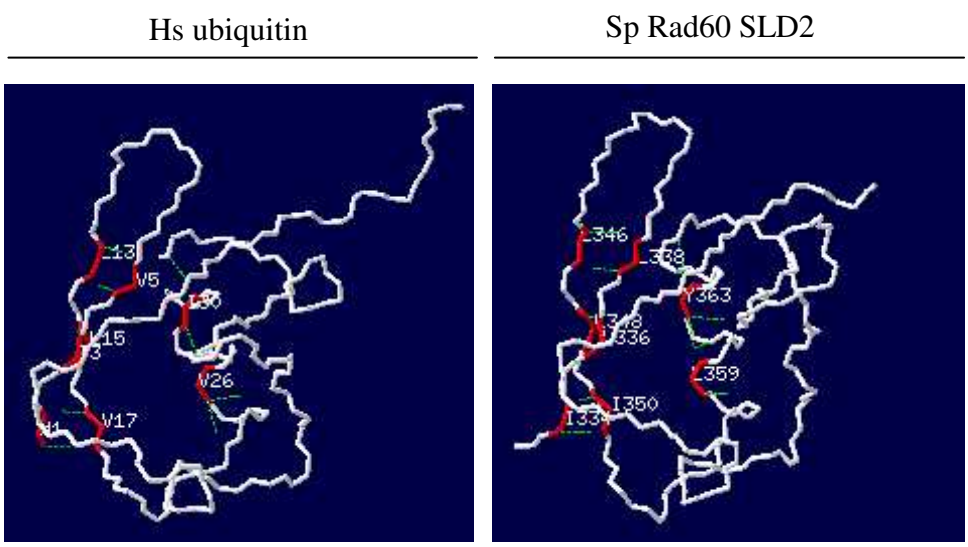

B

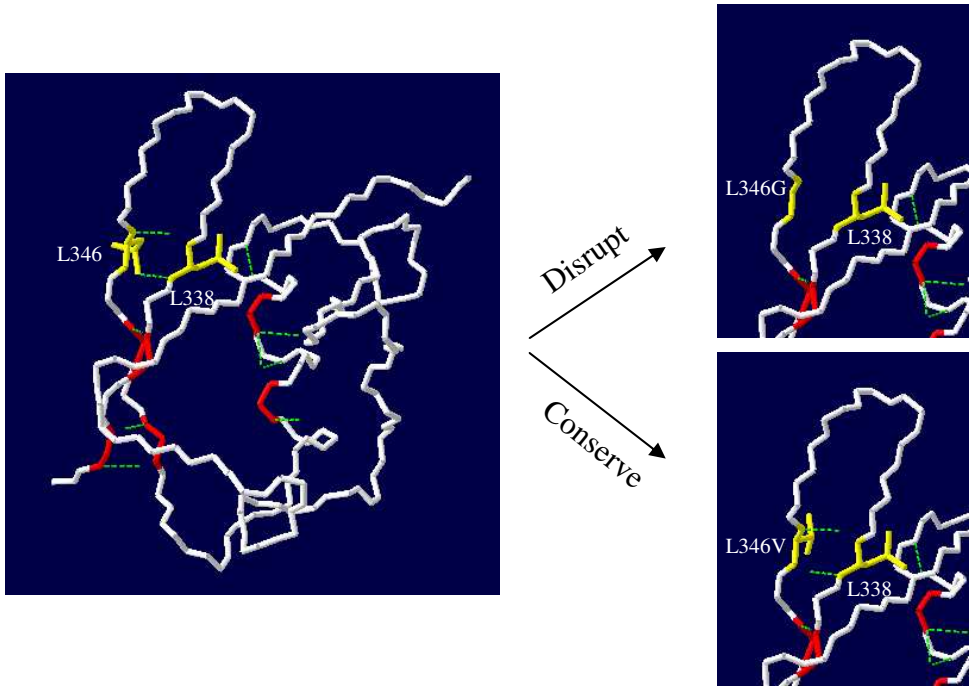

C

ubiquitin	SUMO-1	Rad60 SLD2	SLD2 H-bonding partner (s)	Conservative mutation	Disruptive mutation
M1	I22	I334	I350	I334L	I334G
I3	**L24**	L336	L348	L336V	L336G
F5	K25	L338	L346 (x2)	L338V	L338G
I13	**L34**	L346	L338 (x2)	L346V	L346G
L15	**F36**	L348	L336	L348V	L348G
V17	V38	I350	I334	I350L	I350G
V26	**L47**	L359	Y363	L359V	L359G
I30	**Y51**	Y363	L359	Y363F	Y363G

Figure 6.8: Selecting residues for mutagenesis of Rad60 SLD2

align to M1, I3, V5, I13, L15, V17, V26 and I30 of ubiquitin and compare the phenotype to the Rad60 SLD2 deletion mutant, *rad60-ct*.

6.5.2 Point mutations within the predicted ubiquitin-fold of SLD2 can result in a phenotype similar to that of the Rad60 SLD2 deleted strain, *rad60-ct*

To further test the hypothesis that Rad60 SLD2 can fold to resemble SUMO, strains carrying point mutations in the coding sequence for I334, L336, L338, L346, L348, I350, L359 and Y363 (corresponding to M1, I3, F5, I13, L15, L17, V26 and I30 of *H. sapiens* ubiquitin, respectively) were created. In an attempt to disrupt the SLD2 structure, residues of interest were mutated to glycine. When mutated to glycine, a small non-polar amino acid, the ability to form H-bonds at this position should be abolished. For example, L336 is shown to H-bond to L348. By introducing either an L336G or L348G mutation into SLD2, H-bonding between this pair should be lost. Prior to creating mutant strains the mutations designed to disrupt H-bonding were tested *in silico* using the mutate tool in Swiss-Pdb Viewer. An example of the mutation made for L346 is shown in figure 6.8B.

The RMCE system was used to replace the wild-type copy of *rad60* with a copy of the *rad60* gene carrying the point mutation of interest. Site-directed mutagenesis was used to introduce point mutations into the *rad60* coding sequence of the pAW8p*rad60* construct. Primers used for site-directed mutagenesis are listed in Table 6.2. The *rad60* base strain was transformed with the mutant pAW8p*rad60* constructs and RCME was achieved as described in section 2.1.5. For each construct, two 5-FOA resistant (*ura4*$^-$) isolates were selected and their phenotype tested. Given the HU and MMS sensitivity of the *rad60*-ct strain, spot tests were carried out and the sensitivity of the 5-FOA resistant colonies to HU and MMS examined at 30^{o}C. Of the mutations designed to disrupt H-bonding, and therefore destabilise the SLD2 structure, strains transformed with *rad60-L336G*, *rad60-I350G*, *rad60-Y363G* and *rad60-L359G* constructs show a wild-type sensitivity to HU and MMS (Figure 6.9iA). However, the sensitivity of the strains transformed with the *rad60-L348G*, *rad60-L338G* and *rad60-I334G* constructs is comparable with that seen for *rad60-ct*. At high doses of HU and MMS, cells transformed with the *rad60-L346G* construct is more sensitive than wild-type cells but less sensitive than *rad60-ct*. Following the initial

Table 6.2: Mutagenic primer sequences to mutate residues predicted to be important for maintaining the ββαββαβ fold of Rad60 SLD2

Mutation	Primer	Primer sequence (5'to 3')
L336V	L210 L211	F CAAACGTGTAAACTTATAACGGTGCTTTTG CGTTCGAG R CTCGAACGCAAAAGCACCGTTATAAGTTTACACGTTTG
L336G	L212 L213	F CAAACG TGTAAACTTATAACGGGGCTTTTGCGTTCG AG R CTCGAACGCAAAAGCCCCGTTATAAGTTTACACGTTTG
L348V	L214 L215	F GTGAGGATCTTCGTGTCTCAATACCCGTCG R CGACGGGTATTGAGACACGAAGATCCTCAC
L348G	L216 L217	F GTGAGGATCTTCGTGGCTCAATACCCGTCG R CGACGGGTATTGAGCCACGAAGATCCTCAC
L359V	L219 L220	F CGATTTCACTGTTAAAGATGTGATTAAGAGATATTGTACTG R CAGTACAATATCTCTTAATCACATCTTTAACAGTGAAATGG
L359G	L221 L222	F CGATTTCACTGTTAAAGATGGGATTAAGAGATATTGTACTG R CAGTACAATATCTCTTAATCCCATCTTTAACAGTGAAATGG
Y363F	L223 L224	F GATTTGATTAAGAGATTTTGTACTGAAGTAAAG R CTTTACTTCAGTACAAAATCTCTTAATCAAATC
Y363G	L225 L226	F GATTTGATTAAGAGAGGTTGTACTGAAGTAAAG R CTTTACTTCAGTACAACCTCTCTTAATCAAATC
L338G	L229 L230	F CGTGTATAACGTTGCTTGGGCGTTCGAGTAAGAG R CTCTTACTCGAACGCCCAAGCAACGTTATACACG
L346V	L231 L232	F GTAAGAGTGAGGATGTTCGTCTCTCAATACC R GGTATTGAGAGACGAACATCCTCACTCTTAC
L346G	L233 L234	F GTAAGAGTGAGGATGGTCGTCTCTCAATACC R GGTATTGAGAGACGACCATCCTCACTCTTAC
I350L	L235 L236	F CTTCGTCTCTCACTACCCGTCGATTTCAC R GTGAAATCGACGGGTAGTGAGAGACGAAG
I350G	L237 L238	F CTTCGTCTCTCAGGACCCGTCGATTTCAC R GTGAAATCGACGGGTCCTGAGAGACGAAG
I334L	L239 L240	F GCTCAAACGTGTAAACTTTTAACGTTGCTTTTGCG R CGCAAAAGCAACGTTAAAAGTTTACACGTTTGAGC
I334G	L241 L242	F GCTCAAACGTGTAAACTTGGAACGTTGCTTTTGCG R CGCAAAAGCAACGTTCCAAGTTTACACGTTTGAGC

Figure 6.9: HU and MMS sensitivity of Rad60 SLD2 mutants

(A) Cells transformed with *rad60*-I334G, *rad60*-L338G, *rad60*-L346 and *rad60*-L348G constructs are sensitive to HU and MMS. (Cells indicated in red were transformed with mutated *rad60* constructs but were later sequenced and found to be wild-type). (B) Cells transformed with *rad60*-I334L, *rad60*-L338V, *rad60*-L346V and *rad60*-L348V constructs show wild-type sensitivity to HU and MMS. Cells were grown at 30^{o}C in YE medium to mid-exponential phase. 10 μl of 10 fold serial dilutions were spotted onto YEA plates containing supplements at the indicated doses. Plates were incubated at (i) 30^{o}C, (ii) 36^{o}C and (iii) 25^{o}C for 72 hours and then photographed.

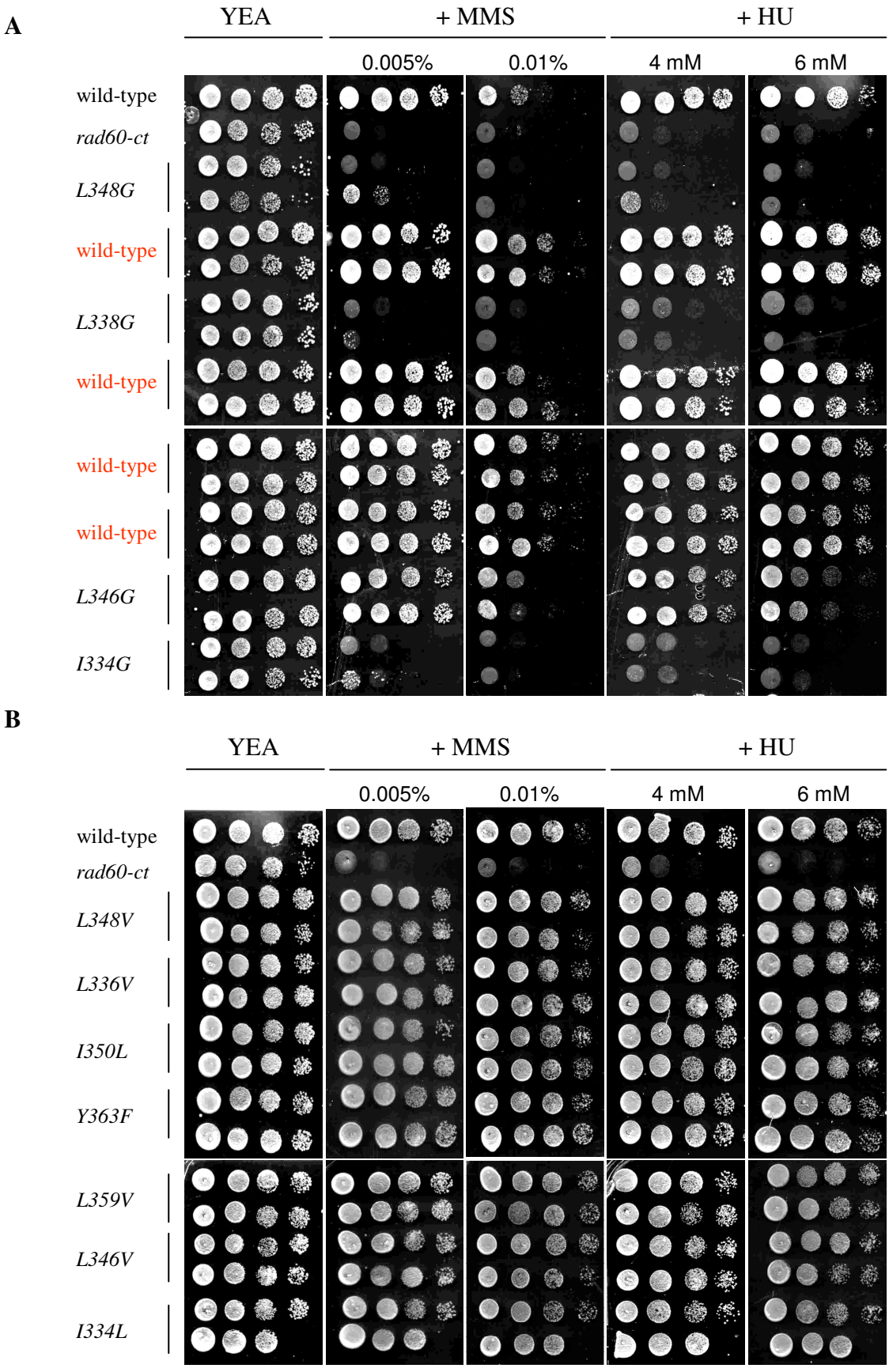

Figure 6.9i: HU and MMS sensitivity of Rad60 SLD2 mutants (30°C)

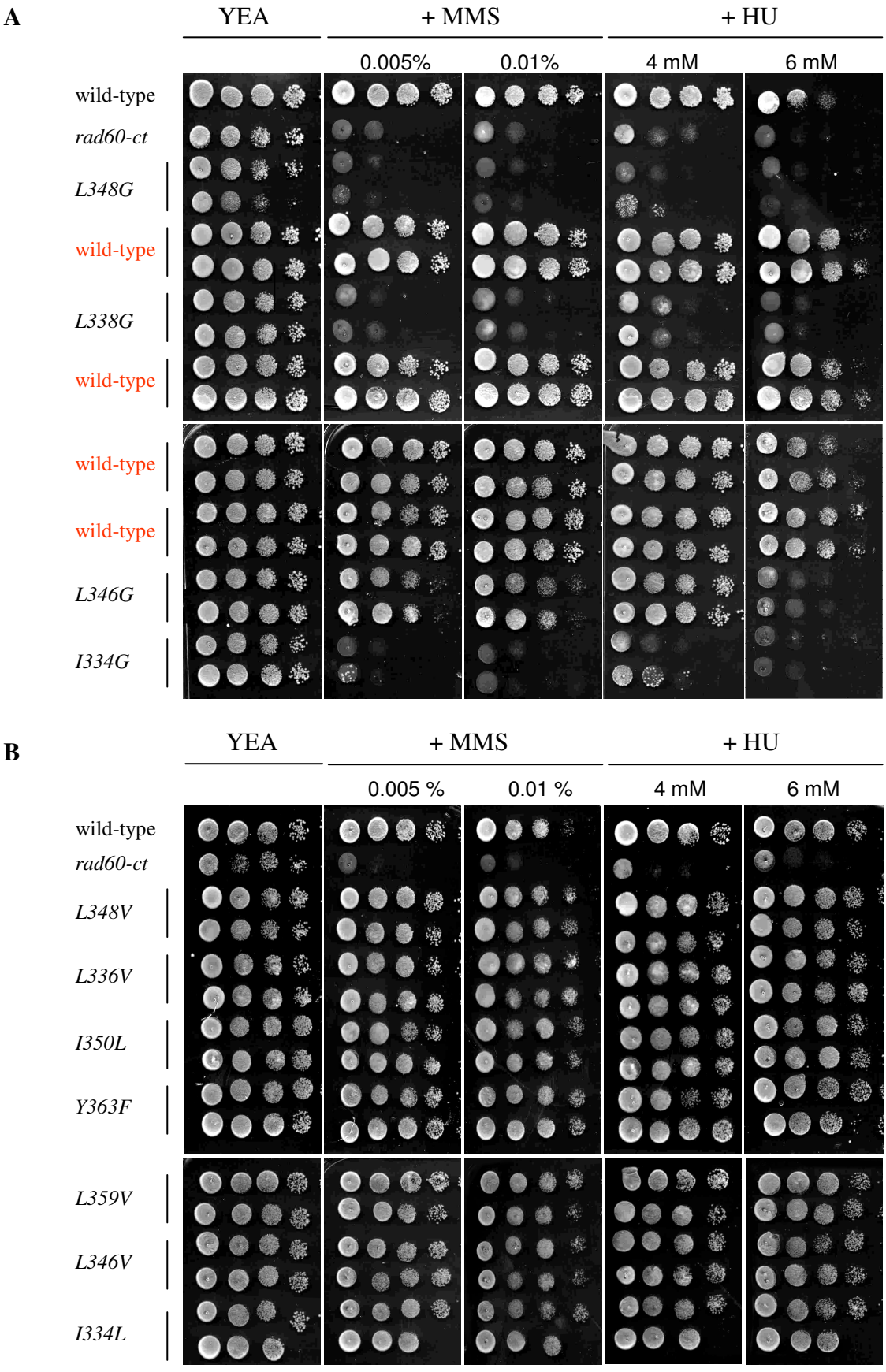

Figure 6.9ii: HU and MMS sensitivity of Rad60 SLD2 mutants (36°C)

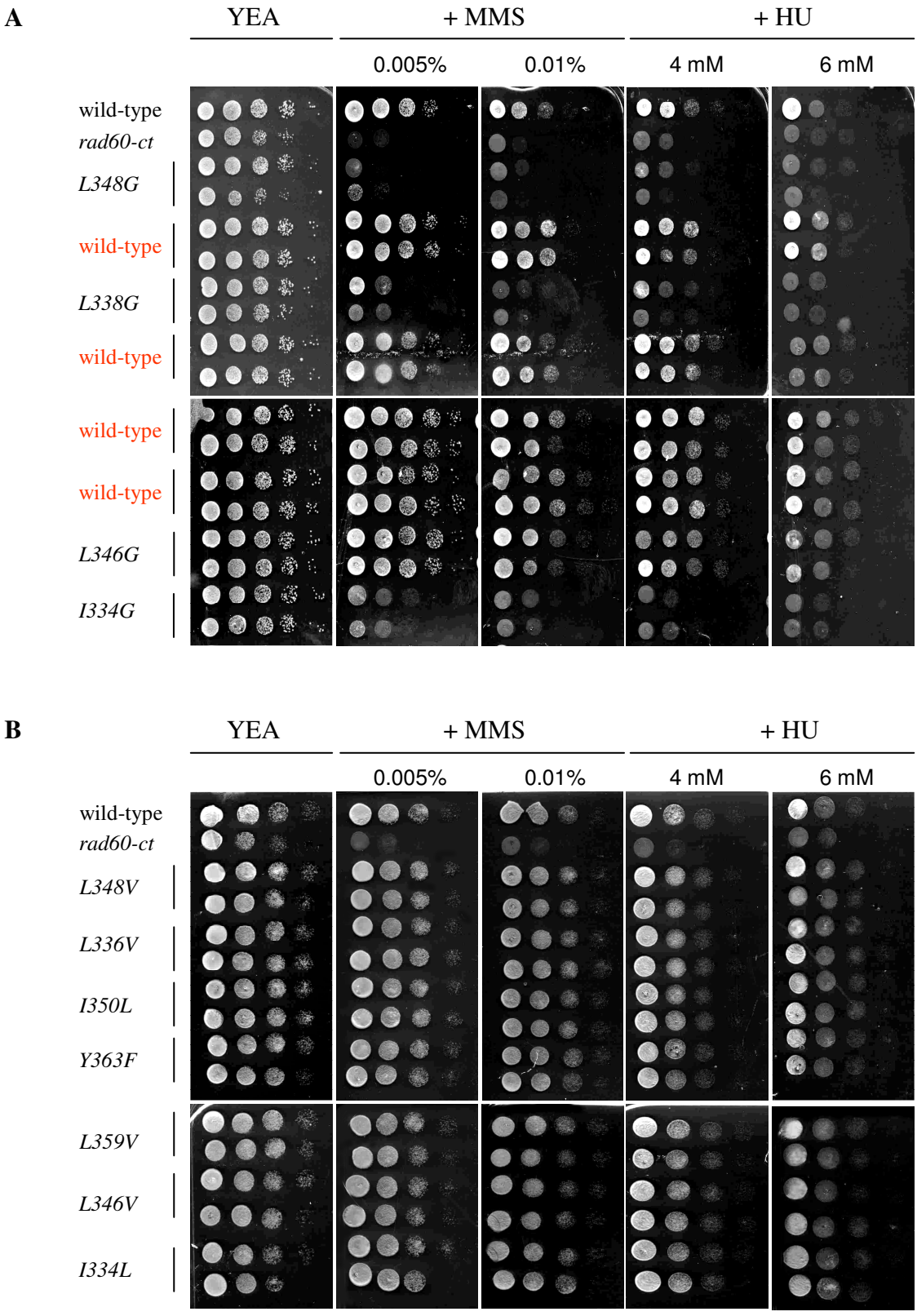

Figure 6.9iii: HU and MMS sensitivity of Rad60 SLD2 mutants (25°C)

screening, colony PCR with primers L41 and L40 was used to amplify *rad60*. Sequencing with primer L18 was used to confirm the mutations of interest had been successfully integrated. Unfortunately, of the strains tested, only those transformed the *rad60-L348G*, *rad60-L338G*, *rad60-I334G* and *rad60-L346G* mutations had been correctly integrated. The remaining strains were wild-type. Interestingly, the strains in which the mutation of interest had been correctly integrated via RMCE, were also the strains that showed an increased sensitivity to HU and MMS as compared to wild-type. This suggests that the single I334G, L338G and L348G mutations are sufficient to disrupt the structure, and therefore the function, of SLD2 to the same extent as deleting SLD2 altogether. The L346G mutation appears to partially disrupt the structure and function of the Rad60 SLD2. To test for temperature sensitive mutations the sensitivity of cells to HU and MMS was also tested at 37^{o}C (Figure 6.9iiA) and 25^{o}C (Figure 6.9iiiA). No difference in sensitivity was observed. The UV and IR sensitivity of cells transformed with the *rad60-I334G*, *rad60-L338G*, *rad60-L346G* and *rad60-L348G* was tested. As seen for the spot tests, the sensitivity of *rad60-I334G* and *rad60-L338G* to UV and IR is similar to that of *rad60-ct* cells. Additionally, *rad60-L346G* cells are more sensitive than wild-type cells but less sensitive than the *rad60-ct* cells. However, the *rad60-L348G* cells exhibit a much greater sensitivity than that seen by the *rad60-ct* cells (Figure 6.10 A, B). Watson *et al* suggest that following RMCE ~10% of 5-FOA resistant colonies will be wild-type (Watson, Garcia et al. 2008). However, given that two colonies were selected at random for each 'mutation', it seems highly likely that the *rad60-L336G*, *rad60-I350G*, *rad60-Y363G* and *rad60-L359G* mutations may be lethal.

To test that the phenotypes described above are the result of the glycine substitutions, specifically designed to disrupt the structure, further mutations were made. The residues of interest (I334, L336, L338, L346, L348, I350, L359 and Y363) were therefore mutated to a residue designed to conserve H-bonding to this site. For example, L336 is shown to H-bond to L348. By mutating L336 or L348 to a residue with a biochemically similar side chain, e.g valine, H-bonding between L336 and L348 should be conserved. Using the mutate tool in Swiss-Pdb, conservation of the H-bonds was first tested *in silico*. An example of the mutation made for L346 is shown in figure 6.8B and the mutations selected are summarised

Figure 6.10: UV and IR sensitivity of Rad60 SLD2 mutants

(A, B) *rad60*-I334G, *rad60*-L338G, *rad60*-L346 and *rad60*-L348G cells are sensitive to (A) UV and (B) IR. Cells were grown at 30^{o}C in YE medium to mid-exponential phase and irradiated with UV (A) or γ (B) rays at the indicated doses. Cells were plated on YEA and grown at 30^{o}C for ~72 hours. Colonies were counted and % survival was calculated.

A

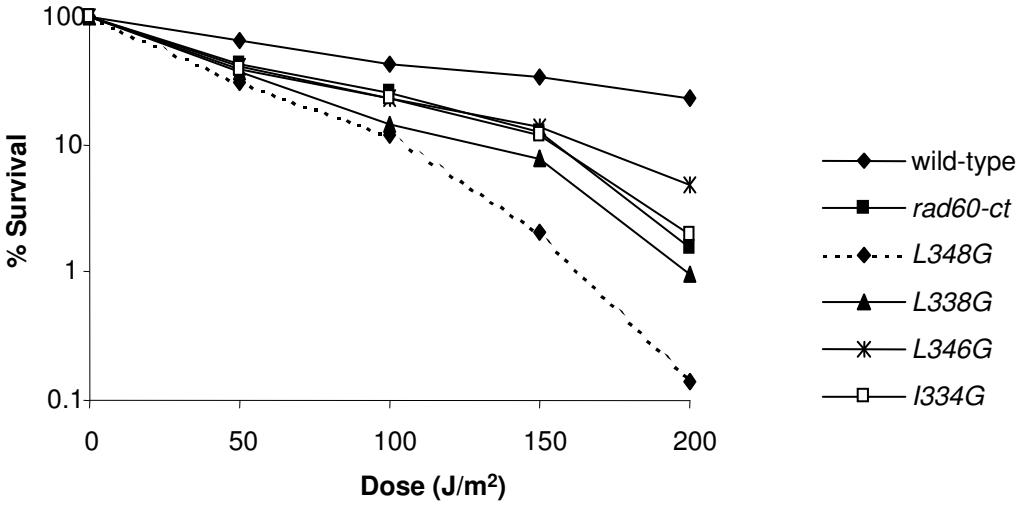

B

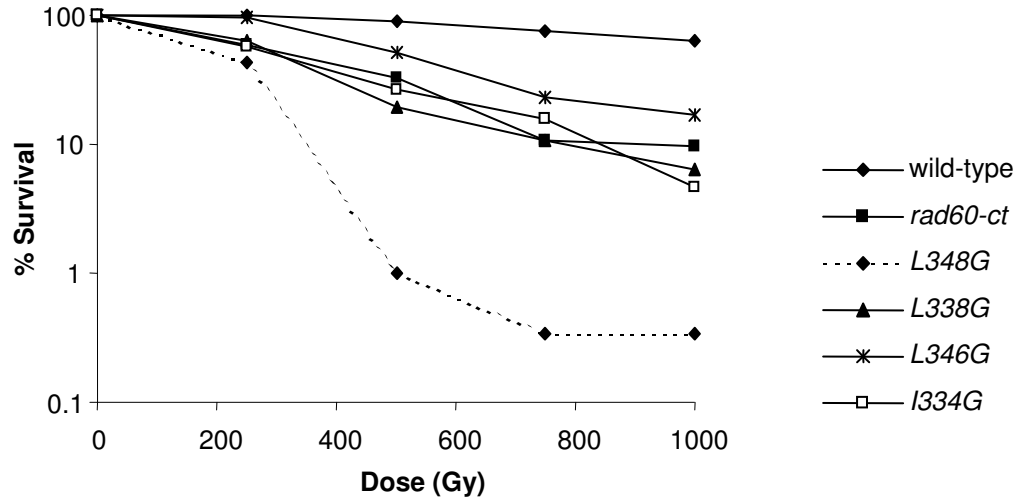

Figure 6.10: UV and IR sensitivity of Rad60 SLD2 mutants

in figure 6.8C. As predicted cells containing the conservative mutations all showed a phenotype similar to that of wild-type cells (Figure 6.9iB). As seen for the disruptive mutations, no difference in the sensitivity at 37^{o}C and 25^{o}C was observed. Unfortunately due to technical problems with mutagenesis, *rad60-L338V* was not tested.

6.6 Discussion

In previous chapters, I have shown the C-terminal SLDs of Rad60 to be important for Rad60 function. However, there is little evidence to show that the SLDs are in fact 'SUMO-like'. In this chapter I have carried out preliminary structure-function studies of the Rad60 SUMO-like domains to support the hypothesis that the Rad60 SLDs can fold to resemble SUMO.

I have previously shown a *rad60* mutant deleted for SLD2 (*rad60-ct*) to be defective in the response to DNA damage (Chapter 3). The SLD2 of Rad60 is also important for the correct localisation of the Rad60 protein (Chapter 5). It has recently been proposed that Rad60 contains three SBMs (Raffa, Wohlschlegel et al. 2006). SMB3 is located within the very C-terminal 6 amino acids of SLD2. A *rad60*-SBM3 mutant strain, containing valine to alanine substitutions in SBM3, showed no significant sensitivity to HU, MMS, UV and IR as compared to wild-type cells. This suggests that the phenotype observed for the SLD2 deletion strain (*rad60-ct*) is not a consequence of deleting SBM3. Similarly a *rad60-SBM1* showed no significant sensitivity to HU, MMS, UV and IR, as compared to wild-type cells. Interestingly, a *rad60-SBM2* mutant is more sensitive to HU, MMS, UV and IR than wild-type cells, but less sensitive than the *rad60-ct* mutant. Visualisation, with Swiss-Pdb Viewer, of the Rad60 SBM2 and SBM3 residues in the predicted structures of SLD1 and SLD2 respectively, suggests that the amino acid residues of SBM2 are not located on the surface of SLD1 (data not shown). Rather, the side chains point towards the hydrophobic core. This is in contrast to the residues of SBM3, which are predicted to be surface residues and, therefore, more likely to contribute to a binding surface for interaction with SUMO. The VVLV motif of SBM2 consists of residues 268-271. L269 aligns to one of the residues identified to be of structural importance in SUMO-1 (Bayer, Arndt et al. 1998). Additionally, F272, immediately after SBM2 also aligns to a Bayer residue. It is therefore

likely that the phenotype observed for the *rad60-SBM2* mutant (V268A, V270A) is a consequence of disrupting the structure of SLD1. Raffa *et al* have suggested that each SBM makes an independent contribution to the homodimerisation of Rad60 via the SUMO-like domains (Raffa, Wohlschlegel et al. 2006). For that reason, I would expect a triple SBM knockout strain to be phenotypically similar to the SLD2 deletion strain *rad60-ct*. Due to time constraints this experiment was not carried out.

Ubiquitin-like domain proteins, such as Rad23 and Dsk2, interact with the proteosome, suggesting that the ubiquitin-like domains act to functionally mimic ubiquitination (Funakoshi, Sasaki et al. 2002; Rao and Sastry 2002; Lambertson, Chen et al. 2003). Unlike for the ubiquitin-like domain proteins, there is little functional evidence to suggest a SUMO-like role for the RENi family of SUMO-like domain proteins. However, previous studies on *S. cerevisiae* Esc2 and *S. pombe* Rad60 suggest a functional importance of SLD1. A region containing SLD1 of *S. cerevisiae* Esc2 and 80 amino acids in the N-terminal fragment has been shown to be sufficient to supply Esc2 function in targeted silencing (Andrulis *et al*, 2004). In addition, the *S. pombe* mutants *rad60-1* (K263E) and *rad60-3* (F272V), which are defective in DSB repair, contain point mutations in SLD1 that align to Q55 and F66 of *H. sapiens* SUMO-1. Residues Q55 and F66 of SUMO-1 have been listed by Bayer *et al* as structurally important residues that contribute to the formation of the hydrophobic core of the ββαββαβ fold (Bayer, Arndt et al. 1998). With the exception of Q53 and Q55, the hydrophobic nature of the Bayer residues is conserved in ubiquitin (Bayer, Arndt et al. 1998). For example, isoleucines, leucines and valines are commonly substituted for one another. The hydrophobic nature of residues aligning to the Bayer positions in SUMO-1 is better conserved in SLD2 than SLD1. Interestingly, Y51 of SUMO-1 is conserved between almost all SUMO-1 homologues. Since this is not the case in ubiquitin proteins, this may suggest a possible SUMO-specific residue. Residues aligning to Y51 are better conserved in SLD2, than SLD1 of RENi proteins. However Y51 is conserved in both Rad60 SLD1 and SLD2. In proteins of the RENi family, the C-terminal region of SLD2 contains a cluster of negatively charged amino acid residues, which is indicative of a SUMO-like protein rather than a ubiquitin-like protein. The negative surface patch formed by these residues has been suggested to form a SUMO-

typical interaction surface (Bayer, Arndt et al. 1998). In proteins of the RENi family, three factors suggest that SLD2 is more 'SUMO-like' than SLD1; 1) SLD2 has a greater sequence identity to SUMO, 2) SLD2 has a cluster of negatively charged amino acid residues (indicative of a SUMO-like protein) and 3) residues aligning to the SUMO specific residue, Y51, are better conserved in SLD2 than SLD1. This suggests that of the two SLDs of the RENi family SLD2 is more likely to adopt a SUMO-like fold and therefore function.

The biological importance of SUMO modification is often mediated by proteins that are able to recognise and interact with SUMO via their SBMs. The SBM-SUMO interaction is stabilised by H-bonds between the SBM sequence and the SUMO surface side chains. The SBM binding surface of SUMO-1 is formed by a deep groove that is lined with hydrophobic and aromatic patches consisting of residues I34, H35, F36, V38, L47, Y51 and E33 (Song, Zhang et al. 2005). The biochemical nature of these residues is largely conserved in both SLD1 and SLD2. Interestingly, F36 of SUMO-1 aligns to F244 of Rad60 SLD1. Substitution of F244 in the Rad60 SBM-binding pocket (F244A) abolishes the interaction between Rad60 and the STUbL, Rfp1 (Prudden, Pebernard et al. 2007). Since Rfp1 contains an SBM, this suggests that if the SLDs do fold to resemble SUMO they may function in a SUMO-specific manner by interacting with proteins containing an SBM.

Comparative modelling of Rad60 SLD1 and SLD2 with SUMO-1 has strengthened the hypothesis that the SLDs of Rad60 are able to fold to resemble SUMO. However, if the ββαββαβ fold is assumed, the surfaces of Rad60 SLD1 and SLD2 would have opposite overall charges. This could indicate either an intra-molecular interaction between the SLDs or an inter-molecular interaction between domains in two different Rad60 molecules. Given that Rad60 has been shown to homodimerise (Raffa, Wohlschlegel et al. 2006), it is more likely that the opposing surface charges could contribute to an inter-molecular interaction between the two SLDs.

In an attempt to support the *in silico* evidence for folding of the Rad60 SLDs, residues predicted to be of key importance in maintaining the hydrophobic core of the predicted

SLD2 structure were mutated. Cells containing I334G, L338G, L346G and L348G substitutions in SLD2 are more sensitive to HU, MMS, UV and IR than wild-type cells. *rad60*-L346G cells are less sensitive that the Rad60 SLD2 deletion mutant, *rad60-ct*, suggesting that the L346G may partially disrupt the structure and function of the Rad60 SLD2. *rad60-I334G*, and *rad60-L338G* cells show a sensitivity comparable with the *rad60-ct* cells. This suggests that the single I334G and L338G mutations are sufficient to disrupt the structure, and therefore function, of SLD2 to the same extent as deleting SLD2 altogether. *rad60-L348G* cells exhibit a much greater sensitivity than that seen by the *rad60-ct* cells. This may suggest that this mutation alters the structure of SLD2 in such a way that the SLD2-independent role of Rad60 protein is affected. Preliminary results of cells carrying mutations in the corresponding residues of SLD1 indicate similar phenotypes (F-X Ogi, University of Sussex-data not shown). The *rad60-L336G*, *rad60-I350G*, *rad60-Y363G* and *rad60-L359G* mutations failed to be introduced into the *S. pombe* genome via RMCE. This suggests that these muations may not be viable. Additionaly, the corresponding residues of SLD1 have also failed to be isolated following RMCE (F-X Ogi, University of Sussex-data not shown). To confirm that these mutations are infact lethal, the substitutions should be introduced into the heterozygous diploid *rad60* base strain (Section 3.5) and the viability tested following sporulation. Due to time constraints this was not carried out.

Interestingly, of the substitutions corresponding to the mutant phenotypes, L346 and L348 of SLD2 align to I34 and F36 of SUMO-1. These residues have been shown to contribute to the SBM-binding pocket of SUMO-1. An F244A substitution in the predicted SBM-binding pocket of SLD1 abolishes the interaction between Rad60 and the STUbL, Rfp1 (Prudden, Pebernard et al. 2007). This may suggest that in the *rad60-L346G* and *rad60-L348G* cells, Rad60 is unable to interact with an unknown regulatory protein through interaction with its SBM. This raises the possibility that the phenotypes observed maybe due to a loss of protein-protein interaction, rather than destabilisation of the hydrophobic core of the SLD.

Whilst the above data support the hypothesis that the Rad60 SLDs fold in a similar manner to SUMO, structural evidence is ultimately required to confirm this. As part of an undergraduate project, His-tagged Rad60 SLD2 (aa 333-406) was expressed and purified from *E. coli.* When the mutations corresponding to I334G, L338G, L346G and L348G point mutations were introduced into the Rad60 SLD2 coding sequence, the levels of all mutant proteins in cells was dramatically reduced compared to the levels of wild-type SLD2. Additionally, mutant proteins were found predominantly in the insoluble fraction, unlike the wild-type SLD2 protein. (T. Ahadome and F. Z. Watts, University of Sussex-data not shown). This is consistent with the belief that these mutants contain an unstable SLD2 and further supports the hypothesis that the Rad60 SLDs can fold in a SUMO-like manner.

CHAPTER 7
DISCUSSION

Ubiquitin and ubiquitin-like proteins are post-translational modifiers that share a characteristic ββαββαβ fold. The best-defined role for ubiquitin conjugation is the targeting of proteins for degradation via the proteasome (Wilkinson 1995; Hochstrasser 1996). SUMO is one of a number of UBLs, sharing ~18% sequence identity with ubiquitin. SUMO is covalently attached to lysine residues of target proteins in a post-translational modification process that is similar to, but distinct from, ubiquitination. Unlike ubiquitin, SUMO does not appear to have a role in protein degradation. Instead it has been shown to have roles in facilitating protein-protein interactions, altering protein localisation and in modulating protein activity. Analysis of protein databases indicates that ubiquitin-like sequences can also be found fused to other open-reading frames. The ubiquitin-fusion proteins, act to functionally mimic ubiquitination by interacting with the proteasome (Funakoshi, Sasaki et al. 2002; Rao and Sastry 2002). During the course of this project a family of SUMO-like domain proteins was identified and termed the RENi family after its best-studied members *S. pombe* Rad60, *S. cerevisiae* Esc2 and *M. musculus* Nip45. Rad60, Esc2 and Nip45 are all ~400 amino acids in length and share two C-terminal SLDs. Unlike SUMO, the SUMO-like domains of the RENi proteins do not have the C-terminal diglycine motif required for covalent attachment to target proteins, suggesting that the SLD2 of these proteins is likely to function as a protein-protein interface and is not conjugated to other proteins.

The gene encoding the essential Rad60 protein was first identified in a screen to identify *S. pombe* mutants hypersensitive to MMS and synthetically lethal with *rad2*, suggesting a role in recombinational repair (Morishita, Tsutsui et al. 2002). Rad60 has been shown to physically and genetically interact with the Smc5/6 complex. Following replication stress, Rad60 is hyperphosphorylated by the checkpoint kinase Cds1 resulting in nuclear delocalisation (Boddy, Shanahan et al. 2003). Rad60 function is required after release from replication arrest, suggesting that Rad60 re-enters the nucleus upon HU release to carry out a late repair role in concert with the Smc5/6 complex (Ampatzidou, Irmisch et al. 2006;

Miyabe, Morishita et al. 2006). Three previously characterised temperature sensitive mutants, *rad60-1* (K263E), *rad60-3* (F272V) and *rad60-4* (T72A, I232S, Q250R, K312N) contain point mutations that map to SLD1. This suggests that this domain is of importance for Rad60 function (Morishita, Tsutsui et al. 2002; Boddy, Shanahan et al. 2003). To determine whether the SLDs are required for cell viability and/or contribute to Rad60 function, domain deletion mutants were created and their phenotypes analysed.

To test the importance of SLD1 for Rad60 function, the RMCE system (Watson, Garcia et al. 2008)was utilised to replace the genomic copy of *rad60* with a copy of *rad60* deleted for SLD1 (aa 228-307). Although the previously published *rad60-1*, *rad60-3* and *rad60-4* strains, carrying mutations within SLD1, are viable, it was possible that deletion of the entire domain would prove to be lethal for cells. For this reason the *rad60-SLD1Δ* allele was introduced into a heterozygous diploid *rad60* base strain. Following sporulation and tetrad dissection, only two spores germinated, implying that deletion of SLD1 is lethal. Furthermore, the heterozygous diploid *rad60-SLD1Δ* cells showed a severely reduced sporulation frequency (~<1% forming zygotes), as compared to the diploid base strain. Analysis of the hypomorphic mutants *nse1-1*, *nse2-1* and *nse3-1* of the Smc5/6 complex has indicated a role for the Smc5/6 complex in meiosis (Pebernard, McDonald et al. 2004). The SLD1 deletion result implies that Rad60 also has a role in meiosis.

Unlike the null and SLD1Δ mutants, a *rad60* mutant deleted for SLD2 (*rad60-ct*) is viable. Initial characterisation of the *rad60-ct* cells showed a phenotype reminiscent of the *smc6-X* and *smc6-74* mutants (Lehmann 1995; Verkade, Bugg et al. 1999). *rad60-ct* cells are elongated and are sensitive to UV, IR, HU and MMS as compared to wild-type cells. This implies that SLD2 is not required for the essential function of Rad60 but is required for the response to DNA damage. Rad60 is known to associate with the Smc5/6 complex and like the *rad60-1* and *rad60-3* mutants, *rad60-ct* is synthetically lethal with both *smc6-X* and *smc6-74* (Morishita, Tsutsui et al. 2002; Boddy, Shanahan et al. 2003). Additionally, expression of *rad60* but not *rad60-ct* in the *smc6-X* background can suppress the sensitivity of *smc6-X* to HU and MMS, suggesting that suppression is dependent on the SLD2 of Rad60. As is the case for other mutants defective in the Smc5/6 complex, *rad60-ct* is

epistatic with *rhp51-d*. This implies a role for *rad60* in homologous recombination that is dependent on SLD2. The *smc6* mutants are also sensitive to 4NQO. In normal cells DNA adducts caused by 4NQO are removed by the NER pathway. However, the *smc6* mutants are not epistatic to mutants in the conserved NER pathway. Instead Smc6 is thought to be involved in UVER, a secondary pathway that involves the *rad2* and *rhp51* genes (Lehmann 1995; Murray, Lindsay et al. 1997). Although *rad60-ct* and *rad60-1* show a similar degree of sensitivity to UV, IR and MMS, unlike *rad60-1*, *rad60-ct* cells are sensitive to 4NQO. This suggests that the functional interaction shared between Rad60 and Smc5/6 may be in the UVER pathway and is SLD2 dependent. Presumably a *rad60-ct rad2-d* mutant would be lethal.

Although Rad60 is a nuclear protein under wild-type conditions, a C-terminally GFP-tagged strain showed that deletion of SLD2 disrupts the nuclear localisation of Rad60. This raises the possibility that the role of SLD2 is in protein localisation. Although I have been unable to confirm this phenotype with either N-terminally tagged strains, or immunofluorescence with anti-Rad60 antibodies, this observation corresponds well with the sensitivity of the strain to DNA damaging agents. Specifically, if Rad60 is not localised to the nucleus it presumably cannot fulfil its DNA repair role. Rad60 has been shown to exit the nucleus both upon treatment of cells with HU and by over-expressing *cds1* (Boddy, Shanahan et al. 2003). HU causes replication forks to stall by causing dNTP starvation resulting in a replication checkpoint arrest that leads to the activation of the effector protein kinase Cds1. Cds1 acts to stabilise stalled forks by enforcing the cell cycle checkpoint that prevents mitosis during a replication arrest. With single stranded regions and DNA ends in close proximity to homologous sequences, stalled forks should be ideal substrates for recombination. It has been suggested that in the event of a stalled fork, Cds1 is activated to phosphorylate and concomitantly delocalise Rad60 from the nucleus to prevent HR (Boddy, Shanahan et al. 2003).

There are two possible explanations as to why the deletion of SLD2 disrupts nuclear localisation; 1) Rad60 is continuously exported from the nucleus, or 2) Rad60 cannot be retained in the nucleus. The possibility that mis-localisation of the truncated Rad60 is the

result of continuous *cds1* activation was tested. If this were the case, Rad60-ct would be nuclear in a *cds1-d* background. However, in the *cds1-d* background Rad60-ct is pan-cellular. This suggests that mis-localisation of Rad60-ct is not the result of constitutive Cds1 activation. By the same argument, the mis-localisation of Rad60-ct is not a consequence of constitutive Chk1 activation. Interestingly, in *chk1-d* cells, full-length Rad60 is not localised to the nucleus. Delocalisation of Rad60 from the nucleus is believed to be S-phase specific and is not observed in G2 cells treated with IR (Boddy, Shanahan et al. 2003). This suggests that Chk1 may have a role in maintaining Rad60 in the nucleus.

Since the mis-localisation of Rad60-ct is not the result of constitutive Cds1 or Chk1 activation, it seems that SLD2 is required for the correct nuclear localisation of Rad60. Another possibility explored was that Rad60 SLD2 has an NLS-like property that when masked, results in delocalisation from the nucleus. Usng over-expression constructs, provision of an NLS to the Rad60-ct protein is capable of restoring wild-type localisation. However, expression of the Rad60-ctNLS protein in *rad60-ct* cells is unable to rescue the DNA damage sensitive phenotype of the *rad60-ct* cells and instead has a dominant negative effect in both wild-type and *rad60-ct* cells. Since a *rad60-4* mutant unable to delocalise from the nucleus is proficient for the survival of UV-induced DNA damage (Boddy, Shanahan et al. 2003), it is unlikely that the dominant-negative phenotype observed is purely a consequence of Rad60-ctNLS being unable to delocalise from the nucleus following replication stress. Rather, it suggests that SLD2 is required not only to localise Rad60 to the nucleus for its role in the DNA damage response, but also for the DNA damage response itself. Unfortunately, over-expressed full-length Rad60 failed to delocalise from the nucleus following HU treatment. This meant that the ability of the over-expressed Rad60-ctNLS protein to delocalise from the nucleus following replication stress could not be confirmed. Typically NLSs are found on the exposed surface of the protein and consist of a few short sequences of positively charged residues. Given that Rad60 does not contain a recognised NLS and that SLD2 alone is unable to localise GFP to the nucleus, it is likely that SLD2 maintains nuclear localisation by facilitating protein-protein interactions or as a result of being modified itself.

The SLDs of Rad60 are clearly important for its function. Despite this, there is little evidence to suggest that the SLDs are in fact 'SUMO-like'. Proving a SUMO-like function is problematic given that SUMO itself does not have a clearly defined role. For this reason a structural perspective was taken. Despite the low sequence identity shared by SUMO and the Rad60 SLDs, there is significant conservation of the biochemical nature of the amino-acid side chains. In proteins of the RENi family SLD2 has a) a greater sequence identity to SUMO than SLD1, b) a cluster of negatively charged amino acid residues, indicative of a SUMO-like protein and not found in SLD1 and c) a more highly conserved residue aligning to the SUMO specific residue, Y51 than SLD1. This suggests that of the two SLDs of the RENi family, SLD2 is more likely to adopt a SUMO-like structure and therefore function. However, comparative modelling suggests that both SLD1 and SLD2 can adopt the characteristic ββαββαβ fold shared by UBLs. The *S. pombe* mutants *rad60-1* (K263E) and *rad60-3* (F272V) contain point mutations in SLD1 that align to Q55 and F66 of *H. sapiens* SUMO-1. Q55 and F66 of SUMO-1 have been identified as structurally important residues that contribute to the formation of the hydrophobic core of the ββαββαβ fold (Bayer, *et al* 1998). This suggests that disrupting the hydrophobic core of the SLDs may affect Rad60 function. A novel 'recombinase-mediated cassette exchange' system was used to mutate residues in SLD2 predicted to help maintain the hydrophobic core of the ββαββαβ fold. The DNA damage sensitive phenotype of L348G, L338G, L346G and I334G substitutions support the hypothesis that the Rad60 SLD2 is able to fold in a manner similar to SUMO. Corresponding mutations have been introduced into SLD1 and their phenotypes analysed (F-X Ogi, University of Sussex). This provides further support for the ββαββαβ fold of the SLDs. Together**,** the sequence analysis, comparative modelling and mutation studies support the hypothesis that the Rad60 SLDs adopt a SUMO/ubiquitin-like fold. However, structural evidence is ultimately required to confirm this. Recombinantly expressed His-tagged SLD2 can be purified in mg quantities and is currently being used for crystallography trials in an attempt to elucidate the structure (F. Z. Watts, T. Freche and B. Vintner, University of Sussex). With the intention of carrying out stability studies, mutations corresponding to those resulting in DNA damage sensitive phenotypes (Chapter 6.5) were introduced into the SLD2 coding sequence cloned into the *E.coli* expression vector pET15b. The I334G, L338G, L346G and L348G point mutations resulted in

dramatically reduced levels of protein as compared to the levels of wild-type SLD2 that could be obtained (T. Ahadome and F. Z. Watts, University of Sussex). Although this prevents structural/folding analysis of the mutated protein, it is further suggestive that the Rad60 SLDs fold in a SUMO-like manner and is consistent with the hypothesis that the point mutants are able to disrupt the hydrophobic core and hence destabilise SLD2.

If Rad60 SLD2 is really SUMO-like in both structure and function, I would expect substitution of SLD2 with authentic Pmt3 (SUMO) to restore nuclear localisation of Rad60 and result in cells with a wild-type response to DNA damaging agents. As is the case when an NLS is provided at the C-terminal of Rad60-ct, replacement of SLD2 with SUMO is able to restore wild-type localisation to Rad60-ct but is unable to rescue the DNA damage sensitive phenotype of *rad60-ct* cells. In addition, expression of Rad60-ctPmt3 in both wild-type and *rad60-ct* cells has a dominant-negative effect. This suggests that once in the nucleus, SUMO (Pmt3) cannot functionally substitute for Rad60 SLD2.

Rad60 has recently been identified as a potential target of the Slx8-Rfp SUMO-targeted ubiquitin ligase (Prudden, Pebernard et al. 2007). STUbLs interact with SUMO in a non-covalent manner to promote the de-sumoylation and/or degradation of sumoylated target proteins. Rad60 is ubiquitinated *in vitro* by Slx8 in an Rfp1-dependent manner (Prudden, Pebernard et al. 2007). Interestingly, a mutation in the predicted SBM binding pocket of Rad60 SLD1 is able to abolish ubiquitination of Rad60 by Slx8 (Prudden, Pebernard et al. 2007). This suggests that SLD1 mimics SUMO in its ability to bind the STUbL and that the Rad60-STUbL interaction is not reliant on SUMO-modification. However, given that a mutant encoding a ligase-dead version of the Nse2 protein, (*nse2-SA*) and *rad60-ct* are epistatic in their response to both UV and IR, the ability of Rad60 to be sumoylated in an Nse2-dependent manner was tested *in vitro*. Rad60 was found to be sumoylated *in vitro* and this was enhanced by the SUMO E3 ligase Pli1, but not by Nse2. Furthermore, Rad60 is sumoylated in a manner dependent on the C-terminus. A K342/357/361/368R quadruple mutant, where all four lysine residues in the C-terminus are knocked out, shows a modification pattern similar to the wild-type Rad60 protein. This suggests that although the site(s) of sumoylation are not within the C-terminal 73 amino acids (SLD2), SUMO

modification of Rad60 is dependent on the C-terminus. Rad60, but not Rad60-ct., is able to interact with the Hus5 conjugator *in vitro*, suggesting that SLD2 is required to recruit the Hus5 conjugator to Rad60. This is further supported by evidence that recombinant SLD2 (aa 334-406) interacts with GST-Hus5 but not a GST control (F.Z.Watts and B. Vintner, University of Sussex). It is therefore possible that the SUMO-like roles of SLD1 and SLD2 are to interact with the Slx8 STUbL and Hus5 conjugator, respectively. The differences identified in the SLD1 and SLD2 peptide sequence and predicted structures may explain their specificity for binding partners. Although the SLDs may fold like SUMO, the surface residues of each domain would be expected to define a different SUMO-/ubiquitin-like role.

It is possible that Rad60 SLD2 not only acts to recruit Hus5 for the SUMO-modification of itself, but may also function as a scaffold to recruit Hus5 to the Smc5/6 complex for use in Nse2 ligase -dependent sumoylation events. This would explain the epistasis between *nse2-SA* and *rad60-ct*; events in which either the ability to correctly localise the conjugator is impaired, or where SUMO ligase activity is lost, would result in loss of sumoylation of one or more specific proteins. The cellular consequence would, therefore, be the same. Given that Smc6 is sumoylated in an Nse2-dependent manner, and sumoylation of Smc6 is abolished in an *nse2-SA* background, it would be informative to know whether sumoylation of Smc6 is also abolished in the *rad60-ct* background. If sumoylation of Smc6 is dependent on Rad60, the transient interaction observed between Rad60 and the Smc5/6 complex could be explained (Morishita, Tsutsui et al. 2002; Boddy, Shanahan et al. 2003). Additionally, by assigning SLD2 a role in recruiting Hus5, the dominant negative effect observed when *rad60* is over-expressed in a *pli1-d* background can be explained. If SLD2 is required to interact with Hus5, over-expression of Rad60 in *pli1-d* cells may result in the titrating out of Hus5 in cells where sumoylation activity is already reduced. The effect therefore might be similar to that observed in *hus5* mutants. This effect is not seen with expression of *rad60-ct*, presumably because Rad60-ct cannot associate with Hus5. A possible experiment, which may give a better insight into the role of the Rad60-Hus5 interaction, may be to tether hus5 to Rad60-ct and assess whether Rad60 function is restored.

The N-terminal ubiquitin-like (UBL) and C-terminal ubiquitin-associated (UBA) domains of *S. cerevisiae* Dsk2 have been shown to interact, suggesting that the full length protein can form a closed conformation mediated by intramolecular binding of the UBL and UBA domains (Lowe, Hasan et al. 2006). The Dsk2 UBL-UBA interaction is weaker than that observed for the Dsk2 UBA-ubiquitin. This suggests that only when the UBA-UBL interaction is disrupted would the UBL domain be available for interaction with the proteasome. The UBA-UBL interaction may therefore play a regulatory role for Dsk2 adaptor function during ubiquitin-mediated proteasomal targeting. A similar proposal has been made for H. *sapiens* Rad23 (Walters, Lech et al. 2003). Rad60 has been proposed to form a homodimer via association of the SLDs of one Rad60 molecule and the SBMs of another (Raffa, Wohlschlegel et al. 2006). However, it is possible that, like Rad23 and Dsk2, Rad60 may form a closed conformation mediated by intramolecular binding of the SBMs and the SLDs. Comparative modelling suggests that Rad60 SLD1 and SLD2 have opposing surface charges. If an intramolecular interaction does exist between the N-terminal SBMs and the C-terminal SLDs, the result would be that the Rad60 molecule would fold back on itself. The opposing surface charges of the two SLDs may contribute to the stability of this strucure. In the closed conformation, the SLD2 surface residues required to interact with Hus5 may still be accessible and may help maintain Rad60 in the nucleus

Although initially the functions of the RENi family proteins do not seem well conserved, there is evidence to suggest that *rad60* and *esc2* may share some genetic interactions and hence may be functional homologues. The *S. pombe rad60* gene was first identified through its synthetic lethal interaction with *rad2*. Unlike *rad60, esc2* is not essential but an *esc2Δ* strain is synthetically lethal with mutations of the *rad27* (*rad2* homologue) gene (Tong, Evangelista et al. 2001). In addition, like *rad60-1 and rad60-3 esc2Δ* is synthetically lethal with *sgs1Δ*, the *S. cerevisiae* homologue of *rqh1* (Tong, Evangelista et al. 2001; Morishita, Tsutsui et al. 2002; Boddy, Shanahan et al. 2003). Recently, the crystal structure of *H. sapiens* Nip45 has been elucidated and shown to adopt a ββαββαβ fold, supporting the hypothesis that the SLDs of the RENi family are SUMO-like. As is the case for Rad60, *H. sapiens* Nip45 interacts with a STUbL. Interaction between RNF4 and Nip45

is increased following treatment with HU (Prudden, Pebernard et al. 2007). This suggests a model for the regulation of Rad60 into and out of the nucleus (Figure 7.1). In the nucleus, in the closed conformation, Rad60 SLD2 binds Hus5 facilitating its own sumoylation in a Pli1-dependent manner, thus maintaining Rad60 in the nucleus. Rad60 SLD2 also acts to recruit Hus5 to the Smc5/6 complex, to perhaps bring about the sumoylation of Smc6. Following replication stress, caused for example by a stalled replication fork, Cds1 is activated and Rad60 is phosphorylated on T72. This phosphorylation event may trigger a conformational change of Rad60 from a closed to an open conformation, allowing recruitment of Slx8 to SLD1. Alternatively, the Cds1-dependent phosphorylation event may act as a signal for the recruitment of Slx8. As is a similar case for the ubiquitin-like domain protein Dsk2, the affinity of Rad60 for the interaction with Slx8 may be greater than for the Rad60 SBM-SLD intramolecular interaction, thus switching from a closed to open conformation. Once bound, Slx8 replaces SUMO with ubiquitin and thus signals for delocalisation and degradation of Rad60. Presumably, in the case of the Rad60-ct protein, Rad60 cannot form a closed formation nor recruit Hus5 and can therefore not be maintained in the nucleus. This suggests a conserved role for the RENi proteins as scaffold proteins to regulate sumoylation and de-sumoylation events in the cell.

Figure 7.1: Proposed model for the control of homologous recombination mediated by alternative post-translational modifications of Rad60.

(A) Rad60 forms a closed conformation in the nucleus. **(B)** Rad60 SLD2 (indicated by red box) binds Hus5 facilitating its own sumoylation in a Pli1-dependent manner, as well as sumoylation of components of the Smc5/6 complex and permitting homologous recombination. **(C)** Following replication stress, Cds1-dependent phosphorylation of Rad60 on T72. signals for the recruitment of Slx8 to SLD1 (indicated by blue box), causing Rad60 to form. an open conformation. **(D)** Slx8 replaces SUMO with ubiquitin **(E)** Ubiquitination signals for delocalisation and degradation of Rad60. (SUMO, phosphorylation and ubiquitin modifications are denoted by S, P and U, respectively).

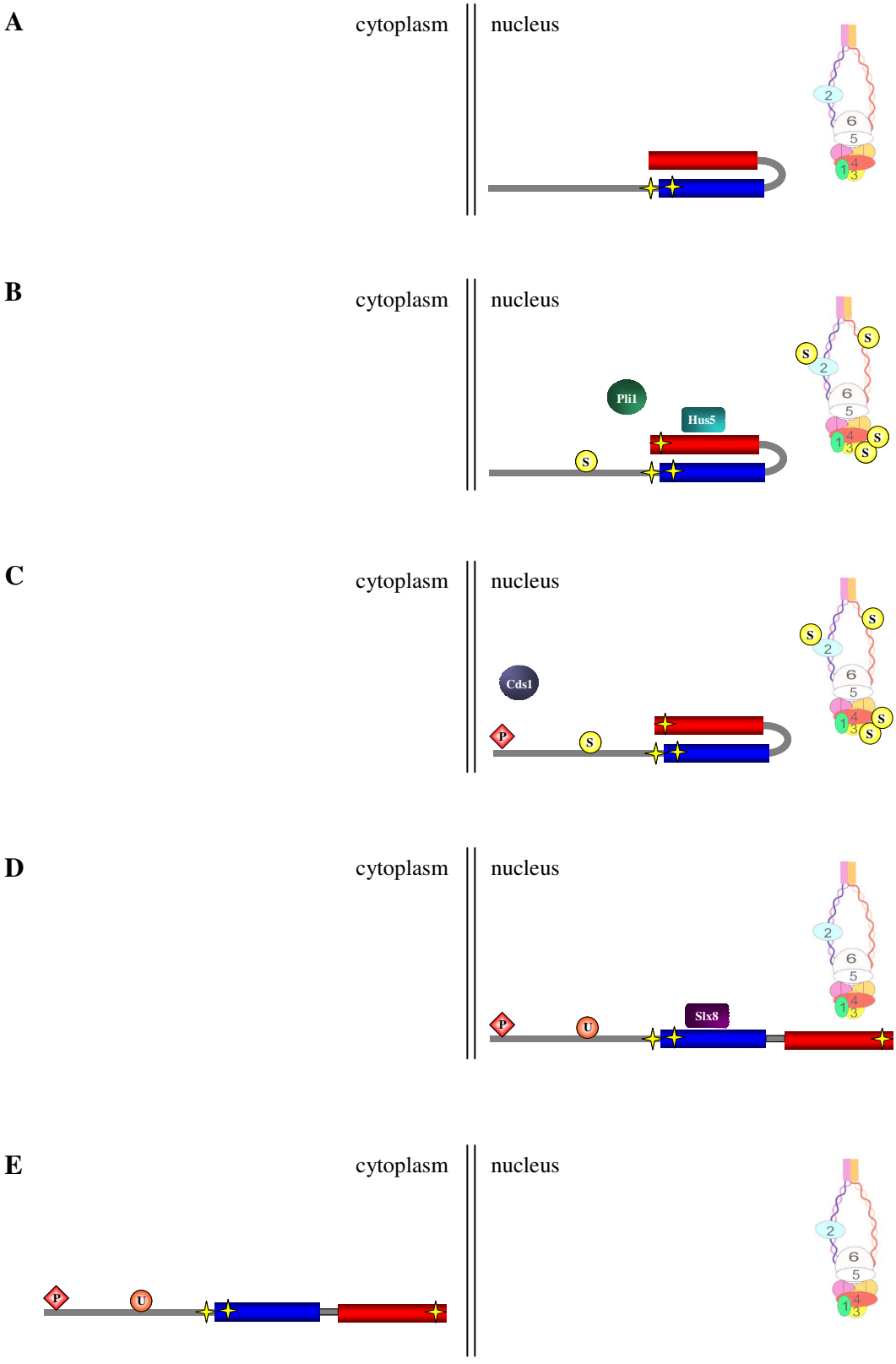

Figure 7.1: Proposed model for the control of homologous recombination mediated by alternative post-translational modifications of Rad60.

CHAPTER 8

REFERENCES

Aboussekhra, A., Biggerstaff, M., Shivji, M. K., Vilpo, J. A., Moncollin, V., Podust, V. N., Protic, M., Hubscher, U., Egly, J. M., and Wood, R. D. (1995). "Mammalian DNA nucleotide excision repair reconstituted with purified protein components." *Cell*, 80(6), 859-68.

al-Khodairy, F., and Carr, A. M. (1992). "DNA repair mutants defining G2 checkpoint pathways in Schizosaccharomyces pombe." *EMBO J*, 11(4), 1343-50.

al-Khodairy, F., Enoch, T., Hagan, I. M., and Carr, A. M. (1995). "The Schizosaccharomyces pombe hus5 gene encodes a ubiquitin conjugating enzyme required for normal mitosis." *J Cell Sci*, 108 (Pt 2), 475-86.

Allers, T., and Lichten, M. (2001). "Differential timing and control of noncrossover and crossover recombination during meiosis." *Cell*, 106(1), 47-57.

Alleva, J. L., and Doetsch, P. W. (1998). "Characterization of Schizosaccharomyces pombe Rad2 protein, a FEN-1 homolog." *Nucleic Acids Res*, 26(16), 3645-50.

Ampatzidou, E., Irmisch, A., O'Connell, M. J., and Murray, J. M. (2006). "Smc5/6 is required for repair at collapsed replication forks." *Mol Cell Biol*, 26(24), 9387-401.

Andrews, E. A., Palecek, J., Sergeant, J., Taylor, E., Lehmann, A. R., and Watts, F. Z. (2005). "Nse2, a component of the Smc5-6 complex, is a SUMO ligase required for the response to DNA damage." *Mol Cell Biol*, 25(1), 185-96.

Araujo, S. J., Tirode, F., Coin, F., Pospiech, H., Syvaoja, J. E., Stucki, M., Hubscher, U., Egly, J. M., and Wood, R. D. (2000). "Nucleotide excision repair of DNA with recombinant human proteins: definition of the minimal set of factors, active forms of TFIIH, and modulation by CAK." *Genes Dev*, 14(3), 349-59.

Azuma, Y., Arnaoutov, A., and Dasso, M. (2003). "SUMO-2/3 regulates topoisomerase II in mitosis." *J Cell Biol*, 163(3), 477-87.

Bachant, J., Alcasabas, A., Blat, Y., Kleckner, N., and Elledge, S. J. (2002). "The SUMO-1 isopeptidase Smt4 is linked to centromeric cohesion through SUMO-1 modification of DNA topoisomerase II." *Mol Cell*, 9(6), 1169-82.

Bahler, J., Wu, J. Q., Longtine, M. S., Shah, N. G., McKenzie, A., 3rd, Steever, A. B., Wach, A., Philippsen, P., and Pringle, J. R. (1998). "Heterologous modules for efficient and versatile PCR-based gene targeting in Schizosaccharomyces pombe." *Yeast*, 14(10), 943-51.

Bailly, V., Lamb, J., Sung, P., Prakash, S., and Prakash, L. (1994). "Specific complex formation between yeast RAD6 and RAD18 proteins: a potential mechanism for targeting RAD6 ubiquitin-conjugating activity to DNA damage sites." *Genes Dev*, 8(7), 811-20.

Bakkenist, C. J., and Kastan, M. B. (2003). "DNA damage activates ATM through intermolecular autophosphorylation and dimer dissociation." *Nature*, 421(6922), 499-506.

Banin, S., Moyal, L., Shieh, S., Taya, Y., Anderson, C. W., Chessa, L., Smorodinsky, N. I., Prives, C., Reiss, Y., Shiloh, Y., and Ziv, Y. (1998). "Enhanced phosphorylation of p53 by ATM in response to DNA damage." *Science*, 281(5383), 1674-7.

Bartek, J., and Lukas, J. (2001). "Pathways governing G1/S transition and their response to DNA damage." *FEBS Lett*, 490(3), 117-22.

Baumann, P., and West, S. C. (1998). "Role of the human RAD51 protein in homologous recombination and double-stranded-break repair." *Trends Biochem Sci*, 23(7), 247-51.

Bayer, P., Arndt, A., Metzger, S., Mahajan, R., Melchior, F., Jaenicke, R., and Becker, J. (1998). "Structure determination of the small ubiquitin-related modifier SUMO-1." *J Mol Biol*, 280(2), 275-86.

Benito, J., Martin-Castellanos, C., and Moreno, S. (1998). "Regulation of the G1 phase of the cell cycle by periodic stabilization and degradation of the p25rum1 CDK inhibitor." *EMBO J*, 17(2), 482-97.

Bernier-Villamor, V., Sampson, D. A., Matunis, M. J., and Lima, C. D. (2002). "Structural basis for E2-mediated SUMO conjugation revealed by a complex between ubiquitin-conjugating enzyme Ubc9 and RanGAP1." *Cell*, 108(3), 345-56.

Bertolaet, B. L., Clarke, D. J., Wolff, M., Watson, M. H., Henze, M., Divita, G., and Reed, S. I. (2001). "UBA domains of DNA damage-inducible proteins interact with ubiquitin." *Nat Struct Biol*, 8(5), 417-22.

Best, J. L., Ganiatsas, S., Agarwal, S., Changou, A., Salomoni, P., Shirihai, O., Meluh, P. B., Pandolfi, P. P., and Zon, L. I. (2002). "SUMO-1 protease-1 regulates gene transcription through PML." *Mol Cell*, 10(4), 843-55.

Bi, H., Song, X., Han, C., Xu, X., and Zhang, H. (2004). "[Studies on the chemical constituents of the essential oil from the leaves of Dalbergia odorifera T. Chen]." *Zhong Yao Cai*, 27(10), 733-5.

Boddy, M. N., Shanahan, P., McDonald, W. H., Lopez-Girona, A., Noguchi, E., Yates, I. J., and Russell, P. (2003). "Replication checkpoint kinase Cds1 regulates recombinational repair protein Rad60." *Mol Cell Biol*, 23(16), 5939-46.

Bohren, K. M., Nadkarni, V., Song, J. H., Gabbay, K. H., and Owerbach, D. (2004). "A M55V polymorphism in a novel SUMO gene (SUMO-4) differentially activates heat shock transcription factors and is associated with susceptibility to type I diabetes mellitus." *J Biol Chem*, 279(26), 27233-8.

Boutros, R., Dozier, C., and Ducommun, B. (2006). "The when and wheres of CDC25 phosphatases." *Curr Opin Cell Biol*, 18(2), 185-91.

Briggs, S. D., Xiao, T., Sun, Z. W., Caldwell, J. A., Shabanowitz, J., Hunt, D. F., Allis, C. D., and Strahl, B. D. (2002). "Gene silencing: trans-histone regulatory pathway in chromatin." *Nature*, 418(6897), 498.

Brondello, J. M., Boddy, M. N., Furnari, B., and Russell, P. (1999). "Basis for the checkpoint signal specificity that regulates Chk1 and Cds1 protein kinases." *Mol Cell Biol*, 19(6), 4262-9.

Bryce, P. J., Oyoshi, M. K., Kawamoto, S., Oettgen, H. C., and Tsitsikov, E. N. (2006). "TRAF1 regulates Th2 differentiation, allergic inflammation and nuclear localization of the Th2 transcription factor, NIP45." *Int Immunol*, 18(1), 101-11.

Busch, H., and Goldknopf, I. L. (1981). "Ubiquitin - protein conjugates." *Mol Cell Biochem*, 40(3), 173-87.

Bustin, M. (2001). "Chromatin unfolding and activation by HMGN(*) chromosomal proteins." *Trends Biochem Sci*, 26(7), 431-7.

Bylebyl, G. R., Belichenko, I., and Johnson, E. S. (2003). "The SUMO isopeptidase Ulp2 prevents accumulation of SUMO chains in yeast." *J Biol Chem*, 278(45), 44113-20.

Byun, T. S., Pacek, M., Yee, M. C., Walter, J. C., and Cimprich, K. A. (2005). "Functional uncoupling of MCM helicase and DNA polymerase activities activates the ATR-dependent checkpoint." *Genes Dev*, 19(9), 1040-52.

Canman, C. E., Lim, D. S., Cimprich, K. A., Taya, Y., Tamai, K., Sakaguchi, K., Appella, E., Kastan, M. B., and Siliciano, J. D. (1998). "Activation of the ATM kinase by ionizing radiation and phosphorylation of p53." *Science*, 281(5383), 1677-9.

Carney, J. P., Maser, R. S., Olivares, H., Davis, E. M., Le Beau, M., Yates, J. R., 3rd, Hays, L., Morgan, W. F., and Petrini, J. H. (1998). "The hMre11/hRad50 protein complex and Nijmegen breakage syndrome: linkage of double-strand break repair to the cellular DNA damage response." *Cell*, 93(3), 477-86.

Carr, A. M., Schmidt, H., Kirchhoff, S., Muriel, W. J., Sheldrick, K. S., Griffiths, D. J., Basmacioglu, C. N., Subramani, S., Clegg, M., Nasim, A., and et al. (1994). "The rad16 gene of Schizosaccharomyces pombe: a homolog of the RAD1 gene of Saccharomyces cerevisiae." *Mol Cell Biol*, 14(3), 2029-40.

Caspari, T., Dahlen, M., Kanter-Smoler, G., Lindsay, H. D., Hofmann, K., Papadimitriou, K., Sunnerhagen, P., and Carr, A. M. (2000). "Characterization of Schizosaccharomyces pombe Hus1: a PCNA-related protein that associates with Rad1 and Rad9." *Mol Cell Biol*, 20(4), 1254-62.

Caspari, T., Murray, J. M., and Carr, A. M. (2002). "Cdc2-cyclin B kinase activity links Crb2 and Rqh1-topoisomerase III." *Genes Dev*, 16(10), 1195-208.

Chen, L., Shinde, U., Ortolan, T. G., and Madura, K. (2001). "Ubiquitin-associated (UBA) domains in Rad23 bind ubiquitin and promote inhibition of multi-ubiquitin chain assembly." *EMBO Rep*, 2(10), 933-8.

Cleaver, J. E. (1968). "Defective repair replication of DNA in xeroderma pigmentosum." *Nature*, 218(5142), 652-6.

Cobb, J. A., Bjergbaek, L., Shimada, K., Frei, C., and Gasser, S. M. (2003). "DNA polymerase stabilization at stalled replication forks requires Mec1 and the RecQ helicase Sgs1." *EMBO J*, 22(16), 4325-36.

Cobbe, N., and Heck, M. M. (2004). "The evolution of SMC proteins: phylogenetic analysis and structural implications." *Mol Biol Evol*, 21(2), 332-47.

Correa-Bordes, J., Gulli, M. P., and Nurse, P. (1997). "p25rum1 promotes proteolysis of the mitotic B-cyclin p56cdc13 during G1 of the fission yeast cell cycle." *EMBO J*, 16(15), 4657-64.

Cost, G. J., and Cozzarelli, N. R. (2006). "Smc5p promotes faithful chromosome transmission and DNA repair in Saccharomyces cerevisiae." *Genetics*, 172(4), 2185-200.

Cuperus, G., and Shore, D. (2002). "Restoration of silencing in Saccharomyces cerevisiae by tethering of a novel Sir2-interacting protein, Esc8." *Genetics*, 162(2), 633-45.

Dao, V., and Modrich, P. (1998). "Mismatch-, MutS-, MutL-, and helicase II-dependent unwinding from the single-strand break of an incised heteroduplex." *J Biol Chem*, 273(15), 9202-7.

Desterro, J. M., Rodriguez, M. S., Kemp, G. D., and Hay, R. T. (1999). "Identification of the enzyme required for activation of the small ubiquitin-like protein SUMO-1." *J Biol Chem*, 274(15), 10618-24.

Desterro, J. M., Thomson, J., and Hay, R. T. (1997). "Ubch9 conjugates SUMO but not ubiquitin." *FEBS Lett*, 417(3), 297-300.

Dhillon, N., and Kamakaka, R. T. (2000). "A histone variant, Htz1p, and a Sir1p-like protein, Esc2p, mediate silencing at HMR." *Mol Cell*, 6(4), 769-80.

Doe, C. L., Ahn, J. S., Dixon, J., and Whitby, M. C. (2002). "Mus81-Eme1 and Rqh1 involvement in processing stalled and collapsed replication forks." *J Biol Chem*, 277(36), 32753-9.

Doetsch, P. W., and Cunningham, R. P. (1990). "The enzymology of apurinic/apyrimidinic endonucleases." *Mutat Res*, 236(2-3), 173-201.

Dohmen, R. J., Stappen, R., McGrath, J. P., Forrova, H., Kolarov, J., Goffeau, A., and Varshavsky, A. (1995). "An essential yeast gene encoding a homolog of ubiquitin-activating enzyme." *J Biol Chem*, 270(30), 18099-109.

Drapkin, R., Reardon, J. T., Ansari, A., Huang, J. C., Zawel, L., Ahn, K., Sancar, A., and Reinberg, D. (1994). "Dual role of TFIIH in DNA excision repair and in transcription by RNA polymerase II." *Nature*, 368(6473), 769-72.

Dulic, V., Kaufmann, W. K., Wilson, S. J., Tlsty, T. D., Lees, E., Harper, J. W., Elledge, S. J., and Reed, S. I. (1994). "p53-dependent inhibition of cyclin-dependent kinase activities in human fibroblasts during radiation-induced G1 arrest." *Cell*, 76(6), 1013-23.

el-Deiry, W. S., Tokino, T., Velculescu, V. E., Levy, D. B., Parsons, R., Trent, J. M., Lin, D., Mercer, W. E., Kinzler, K. W., and Vogelstein, B. (1993). "WAF1, a potential mediator of p53 tumor suppression." *Cell*, 75(4), 817-25.

Essers, J., Houtsmuller, A. B., van Veelen, L., Paulusma, C., Nigg, A. L., Pastink, A., Vermeulen, W., Hoeijmakers, J. H., and Kanaar, R. (2002). "Nuclear dynamics of RAD52 group homologous recombination proteins in response to DNA damage." *EMBO J*, 21(8), 2030-7.

Ferguson, D. O., and Holloman, W. K. (1996). "Recombinational repair of gaps in DNA is asymmetric in Ustilago maydis and can be explained by a migrating D-loop model." *Proc Natl Acad Sci U S A*, 93(11), 5419-24.

Finucane, M. D., and Woolfson, D. N. (1999). "Core-directed protein design. II. Rescue of a multiply mutated and destabilized variant of ubiquitin." *Biochemistry*, 38(36), 11613-23.

Fishel, R., Lescoe, M. K., Rao, M. R., Copeland, N. G., Jenkins, N. A., Garber, J., Kane, M., and Kolodner, R. (1993). "The human mutator gene homolog MSH2 and its association with hereditary nonpolyposis colon cancer." *Cell*, 75(5), 1027-38.

Fousteri, M., Vermeulen, W., van Zeeland, A. A., and Mullenders, L. H. (2006). "Cockayne syndrome A and B proteins differentially regulate recruitment of chromatin remodeling and repair factors to stalled RNA polymerase II in vivo." *Mol Cell*, 23(4), 471-82.

Fousteri, M. I., and Lehmann, A. R. (2000). "A novel SMC protein complex in Schizosaccharomyces pombe contains the Rad18 DNA repair protein." *EMBO J*, 19(7), 1691-702.

Frampton, J., Irmisch, A., Green, C. M., Neiss, A., Trickey, M., Ulrich, H. D., Furuya, K., Watts, F. Z., Carr, A. M., and Lehmann, A. R. (2006). "Postreplication repair and PCNA modification in Schizosaccharomyces pombe." *Mol Biol Cell*, 17(7), 2976-85.

Freyer, G. A., Davey, S., Ferrer, J. V., Martin, A. M., Beach, D., and Doetsch, P. W. (1995). "An alternative eukaryotic DNA excision repair pathway." *Mol Cell Biol*, 15(8), 4572-7.

Fujioka, Y., Kimata, Y., Nomaguchi, K., Watanabe, K., and Kohno, K. (2002). "Identification of a novel non-structural maintenance of chromosomes (SMC) component of the SMC5-SMC6 complex involved in DNA repair." *J Biol Chem*, 277(24), 21585-91.

Funakoshi, M., Sasaki, T., Nishimoto, T., and Kobayashi, H. (2002). "Budding yeast Dsk2p is a polyubiquitin-binding protein that can interact with the proteasome." *Proc Natl Acad Sci U S A*, 99(2), 745-50.

Furuse, M., Nagase, Y., Tsubouchi, H., Murakami-Murofushi, K., Shibata, T., and Ohta, K. (1998). "Distinct roles of two separable in vitro activities of yeast Mre11 in mitotic and meiotic recombination." *EMBO J*, 17(21), 6412-25.

Furuya, K., Poitelea, M., Guo, L., Caspari, T., and Carr, A. M. (2004). "Chk1 activation requires Rad9 S/TQ-site phosphorylation to promote association with C-terminal BRCT domains of Rad4TOPBP1." *Genes Dev*, 18(10), 1154-64.

Gagne, J. M., Downes, B. P., Shiu, S. H., Durski, A. M., and Vierstra, R. D. (2002). "The F-box subunit of the SCF E3 complex is encoded by a diverse superfamily of genes in Arabidopsis." *Proc Natl Acad Sci U S A*, 99(17), 11519-24.

Garcia, V., Furuya, K., and Carr, A. M. (2005). "Identification and functional analysis of TopBP1 and its homologs." *DNA Repair (Amst)*, 4(11), 1227-39.

Giaccia, A. J., and Kastan, M. B. (1998). "The complexity of p53 modulation: emerging patterns from divergent signals." *Genes Dev*, 12(19), 2973-83.

Goldknopf, I. L., and Busch, H. (1977). "Isopeptide linkage between nonhistone and histone 2A polypeptides of chromosomal conjugate-protein A24." *Proc Natl Acad Sci U S A*, 74(3), 864-8.

Gong, L., Li, B., Millas, S., and Yeh, E. T. (1999). "Molecular cloning and characterization of human AOS1 and UBA2, components of the sentrin-activating enzyme complex." *FEBS Lett*, 448(1), 185-9.

Gostissa, M., Hengstermann, A., Fogal, V., Sandy, P., Schwarz, S. E., Scheffner, M., and Del Sal, G. (1999). "Activation of p53 by conjugation to the ubiquitin-like protein SUMO-1." *EMBO J*, 18(22), 6462-71.

Gottlieb, T. M., and Jackson, S. P. (1993). "The DNA-dependent protein kinase: requirement for DNA ends and association with Ku antigen." *Cell*, 72(1), 131-42.

Gregoire, S., Tremblay, A. M., Xiao, L., Yang, Q., Ma, K., Nie, J., Mao, Z., Wu, Z., Giguere, V., and Yang, X. J. (2006). "Control of MEF2 transcriptional activity by coordinated phosphorylation and sumoylation." *J Biol Chem*, 281(7), 4423-33.

Haas, A. L., and Siepmann, T. J. (1997). "Pathways of ubiquitin conjugation." *FASEB J*, 11(14), 1257-68.

Haber, J. E. (1999). "DNA recombination: the replication connection." *Trends Biochem Sci*, 24(7), 271-5.

Haering, C. H., Lowe, J., Hochwagen, A., and Nasmyth, K. (2002). "Molecular architecture of SMC proteins and the yeast cohesin complex." *Mol Cell*, 9(4), 773-88.

Hagan, I. M. (1998). "The fission yeast microtubule cytoskeleton." *J Cell Sci*, 111 (Pt 12), 1603-12.

Hanahan, D. (1983). "Studies on transformation of Escherichia coli with plasmids." *J Mol Biol*, 166(4), 557-80.

Haracska, L., Torres-Ramos, C. A., Johnson, R. E., Prakash, S., and Prakash, L. (2004). "Opposing effects of ubiquitin conjugation and SUMO modification of PCNA on

replicational bypass of DNA lesions in Saccharomyces cerevisiae." *Mol Cell Biol*, 24(10), 4267-74.

Hardeland, U., Steinacher, R., Jiricny, J., and Schar, P. (2002). "Modification of the human thymine-DNA glycosylase by ubiquitin-like proteins facilitates enzymatic turnover." *EMBO J*, 21(6), 1456-64.

Harper, J. W., Adami, G. R., Wei, N., Keyomarsi, K., and Elledge, S. J. (1993). "The p21 Cdk-interacting protein Cip1 is a potent inhibitor of G1 cyclin-dependent kinases." *Cell*, 75(4), 805-16.

Hazbun, T. R., Malmstrom, L., Anderson, S., Graczyk, B. J., Fox, B., Riffle, M., Sundin, B. A., Aranda, J. D., McDonald, W. H., Chiu, C. H., Snydsman, B. E., Bradley, P., Muller, E. G., Fields, S., Baker, D., Yates, J. R., 3rd, and Davis, T. N. (2003). "Assigning function to yeast proteins by integration of technologies." *Mol Cell*, 12(6), 1353-65.

Hecker, C. M., Rabiller, M., Haglund, K., Bayer, P., and Dikic, I. (2006). "Specification of SUMO1- and SUMO2-interacting motifs." *J Biol Chem*, 281(23), 16117-27.

Hershko, A., and Ciechanover, A. (1998). "The ubiquitin system." *Annu Rev Biochem*, 67, 425-79.

Hietakangas, V., Anckar, J., Blomster, H. A., Fujimoto, M., Palvimo, J. J., Nakai, A., and Sistonen, L. (2006). "PDSM, a motif for phosphorylation-dependent SUMO modification." *Proc Natl Acad Sci U S A*, 103(1), 45-50.

Hirano, M., and Hirano, T. (1998). "ATP-dependent aggregation of single-stranded DNA by a bacterial SMC homodimer." *EMBO J*, 17(23), 7139-48.

Hirano, M., and Hirano, T. (2002). "Hinge-mediated dimerization of SMC protein is essential for its dynamic interaction with DNA." *EMBO J*, 21(21), 5733-44.

Hirano, T. (1999). "SMC-mediated chromosome mechanics: a conserved scheme from bacteria to vertebrates?" *Genes Dev*, 13(1), 11-9.

Hirano, T. (2006). "At the heart of the chromosome: SMC proteins in action." *Nat Rev Mol Cell Biol*, 7(5), 311-22.

Ho, J. C., Warr, N. J., Shimizu, H., and Watts, F. Z. (2001). "SUMO modification of Rad22, the Schizosaccharomyces pombe homologue of the recombination protein Rad52." *Nucleic Acids Res*, 29(20), 4179-86.

Ho, J. C., and Watts, F. Z. (2003). "Characterization of SUMO-conjugating enzyme mutants in Schizosaccharomyces pombe identifies a dominant-negative allele that severely reduces SUMO conjugation." *Biochem J*, 372(Pt 1), 97-104.

Hochstrasser, M. (1996). "Ubiquitin-dependent protein degradation." *Annu Rev Genet*, 30, 405-39.

Hochstrasser, M. (2001). "SP-RING for SUMO: new functions bloom for a ubiquitin-like protein." *Cell*, 107(1), 5-8.

Hoege, C., Pfander, B., Moldovan, G. L., Pyrowolakis, G., and Jentsch, S. (2002). "RAD6-dependent DNA repair is linked to modification of PCNA by ubiquitin and SUMO." *Nature*, 419(6903), 135-41.

Huang, W. P., and Klionsky, D. J. (2002). "Autophagy in yeast: a review of the molecular machinery." *Cell Struct Funct*, 27(6), 409-20.

Imai, S., Armstrong, C. M., Kaeberlein, M., and Guarente, L. (2000). "Transcriptional silencing and longevity protein Sir2 is an NAD-dependent histone deacetylase." *Nature*, 403(6771), 795-800.

Jackson, D., Dhar, K., Wahl, J. K., Wold, M. S., and Borgstahl, G. E. (2002). "Analysis of the human replication protein A:Rad52 complex: evidence for crosstalk between RPA32, RPA70, Rad52 and DNA." *J Mol Biol*, 321(1), 133-48.

Johnson, E. S., and Blobel, G. (1997). "Ubc9p is the conjugating enzyme for the ubiquitin-like protein Smt3p." *J Biol Chem*, 272(43), 26799-802.

Johnson, E. S., and Blobel, G. (1999). "Cell cycle-regulated attachment of the ubiquitin-related protein SUMO to the yeast septins." *J Cell Biol*, 147(5), 981-94.

Johnson, E. S., and Gupta, A. A. (2001). "An E3-like factor that promotes SUMO conjugation to the yeast septins." *Cell*, 106(6), 735-44.

Junop, M. S., Obmolova, G., Rausch, K., Hsieh, P., and Yang, W. (2001). "Composite active site of an ABC ATPase: MutS uses ATP to verify mismatch recognition and authorize DNA repair." *Mol Cell*, 7(1), 1-12.

Kagey, M. H., Melhuish, T. A., and Wotton, D. (2003). "The polycomb protein Pc2 is a SUMO E3." *Cell*, 113(1), 127-37.

Kai, M., Furuya, K., Paderi, F., Carr, A. M., and Wang, T. S. (2007). "Rad3-dependent phosphorylation of the checkpoint clamp regulates repair-pathway choice." *Nat Cell Biol*, 9(6), 691-7.

Kai, M., and Wang, T. S. (2003). "Checkpoint responses to replication stalling: inducing tolerance and preventing mutagenesis." *Mutat Res*, 532(1-2), 59-73.

Kamitani, T., Kito, K., Fukuda-Kamitani, T., and Yeh, E. T. (2001). "Targeting of NEDD8 and its conjugates for proteasomal degradation by NUB1." *J Biol Chem*, 276(49), 46655-60.

Kamitani, T., Nguyen, H. P., and Yeh, E. T. (1997). "Preferential modification of nuclear proteins by a novel ubiquitin-like molecule." *J Biol Chem*, 272(22), 14001-4.

Karahalil, B., Hogue, B. A., de Souza-Pinto, N. C., and Bohr, V. A. (2002). "Base excision repair capacity in mitochondria and nuclei: tissue-specific variations." *FASEB J*, 16(14), 1895-902.

Kirkin, V., and Dikic, I. (2007). "Role of ubiquitin- and Ubl-binding proteins in cell signaling." *Curr Opin Cell Biol*, 19(2), 199-205.

Kitamura, K., Maekawa, H., and Shimoda, C. (1998). "Fission yeast Ste9, a homolog of Hct1/Cdh1 and Fizzy-related, is a novel negative regulator of cell cycle progression during G1-phase." *Mol Biol Cell*, 9(5), 1065-80.

Kosoy, A., Calonge, T. M., Outwin, E. A., and O'Connell, M. J. (2007). "Fission yeast Rnf4 homologs are required for DNA repair." *J Biol Chem*, 282(28), 20388-94.

Krokan, H. E., Nilsen, H., Skorpen, F., Otterlei, M., and Slupphaug, G. (2000). "Base excision repair of DNA in mammalian cells." *FEBS Lett*, 476(1-2), 73-7.

Kubota, Y., Nash, R. A., Klungland, A., Schar, P., Barnes, D. E., and Lindahl, T. (1996). "Reconstitution of DNA base excision-repair with purified human proteins: interaction between DNA polymerase beta and the XRCC1 protein." *EMBO J*, 15(23), 6662-70.

Kumagai, A., Kim, S. M., and Dunphy, W. G. (2004). "Claspin and the activated form of ATR-ATRIP collaborate in the activation of Chk1." *J Biol Chem*, 279(48), 49599-608.

Lallemand-Breitenbach, V., Jeanne, M., Benhenda, S., Nasr, R., Lei, M., Peres, L., Zhou, J., Zhu, J., Raught, B., and de The, H. (2008). "Arsenic degrades PML or PML-RARalpha through a SUMO-triggered RNF4/ubiquitin-mediated pathway." *Nat Cell Biol*, 10(5), 547-55.

Lambertson, D., Chen, L., and Madura, K. (2003). "Investigating the importance of proteasome-interaction for Rad23 function." *Curr Genet*, 42(4), 199-208.

Laursen, L. V., Ampatzidou, E., Andersen, A. H., and Murray, J. M. (2003). "Role for the fission yeast RecQ helicase in DNA repair in G2." *Mol Cell Biol*, 23(10), 3692-705.

Leach, F. S., Tokino, T., Meltzer, P., Burrell, M., Oliner, J. D., Smith, S., Hill, D. E., Sidransky, D., Kinzler, K. W., and Vogelstein, B. (1993). "p53 Mutation and MDM2 amplification in human soft tissue sarcomas." *Cancer Res*, 53(10 Suppl), 2231-4.

Lee, J. H., and Paull, T. T. (2005). "ATM activation by DNA double-strand breaks through the Mre11-Rad50-Nbs1 complex." *Science*, 308(5721), 551-4.

Lehmann, A. R. (1995). "Nucleotide excision repair and the link with transcription." *Trends Biochem Sci*, 20(10), 402-5.

Lehmann, A. R. (2003). "DNA repair-deficient diseases, xeroderma pigmentosum, Cockayne syndrome and trichothiodystrophy." *Biochimie*, 85(11), 1101-11.

Lehmann, A. R., Walicka, M., Griffiths, D. J., Murray, J. M., Watts, F. Z., McCready, S., and Carr, A. M. (1995). "The rad18 gene of Schizosaccharomyces pombe defines a new subgroup of the SMC superfamily involved in DNA repair." *Mol Cell Biol*, 15(12), 7067-80.

Li, S. J., and Hochstrasser, M. (1999). "A new protease required for cell-cycle progression in yeast." *Nature*, 398(6724), 246-51.

Li, S. J., and Hochstrasser, M. (2000). "The yeast ULP2 (SMT4) gene encodes a novel protease specific for the ubiquitin-like Smt3 protein." *Mol Cell Biol*, 20(7), 2367-77.

Lieberson, R., Mowen, K. A., McBride, K. D., Leautaud, V., Zhang, X., Suh, W. K., Wu, L., and Glimcher, L. H. (2001). "Tumor necrosis factor receptor-associated factor (TRAF)2 represses the T helper cell type 2 response through interaction with NFAT-interacting protein (NIP45)." *J Exp Med*, 194(1), 89-98.

Lin, D., Tatham, M. H., Yu, B., Kim, S., Hay, R. T., and Chen, Y. (2002). "Identification of a substrate recognition site on Ubc9." *J Biol Chem*, 277(24), 21740-8.

Lindroos, H., Vinnere, O., Mira, A., Repsilber, D., Naslund, K., and Andersson, S. G. (2006). "Genome rearrangements, deletions, and amplifications in the natural population of Bartonella henselae." *J Bacteriol*, 188(21), 7426-39.

Lindsay, H. D., Griffiths, D. J., Edwards, R. J., Christensen, P. U., Murray, J. M., Osman, F., Walworth, N., and Carr, A. M. (1998). "S-phase-specific activation of Cds1 kinase defines a subpathway of the checkpoint response in Schizosaccharomyces pombe." *Genes Dev*, 12(3), 382-95.

Liu, L. Q., Ilaria, R., Jr., Kingsley, P. D., Iwama, A., van Etten, R. A., Palis, J., and Zhang, D. E. (1999). "A novel ubiquitin-specific protease, UBP43, cloned from leukemia fusion protein AML1-ETO-expressing mice, functions in hematopoietic cell differentiation." *Mol Cell Biol*, 19(4), 3029-38.

Liu, Q., Guntuku, S., Cui, X. S., Matsuoka, S., Cortez, D., Tamai, K., Luo, G., Carattini-Rivera, S., DeMayo, F., Bradley, A., Donehower, L. A., and Elledge, S. J. (2000). "Chk1 is an essential kinase that is regulated by Atr and required for the G(2)/M DNA damage checkpoint." *Genes Dev*, 14(12), 1448-59.

Lowe, E. D., Hasan, N., Trempe, J. F., Fonso, L., Noble, M. E., Endicott, J. A., Johnson, L. N., and Brown, N. R. (2006). "Structures of the Dsk2 UBL and UBA domains and their complex." *Acta Crystallogr D Biol Crystallogr*, 62(Pt 2), 177-88.

Ma, H., Gamper, M., Parent, C., and Firtel, R. A. (1997). "The Dictyostelium MAP kinase kinase DdMEK1 regulates chemotaxis and is essential for chemoattractant-mediated activation of guanylyl cyclase." *EMBO J*, 16(14), 4317-32.

Madura, K. (2004). "Rad23 and Rpn10: perennial wallflowers join the melee." *Trends Biochem Sci*, 29(12), 637-40.

Mahajan, R., Delphin, C., Guan, T., Gerace, L., and Melchior, F. (1997). "A small ubiquitin-related polypeptide involved in targeting RanGAP1 to nuclear pore complex protein RanBP2." *Cell*, 88(1), 97-107.

Malakhov, M. P., Kim, K. I., Malakhova, O. A., Jacobs, B. S., Borden, E. C., and Zhang, D. E. (2003). "High-throughput immunoblotting. Ubiquitiin-like protein ISG15 modifies key regulators of signal transduction." *J Biol Chem*, 278(19), 16608-13.

Marti, T. M., Kunz, C., and Fleck, O. (2002). "DNA mismatch repair and mutation avoidance pathways." *J Cell Physiol*, 191(1), 28-41.

Masutani, C., Araki, M., Sugasawa, K., van der Spek, P. J., Yamada, A., Uchida, A., Maekawa, T., Bootsma, D., Hoeijmakers, J. H., and Hanaoka, F. (1997). "Identification and characterization of XPC-binding domain of hHR23B." *Mol Cell Biol*, 17(12), 6915-23.

Matic, I., van Hagen, M., Schimmel, J., Macek, B., Ogg, S. C., Tatham, M. H., Hay, R. T., Lamond, A. I., Mann, M., and Vertegaal, A. C. (2008). "In vivo identification of human small ubiquitin-like modifier polymerization sites by high accuracy mass spectrometry and an in vitro to in vivo strategy." *Mol Cell Proteomics*, 7(1), 132-44.

Matunis, M. J., Coutavas, E., and Blobel, G. (1996). "A novel ubiquitin-like modification modulates the partitioning of the Ran-GTPase-activating protein RanGAP1 between the cytosol and the nuclear pore complex." *J Cell Biol*, 135(6 Pt 1), 1457-70.

Maundrell, K. (1993). "Thiamine-repressible expression vectors pREP and pRIP for fission yeast." *Gene*, 123(1), 127-30.

McCready, S., Carr, A. M., and Lehmann, A. R. (1993). "Repair of cyclobutane pyrimidine dimers and 6-4 photoproducts in the fission yeast Schizosaccharomyces pombe." *Mol Microbiol*, 10(4), 885-90.

McCready, S. J., Osman, F., and Yasui, A. (2000). "Repair of UV damage in the fission yeast Schizosaccharomyces pombe." *Mutat Res*, 451(1-2), 197-210.

McDonald, W. H., Pavlova, Y., Yates, J. R., 3rd, and Boddy, M. N. (2003). "Novel essential DNA repair proteins Nse1 and Nse2 are subunits of the fission yeast Smc5-Smc6 complex." *J Biol Chem*, 278(46), 45460-7.

McLaughlin, P. M., Helfrich, W., Kok, K., Mulder, M., Hu, S. W., Brinker, M. G., Ruiters, M. H., de Leij, L. F., and Buys, C. H. (2000). "The ubiquitin-activating enzyme E1-like protein in lung cancer cell lines." *Int J Cancer*, 85(6), 871-6.

Melby, T. E., Ciampaglio, C. N., Briscoe, G., and Erickson, H. P. (1998). "The symmetrical structure of structural maintenance of chromosomes (SMC) and MukB proteins: long, antiparallel coiled coils, folded at a flexible hinge." *J Cell Biol*, 142(6), 1595-604.

Melchionna, R., Chen, X. B., Blasina, A., and McGowan, C. H. (2000). "Threonine 68 is required for radiation-induced phosphorylation and activation of Cds1." *Nat Cell Biol*, 2(10), 762-5.

Melchior, F., Schergaut, M., and Pichler, A. (2003). "SUMO: ligases, isopeptidases and nuclear pores." *Trends Biochem Sci*, 28(11), 612-8.

Melo, J. A., Cohen, J., and Toczyski, D. P. (2001). "Two checkpoint complexes are independently recruited to sites of DNA damage in vivo." *Genes Dev*, 15(21), 2809-21.

Meluh, P. B., and Koshland, D. (1995). "Evidence that the MIF2 gene of Saccharomyces cerevisiae encodes a centromere protein with homology to the mammalian centromere protein CENP-C." *Mol Biol Cell*, 6(7), 793-807.

Michaelis, C., Ciosk, R., and Nasmyth, K. (1997). "Cohesins: chromosomal proteins that prevent premature separation of sister chromatids." *Cell*, 91(1), 35-45.

Minty, A., Dumont, X., Kaghad, M., and Caput, D. (2000). "Covalent modification of p73alpha by SUMO-1. Two-hybrid screening with p73 identifies novel SUMO-1-interacting proteins and a SUMO-1 interaction motif." *J Biol Chem*, 275(46), 36316-23.

Miyabe, I., Morishita, T., Hishida, T., Yonei, S., and Shinagawa, H. (2006). "Rhp51-dependent recombination intermediates that do not generate checkpoint signal are accumulated in Schizosaccharomyces pombe rad60 and smc5/6 mutants after release from replication arrest." *Mol Cell Biol*, 26(1), 343-53.

Mizushima, N., Noda, T., Yoshimori, T., Tanaka, Y., Ishii, T., George, M. D., Klionsky, D. J., Ohsumi, M., and Ohsumi, Y. (1998). "A protein conjugation system essential for autophagy." *Nature*, 395(6700), 395-8.

Modrich, P., and Lahue, R. (1996). "Mismatch repair in replication fidelity, genetic recombination, and cancer biology." *Annu Rev Biochem*, 65, 101-33.

Moreau, S., Ferguson, J. R., and Symington, L. S. (1999). "The nuclease activity of Mre11 is required for meiosis but not for mating type switching, end joining, or telomere maintenance." *Mol Cell Biol*, 19(1), 556-66.

Moreno, S., Klar, A., and Nurse, P. (1991). "Molecular genetic analysis of fission yeast Schizosaccharomyces pombe." *Methods Enzymol*, 194, 795-823.

Moreno, S., Nurse, P., and Russell, P. (1990). "Regulation of mitosis by cyclic accumulation of p80cdc25 mitotic inducer in fission yeast." *Nature*, 344(6266), 549-52.

Morikawa, H., Morishita, T., Kawane, S., Iwasaki, H., Carr, A. M., and Shinagawa, H. (2004). "Rad62 protein functionally and physically associates with the smc5/smc6 protein complex and is required for chromosome integrity and recombination repair in fission yeast." *Mol Cell Biol*, 24(21), 9401-13.

Morishita, T., Tsutsui, Y., Iwasaki, H., and Shinagawa, H. (2002). "The Schizosaccharomyces pombe rad60 gene is essential for repairing double-strand DNA breaks spontaneously occurring during replication and induced by DNA-damaging agents." *Mol Cell Biol*, 22(10), 3537-48.

Mossessova, E., and Lima, C. D. (2000). "Ulp1-SUMO crystal structure and genetic analysis reveal conserved interactions and a regulatory element essential for cell growth in yeast." *Mol Cell*, 5(5), 865-76.

Mullen, J. R., Kaliraman, V., Ibrahim, S. S., and Brill, S. J. (2001). "Requirement for three novel protein complexes in the absence of the Sgs1 DNA helicase in Saccharomyces cerevisiae." *Genetics*, 157(1), 103-18.

Muller, S., Berger, M., Lehembre, F., Seeler, J. S., Haupt, Y., and Dejean, A. (2000). "c-Jun and p53 activity is modulated by SUMO-1 modification." *J Biol Chem*, 275(18), 13321-9.

Muller, S., Matunis, M. J., and Dejean, A. (1998). "Conjugation with the ubiquitin-related modifier SUMO-1 regulates the partitioning of PML within the nucleus." *EMBO J*, 17(1), 61-70.

Murray, J. M., Doe, C. L., Schenk, P., Carr, A. M., Lehmann, A. R., and Watts, F. Z. (1992). "Cloning and characterisation of the S. pombe rad15 gene, a homologue to the S. cerevisiae RAD3 and human ERCC2 genes." *Nucleic Acids Res*, 20(11), 2673-8.

Murray, J. M., Lindsay, H. D., Munday, C. A., and Carr, A. M. (1997). "Role of Schizosaccharomyces pombe RecQ homolog, recombination, and checkpoint genes in UV damage tolerance." *Mol Cell Biol*, 17(12), 6868-75.

Murray, J. M., Tavassoli, M., al-Harithy, R., Sheldrick, K. S., Lehmann, A. R., Carr, A. M., and Watts, F. Z. (1994). "Structural and functional conservation of the human homolog of the Schizosaccharomyces pombe rad2 gene, which is required for chromosome segregation and recovery from DNA damage." *Mol Cell Biol*, 14(7), 4878-88.

Nakatsu, Y., Asahina, H., Citterio, E., Rademakers, S., Vermeulen, W., Kamiuchi, S., Yeo, J. P., Khaw, M. C., Saijo, M., Kodo, N., Matsuda, T., Hoeijmakers, J. H., and Tanaka, K. (2000). "XAB2, a novel tetratricopeptide repeat protein involved in transcription-coupled DNA repair and transcription." *J Biol Chem*, 275(45), 34931-7.

Nasmyth, K., and Haering, C. H. (2005). "The structure and function of SMC and kleisin complexes." *Annu Rev Biochem*, 74, 595-648.

Nick McElhinny, S. A., Snowden, C. M., McCarville, J., and Ramsden, D. A. (2000). "Ku recruits the XRCC4-ligase IV complex to DNA ends." *Mol Cell Biol*, 20(9), 2996-3003.

Norbury, C., and Nurse, P. (1992). "Animal cell cycles and their control." *Annu Rev Biochem*, 61, 441-70.

Norbury, C. J., and Hickson, I. D. (2001). "Cellular responses to DNA damage." *Annu Rev Pharmacol Toxicol*, 41, 367-401.

Novatchkova, M., Bachmair, A., Eisenhaber, B., and Eisenhaber, F. (2005). "Proteins with two SUMO-like domains in chromatin-associated complexes: the RENi (Rad60-Esc2-NIP45) family." *BMC Bioinformatics*, 6, 22.

O'Donovan, A., Davies, A. A., Moggs, J. G., West, S. C., and Wood, R. D. (1994). "XPG endonuclease makes the 3' incision in human DNA nucleotide excision repair." *Nature*, 371(6496), 432-5.

Osaka, F., Kawasaki, H., Aida, N., Saeki, M., Chiba, T., Kawashima, S., Tanaka, K., and Kato, S. (1998). "A new NEDD8-ligating system for cullin-4A." *Genes Dev*, 12(15), 2263-8.

Palecek, J., Vidot, S., Feng, M., Doherty, A. J., and Lehmann, A. R. (2006). "The Smc5-Smc6 DNA repair complex. bridging of the Smc5-Smc6 heads by the KLEISIN, Nse4, and non-Kleisin subunits." *J Biol Chem*, 281(48), 36952-9.

Papadopoulos, N., Nicolaides, N. C., Wei, Y. F., Ruben, S. M., Carter, K. C., Rosen, C. A., Haseltine, W. A., Fleischmann, R. D., Fraser, C. M., Adams, M. D., and et al. (1994). "Mutation of a mutL homolog in hereditary colon cancer." *Science*, 263(5153), 1625-9.

Papouli, E., Chen, S., Davies, A. A., Huttner, D., Krejci, L., Sung, P., and Ulrich, H. D. (2005). "Crosstalk between SUMO and ubiquitin on PCNA is mediated by recruitment of the helicase Srs2p." *Mol Cell*, 19(1), 123-33.

Park, C. H., Mu, D., Reardon, J. T., and Sancar, A. (1995). "The general transcription-repair factor TFIIH is recruited to the excision repair complex by the XPA protein independent of the TFIIE transcription factor." *J Biol Chem*, 270(9), 4896-902.

Paz, Y., Elazar, Z., and Fass, D. (2000). "Structure of GATE-16, membrane transport modulator and mammalian ortholog of autophagocytosis factor Aut7p." *J Biol Chem*, 275(33), 25445-50.

Pebernard, S., McDonald, W. H., Pavlova, Y., Yates, J. R., 3rd, and Boddy, M. N. (2004). "Nse1, Nse2, and a novel subunit of the Smc5-Smc6 complex, Nse3, play a crucial role in meiosis." *Mol Biol Cell*, 15(11), 4866-76.

Pebernard, S., Wohlschlegel, J., McDonald, W. H., Yates, J. R., 3rd, and Boddy, M. N. (2006). "The Nse5-Nse6 dimer mediates DNA repair roles of the Smc5-Smc6 complex." *Mol Cell Biol*, 26(5), 1617-30.

Perry, J. J., Tainer, J. A., and Boddy, M. N. (2008). "A SIM-ultaneous role for SUMO and ubiquitin." *Trends Biochem Sci*, 33(5), 201-8.

Pfander, B., Moldovan, G. L., Sacher, M., Hoege, C., and Jentsch, S. (2005). "SUMO-modified PCNA recruits Srs2 to prevent recombination during S phase." *Nature*, 436(7049), 428-33.

Pichler, A., Gast, A., Seeler, J. S., Dejean, A., and Melchior, F. (2002). "The nucleoporin RanBP2 has SUMO1 E3 ligase activity." *Cell*, 108(1), 109-20.

Pierce, A. J., Stark, J. M., Araujo, F. D., Moynahan, M. E., Berwick, M., and Jasin, M. (2001). "Double-strand breaks and tumorigenesis." *Trends Cell Biol*, 11(11), S52-9.

Pines, J. (1995). "Cyclins and cyclin-dependent kinases: a biochemical view." *Biochem J*, 308 (Pt 3), 697-711.

Potts, P. R., Porteus, M. H., and Yu, H. (2006). "Human SMC5/6 complex promotes sister chromatid homologous recombination by recruiting the SMC1/3 cohesin complex to double-strand breaks." *EMBO J*, 25(14), 3377-88.

Potts, P. R., and Yu, H. (2005). "Human MMS21/NSE2 is a SUMO ligase required for DNA repair." *Mol Cell Biol*, 25(16), 7021-32.

Prudden, J., Pebernard, S., Raffa, G., Slavin, D. A., Perry, J. J., Tainer, J. A., McGowan, C. H., and Boddy, M. N. (2007). "SUMO-targeted ubiquitin ligases in genome stability." *EMBO J*, 26(18), 4089-101.

Raffa, G. D., Wohlschlegel, J., Yates, J. R., 3rd, and Boddy, M. N. (2006). "SUMO-binding motifs mediate the Rad60-dependent response to replicative stress and self-association." *J Biol Chem*, 281(38), 27973-81.

Ramilo, C., Gu, L., Guo, S., Zhang, X., Patrick, S. M., Turchi, J. J., and Li, G. M. (2002). "Partial reconstitution of human DNA mismatch repair in vitro: characterization of the role of human replication protein A." *Mol Cell Biol*, 22(7), 2037-46.

Ramsden, D. A., and Gellert, M. (1998). "Ku protein stimulates DNA end joining by mammalian DNA ligases: a direct role for Ku in repair of DNA double-strand breaks." *EMBO J*, 17(2), 609-14.

Rao, H., and Sastry, A. (2002). "Recognition of specific ubiquitin conjugates is important for the proteolytic functions of the ubiquitin-associated domain proteins Dsk2 and Rad23." *J Biol Chem*, 277(14), 11691-5.

Ritchie, K. J., Malakhov, M. P., Hetherington, C. J., Zhou, L., Little, M. T., Malakhova, O. A., Sipe, J. C., Orkin, S. H., and Zhang, D. E. (2002). "Dysregulation of protein modification by ISG15 results in brain cell injury." *Genes Dev*, 16(17), 2207-12.

Rodriguez, M. S., Dargemont, C., and Hay, R. T. (2001). "SUMO-1 conjugation in vivo requires both a consensus modification motif and nuclear targeting." *J Biol Chem*, 276(16), 12654-9.

Rogakou, E. P., Pilch, D. R., Orr, A. H., Ivanova, V. S., and Bonner, W. M. (1998). "DNA double-stranded breaks induce histone H2AX phosphorylation on serine 139." *J Biol Chem*, 273(10), 5858-68.

Rosenberg, M. I., and Parkhurst, S. M. (2002). "Drosophila Sir2 is required for heterochromatic silencing and by euchromatic Hairy/E(Spl) bHLH repressors in segmentation and sex determination." *Cell*, 109(4), 447-58.

Sachdev, S., Bruhn, L., Sieber, H., Pichler, A., Melchior, F., and Grosschedl, R. (2001). "PIASy, a nuclear matrix-associated SUMO E3 ligase, represses LEF1 activity by sequestration into nuclear bodies." *Genes Dev*, 15(23), 3088-103.

Saitoh, H., and Hinchey, J. (2000). "Functional heterogeneity of small ubiquitin-related protein modifiers SUMO-1 versus SUMO-2/3." *J Biol Chem*, 275(9), 6252-8.

Saka, Y., Esashi, F., Matsusaka, T., Mochida, S., and Yanagida, M. (1997). "Damage and replication checkpoint control in fission yeast is ensured by interactions of Crb2, a protein with BRCT motif, with Cut5 and Chk1." *Genes Dev*, 11(24), 3387-400.

Sali, A., Potterton, L., Yuan, F., van Vlijmen, H., and Karplus, M. (1995). "Evaluation of comparative protein modeling by MODELLER." *Proteins*, 23(3), 318-26.

Sampson, D. A., Wang, M., and Matunis, M. J. (2001). "The small ubiquitin-like modifier-1 (SUMO-1) consensus sequence mediates Ubc9 binding and is essential for SUMO-1 modification." *J Biol Chem*, 276(24), 21664-9.

Sanchez, R., and Sali, A. (2000). "Comparative protein structure modeling. Introduction and practical examples with modeller." *Methods Mol Biol*, 143, 97-129.

Santa Maria, S. R., Gangavarapu, V., Johnson, R. E., Prakash, L., and Prakash, S. (2007). "Requirement of Nse1, a subunit of the Smc5-Smc6 complex, for Rad52-dependent postreplication repair of UV-damaged DNA in Saccharomyces cerevisiae." *Mol Cell Biol*, 27(23), 8409-18.

Seeler, J. S., and Dejean, A. (2003). "Nuclear and unclear functions of SUMO." *Nat Rev Mol Cell Biol*, 4(9), 690-9.

Sergeant, J., Taylor, E., Palecek, J., Fousteri, M., Andrews, E. A., Sweeney, S., Shinagawa, H., Watts, F. Z., and Lehmann, A. R. (2005). "Composition and architecture of the Schizosaccharomyces pombe Rad18 (Smc5-6) complex." *Mol Cell Biol*, 25(1), 172-84.

Seufert, W., Futcher, B., and Jentsch, S. (1995). "Role of a ubiquitin-conjugating enzyme in degradation of S- and M-phase cyclins." *Nature*, 373(6509), 78-81.

Shalizi, A., Gaudilliere, B., Yuan, Z., Stegmuller, J., Shirogane, T., Ge, Q., Tan, Y., Schulman, B., Harper, J. W., and Bonni, A. (2006). "A calcium-regulated MEF2 sumoylation switch controls postsynaptic differentiation." *Science*, 311(5763), 1012-7.

Shayeghi, M., Doe, C. L., Tavassoli, M., and Watts, F. Z. (1997). "Characterisation of Schizosaccharomyces pombe rad31, a UBA-related gene required for DNA damage tolerance." *Nucleic Acids Res*, 25(6), 1162-9.

Shieh, S. Y., Taya, Y., and Prives, C. (1999). "DNA damage-inducible phosphorylation of p53 at N-terminal sites including a novel site, Ser20, requires tetramerization." *EMBO J*, 18(7), 1815-23.

Shih, H. M., Chang, C. C., Kuo, H. Y., and Lin, D. Y. (2007). "Daxx mediates SUMO-dependent transcriptional control and subnuclear compartmentalization." *Biochem Soc Trans*, 35(Pt 6), 1397-400.

Shiloh, Y. (1997). "Ataxia-telangiectasia and the Nijmegen breakage syndrome: related disorders but genes apart." *Annu Rev Genet*, 31, 635-62.

Shiozaki, K., and Yanagida, M. (1992). "Functional dissection of the phosphorylated termini of fission yeast DNA topoisomerase II." *J Cell Biol*, 119(5), 1023-36.

Shivji, M. K., Podust, V. N., Hubscher, U., and Wood, R. D. (1995). "Nucleotide excision repair DNA synthesis by DNA polymerase epsilon in the presence of PCNA, RFC, and RPA." *Biochemistry*, 34(15), 5011-7.

Sijbers, A. M., van der Spek, P. J., Odijk, H., van den Berg, J., van Duin, M., Westerveld, A., Jaspers, N. G., Bootsma, D., and Hoeijmakers, J. H. (1996). "Mutational analysis of the human nucleotide excision repair gene ERCC1." *Nucleic Acids Res*, 24(17), 3370-80.

Singleton, B. K., Torres-Arzayus, M. I., Rottinghaus, S. T., Taccioli, G. E., and Jeggo, P. A. (1999). "The C terminus of Ku80 activates the DNA-dependent protein kinase catalytic subunit." *Mol Cell Biol*, 19(5), 3267-77.

Sobko, A., Ma, H., and Firtel, R. A. (2002). "Regulated SUMOylation and ubiquitination of DdMEK1 is required for proper chemotaxis." *Dev Cell*, 2(6), 745-56.

Sokhansanj, B. A., Rodrigue, G. R., Fitch, J. P., and Wilson, D. M., 3rd. (2002). "A quantitative model of human DNA base excision repair. I. Mechanistic insights." *Nucleic Acids Res*, 30(8), 1817-25.

Song, J., Durrin, L. K., Wilkinson, T. A., Krontiris, T. G., and Chen, Y. (2004). "Identification of a SUMO-binding motif that recognizes SUMO-modified proteins." *Proc Natl Acad Sci U S A*, 101(40), 14373-8.

Song, J., Zhang, Z., Hu, W., and Chen, Y. (2005). "Small ubiquitin-like modifier (SUMO) recognition of a SUMO binding motif: a reversal of the bound orientation." *J Biol Chem*, 280(48), 40122-9.

Stelter, P., and Ulrich, H. D. (2003). "Control of spontaneous and damage-induced mutagenesis by SUMO and ubiquitin conjugation." *Nature*, 425(6954), 188-91.

Stewart, E., Chapman, C. R., Al-Khodairy, F., Carr, A. M., and Enoch, T. (1997). "rqh1+, a fission yeast gene related to the Bloom's and Werner's syndrome genes, is required for reversible S phase arrest." *EMBO J*, 16(10), 2682-92.

Stewart, G. S., Wang, B., Bignell, C. R., Taylor, A. M., and Elledge, S. J. (2003). "MDC1 is a mediator of the mammalian DNA damage checkpoint." *Nature*, 421(6926), 961-6.

Stucki, M., and Jackson, S. P. (2004). "MDC1/NFBD1: a key regulator of the DNA damage response in higher eukaryotes." *DNA Repair (Amst)*, 3(8-9), 953-7.

Subramanian, L., Benson, M. D., and Iniguez-Lluhi, J. A. (2003). "A synergy control motif within the attenuator domain of CCAAT/enhancer-binding protein alpha inhibits transcriptional synergy through its PIASy-enhanced modification by SUMO-1 or SUMO-3." *J Biol Chem*, 278(11), 9134-41.

Sugasawa, K., Ng, J. M., Masutani, C., Maekawa, T., Uchida, A., van der Spek, P. J., Eker, A. P., Rademakers, S., Visser, C., Aboussekhra, A., Wood, R. D., Hanaoka, F.,

Bootsma, D., and Hoeijmakers, J. H. (1997). "Two human homologs of Rad23 are functionally interchangeable in complex formation and stimulation of XPC repair activity." *Mol Cell Biol*, 17(12), 6924-31.

Sugasawa, K., Okamoto, T., Shimizu, Y., Masutani, C., Iwai, S., and Hanaoka, F. (2001). "A multistep damage recognition mechanism for global genomic nucleotide excision repair." *Genes Dev*, 15(5), 507-21.

Sun, H., Leverson, J. D., and Hunter, T. (2007). "Conserved function of RNF4 family proteins in eukaryotes: targeting a ubiquitin ligase to SUMOylated proteins." *EMBO J*, 26(18), 4102-12.

Sun, Z. W., and Allis, C. D. (2002). "Ubiquitination of histone H2B regulates H3 methylation and gene silencing in yeast." *Nature*, 418(6893), 104-8.

Takahashi, Y., Iwase, M., Konishi, M., Tanaka, M., Toh-e, A., and Kikuchi, Y. (1999). "Smt3, a SUMO-1 homolog, is conjugated to Cdc3, a component of septin rings at the mother-bud neck in budding yeast." *Biochem Biophys Res Commun*, 259(3), 582-7.

Tanaka, K., Nishide, J., Okazaki, K., Kato, H., Niwa, O., Nakagawa, T., Matsuda, H., Kawamukai, M., and Murakami, Y. (1999). "Characterization of a fission yeast SUMO-1 homologue, pmt3p, required for multiple nuclear events, including the control of telomere length and chromosome segregation." *Mol Cell Biol*, 19(12), 8660-72.

Tatham, M. H., Geoffroy, M. C., Shen, L., Plechanovova, A., Hattersley, N., Jaffray, E. G., Palvimo, J. J., and Hay, R. T. (2008). "RNF4 is a poly-SUMO-specific E3 ubiquitin ligase required for arsenic-induced PML degradation." *Nat Cell Biol*, 10(5), 538-46.

Tatham, M. H., Jaffray, E., Vaughan, O. A., Desterro, J. M., Botting, C. H., Naismith, J. H., and Hay, R. T. (2001). "Polymeric chains of SUMO-2 and SUMO-3 are conjugated to protein substrates by SAE1/SAE2 and Ubc9." *J Biol Chem*, 276(38), 35368-74.

Taylor, D. L., Ho, J. C., Oliver, A., and Watts, F. Z. (2002). "Cell-cycle-dependent localisation of Ulp1, a Schizosaccharomyces pombe Pmt3 (SUMO)-specific protease." *J Cell Sci*, 115(Pt 6), 1113-22.

Taylor, E. M., Moghraby, J. S., Lees, J. H., Smit, B., Moens, P. B., and Lehmann, A. R. (2001). "Characterization of a novel human SMC heterodimer homologous to the Schizosaccharomyces pombe Rad18/Spr18 complex." *Mol Biol Cell*, 12(6), 1583-94.

Tong, A. H., Evangelista, M., Parsons, A. B., Xu, H., Bader, G. D., Page, N., Robinson, M., Raghibizadeh, S., Hogue, C. W., Bussey, H., Andrews, B., Tyers, M., and Boone, C. (2001). "Systematic genetic analysis with ordered arrays of yeast deletion mutants." *Science*, 294(5550), 2364-8.

Torres-Rosell, J., Machin, F., and Aragon, L. (2005a). "Smc5-Smc6 complex preserves nucleolar integrity in S. cerevisiae." *Cell Cycle*, 4(7), 868-72.

Torres-Rosell, J., Machin, F., Farmer, S., Jarmuz, A., Eydmann, T., Dalgaard, J. Z., and Aragon, L. (2005b). "SMC5 and SMC6 genes are required for the segregation of repetitive chromosome regions." *Nat Cell Biol*, 7(4), 412-9.

Uhlmann, F., Wernic, D., Poupart, M. A., Koonin, E. V., and Nasmyth, K. (2000). "Cleavage of cohesin by the CD clan protease separin triggers anaphase in yeast." *Cell*, 103(3), 375-86.

Ulrich, H. D., and Jentsch, S. (2000). "Two RING finger proteins mediate cooperation between ubiquitin-conjugating enzymes in DNA repair." *EMBO J*, 19(13), 3388-97.

Uziel, T., Lerenthal, Y., Moyal, L., Andegeko, Y., Mittelman, L., and Shiloh, Y. (2003). "Requirement of the MRN complex for ATM activation by DNA damage." *EMBO J*, 22(20), 5612-21.

Uzunova, K., Gottsche, K., Miteva, M., Weisshaar, S. R., Glanemann, C., Schnellhardt, M., Niessen, M., Scheel, H., Hofmann, K., Johnson, E. S., Praefcke, G. J., and Dohmen, R. J. (2007). "Ubiquitin-dependent proteolytic control of SUMO conjugates." *J Biol Chem*, 282(47), 34167-75.

Vaziri, H., Dessain, S. K., Ng Eaton, E., Imai, S. I., Frye, R. A., Pandita, T. K., Guarente, L., and Weinberg, R. A. (2001). "hSIR2(SIRT1) functions as an NAD-dependent p53 deacetylase." *Cell*, 107(2), 149-59.

Verkade, H. M., Bugg, S. J., Lindsay, H. D., Carr, A. M., and O'Connell, M. J. (1999). "Rad18 is required for DNA repair and checkpoint responses in fission yeast." *Mol Biol Cell*, 10(9), 2905-18.

Vertegaal, A. C., Ogg, S. C., Jaffray, E., Rodriguez, M. S., Hay, R. T., Andersen, J. S., Mann, M., and Lamond, A. I. (2004). "A proteomic study of SUMO-2 target proteins." *J Biol Chem*, 279(32), 33791-8.

Volker, M., Mone, M. J., Karmakar, P., van Hoffen, A., Schul, W., Vermeulen, W., Hoeijmakers, J. H., van Driel, R., van Zeeland, A. A., and Mullenders, L. H. (2001). "Sequential assembly of the nucleotide excision repair factors in vivo." *Mol Cell*, 8(1), 213-24.

Walters, K. J., Lech, P. J., Goh, A. M., Wang, Q., and Howley, P. M. (2003). "DNA-repair protein hHR23a alters its protein structure upon binding proteasomal subunit S5a." *Proc Natl Acad Sci U S A*, 100(22), 12694-9.

Walworth, N. C., and Bernards, R. (1996). "rad-dependent response of the chk1-encoded protein kinase at the DNA damage checkpoint." *Science*, 271(5247), 353-6.

Wang, C., Deng, L., Hong, M., Akkaraju, G. R., Inoue, J., and Chen, Z. J. (2001). "TAK1 is a ubiquitin-dependent kinase of MKK and IKK." *Nature*, 412(6844), 346-51.

Wang, Z., Buratowski, S., Svejstrup, J. Q., Feaver, W. J., Wu, X., Kornberg, R. D., Donahue, T. F., and Friedberg, E. C. (1995). "The yeast TFB1 and SSL1 genes, which encode subunits of transcription factor IIH, are required for nucleotide excision repair and RNA polymerase II transcription." *Mol Cell Biol*, 15(4), 2288-93.

Watson, A. T., Garcia, V., Bone, N., Carr, A. M., and Armstrong, J. (2008). "Gene tagging and gene replacement using recombinase-mediated cassette exchange in Schizosaccharomyces pombe." *Gene*, 407(1-2), 63-74.

Weinert, T. A., and Hartwell, L. H. (1988). "The RAD9 gene controls the cell cycle response to DNA damage in Saccharomyces cerevisiae." *Science*, 241(4863), 317-22.

Werler, P. J., Hartsuiker, E., and Carr, A. M. (2003). "A simple Cre-loxP method for chromosomal N-terminal tagging of essential and non-essential Schizosaccharomyces pombe genes." *Gene*, 304, 133-41.

Wilkinson, K. D. (1995). "Roles of ubiquitinylation in proteolysis and cellular regulation." *Annu Rev Nutr*, 15, 161-89.

Wood, V., Gwilliam, R., Rajandream, M. A., Lyne, M., Lyne, R., Stewart, A., Sgouros, J., Peat, N., Hayles, J., Baker, S., Basham, D., Bowman, S., Brooks, K., Brown, D., Brown, S., Chillingworth, T., Churcher, C., Collins, M., Connor, R., Cronin, A., Davis, P., Feltwell, T., Fraser, A., Gentles, S., Goble, A., Hamlin, N., Harris, D.,

Hidalgo, J., Hodgson, G., Holroyd, S., Hornsby, T., Howarth, S., Huckle, E. J., Hunt, S., Jagels, K., James, K., Jones, L., Jones, M., Leather, S., McDonald, S., McLean, J., Mooney, P., Moule, S., Mungall, K., Murphy, L., Niblett, D., Odell, C., Oliver, K., O'Neil, S., Pearson, D., Quail, M. A., Rabbinowitsch, E., Rutherford, K., Rutter, S., Saunders, D., Seeger, K., Sharp, S., Skelton, J., Simmonds, M., Squares, R., Squares, S., Stevens, K., Taylor, K., Taylor, R. G., Tivey, A., Walsh, S., Warren, T., Whitehead, S., Woodward, J., Volckaert, G., Aert, R., Robben, J., Grymonprez, B., Weltjens, I., Vanstreels, E., Rieger, M., Schafer, M., Muller-Auer, S., Gabel, C., Fuchs, M., Dusterhoft, A., Fritzc, C., Holzer, E., Moestl, D., Hilbert, H., Borzym, K., Langer, I., Beck, A., Lehrach, H., Reinhardt, R., Pohl, T. M., Eger, P., Zimmermann, W., Wedler, H., Wambutt, R., Purnelle, B., Goffeau, A., Cadieu, E., Dreano, S., Gloux, S., et al. (2002). "The genome sequence of Schizosaccharomyces pombe." *Nature*, 415(6874), 871-80.

Xhemalce, B., Seeler, J. S., Thon, G., Dejean, A., and Arcangioli, B. (2004). "Role of the fission yeast SUMO E3 ligase Pli1p in centromere and telomere maintenance." *EMBO J*, 23(19), 3844-53.

Xiao, Z., Chen, Z., Gunasekera, A. H., Sowin, T. J., Rosenberg, S. H., Fesik, S., and Zhang, H. (2003). "Chk1 mediates S and G2 arrests through Cdc25A degradation in response to DNA-damaging agents." *J Biol Chem*, 278(24), 21767-73.

Xie, Y., Kerscher, O., Kroetz, M. B., McConchie, H. F., Sung, P., and Hochstrasser, M. (2007). "The yeast Hex3.Slx8 heterodimer is a ubiquitin ligase stimulated by substrate sumoylation." *J Biol Chem*, 282(47), 34176-84.

Yamaguchi, S., Murakami, H., and Okayama, H. (1997). "A WD repeat protein controls the cell cycle and differentiation by negatively regulating Cdc2/B-type cyclin complexes." *Mol Biol Cell*, 8(12), 2475-86.

Yang, S. H., Galanis, A., Witty, J., and Sharrocks, A. D. (2006). "An extended consensus motif enhances the specificity of substrate modification by SUMO." *EMBO J*, 25(21), 5083-93.

Yang, S. H., Jaffray, E., Hay, R. T., and Sharrocks, A. D. (2003). "Dynamic interplay of the SUMO and ERK pathways in regulating Elk-1 transcriptional activity." *Mol Cell*, 12(1), 63-74.

Yang, S. H., and Sharrocks, A. D. (2004). "SUMO promotes HDAC-mediated transcriptional repression." *Mol Cell*, 13(4), 611-7.

Yeh, E. T., Gong, L., and Kamitani, T. (2000). "Ubiquitin-like proteins: new wines in new bottles." *Gene*, 248(1-2), 1-14.

Yonemasu, R., McCready, S. J., Murray, J. M., Osman, F., Takao, M., Yamamoto, K., Lehmann, A. R., and Yasui, A. (1997). "Characterization of the alternative excision repair pathway of UV-damaged DNA in Schizosaccharomyces pombe." *Nucleic Acids Res*, 25(8), 1553-8.

Zhao, H., Watkins, J. L., and Piwnica-Worms, H. (2002). "Disruption of the checkpoint kinase 1/cell division cycle 25A pathway abrogates ionizing radiation-induced S and G2 checkpoints." *Proc Natl Acad Sci U S A*, 99(23), 14795-800.

Zhao, X., and Blobel, G. (2005). "A SUMO ligase is part of a nuclear multiprotein complex that affects DNA repair and chromosomal organization." *Proc Natl Acad Sci U S A*, 102(13), 4777-82.

Zhao, Y., Kwon, S. W., Anselmo, A., Kaur, K., and White, M. A. (2004). "Broad spectrum identification of cellular small ubiquitin-related modifier (SUMO) substrate proteins." *J Biol Chem*, 279(20), 20999-1002.

Zhong, S., Muller, S., Ronchetti, S., Freemont, P. S., Dejean, A., and Pandolfi, P. P. (2000). "Role of SUMO-1-modified PML in nuclear body formation." *Blood*, 95(9), 2748-52.

Zou, L., and Elledge, S. J. (2003). "Sensing DNA damage through ATRIP recognition of RPA-ssDNA complexes." *Science*, 300(5625), 1542-8.